UNIVERSITÀ DELLA CALABRIA

UNIVERSITY OF CALABRIA

Department of Pharmacy and Health and Nutritional Sciences

PHD IN TRANSLATIONAL MEDICINE

XXXII cycle

ADVANCED AND SMART NANOCARRIERS FOR PHARMACEUTICAL APPLICATIONS

CHIM/09

Coordinator: Prof. Sebastiano Andò

ANDO'
SEBASTIANO
20.04.2020
09:49:13 UTC

Supervisor/Tutor: Prof. Rita Muzzalupo

Rita Muzzalupo

PhD Student: Elisabetta Mazzotta

Elisabetta Mazzotta

ABSTRACT

The application of nanotechnology in drug formulation has made significant headway over the last decade. Nanoscale controlled release systems allow to revalue and reformulate old drugs through targeted delivery to the desired pathological site, improving therapeutic efficiency and reducing side effects. This innovative modality of drug delivery aims to create personalized, safer and effective treatments. A great interest of the academic and industrial research is focused on the design and development of advanced nanocarriers since is a profitable way in terms of costs, times and risks than the discovery of new drugs. Herein, an extensive variety of nanocarriers systems composed of different materials including lipids, polymers and non-ionic surfactants have been proposed for different pharmaceutical applications. Specifically, the carriers have been tailor-made designed to improve drug photostability, enhance skin permeation and realize smart tools for tumor target therapy.

1

INTRODUCTION

1.0 Main contributions

The current century has witnessed a growing interest in the design and synthesis of advanced nanomaterials for pharmaceutical purpose. The nanotechnology has revolutionized the conventional delivery of drugs offering several implementations from numerous point of view. The present thesis deals about the design of new advanced nanodevices useful for pharmaceutical applications and the evaluation of their potentiality as drug delivery systems through tests *in vitro*.

1.1 Structure of the thesis

In the framework of a long-standing research activity ongoing in the Pharmaceutical Technology group of Department of Pharmacy, Health and Nutritional Sciences (University of Calabria), the present thesis is divided into three self-contained sections focused on the development of novel macromolecular systems for several pharmaceutical applications. Specifically, the developed nanocarriers were designed for a potential application in topical delivery (Chapter 2), in cancer therapy (Chapter 3) and in drug photoprotection (Chapter 4).

1.2 Nanotechnology in Drug Formulation

Over the last few years, nanotechnology has found an unprecedented attention in broad areas of the science. According to the National Nanotechnology Initiative, nanotechnology is the research and technology development at the atomic, molecular, or macromolecular levels to create and use structures, devices, and systems in the length scale of 1-100 nm range (Figure 1). Unlike the properties of the bulk materials which follow the classic laws, nanoscale size particles exhibit unique and novel properties due to the influence of quantum effect and the higher surface area [1]. Particularly, nanotechnology has revolutionized the manipulation of the materials used for drug delivery. The application of knowledges and techniques of nanoscience in pharmaceutical formulation has, indeed, been well appreciated for the ability to engineer molecules or supramolecular structures and to produce devices with programmed functions. Nanomedicines for pharmaceutical purposes are defined by the Encyclopaedia of Pharmaceutical Technology as solid colloidal particles in the range size around 1-1000 nm. They consist in macromolecular materials in which a therapeutic or diagnostic agent can be dissolved, entrapped, adsorbed or attached [2]. The advancements of nanomedicine are making the old drugs work better and delivering novel classes of drugs those were previously considered unmarketable due to the low solubility and bioavailability, high toxicity and marked side effects. Different factors such as size and surface characteristics support the countless advantages of the use of nanoparticles in biomedical field. The most benefits of nano sized drug formulation are known, indeed, to be directly related to particle size that majorly affect the distribution in the body. It has been reported that nanoscale size particles cellular

uptake is much higher than that of large particles with size ranging between 1 and 10 μm [3]. Due to their small size, nanoparticles, indeed, are able to penetrate in the tissue system, cross the blood brain barrier (BBB), be absorbed through the tight junctions of skin endothelial cells and enter the pulmonary systems [3]. Consequently, this technology has yielded the opportunity to reach new targets and to control drug distribution manipulating the carrier size.

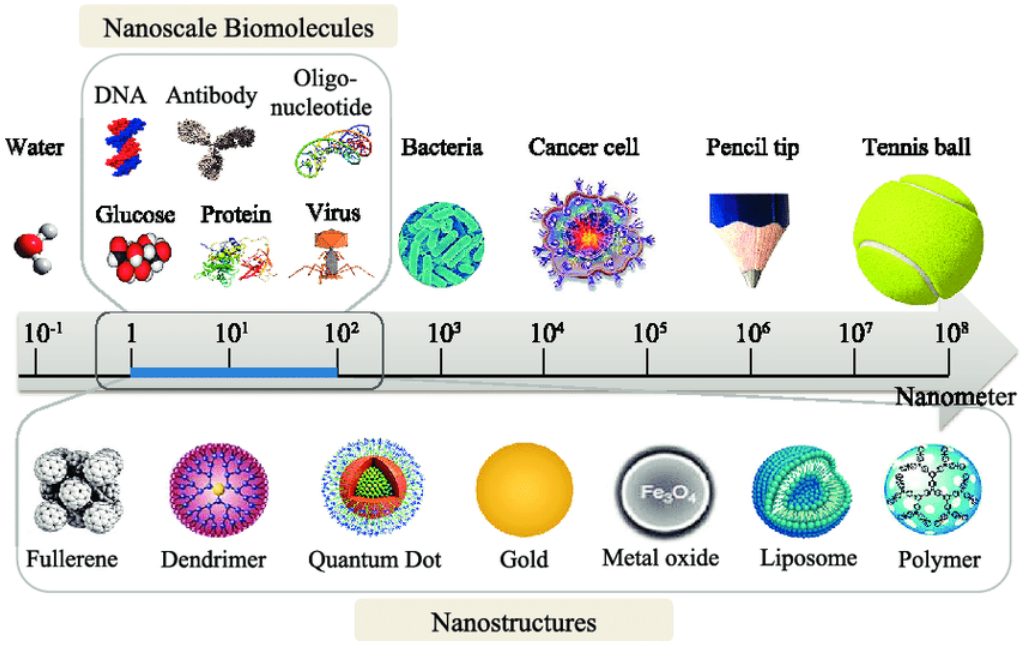

Figure 1. Size scale for nanoparticles as compared to other materials.

Not only it is possible to reach new targets, but the small size of nanodevices allows to avoid the immediate clearance by the lymphatic system and increase circulation times in bloodstream. Another advantage associated with small size is the larger surface area that makes available higher amount of drug near the surface of and, therefore, leads to a faster drug release. Additionally, the surface charges of nanocarriers affect aggregation, stability, and drug distribution and, consequently, the manipulation of this property must be also opportunely considered in the design of drug carriers. Hydrophilic surface and higher surface charges are, indeed, known to hinder the binding of plasma protein (opsonization) and prolong circulation in the bloodstream of nanoformulations [4]. In summary, an ideal system for drug delivery must have size large enough to avoid leakage in blood capillaries but not too large to be recognized by the lymphatic systems and hydrophilic surfaces in order to avoid the binding of blood components. By controlling these features with nanotechnology approaches, it is possible to obtain smart and tailor-made nanodevices for specific therapeutic or diagnostic purposes which is the main goal of an ideal pharmaceutical formulation.

1.3 Target Drug delivery

The application of nanotechnology approaches in drug delivery allows to overcome the typical limitations of conventional pharmaceutical formulations. The efficacy of a drug is, indeed, significantly influenced by the way which is delivered and its biopharmaceutical properties. Physicochemical or metabolic instability, poor aqueous solubility or permeability, insufficient drug concentration at the target tissue, non-specific adverse toxic effects are common factors that limit the drug clinical efficacy. To overcome these drawbacks, nanoscale size particles are used as delivery agents by loading drug and deliver them to target tissues more selectively with a controlled release [5]. Drug delivery systems (DDS) are designed with the aim to enhance solubility and bioavailability, control pharmacokinetics and pharmacodynamics drug profiles. Moreover, the delivery of drug using DDS protects them from harsh physiological environments such as the acidic environment of the stomach or lysosomes and from the high levels of proteases or others enzymes present in bloodstream [6]. DDS allow also to explore new administration routes of old drugs. Overall these reasons (Figure 2) support the advancement of DDS in a wide range of outstanding applications in the treatment of various diseases.

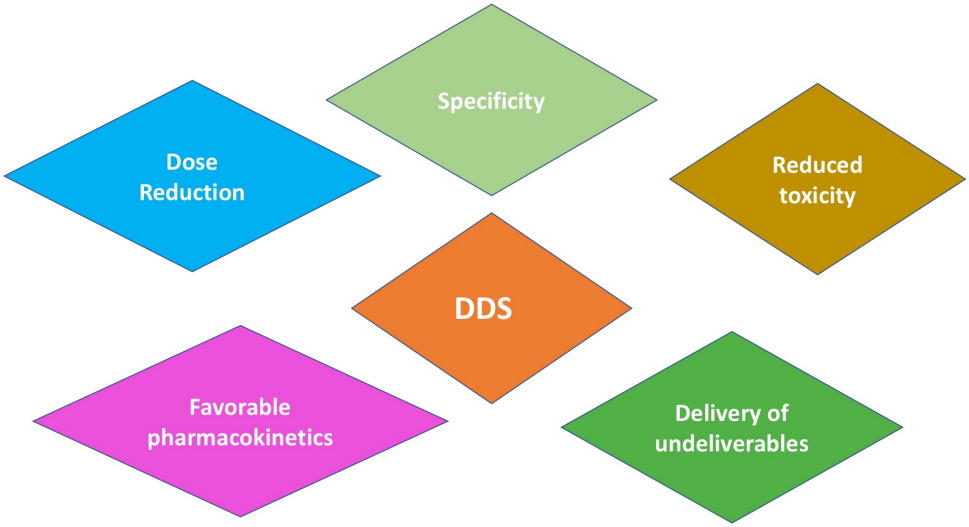

Figure 2. Advantages of DDS

It has been claimed that the main advantage of DDS is the ability to reduce drug dose by increasing the specificity for the interest target site. The pioneer idea of targeted drug delivery was first developed by the “magic bullet” concept of Paul Ehrlich in the early 1900s [7]. Targeting delivery approach is the ability of DDS to reach, recognize, bind and deliver its payload to specific pathologic tissues, and minimize or avoid toxic effects to healthy tissues. Several strategies have been used to target drug at the interest site such as active and passive targeting. Passive targeting refers

to the accumulation of drug-carrier system taking advantage of the unique pathophysiological characteristics of the target site, not normally present in healthy tissues. The most classical example is the enhanced permeation and retention (EPR) effect, which results in accumulation of macromolecules in the tumor through an altered vasculature and lymphatic drainage. The increased vascular permeability due to abnormal pores of capillary membrane with size ranged from 100 to 700 nm and impaired lymphatic drainage of cancer cell allow a preferential accumulation of nano-sized structures [8]. The efficacy of this targeting approach is influenced by nanoparticles properties including size, surface charge, shape, circulation time and by the anatomical and physiological characteristics of the target site [9]. However, EPR effect is restricted by several factors such as non-specific uptake of the particles and non-specific delivery of the drug. It has been reported in literature, indeed, that, some of passively targeted nanocarriers fail to reach the tumor when administered intravenously [10]. Consequently, active targeting strategy has been advanced to overcome the lack of specificity and limitations of passive targeting. Active targeting relies on specific interaction between a ligand on nanocarrier surface and the target site in order to improve uptake selectivity (Figure 3). This approach, indeed, is based on the conjugation of a targeting moiety on carrier surface having a selective affinity for recognizing and interacting with a specific cell, tissue or organ in the body. A large number of disease-associated biomarkers has been identified and investigated as targeting agents. Targeting ligands can be chemically conjugated or physically adsorbed on carriers after formation or can be linked with nanodevices components, such as polymers and surfactants before formation [11]. Independently of the used conjugation approaches, the devices can be functionalized using targeting ligands of different nature including aptamers, small molecules, proteins, peptides, antibodies, carbohydrates or glycoproteins in function of target cell characteristics. Physicochemical properties such as size and shape are very important parameters influencing the *in vivo* nanoparticle distribution. Consequently, it is fundamental to keep unchanged them during the conjugation process [12].

DDS can be engineered to have different drug release profiles depended on therapeutic needs. The drug controlled release can be enclosed into two major categories: extended and stimuli-responsive release [13]. Extended drug release relies on the delivery of drugs over a sustained period maintaining constant their concentration in the plasma or target tissue. This mechanism involves often polymers that release the drugs at controlled rate due to the diffusion out of the carrier or by degradation of the matrix over the time. On the other hand, stimuli-responsive release is based on the modification of the structural composition or conformation of the nanocarriers resulting in the release of drug entrapped within them in response to specific stimuli. The signals common used can be external (temperature, light, magnetic, ultrasound) or internal due to specific features of the pathologic tissue (variation of pH, enzyme and redox state).

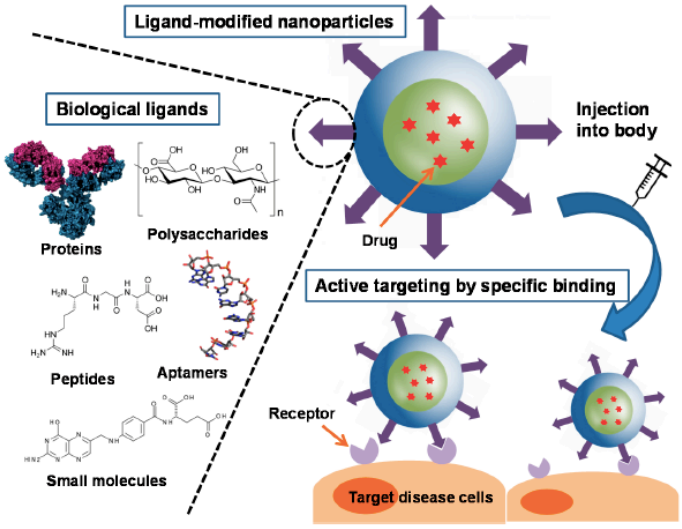

Figure 3. Illustration of ligands for active targeting of DDS.

1.4 Nanotechnology in Skin delivery

In the last decades, the use of nanocarriers as tools to improve skin drug delivery has attracted a large interest. As one of the widest organ in human body, the skin exhibits many functions: it acts as barrier protecting body from external substances, plays a role in temperature regulation, in immunological response, in neurosensory functions and in biosynthesis of constitutive substances such as keratin, collagen, melanin, lipids and carbohydrates [14]. Skin delivery offers a number of advantages compared to other conventional routes: bypassing hepatic metabolism, avoiding toxic effect related to drug oral delivery, sustained drug release, patient compliance and a suitable route for unconscious or vomiting patients. The skin has a complex structure composed of two layers: the epidermis and the dermis. The epidermis contains various histologically distinct layers, stratum basal, spinosum, granulosum, lucidum and corneum. Stratum corneum (SC) is the outermost layer made up of densely packed dead keratin-filled corneocytes that acts as the first barrier to external agents modulating drugs absorption into the deeper skin layers. Each cells of the SC, indeed, has approximately a diameter of 30 μm and a thickness in the range between 0.5 and 0.8 μm. This structure proposed by various authors as a "brick and mortar" model represents, thus, the main permeation rate-limiting barrier of drugs administered via topical route [15]. Because of this peculiar organization, conventional topical formulations are often inadequate to achieve therapeutic drug concentrations. Several chemical and physical methods, thus, have been advanced to overcome the main drawbacks of classical skin delivery. Among physical enhancers, micro-needles, heating, iontophoresis, electroporation, radiofrequency and ultrasound are extensively applied. On the other hand, nanotechnology has shown remarkable potential in target specific delivery of drugs to the skin. Different types of nanocarriers such as niosomes, liposomes, solid lipid nanoparticles, polymeric

nanoparticles, indeed, have been designed by researchers to increase skin penetration, control the release, and target drugs to specific areas of skin. There are different possible pathways of molecular penetration of nanocarriers across the SC:

- intercellular route with partitioning into the lipid matrix;
- intracellular route through epidermis cell membrane;
- appendageal route through sweat glands and hair follicles;

Several mechanisms such as alteration of physicochemical and hydrating properties of SC, fusion with skin components and better drug partitioning have been proposed to explain the role of nanoparticles in skin penetration and permeation [16]. Many characteristics of nanodevices including size, shape, charge, surface properties affect skin permeation. For instance, several researchers have highlighted that drug penetration can be influenced by surface charge. The lipid layer in the SC contains a high ratio of negatively charged lipids and, thus, positive charges on particle surface enhance the electrostatic interaction with cell membrane and their internalization, while the diffusion of negative charged nanoparticles seems to be slowed in cellular matrix allowing a skin drug depot [17]. Moreover, spherical and deformable nanoparticles resulted be able to penetrate through skin more fast than ellipsoid shaped and rigid carriers [18], [19]. Different qualitative and semi-quantitative techniques have been advanced and employed to evaluate the *in vitro* skin permeation ability. Standard quantitative tools include Franz-type diffusion cell experiments and differential tape-stripping of the SC aiming to measure the amount of drug permeated trough a membrane over time or accumulated in skin layers. Qualitative techniques such as laser scanning confocal microscopy (LSCM) multi-photon fluorescence microscopy (MFM) and transmission electron microscopy (TEM) are, instead, addressed to estimate drug distribution in the various skin layers.
Commonly, permeation enhancers are employed in the composition of nanocarriers aimed to alter temporarily the physicochemical structure of SC and, consequently, improve drug permeation. Many compounds including surfactants, small molecules, lipids and solvents have been investigated and proposed as chemical penetration enhancers (Table 2). An ideal chemical enhancer should be pharmacologically inert, non-toxic, non-allergenic, chemically and physically compatible with the DDS, inexpensive and cosmetically. Moreover, following its removal, SC should immediately and fully recover its normal barrier function. Structure-activity studies indicated several mechanism by which skin enhancers may act. One is the ability to increase drug diffusivity within the cutaneous membrane and drug partitioning. Another proposed mechanism is the ability to modify skin polarity [20].

Surfactants	Anionic surfactants Cationic surfactant Non-ionic surfactants Span80, Tween 80 Sodium lauryl sulphate
Alcohols	Ethanol Isopropyl alcohol Decanol Hexanol Octanol Myristil alcohol
Fatty acids	Lauric acid Linoleic acid Oleic acid Palmitic acid Isostearic acid
Sulfoxide	Dymethilsulphoxides Decylmethilsuphoxides
Terpenes	Cineole Eugeneol Menthol D-Limonene Linalool
Glycols	Propylen glycole Dypropylene glycol
Polymer	Chitosan Trimethyl chitosan
Cyclodextrins	α-, β-, γ- cyclodextrins, Methylated β-cyclodextrins

Table 2. Examples of penetration enhancers investigated in literature.

Delivery through skin can be classified into topical aimed to treat local diseases and transdermal aimed, instead, to treat systemic pathologies. Nanocarriers can be properly engineered for the desired therapeutic response varying their composition thanks the large availability of materials suitable for drug delivery applications. For instance, more hydrophobic formulations due to the use of surfactant with low HLB result in a higher drug retention capacity and in a more delayed permeation. On the contrary, hydrophilic formulations may be preferred to achieve systemic effect [21]. Several types of delivery systems such as vesicular systems (liposomes, niosomes, transfersomes), emulsions (microemulsions and nanoemulsions), and nanoparticle systems (microparticles, nanoparticles) have been widely investigated as drug carriers for skin delivery both for topical and systemic therapy and cosmetic care [22]. The first transdermal drug delivery systems approved was the scopolamine patch for motion sickness in 1979. Since then, a few other drugs such as non-steroidal antinflammatory, antimicrobial, antioxidant, anticancer agents have been successfully formulated into DDS. Some of the dermal and transdermal DDS currently available in the market are presented in Table 3.

Name	Drug	Delivery Systems	Company
Transderm Scop®	Scopolamine	Transdermal patch	Novartis
Qutenza®	Capsaicin	Topical patch	NeurogesX, Inc.
Revitalift	Pro-Retinol A	Nanosome	L'Oreal
Renergie Microlift	Silica and protein	Nanoparticles	Lancome
Nano-Golds® Energizing Cream	24-karat gold	Nanoparticles	Neiman Marcus
Lipobelle Soyaglycone	Genstein	Liposomes	Mibelle Biochemistry

Table 3. Some examples of cosmetic and transdermal DDS formulation available in market.

1.5 Nanotechnology in Cancer

Cancer is one of the most fatal disease diagnosed in more of ten million people every year. It is a complex biological process caused by uncontrollably division of cells and rapid spread into surrounding tissues. Conventional treatment are surgery, radiotherapy and chemotherapy. In the last century, chemotherapy has arisen as a viable and adjuvant therapeutic modality aimed to destroy all rapidly proliferating cells. The main drawback of this therapy is that healthy cells are also killed and, thus, side effects in normal tissues such as alopecia, nephrotoxicity, neurotoxicity, cardiotoxicity commonly occur. In addition, multidrug resistance mechanism in cancer cell is a typical observed phenomenon that reduces drug concentration at the target site and, consequently, its efficacy. Chemotherapy still need further improvement and the development of nanotechnological approaches has provided a new avenue in cancer treatment. Smartly designed nanoparticles can alter the anticancer drug distribution in the body and promote selectively the accumulation in pathological sites. Nanocarriers if opportunely designed can, thus, reduce drug dose while maintaining effective intracellular concentrations, thereby widening the therapeutic window of anticancer agents. Consequently, an improved therapeutic efficacy and reduced toxic effects can be achieved. A deep interest has been addressed to the identification of optimal carrier characteristics in terms of size, composition, surface charge to allow a specific delivery to cancer tissues. Different strategies such as active, passive and local stimuli-triggered drug release have been used to selectively target tumor. Indeed, the nanocarriers can be differently engineered combining multiple functions at the same time in order to provide:

- Prolonged blood circulation and spontaneous accumulation to tumor site;
- Recognition of target cells through specific ligands on nanocarriers surface;
- Responsivity to local or external stimuli (e.g. pH, temperature, redox potential, ultrasound, etc..).

The drug accumulation at the desired site depends on physic-chemical and physiological factors such as carrier size and tumor vasculature characteristics. Tumor vasculature is abnormal and exhibits wide fenestrations, high vascular permeability and impaired lymphatic drenage that decreases the clearance of

macromolecules giving, consequently, extended retention times in the tumor interstitium (Figure 4). This effect, named EPR, is a molecular weight and size-dependent phenomenon: particles larger than 40 kDa show prolonged half-life, whereas nanoparticles with size between 60 and 500 nm are able to extravasate in tumor tissue [23]. Several passive targeted nanomedicines such as Myocet®, Doxil®, Daunoxome®, Abraxane® and Genexol-PM® have been already approved for clinical use and other are currently in clinical trials.

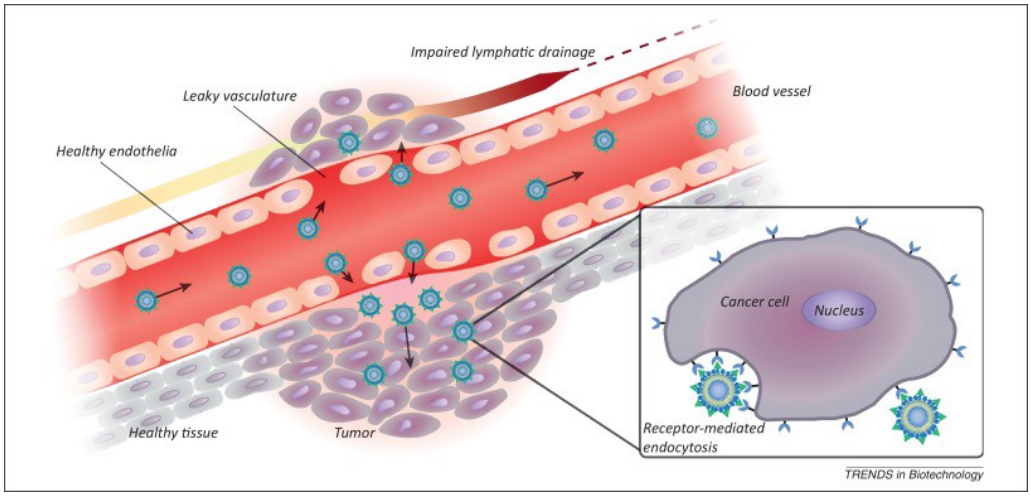

Figure 4. Passive targeting strategy

To improve drug delivery accuracy, the conjugation of target specific ligands is another important strategy employed. Indeed, target systems recognize and bind specific cell surface receptors overexpressed in tumors and, subsequently, are internalized via receptor-mediated endocytosis. Researchers have identified and studies a large number of tumor targeting ligands including antibodies, aptamers, peptides, and small molecules (Table 4).

Type	Ligands
Proteins	Transferrin
Antibodies	anti-Her-2 , anti-MUC-1, Trastuzumab
Small molecules	Folic acid, Sugars
Aptamers	AS-1411, GBI-10
Polysaccharides	Hyaluronic acid
Peptides	IL4RPep-1, cRGD, cNGR and CREKA

Table 4. Ligands for active targeting of DDS.

Moreover, the use of devices with the presence on surface of more than one targeting moiety has been advanced to promote binding and cellular uptake through the multivalent effect and to prevent receptors saturation [24]. The progress of nanotechnology in cancer therapy resulted in the possibility to control drug biodistribution in time and spatial. This has become possible through the

development of nanomaterials sensitive to specific stimuli. Nanocarriers, in fact, can be built to experience rapid changes in their structure and physical properties under exposure to special conditions and release their payload. The main advantage of this approach is the possibility to obtain a localize drug release in response to specific disease-related biomarkers and prevent premature drug leakage in circulation responsible of side toxic effects. The microenvironment of metastatic disease typically exhibits variations in pH, redox potentials or concentrations of enzymes and these factors can be successfully used to achieve an intracellular drug release [25]. Moreover, stimuli can be applied externally at the target site. Among them, magnetic field, light, ultrasounds and temperature have been extensively investigated to trigger drug release from nanodevices in oncology.

The pioneer stimuli-responsive drug delivery formulation was first suggested in the late 1970s with the use of thermosensitive liposomes and from them, more evolved formulations have been provided and employed in several clinical trials (ThermoDox, Celsion Corporation) [26]. Thermo-responsiveness allows to achieve a drug release control at the desired site and time by the use of an external biomedical devices (radiofrequency, microwave, and high intensity focused ultrasounds) and the inclusion in nanocarriers of molecules with a transition temperatures close to physiological body temperature (40–43◦C) [27]. Another possibility of release triggered by externally stimuli involves the application of a magnetic field on the biological target during injection of magnetically responsive nanocarriers. Among the endogenous stimuli, instead, pH-sensitive and redox sensitive are two main strategies used in intracellular tumor drug delivery. It is well known that in tumor cell there is a special microenvironment such as low pH and high level of glutathione (GSH) which is different to normal cells. The introduction, thus, of pH labile linkages based on the diorthoesters, vinyl esters, cysteine-cleavable polymers, double esters, and hydrazones or disulphide bonds prone to fast cleavage by GSH has been widely used to attain pH sensitivity and redox sensitivity [28]. Moreover, because of the coexistence of different conditions in tumor microenvironment, more than one stimuli can be used in combination to further improve drug delivery.

In the most evolved context, smart delivery systems which incorporate multiple complementary targeting strategies, including passive, active, and stimuli-responsive targeting in the same systems have been emerging as safer and effective tools for antitumor therapy (Figure 5).

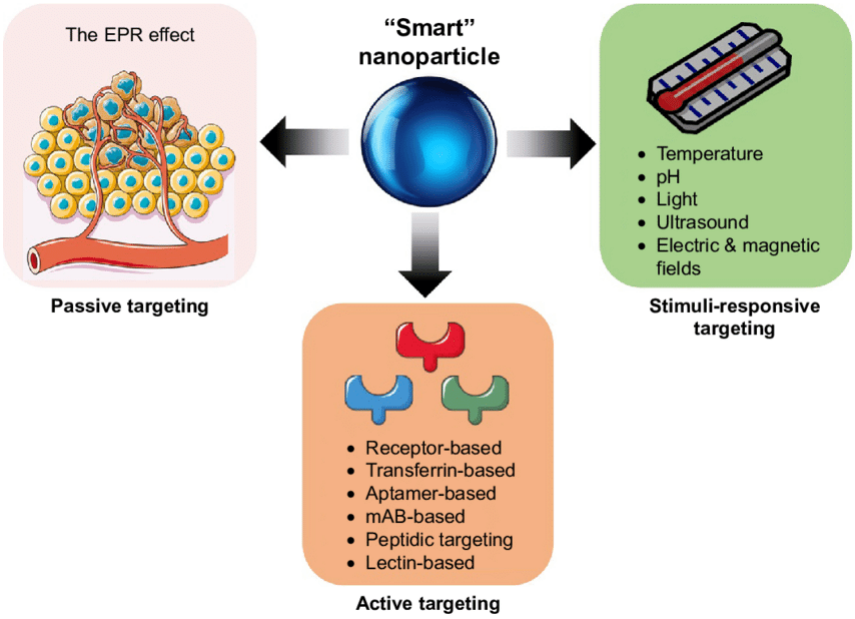

Figure 5. Multifunctional targeting nanoparticles.

Various combinations of targeting strategies have been analysed, investigated and have shown exciting results in preclinical studies, demonstrating their potential as therapeutics carriers. Particular appealing is also the possibility to combine specific targeting approaches with nanoparticles for imaging (such as quantum dots or magnetic NPs), in order to obtain a theranostic system that can be used for simultaneously tumor imaging, diagnosis and treatment.

Recent interests for cancer treatment are currently addressing to new therapeutic approaches such as immunotherapy and gene therapy. Nanotechnologies have been also implemented in these fields. Nanoparticles can be used for delivery of immunostimulatory or immunomodulatory molecules in combination with chemo- or radiotherapy or as adjuvants to other immunotherapies. Unlike conventional nanomedicines that directly target cancer cells, nanoparticles designed for cancer immunotherapy also target lymphocytes or lymphoid tissues. On the other hands, gene therapy involves the transfer of genetic material responsible of activation of apoptosis into a host cell through viral (or bacterial) and non-viral vectors. The most common used non-viral vectors are polymeric or inorganic nanoparticles, which have biological and physicochemical properties that allow them to carry the DNA into tumor cells. Furthermore, these nanodevices may be functionalized with specific molecules for the recognition of molecular markers on tumor cells surface, inducing a better selectivity.

1.6 Nanotechnology in Drug Photoprotection

In the last decade, a wide-reaching impact of nanotechnology is becoming more apparent in the management of photolabile drugs. The European Pharmacopoeia indicates that efficacy and safety of over 250 drugs are adversely affected by light

exposure through their life cycle. Exposure to light can cause changes in the physicochemical properties of the active compounds with loss or the reduction of therapeutic effect and formation of toxic by-products. Consequently, the development of optimal photostabilization methods is a main pharmaceutical research topic and stress testing according to the guidelines given in the International Conference on Harmonization of Technical Requirements for Pharmaceuticals for Human Use (ICH) are necessary to attest the safety and efficacy of all new drugs. Common photoprotective strategies involve the use of light protective packaging or formulations with appropriate coatings. Anyway, these techniques cannot be used for topical formulations since this route of administration contributes to a higher exposure of photolabile compounds to sunlight.

In these cases, the use of supramolecular systems able to encapsulate drugs has aroused a lively interest for their ability to provide a valid photoprotection. The materials and architecture of supramolecular structures capable of protecting active compounds from light vary immensely. Particularly, there is a preference for nanostructures prepared with biodegradable materials such as lipids or biodegradable polymers. From literature data, cyclodextrin (CD), liposomes, solid lipid nanoparticles, microparticles, niosomes, microemulsion and mesoporous silica nanoparticles are the main photoprotective carriers used. CD are cyclic oligosaccharides formed of glucopyranose monomers linked by a-(1,4)- glyosidic bonds forming a central cavity in which the drug is incorporated. Depending on the number of glycopyranosilic units, CD are distinguished in α-CD consisting of six carbon units; β-CD consisting of seven carbon units; and γ−Cd consisting of eight carbon units. The spatial arrangement of CD defines a sort of cone rigid shape with a hydrophobic cavity capable to incorporate appropriately sized lipophilic compounds by a non-covalent complexation phenomenon (Figure 6). A large number of molecules such as 1,4-dihydropyridine, diclofenac, naproxen, methotrexate, quercetine, ranitidine, tretinoin, entrapped in CD matrices have shown an improved light stability [29]. Additionally, the use of both liposomes and niosomes as photoprotection systems has been extensively investigated. The selection of vesicular matrix is often very difficult because the drug photostability is affected by the carrier stability itself, which in turn depends on the vesicle bilayer composition. Many study have compared the efficacy of liposomes and niosomes to improve drug photostability. For instance, treitoin has shown high degradation when incorporated in liposomes made from soy phosphatidylcholines as a consequence of the bilayer degradation in presence of water and light. On the contrary, tretinoin-loaded niosomes prepared from polyoxyethylene lauryl ether, sorbitan esters and a mixture of octyl/decylpolyglucosides demonstrated a more efficient protection [30].

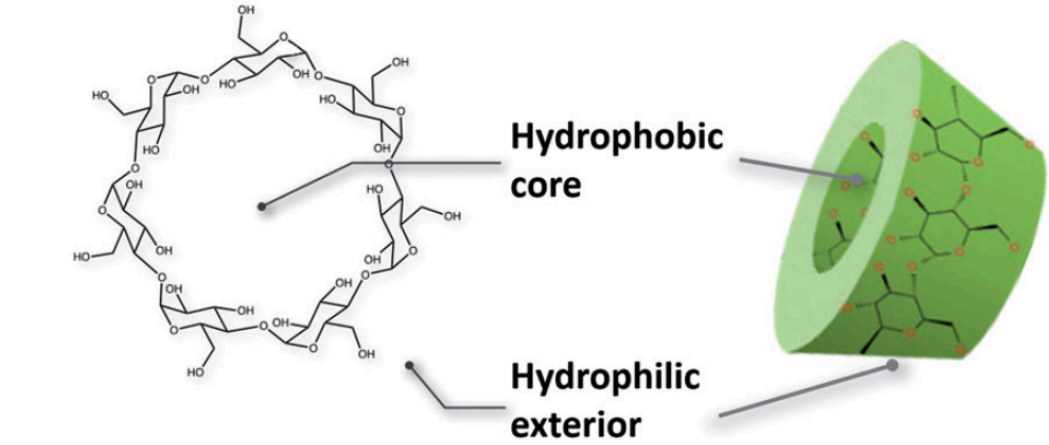

Figure 6. Chemical and toroides structures of Cyclodextrin

In addition, simultaneous use of different kind of photoprotective strategies has been proposed to increase drug photoprotection and, thus, minimize the light effects on therapeutic activity than the same strategies used separately. For instance, drug–CD complex incorporated in the aqueous core of liposomes or the combination of supramolecular systems with solar filters or antioxidant agents are commonly employed to improve the photostability effectiveness. Antioxidants, such as ascorbic acid and α-tocopherol are typically combined with niosomes or CD due to their ability to prevent free radicals and singlet-oxygen intermediates formation and, consequently, increase photoprotection efficacy. Finally, it is crucial for the selection and effectiveness of the suitable photostabilization strategy the knowledge of the photodegradation mechanism of investigated drug. The studies, indeed, made with molecules for which the photodegradation mechanism is well known presented higher photostabilization effectiveness.

1.7 Nanocarriers for drug delivery

Nowadays, a large number of nanosized carriers made of different materials such as lipids, polymers, surfactants, have been proposed in the biomedical field as diagnostic and therapeutic tools. In the following sections, I will discuss the main features of different types of nanocarriers used in the current thesis work.

1.7.1 Emulsions and Microemulsions

Emulsions (E) and microemulsions (ME) are dispersed systems composed of water, oil and surfactant useful for pharmaceutical applications for their capacity to carry both hydrophilic and lipophilic drugs. ME and E are classified as water in oil (w/o) or oil in water (o/w), each designating the dispersed phase within the continuous phase. Pseudo ternary phase diagrams are often constructed to indicate the existence of different phases as a function of the composition of aqueous, oil and surfactant/cosurfactant components.

A wide range of surfactants, together with a variety of oils and cosurfactants have been investigated for a potential use in the design of these systems (Table 4).

OILS	
Saturated fatty acid.	lauric acid, myristic acid, capric acid
Unsaturated fatty acid	oleic acid, linoleic acid, linolenic acid
Fatty acid esters	ethyl or methyl esters of lauric, myristic and oleic acid.
SURFACTANTS	
Natural surfactants	egg lecithin, lyso lecithin, Soybean lecithin, alkyl glucosides, alkylesters
Non-ionic surfactants	Polyoxyethylene/Polysorbate/Tween 20,40,60,80 Sorbitan Monolaurate (Span) Poloxamer,
Others	Labrasol (Polyethylene glycol–8–caprylic acid), Sodium dodecyl sulphate (SDS), Sodium bis (2–ethylhexyl) sulphosuccinate (Aerosol OT), Dioctyl sodium sulphosuccinate, Sodium dexoycholate TritonX–100

Table 4. Commonly used components of E and ME.

Despite their similar composition, there are a lot of factors that differ ME from E, that are given in Table 5. E consist of relatively large droplets in the range between 100 nm and 10 μm, whereas ME show droplet size distribution in the range around 10-100 nm [31]. In addition to their obvious droplet size difference, ME are transparent, form spontaneously, have low interfacial energy and are thermodynamically stable, unlike E that are milky, require energy during preparation, have high interfacial energy and are kinetically stable [32]. ME also need more amount of surfactant to stabilize the systems and the use of co-surfactant (none for emulsions) due to the lower interfacial tension (about 1000 times) and higher surface [33].

Parameters	Emulsion	Microemulsion
Droplet size	Large (100 nm-10 μm)	Small (10-100 nm)
Appearance	Cloudy	Transparent
Interfacial tensions	Low	Ultra-low
Surfactant concentration	Low	High
Co-surfactant type	None	Short chain alcohol

Table 5. Characteristic differences between emulsions and microemulsions.

The ME and E efficacy has already been proved in various routes of admistration such as ocular, vaginal, rectal, buccal, periodontal, parenteral, and nasal. Particularly, they offer considerable opportunities for targeted drug delivery to and

via the skin. In fact, ME and E have been demonstrated to improve transdermal delivery of different drug compared to conventional formulations. The increased percutaneous drug delivery of these systems seems to be related to different mechanisms dependent on the properties of the drug and formulation. According to a first mechanism, the drug penetrates to skin only from outer phase. Afterwards, the drug in the outer phase is replaced by the drug released from the dispersed phase to the continuous phase. This means that droplets act as drug reservoir able to allow a constant drug concentration gradient on the continuous phase and prolong absorption [34]. In the second mechanism, droplets break down upon contact with skin and then release their content. Finally, another possible mechanism is the droplet fusion with skin components. Indeed, in E and ME composition can be used substances with natural ability to fluidize stratum corneum and improve drug partitioning into skin acting as penetration enhancers. Due to the widely availability of material with permeation enhancer properties, there is considerable scope to manipulate the formulation components and characteristics to achieve a skin drug depot or optimal systemic bioavailability depending on the desired therapeutic purpose.

1.7.2 Polymeric nanoparticles

Polymeric nanoparticles (NPs) are colloidal devices ranging in size from 10 to 1000 nm made up of natural or synthetic polymers. According to the method used for NPs preparation, nanospheres (matrix-type NPs) or nanocapsules (reservoir-type NPs) can be obtained. Several preparation techniques are available and can be divided in two major groups: top-down and bottom up methodologies. In the top-down approach, NPs are produced from preformed polymers using different method such as emulsification, extrusion, solvent displacement, ionic gelation, salting out, dialysis, and supercritical fluid technology. On the other hand, in bottom-up procedures NPs are obtained directly from the monomers after polymerization with the use of an initiator or by self-assembly in response to changes of environmental parameters such as temperature, ionic strength, pH or concentration. Among bottom-up procedures, coacervation, inclusion complexation and nanoprecipitation are the most employed [35].

The drug of interest can be dissolved, entrapped, adsorbed, covalently attached or encapsulated in the NPs [36]. Depending on the NPs structure, polymers used and drug physicochemical properties, the release can take place by polymer degradation and erosion or drug desorption and diffusion [37]. Polymeric NPs have been widely employed as drug carriers for topical applications and cancer treatment. It is extensively demonstrated, indeed, that the delivery of common chemotherapeutic drug such as doxorubicin, paclitaxel and methotrexate trough polymeric NPs improve their antiproliferative effect against cancer cells [38]. Moreover, polymeric NPs have emerged as appealing carriers for topical applications. Considering the data available up to now in literature, polymeric NPs show better ability to enhance

skin retention rather than the transdermal drug delivery in systemic circulation. Consequently, they are better suitable for topical treatment of skin diseases such as dermatitis, acne, atopic eczema and psoriasis [39].
The main requirement for a polymer to be used in the design of NPs is a high biocompatibility and rapid degradation *in vivo* without causing inflammatory response. Various natural and synthetic polymers have been attracted attention for drug controlled delivery. The most explored natural and synthetic polymers for NPs preparation are chitosan gelatine, alginate, dextran, albumin, poly(acrylate) and poly (lactide-co-glycolic) acid (PLGA), [40], [41]. Chitosan NPs are particular interesting devices investigated in various drug delivery applications such as the treatment of dermatologic and gastrointestinal diseases, pulmonary diseases, and drug delivery to the brain, colon, ocular infections and gene/vaccines delivery [42]. Recent investigations, instead, are focused on the use of chitosan NPs for tumor targeting, imaging and therapy applications and the development of multifunctional DDS [43]. Chitosan offers, indeed, different advantages for drug delivery applications. First, chitosan has chemical functional groups that can be modified to achieve specific goals, making it a polymer with a tremendous range of potential applications. Furthermore, chitosan has a positive surface charge and mucoadhesive properties such that can adhere to mucus membranes and release the drug payload in a sustained release manner. Chitosan acts, also, as a penetration enhancer by opening epithelium tight junctions improving both paracellular and transcellular transport of drugs. Several methods are available for the synthesis of chitosan NPs, but the most widely used is ionotropic gelation because is a simple technique which not apply high shear force or the use of organic solvents [44]. Overall these factors support a high potential of this polymer in DDS formulation.

1.7.3. Lyotropic liquid crystals

Lyotropic liquid crystals (LLC) are a state of matter which exhibit simultaneously properties of a liquid and those of an order crystalline structure. In fact, they possess anisotropic physical properties such as their refractive index, dielectric constant, elastic behaviour or viscosity. But at the same time, LLCs also exhibit flow properties like a liquid; they are thus anisotropic fluids. LLCs have gained considerable attention in the last few decades due to their potential as DDS. Higher solubility capacity compared with traditional carriers, high carrying capacity for a range of water-insoluble drugs, protection of sensitive drugs from enzymatic degradation are the main advantages of these systems in pharmaceutical applications.
LLC are formed by the swelling of amphiphilic molecules in excess of water. When exposed to aqueous environment, amphiphilic lipids spontaneously form thermodynamically stable self-assembled structures. Monoolein, glycerol monooleate, phosphatidylcolines, oleyl glycerate, polaxamer block copolymers and

some non-ionic surfactants are commonly materials forming LLC for drug delivery [45]. In particular, by varying the temperature and the concentrations, amphiphilics can self-assembly in various forms such as lamellar, hexagonal and cubic phases (Figure 7).

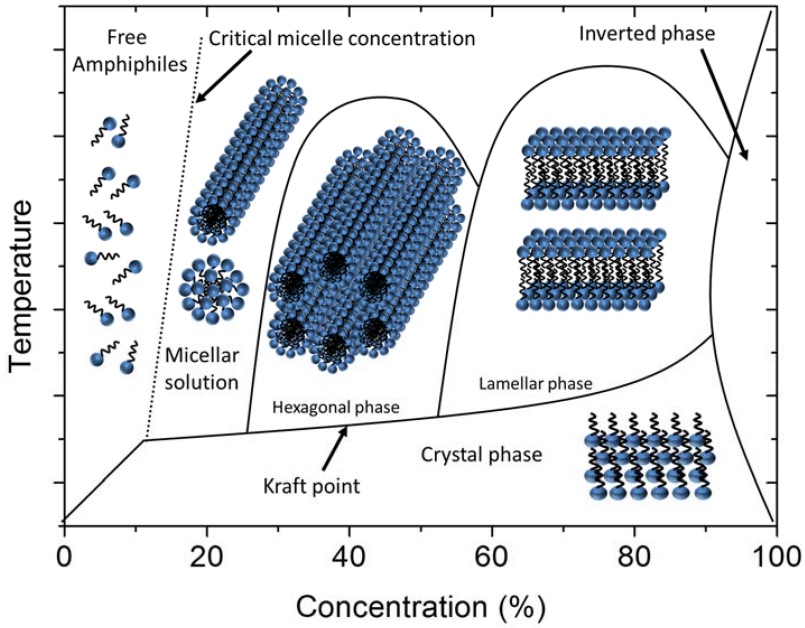

Figure 7. Illustration of the phase diagram of an amphiphilic molecule forming Lyotropic phases.

Lamellar phase is normally present in the organism because is the typical organization of cell membranes. In fact, it is a surfactant bilayer structure separated by water layers where the head polar groups are directly in contact with water, whereas the hydrophobic chains are interdigitated in order to avoid water (Figure 8). Lamellar phases have received particular attention for topical administration of drugs due to the similarity with skin structure and high stability [46].

The hexagonal phase is made up by densely packed cylindrical aggregates of amphiphilic molecules filled with water and disposed on a hexagonal lattice. Two different type of hexagonal phase are possible: normal (Figure 8) in which the hydrophobic chains are within the cylindrical structures and reversed in which water are within the cylindrical aggregates and the hydrocarbon chains fill the voids between the hexagonally packed cylinders.

Cubic phases, instead, are based on continuous curved bilayers and interpenetrating non-intersecting aqueous channels separated by each other. Cubic phase has spherical packing and the polar part of molecule is located on sphere surface and the non-polar portion within the centre of the sphere (Figure 8). This unique microstructure offers different advantages for drug delivery applications making it optimal for gastrointestinal, pulmonary, nasal, oral, buccal, rectal, and vaginal drug delivery [47].

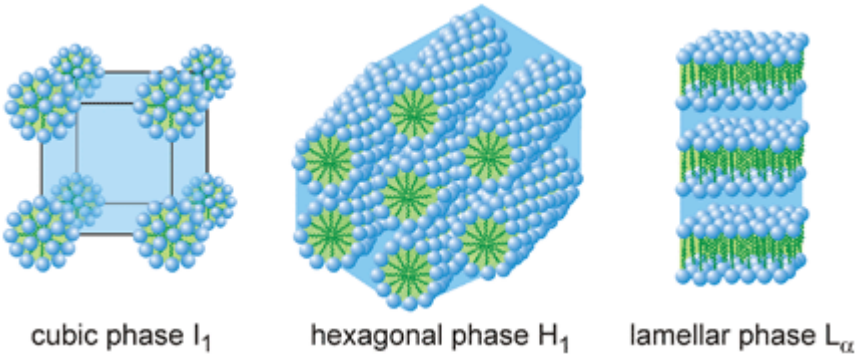

Figure 8. Examples of LLCs

The cubic structure is, indeed, formed spontaneously and is characterized by a high stiffness and bio-adhesive properties that allow a prolonged retention time onto the skin. Cubic and hexagonal phases provide a slow drug release and protect peptides, proteins, and nucleic acids from chemical and physical degradation. A wide range of drugs with different molecular weights and water solubility have demonstrated improved transdermal/topical delivery in cubic phases, such as Tetracycline, Propranolol hydrochloride, Capsaicin, Diclofenac salts and Acyclovir [48].
Furthermore, because of the ability of some materials to switch between the cubic phase and hexagonal phase by adjusting temperature and/or pH, researchers have designed a series of stimuli responsive LLC as DDS for specific target.

1.7.4 Liposomes and Niosomes

Liposomes, phospholipids based vesicles, have been discovered by Bangham in 1960 and have attracted much attention as DDS due to their biocompatibility, biodegradability and non-toxicity. Indeed, liposomes are promising DDS due to their small size and the ability to carry both hydrophilic and lipophilic drugs in aqueous core and lipid bilayer, respectively [49]. Liposomes can be classified in four types:1) conventional type liposomes based on anionic, cationic and neutral phospholipids; 2) PEGylated types based on the inclusion of PEG; 3) ligand-targeted type based on the linking of a targeting moiety to liposomal surface; 4) theranostic liposome types involving the simultaneous presence of a targeting, imaging and therapeutic element [50]. Their properties can be accurately modified by the choice of bilayer components and therefore changing the superficial charge, size and functionalization. Indeed, the liposome surface is amenable to modification with targeting ligands and polymers. The Food and Drug Administration approved several liposomal formulations, some example available in the market are Doxil® and AmBisome®, liposomal Doxorubicin and Amphotericin B used for the treatment of cancer and fungal infections, respectively. Anyway, liposomes present some disadvantages like the fast elimination from blood circulation by reticulo-endothelial system and macrophages [51], [52], the physical and chemical instability

(aggregation, fusion, degradation, hydrolysis and oxidation of phospholipids) and high cost of production [53].

Niosomes, non-ionic surfactant based vesicles, are functionally analogous to liposomes and can be used for target and sustained release of both hydrophilic and lipophilic drugs. Anyway, the different chemical nature of their structure units make niosomes a powerful device with several advantages with respect to liposomes. Non-ionic surfactant indeed, have greater stability, low cost, high availability and no special conditions are necessary during storage. Moreover, niosomes showed intrinsic skin penetration-enhancing properties. Overall these features make niosomes more attractive for industrial manufacturing. In literature, a large number of studies highlighted the potential of niosomes for transdermal delivery of numerous pharmacological agents, including antioxidant, anticancer, anti-inflammatory, antimicrobial and antibacterial molecules. In the following sections, I report our expert view of the current applications of niosomes and the developments that are likely to be important in the future.

1.7.4.1 Do niosomes have a place in the field of drug delivery?
(Editorial)

Rita Muzzalupo[a] and Elisabetta Mazzotta[a]

[a] Department of Pharmacy, Health and Nutritional Sciences, University of Calabria, Via Savinio, Ed. Polifunzionale, 87036 Arcavacata di Rende, Italy

Published on Expert Opinion on Drug Delivery 16, (2019), 1145–1147.

1. Niosomes: a next attractive generation of drug delivery carriers

In the field of nanotechnology, niosomes are gaining increasing scientific interest as useful drug delivery systems for several therapeutic applications due to their unique versatility. Niosomes are vesicular nanocarriers made up of non-ionic surfactants, developed from scientists as the best alternative to liposomes. Niosomes and liposomes are both amphiphilic carriers with similar physicochemical properties, pharmaceutical applications and, also, equal *in vivo* behaviour. Despite these comparable features, niosomes differ in chemical composition of the bilayer and this offers several advantages over liposomes. Liposomes are based on phospholipids, whereas niosomes are made of surfactants with improved physical, chemical and biological stability. Furthermore, higher drug entrapment can be achieved by modulating the composition of niosomes bilayers and their industrial manufacture is less expensive because does not require special handling methods and storage conditions due to the higher stability. Most of the published papers focused on niosomes, highlighting their optimal skin permeation potential, sustained release characteristics, long shelf life and, high drug photo-protective activity as compared to liposomes [1]. Niosomes production was first reported in the 70s in cosmetic industry, but then potential applications of niosomes were expanded for the delivery of several pharmacological agents such as anticancer, antioxidants, anti-inflammatory, antiasthma, antimicrobial, antiviral, antibacterial molecules and oligonucleotides. At the present state of the art, most of the publications in scientific literature and the first clinical trials about niosomes, highlight the great potential of these systems in dermal/transdermal applications but showed, also, the niosomal potentialities as oral formulations for blood glucose lowering or antihypertensive or analgesic drugs [2, 3]. Enhanced skin permeation, direct vesicle fusion with the stratum corneum, formation of a drug reservoir into the skin and, sustained pattern of drug release, seem to be the main characteristics that have attracted the interest of academia and industry [4]. Common non-ionic surfactants, used in the design of vesicular delivery systems, include alkyl ethers, alkyl glyceryl ethers, sorbitan fatty acid esters and polyoxyethylene fatty acid esters. The choice of surfactant is a critical

factor to be considered during the design of non-ionic vesicular systems. It is well known, indeed, how the surfactant molecular structure clearly affects the size, stability, entrapment efficiency, pharmacokinetics, pharmacodynamics and targeting properties of vesicular systems. A large selection of surfactants displaying favourable properties for specific drug delivery applications is readily available. This offers the possibility to select the more suitable surfactant in order to achieve tailor-made niosomes for the desired therapeutic response. Anyway, research is keeping to explore new materials in order to customize and optimize niosomes for different therapeutic purposes and for a potential translation in human clinical trials (Figure 1). One of the advantages of classical non-ionic surfactants is the easy chemical modification aimed to improve the selectivity towards specific organs and cells already without affecting healthy tissues. In the last few years, the discovery of therapeutic targets involved in several diseases, has greatly expanded and the use of these target molecules on niosomes surface allows an increased specificity and selectivity of the nanodevices. Different ligands, as small-molecules, proteins, cell penetrating peptides, sugars, monoclonal antibodies and their fragments, are usually involved in the design of niosomes with specific targeting properties to brain, tumour, colon, liver, lung and eyes. Recent *in vivo* studies reported the ability of these engineered vesicular to selectively target tumour cells.

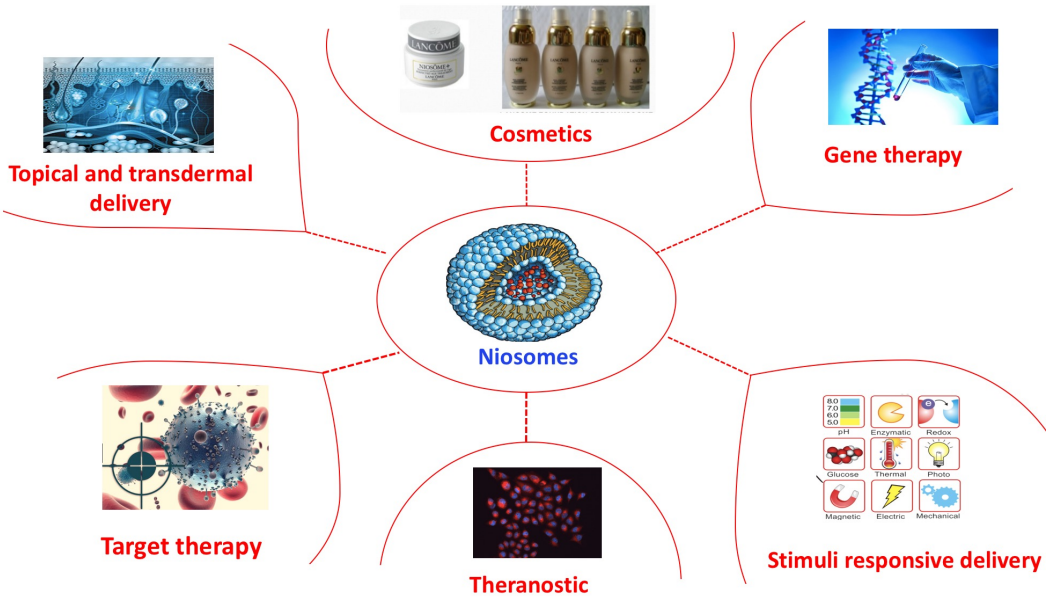

Figure 1: Representation of different niosomes applications

Particularly, the design of potent candidates was attractive for targeting the glioblastoma cells of brain tumour via niosomal surface modification with peptide derived from the Israeli yellow scorpion's venom due to its ability to penetrate the blood-brain barrier [5]. Sugar surfactant systems, instead, are becoming popular in

the design of niosomes for their natural ability to target brain or tumour tissues [6]. In recent years, particular attention has been paid on the design of more sophisticated stimuli responsive surfactants able to take advantage of the physio-pathological differences occurring in several altered conditions such as cancer, inflammation, ischemia and infections compared to healthy cells. Much of the ongoing works focuses on the development of pH sensitive surfactants able to undergo protonation once penetrated into acid compartments of pathological cells destabilizing their structure and improving intracellular release. Several studies proved the pH responsivity of niosomes based on Span® 20 and coated with pH insertion peptide or made of derivatives of Tween® 20 with different pH sensitive moieties like glycine, Nmethyl-glycine, N, N-dimethyl-glycine [7, 8]. These showed a better cytotoxicity than conventional niosomes on cancer cells suggesting the role as useful tools for enhanced intracellular target delivery. Based on their peculiar acid-base properties, these systems are also able to interact with DNA and other biologically relevant molecules like oligonucleotides and RNA with a consequent potential application as gene vectors for transfection. Other stimuli, typical used to manipulate the surfactant properties, consist on temperature, light, glutathione, enzymes and magnetic field. Recent studies focused on the determination of the suitable niosomal compositions for gene therapies. Generally, cationic lipids are incorporated into niosome formulations in order to create positively charged vesicles. Recently, Pengnam et al. [9] synthesized a new gemini surfactant plier-like with an ethylenediamine head group and the preliminary results showed that the niosomes based on Span® 20/cholesterol and their cationic gemini surfactant represent promising vehicles for nucleic acid delivery. Instead, Yang et al. [10] proposed the combination of gene delivery and cell labelling capacity into a single niosomal formulation based on Span® 80 and DOTAP to achieve a theranostic platform for stem cells-based therapy and regenerative medicine. The obtained results suggested optimal labelling ability and *in vivo* gene silencing of negative regulator of osteoblast differentiation of these devices after their implantation in mouse and, consequently, a promising utility in improving cellular regeneration. Furthermore, a depth interest was focused on the develop of innovative surfactants from alternative renewable raw materials at competitive prices, to meet the required safety and environmental criteria. Among these, amino-acid-based surfactants have emerged as a novel and attractive class of surfactants derived from amino acids such as cysteine, lysine and arginine, which showed promising results in several scientific works. These derivatives showed high biodegradability, low toxicity, and excellent antimicrobial activity against Gram-positive and Gram-negative microorganisms with huge potential applications in pharmaceutical, cosmetic and nutrition fields [11]. A great innovation in niosomal formulation was also represented by the use of some amphiphilic drugs with surface active properties as main component of the bilayer. These synthetic compounds similar to a surfactant and known as “surfadrug”, playing the role of both carrier and drug, resulted able to form vesicular systems

bypassing the use of other excipient and improving formulation biocompatibility [12].

2. Expert opinion

Niosomes are certainly a great and innovative promise for drug delivery and their near future could be very bright with several pharmacological therapies and other applications. Considering the above mentioned properties of niosome as drug carriers, they can represent a valid alternative to liposomes. The pioneer topic formulation was launched into the market by Lancome in 1987 and the benefits of these systems in cosmetic field are largely validated. However, the niosomal nanotechnology is still premature and a lot of work is still needed to guide their future applications in different clinical fields. Effectively, niosomes are young systems and few papers in literature have focused on these carriers. Since their birth, as evidenced by Scopus database only 4896 scientific reports focus on niosomes in drug delivery against 95705 ones dealing with liposomes. In most of these works, the pharmaceutical researches have taken advantage of versatility and adaptability of easy modified and functionalized non-ionic surfactants, to obtain specific targeting tools or with intrinsic stimuli responsive properties. The versatility of their constituents has led researchers to study their behaviour as anti-cancer carriers or for applications in gene therapy. These reports and our experience in the pharmaceutical fields underline the importance of creativity and innovation to tailor-made the niosomes suitable for various therapeutic purposes. Furthermore, multi-functional niosomes have been proposed as a further evolution of traditional “magic bullet” and the way to open new possibilities to achieve personalized therapies [13, 14]. These strategies were also extensively explored for liposomes but the incorporation of non-ionic surfactant in the composition of lipid-based vesicular systems was largely reported in many studies as the main reason to improve their major limitations of phospholipids. Then, why do not replace fully phospholipids in vesicular bilayers after seeing their important drawbacks? The niosomes potentiality is already recognized in dermatological therapy, indeed clinical trials for treatment of acne [15], psoriasis [16], leishmaniosis [17], wart [18] and oromucosal ulcers [19] are currently ongoing, but it would be desirable that the same interest is directed to different applications, such as diagnostics or therapeutics or also theranostic devices. Therefore, it is essential to focus on the discovery of novel and innovative surfactants able to form niosomal formulations, adequate for preclinal studies and switch after to clinical studies. The niosomes, despite their similarity to liposomes, have peculiar characteristics worth to be considered in order to increase availability pharmaceutical formulations more efficacy and less expensive. The real opportunities of these vesicular systems should be effectively considered and, in the near future, it will be important to spend more financial resources on their studies.

References

[1] Kazi KM, Mandal A S, Biswas N, et al. A future of targeted drug delivery systems. J Adv Pharm Technol Res. 2010; 1:374–380
[2] Saraswathi TS, Mothilal M, Jaga Nathan MK. Niosomes as an emerging formulation tool for drug delivery -A review. Int J App Pharm. 2019; 11:7-15
[3] Ge X, Wei M, He S, et al. Advances of Non-Ionic Surfactant Vesicles (Niosomes) and Their Application in Drug Delivery. Pharmaceutics 2019, 11, 55
[4] Mazzotta E, Oliviero Rossi C, Muzzalupo R. Different BRIJ97 colloid systems as potential enhancers of acyclovir skin permeation and depot. Colloids Surf B. 2019; 173:623-631
[5] De A, Venkatesh N, Senthil M, et al. Smart niosomes of temozolomide for enhancement of brain targeting. Nanobiomedicine 2018; 5:1-11
[6] Imran M, Shah MR, Ullah F, et al. Sugar-based novel niosomal nanocarrier system for enhanced oral bioavailability of levofloxacin. Drug Deliv. 2016; 23:3653-3664
[7] Pereira MC, Pianella M, Wei, D, et al. pH sensitive pHLIP® coated niosomes. Mol Membr Biol. 2016; 33:51-63
[8] Masotti A, Vicennati P, Alisi, A, et al. Novel Tween 20 derivatives enable the formation of efficient pH-sensitive drug delivery vehicles for human hepatoblastoma. Bioorg Med Chem Lett. 2010; 20:3021–25
[9] Pengnam S, Patrojanasophon P, Rojanarata T, et al. A novel plier-like gemini cationic niosome for nucleic acid delivery. J Drug Deliv Sci Technol. 2019;52: 325–333
[10] Yang C, Gao S, Song P, et al. Theranostic Niosomes for Efficient siRNA/MicroRNA Delivery and Activatable Near-Infrared Fluorescent Tracking of Stem Cells. ACS Appl Mater Interfaces. 2018; 10:19494−19503
[11] Pinazo A, Pons R, Perez L, et al. Amino Acids as Raw Material for Biocompatible Surfactants. Ind Eng Chem Res. 2011; 50:4805–4817
[12] Tavano L, Mazzotta E, Muzzalupo R, Innovative topical formulations from diclofenac sodium used as surfadrug: The birth of Diclosomes. Colloids Surf B. 2018; 164:177–184
[13] Muzzalupo R, Tavano L, La Mesa C. Alkyl glucopyranoside-based niosomes containing methotrexate for pharmaceutical applications: Evaluation of physico-chemical and biological properties Int J Pharm. 2013; 458:224-229
[14] Tavano L, Muzzalupo R Multi-functional vesicles for cancer therapy: the ultimate magic bullet. Colloids Surf B. 2016; 146:161-171
[15] Mohammadi S, Farajzadeh S, Pardakhti A, et al. A Survey to Compare the Efficacy of Niosomal Erythromycin Alone versus Combination of Erythromycin and Zinc Acetate in the Treatment of Acne Vulgaris. J Kerman Univ Med Sci. 2017; 24:420-430
[16] Lakshmi PK, Bhaskaran S, Phase II study of topical niosomal urea gel- an adjuvant in the treatment of psoriasis. Int J Pharm Sci Rev Res. 2011; 7:1-7
[17] Farajzadeh S, Ahmadi R, Mohammadi, S, et al. Evaluation of the efficacy of intralesional Glucantime plus niosomal zinc sulphate in comparison with intralesional Glucantime plus cryotherapy in the treatment of acute cutaneous leishmaniasis, a randomized clinical trial. J Parasit Dis. 2018; 42:616–620
[18] Farajzadeh S, Pardakhti A, Mohammadi S, et al. A randomized clinical trial of using niosomal zinc sulfate plus cryotherapy in comparison with placebo along with cryotherapy in treatment of common wart. J Kerman Univ Med Sci. 2018; 25:1-8
[19] Arafa MG, Ghalwash D, El-Kersh DM, et al. Propolis-based niosomes as oromucoadhesive films: A randomized clinical trial of a therapeutic drug delivery platform for the treatment of oral recurrent aphthous ulcers. Sci Rep. 2018; 8:18056

1.8 References

[1] Balogh, L.P. Nanomedicine in Health and Disease. Taylor &Francis Inc.: U.S., 2011.

[2] Kreuter, J. Encyclopedia of Pharmaceutical Technology; Marcel Dekker: New York, 1994,165.
[3] Rizvi, S.A.A., Saleh, A.M. Applications of nanoparticle systems in drug delivery technology. Pharm. J., 2018, 26, 64–70.
[4] Ernsting, M.J., Murakami,M., Roy, A., Li, S. D. Factors Controlling the Pharmacokinetics, Biodistribution and Intratumoral Penetration of Nanoparticles J Control Release. 2013, 172, 782-94.
[5] Balmayor, E.R., Azevedo, H.S., Reis, R.L. Controlled delivery systems: from pharmaceuticals to cells and genes. Pharm. Res., 2011, 28, 1241.
[6] Couvreur, P. Nanoparticles in drug delivery: past, present and future. Adv Drug Deliv Rev, 2013, 65,21-23.
[7] Tan, S. Y.; Grimes, S. Paul Ehrlich (1854-1915): man with the magic bullet. Singapore Med. J., 2010, 51, 842.
[8] Maeda, H., Nakamura, H., Fang, J. The EPR effect for macromolecular drug delivery to solid tumors: Improvement of tumor uptake, lowering of systemic toxicity, and distinct tumor imaging *in vivo*. Adv. Drug Deliv. Rev., 2013, 65, 71-79.
[9] Albanese, A., Tang, P. S., Chan, W. C. W. The effect of nanoparticle size, shape, and surface chemistry on biological systems. Annual Review of Biomedical Engineering. 2012, 14, 1–16.
[10] Bae, Y. H. Park, K. Targeted drug delivery to tumors: myths, reality and possibility. J. Control. Release. 2011, 153, 198–205.
[11] Liu, Y.; Hui, Y.; Ran, R.; Yang, G.-Z.; Wibowo, D.; Wang, H.-F.; Middelberg, A.P.J.; Zhao, C.-X. Synergetic Combinations of Dual-Targeting Ligands for Enhanced In Vitro and *In Vivo* Tumor Targeting. Adv. Healthc.Mater. 2018, 7.
[12] Bertrand, N., Wu, J., Xu, X., Kamaly, N., Farokhzad, O. C. Cancer nanotechnology: The impact of passive and active targeting in theera of modern cancer biology. Advanced Drug Delivery Reviews. 2014, 66:2-25.
[13] Bhowmik, D., Gopinath, H., Kumar, B. P., Duraivel, S., Kumar, K. P. S. Controlled Release Drug Delivery Systems. Pharma innoation. 2012, 1, 24-32.
[14] Larese Filon, F., Mauro, M., Adami, G., Bovenzi, M., Crosera, M. Nanoparticles skin absorption: New aspects for a safety profile evaluation. Regulatory Toxicology and Pharmacology . 2015, 72, 310–322
[15] Prow, T.W., Grice, J.E., Lin, L.L., Faye, R., Butler, M., Becker, W., Wurm, E.M., Yoong, C., Robertson, T.A., Soyer, H.P., Roberts, M.S. Nanoparticles and microparticles for skin drug delivery. Adv Drug Deliv Rev. 2011, 30, 470-91.
[16] Morrow, D.I.J., McCarron, P.A., Woolfron, A.D. Innovative Strategies for Enhancing Topical and Transdermal Drug Delivery. The Open Drug Delivery Journal. 2007, *1,* 36-59 Woolfson and R.F. Donnelly
[17] Lee, O., Jeong, S.H., Shin, W.U., Lee, G., Oh, C., Son, S.W. Influence of surface charge of gold nanorods on skin penetration. Skin Res. Technol. 2013. 19,390–396.
[18]Ryman-Rasmussen, J.P, Riviere, J.E., Monteiro-Riviere, N.A. penetration of intact skin by quantum dots with diverse physicochemical properties. Toxicol Sci. 2006,91,159-65.
[19] Cevc, G., Blume, G. Lipid vesicles penetrate into intact skin owing to the transdermal osmotic gradients and hydration force. Biochim Biophys Acta. 1992, 17,226-32.
[20] Fox, L.T., Gerber, M., Du Plessis, J., Hamman, J.H. Transdermal Drug Delivery Enhancement by Compounds of Natural Origin. Molecules. 2011, 16, 10507–10540.
[21] Tavano, L., Picci, N., Ioele, G., Muzzalupo, R.* Tetracycline-niosomes versus Tetracycline Hydrochloride-niosomes: How to Modulate Encapsulation and Percutaneous Permeation Properties J. Drug. 2017,1, 1-6.
[22] Uchechi, O., Ogbonna J. D. N., Anthony A. Attama, A.A. Nanoparticles for Dermal and Transdermal Drug Delivery. In book: Application of Nanotechnology in Drug Delivery 2014

[23] Tavano, L., Muzzalupo, R. Multi-functional vesicles for cancer therapy: The ultimate magic bullet .Colloids Surf B Biointerfaces. 2016,1,161-171.
[24] Liu, Y.; Hui, Y., Ran, R., Yang, G.Z., Wibowo, D., Wang, H.F., Middelberg, A.P.J., Zhao, C.X. Synergetic Combinations of Dual-Targeting Ligands for Enhanced *In Vitro* and In Vivo Tumor Targeting. Adv. Healthc. Mater. 2018, 7.
[25] Fernandes, C., Suares, D., Yergeri, M.C. Tumor Microenvironment Targeted Nanotherapy Front Pharmacol. 2018, 9, 1230.
[26] Mazzotta, E., Tavano, L., muzzalupo, R. Thermo-Sensitive Vesicles in Controlled Drug Delivery for Chemotherapy Pharmaceutics 2018, 10, 150
[27] Lindner, L.H., Eichhorn, M.E., Eibl, H., Teichert, N., Schmitt-Sody M., Issels, R.D., Dellian, M. Novel temperature-sensitive liposomes with prolonged circulation time. Clin. Cancer Res. 2004,10, 2168-2178.
[28] Deshpande, P. P., Biswas,S., Torchilin, V. P. Current trends in the use of liposomes for tumor targeting Nanomedicine (Lond). 2013, 8, 1509-28.
[29] Ioele, G., De Luca, M., Garofalo, A., Ragno, G. Photosensitive drugs: a review on their photoprotection by liposomes and cyclodextrins Drug delivery. 2017, 24, 33–44.
[30] Ioele, G., Tavano, L., De Luca, M., Ragno, G., Picci, N., Muzzalupo, R. Photostability and *ex-vivo* permeation studies on diclofenac in topical niosomal formulations. Int J Pharm. 2015, 15, 490-7
[31] McClements, D.J. Nanoemulsions versus microemulsions: terminology, differences and similarities. Soft Matter. 2012, 8, 1719.
[32] Santos, P., Watkinson, A.C., Hadgraft, J., Lane, M.E. Application of microemulsions in dermal and transdermal drug delivery. Skin Pharmacol. Physiol. 2008, 21, 246–259.
[33] Burguera, J. L., Burguera, M. Analytical applications of emulsions and microemulsions, Talanta. 2012, 96, 11-20
[34] Peira, E., Scolari, P., Gasco, M. R. Transdermal permeation of apomorphine through hairless mouse skin from microemulsions. Intern. J. Pharmac.2001, 226, 47-51
[35] Calzoni, E., Cesaretti, A., Polchi, A., Di Michele, A., Tancini, B., Emiliani, C. Biocompatible Polymer Nanoparticles for Drug Delivery Applications in Cancer and Neurodegenerative Disorder Therapies. J Funct Biomater. 2019, 10, 4.
[36] Alonso, M. J., Losa, C., Calvo, P., Vila-Jato, J. L. Approaches to improve the association of amikacin sulfate to poly(alkylcyanoacrylate) nanoparticles. Int. J. Pharm. 1991, 68, 69.
[37] Kamaly, N., Yameen, B., Wu, J., Farokhzad, O. C. Degradable Controlled-Release Polymers and Polymeric Nanoparticles: Mechanisms of Controlling Drug Release. Chem. Rev. 2016, 116, 2602-2663
[38] Masood, F. Polymeric nanoparticles for targeted drug delivery system for cancer therapy. Materials Science and Engineering: C.2016, 60, 569-578
[39] Zhang, Z., Tsai, P. C., Ramezanli,T., Michniak-Kohna,B. B. Polymeric nanoparticles-based topical delivery systems for the treatment of dermatological diseases. Wiley Interdiscip Rev Nanomed Nanobiotechnol. 2013,5,205-18.
[40] Kumar, M. N., Muzzarelli, R. A.; Muzzarelli, C.; Sashiwa, H.; Domb, A. J. Chitosan chemistry and pharmaceutical perspectives. Chem. Rev. 2004, 104, 6017.
[41] Lu, J. M., Wang, X., Marin-Muller, C., Wang, H., Lin, P. H.,
Yao, Q., Chen, C. Current advances in research and clinical applications of PLGA-based nanotechnology. Expert Rev. Mol. Diagn. 2009, 9, 325.
[42] Li, J., Cai, C., Li, J., Li, J., Li, J., Sun, T., Wang, L., Wu, H., Yu, G. Chitosan-Based Nanomaterials for Drug Delivery. Molecules 2018, 23, 2661
[43] Lombardo,D., Kiselev, M. A., Caccamo, M. T. Smart Nanoparticles for Drug Delivery Application: Development of Versatile Nanocarrier Platforms in Biotechnology and Nanomedicine. J. Nanomaterials. 2019

[44] Mohammed, M.A., Syeda, J.T.M., Wasan, K.M., Wasan, E.K.An Overview of Chitosan Nanoparticles and Its Application in Non-Parenteral Drug Delivery. Pharmac. 2017,9, 53.
[45] Kim, D.H., Jahn, A., Cho, S. J., Kim, J. S., Ki, M.H., Kim, D.D. Lyotropic liquid crystal systems in drug delivery: a review. J. Pharm. Investig. 2015, 45, 1–11.
[46] Wahlgren, S., Lindstrom, A.L., Friberg, S.E. Liquid crystals as a potential ointment vehicle. J Pharm Sci. 1984,73,1484-6.
[47] Rajak, P., Nath, L. K., Bhuyan. B. Liquid Crystals: An Approach in Drug Delivery. Indian J Pharm Sci. 2019,81,11-21.
[48] Chaudhary, K. K., Kannojia, P., Mishra, N. Liquid Crystal Systems in Drug Delivery In book: Novel Approaches for drug Delivery. 2016
[49] Quemeneur, F., Rinaudo, M., Pèpin-Donat,B. Influence of Polyelectrolyte Chemical Structure on their Interaction with Lipid Membrane of Zwitterionic LiposomesmBiomacromolecules.2008,9,2237–2243.
[50] Patra, J.K., Das, G., Fraceto, L. F., Campos, E.V.R., Torres, M.P.R. ,-Torres, L. S. A. , Torres, L. A. D., Grillo, R., Swamy, M. K., Sharma, S., Habtemariam, S., Shin, H. S. Nano based drug delivery systems:recent developments and future prospects. Nanobiotechnol.2018, 16,71.
[51] Gabizon, A., Shmeeda, H., Barenholz, Y. Pharmacokinetics of pegylated liposomal doxorubicin, Clin. Pharmacokinet. 2012, 42, 419–436.
[52] Even-Or, O., Joseph, A., Itskovitz-Cooper, N., Samira, S., Rochlin, E., Eliyahu,H., Goldwaser, I., Balasingam, S., Mann, A.J., Lambkin-Williams, R., Kedar, E., Barenholz, Y. A new intranasal influenza vaccine based on a novel polycationic lipid-ceramide carbamoyl -spermine (CCS). II. Studies in mice and ferrets and mechanism of adjuvanticity, Vaccine. 2011, 29,2474–2486.
[53] Tantisripreecha, C., Jaturanpinyo, M., Panyarachun, B., Sarisuta, N. Development of delayed-release proliposomes tablets for oral protein drug delivery. Drug Dev. Ind. Pharm.2012, 38, 718–727.

2

NANOCARRIERS FOR SKIN DELIVERY

This section reviews the scientific projects regarding the design and characterization of nanocarriers for a potential application for skin delivery

2.1 Different BRIJ97 colloid systems as potential enhancers of acyclovir skin permeation and depot

Elisabetta Mazzotta[a], Cesare Oliviero Rossi[b], Rita Muzzalupo[a]

[a] Department of Pharmacy, Health and Nutritional Sciences, University of Calabria, Via Savinio, Ed. Polifunzionale, 87036 Arcavacata di Rende, Italy
[b] Department of Chemistry and Chemical Technologies, University of Calabria, Via P. Bucci, Cubo 14/D, Rende (Cs), Italy

Published on Colloids and Surfaces B: Biointerfaces 173 (2019) 623–631

GRAPHICAL ABSTRACT

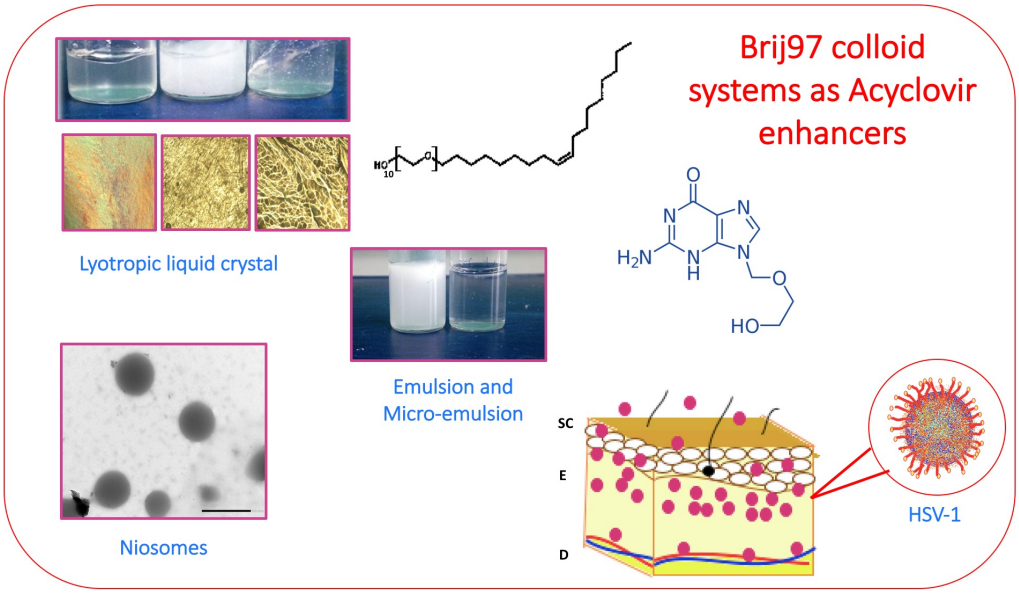

ABSTRACT

The low efficacy of Acyclovir topical therapy is due to its physicochemical properties that limit the permeation across the stratum corneum. The goal of this research was to evaluate the ability of biodegradable surfactant, Brij97, to self-assembly in different types of colloid systems which can improve the Acyclovir permeation and accumulation at the target site (the basal epidermis). New Acyclovir formulation based on Brij97 have been analysed in order to investigate the effect of drug encapsulation on the structure. After that, the *in vitro* percutaneous permeation of Acyclovir has been compared with that one of the commercial specialty Zovirax® 5%. To estimate the potential of the new formulations proposed as topical delivery,

it has been essential to quantify the Acyclovir in the skin layers. The results confirmed that the self-assembly of the surfactant in different nanosized structures improved the amount of permeated Acyclovir and the formation of intracutaneous drug reservoir. Furthermore, the different lipophilicity and structural organization of carriers based on Brij97 showed different influence on the promotion of permeation. The experimental data suggest that the designed carriers could be a valid alternative to improve the efficacy of the current antiviral therapy.

1. Introduction

Acyclovir (ACV) is a potent antiviral agent used as drug of choice to treat Herpes labialis that is the main clinical manifestation of herpes simplex virus type 1 (HSV-1). Herpes simplex virus (HSV) infection is one of the most common chronic viral infection in humans and it is estimated that one third of world's population is affected by this disease [1]. The virus penetrates the epidermis cells, replicates within destroying them and manifests pathologically as painful and vesicular lesions. After this first manifestation, HSV-1 establishes a persistent and latent infection in neuronal ganglia from which it can become active causing, consequently, recurrent infections. The target site for ACV is the basal epidermis. It is necessary, then, a sufficient amount of the drug to reach this site in order to suppress the viral replication [2]. The currently available therapies have various limitations due to the characteristics of the drug and the biological membrane. The skin, in fact, is an effective barrier that protects the body from the outside environment and this natural defence function limits the diffusion of most drugs across it. The drug absorption is affected by the arrangement and composition of the stratum corneum (SC). It is made by a multi-layered wall-like structure, in which corneocytes are embedded in a matrix of highly selective lipids [3], that can be crossed only by small and lipophilic molecules. ACV does not possess biopharmaceutical characteristics that guarantee therapeutic concentrations of the drug at the target site. Consequently, frequent applications of the actual commercial topical formulations are necessary to have an enough drug accumulation at the basal epidermis [4]. The low and marginal ACV permeation, in fact, pushed the researchers to develop alternative drug delivery systems (DDS). Moreover, topical administration is becoming a very attractive way for the local delivery of therapeutic agent. In fact, the skin as potential site of drug absorption offers several benefits as targeted therapy and patient compliance.

Niosomes, emulsion, micro-emulsion and lyomesophases are very interesting as topical drug delivery and they are receiving attention from the pharmaceutical industry for its ability to improve the drug transport and targeting to the skin layers. Niosomes are vesicular carriers widely used as effective dermal drug vehicle in the treatment of skin disorders due to ability to enhance drug permeation and create a localized depot in the inner layer of skin which ensure prolonged drug release over

time, reducing systemic absorption and, thus, minimizing side effects compared to conventional dosage form [5].

Emulsion (E) and micro-emulsion (ME) are widely used in the pharmaceutical field for their countless benefits, enhance long term stability and increased bioavailability [6], [7]. These dispersed systems have different features such as the stability and drop size. ME are thermodynamically stable, clear and translucent due to small drop size ranging from about 10–150 nm [8]. A combination of different mechanisms has been proposed to explain the ability of the ME to improve penetration, e.g. small droplet size, large surface area/volume ratio, action of individual constituent, the increase of skin hydration and high drug loading capacity [9]. Many drugs such as lidocaine [10], alpha- tocopherol [11] and ibuprofene [12] are delivered into the skin using ME and appeared to be ideal drug carrier for a wide range of dermatological disease.

The Emulsions (E) are generally cloudy due to larger drop size. They are kinetically but not thermodynamically stable. It is possible to form kinetically stable (metastable) emulsions for a reasonable period of time, if their destabilization rate is adequately low in comparison with the expended lifespan [13]. The term "emulsion stability" has been described as emulsion aptitude to resist changes in its properties over time, either chemically or physically.

Lyotropic liquid crystals (LLC), a supramolecular aggregation of amphiphilic surfactants, are thermodynamically stable phases whose production is quite simple and cheap. The high viscous structural organization of such colloidal aggregates allows a localized application of the drugs and maintenance on the skin surface [14].

During the last past decades, various type of ACV nanosized drug delivery systems such as niosomes [15], microparticles [16], nanoparticle [17], cyclodextrins [18] have been proposed to overcoming the ACV pharmacokinetic drawbacks and to improve the current available formulation. As far as we are aware, there is a lack of comparative analysis on the permeation of the ACV from the different colloidal nanostructures based on the same surfactant.

Therefore, the objective of this study is to investigate the ability of colloids based on a biodegradable non-ionic surfactant Brij-97 as effective ACV drug delivery system. To this purpose, we developed and compared four colloid systems: niosomes, emulsion, micro-emulsion and lyotropic liquid crystals. The vesicular carriers have been prepared at different molar ratio of Brij97 and cholesterol. All investigated systems have been characterized in terms of dimension, polydispersity index and ACV entrapment efficiency. In addition, considering the well- known percutaneous enhancer properties of Isopropyl myristate (IPM) [19], we hypothesized that its use increase the amount of drug permeated. For this reason, emulsion, micro-emulsion and lyotropic liquid crystal have been realized considering the ternary diagram phase Brij97/IPM/H2O reported in the reference [20]. *Ex-vivo* permeation studies have been performed using diffusion Franz cells and the quantification of ACV deposited

in the skin layer has been determined by extractions. All obtained results were compared to that one obtained using the commercial specialty Zovirax® 5%.

2. Materials and methods

2.1. Chemicals

Brij97, cholesterol (Ch), isopropyl myristate (IPM) and F127 were purchased from Fluka (Sigma-Aldrich, Milan, Italy, 98% purity). All organic solvents were supplied from Sigma-Aldrich (Milan, Italy) and are of high performance liquid chromatography grade. Pharmaceutical specialty Zovirax® 5% (GlaxoSmithKline S.p.A.) was obtained commercially.

2.2. Vesicles preparation

Acyclovir niosomes were prepared using the hydration of lipid film method [21]. Accurately weighed quantities of surfactant (Brij97) and cholesterol in different molar ratio were dissolved in ethanol in a round bottom flask; details of composition are reported in Table 1. The organic solvents were vacuum evaporated at 40 °C under constant rotation to form a thin film on the wall of the flask. This film was then hydrated under mechanical stirring at 60 °C for 30 min with 10 mL of distilled water (empty niosomes) or drug solution (1×10^{-3} M). After preparation, the dispersion was left to equilibrate at room temperature overnight to allow the complete annealing and partitioning of the drug between the lipid bilayer and the aqueous core. Small unilamellar vesicles (SUV) were prepared starting from MLV by sonication in an ultrasonic bath for 30 min at 60 °C.

Formulation	Brij97 (g) x10^{-3}	Chol (g) x 10^{-3}	Diameter (nm ± SD)	P. I.	ξ-potential (mV± SD)	ACV E%
N	71.0±0.3	-	518.1 ± 21	0.246	-18.0±1.4	-
N^A	71.0±0.3	-	585.4 ± 19	0.230	-13.3±1.0	44.0±5
N_1	57.2 ± 0.3	7.2 ± 0.3	305.8 ± 22	0.236	-13.2±1.0	-
N_1^A	57.2 ± 0.3	7.2 ± 0.3	389.2 ±18	0.249	-16.5±1.2	56.54±3
N_2	35.1±0.3	19.0 ± 0.3	227.0 ±21	0.199	-15.1±1.2	-
N_2^A	35.1±0.3	19.0 ± 0.3	245.37 ± 22	0.254	-15.4±1.2	49.0± 3

Table 1. Composition, hydrodynamic diameter, polydispersity index, ζ-potential of empty and loaded niosomes and ACV entrapment efficiency. The total lipid concentration was 1 x 10^{-2}M for each sample.

2.3. Emulsion and micro-emulsion preparation

Once the emulsion and micro-emulsion region was identified in pseudo-ternary phase diagram [20], the formulations at desired component ratios were prepared with or without ACV. Details on the composition of formulation are given in Table 2.

In the first step, ACV was mixed with water at different concentrations. The mixtures of IPM (oil phase) and surfactant were heated for 3 min in a hot water bath set at 70 °C and, then, added to aqueous phase dropwise. Finally, the systems were mixed using a vortex mixing at 2200 rpm for 5 min, followed by 2 min centrifugation at 3500 rpm. The E samples have the following percentage of ACV: 0.07, 0.1, 0.2, 0.5, 0.8 and 1.2% (w/w). The ME are prepared only at 0.07, 0.1 and 0.2% of ACV due to the different drug solubility in these systems.

Formulation	Brij97(g)	IPM (g)	H_2O (g)	ACV (g) x 10^{-3}	Diameter (nm ± SD)	P. I.	ACV skin depot (moles)
E	0.170± 0.005	0.230 ±0.002	1.600±0.005	-	365.1± 5.2	0.182	-
E1	0.170± 0.002	0.230 ±0.002	1.600±0.005	1.400±0.003	148.8± 4.1	0.251	3.77×10^{-7}
E2	0.170± 0.005	0.230 ±0.002	1.600±0.005	2.000 ±0.003	130.4± 3.8	0.240	9.03×10^{-7}
E3	0.170± 0.004	0.230 ±0.003	1.600±0.005	4.000 ±0.005	195.9± 4.2	0.171	5.65×10^{-7}
E4	0.170± 0.001	0.230± 0.001	1.600±0.005	10.000 ±0.003	168.4± 2.7	0.220	1.91×10^{-6}
E5	0.170± 0.002	0.230± 0.002	1.600±0.005	16.000 ±0.003	172.4± 4.0	0.057	6.37×10^{-6}
E6	0.170± 0.005	0.230± 0.001	1.600±0.005	24.000±0.002	155.7± 3.5	0.239	2.16×10^{-5}
ME	0.380± 0.003	0.100± 0.003	1.520±0.005	-	20.8± 3.3	0.233	-
ME1	0.380± 0.003	0.100± 0.002	1.520±0.005	1.400 ±0.001	13.7 ±2.4	0.207	3.93×10^{-7}
ME2	0.380± 0.001	0.100± 0.002	1.520±0.005	2.000 ±0.005	13.6 ±3.0	0.114	3.00×10^{-7}
ME3	0.380± 0.005	0.100± 0.001	1.520±0.005	4.000 ±0.003	14.5 ±1.2	0.230	6.04×10^{-7}

Table 2. Compositions, particle size, polydispersity index and amount of ACV skin depot of emulsion and micro-emulsion formulations.

2.4. Acyclovir LLC preparation

LLC were prepared using an accurate ratio between surfactants, oil phase and water in order to obtain the different Brij97 liquid crystalline structures. The composition of each sample considering the ternary diagram phase Brij97/IPM/H2O [20] is reported in Table 3. The LLC gels were realized using two different fixed drug percentage: 0.1% and 1%. The samples were prepared as follow: the oil phase and the surfactant were mixed and heated at 70° for 10 min to homogenize them. The ACV was dissolved in the water and, consequently, added at the mixture of IPM and surfactant. In order to homogenize the samples, firstly the samples were subjected to various cycles of centrifugation at 3000 rpm for 5 min, after they were mixed by vortex and heat at 70 °C for 10 min.

Phases	Brij97 wt %	H_2O wt%	IPM wt %	ACV %	ACV skin depot (moles)
LLC₁	56.0	30.0	14.0	0.1	7.08×10^{-7}
				1	1.40×10^{-6}
LLC₂	38.4	52.0	9.6	0.1	8.06×10^{-7}
				1	1.13×10^{-6}
LLC₃	30.4	62.0	7.6	0.1	1.01×10^{-6}
				1	9.43×10^{-7}
Zovirax®				5	2.11×10^{-7}

Table 3. Composition and amount of ACV skin depot of liquid crystalline phase.

2.5. Size distribution analysis

The average particle size of E, ME and niosomes were determined by dynamic light scattering (DLS) using a 90 Plus Particle Size Analyzer (Brookhaven Instruments Corporation, New York, USA) at 25.0 ± 0.1 °C. The autocorrelation function was measured at 90°, while the laser beam was operating at 658 nm. The mean size and standard deviation (± S.D.) were directly obtained from the instrument fitting data by the inverse "Laplace transformation" method and by Contin [22]. The polydispersity index (P.I.) was used as a measure of the size distribution and P.I. values ≤0.3 indicate homogenous and monodisperse populations, in the case of colloidal systems. All analyses were done in triplicate and expressed as mean ± standard deviation.

2.6. Transmission electron microscopy (TEM)

The morphology of niosomes sample was carried out by transmission electron microscopy (TEM), using a ZEISS EM 10 electron micro- scope at an accelerating voltage of 80 kV. A drop of dispersion was placed onto a carbon-coated copper grid and left to adhere on the carbon substrate for about 1 min. The dispersion in excess was removed by a piece of filter paper. A drop of 2% phosphotungstic acid solution was stratified and, again, the solution in excess was removed by a tip of filter paper. The sample was air-dried and the film of stained niosomes was observed.

2.7. ζ-potential

The ζ-potential is a very important index of the stability of colloidal systems [23]. The presence of particle surface charge causes, between similar and adjacent charged particles, the development of electrostatic repulsion forces, their degree being related to the ζ-potential. High ζ-potential values indicate, in fact, that the particles repel one another, and this stabilizes the system against aggregation. The ζ-potential of the formulations was measured with the laser Doppler electrophoretic mobility measurements using the Zeta-sizer ZS (Malvern Instrument Ltd., Malvern, U.K.), at 25.0 ± 0.1 °C and the values were calculated by the instrument software, using Helmholtz–Smoluchosky

equation. The results are reported as the means of three independent experiments performed in triplicate.

2.8. Acyclovir entrapment efficiency

The amount of ACV retained in the vesicles was determined as follow. The un-trapped (free) drug was removed using the dialysis technique. According to this method, 3 mL of ACV-loaded niosomes dispersion were dropped in a dialysis bag (Spectra/Por, MW cut-off 12,000, Spectrum, Canada) immersed in 100 mL of distilled water and magnetically stirred. Free drug was removed by exhaustive dialysis. The percent of encapsulation efficiency (E%) was expressed as the percentage of the drug not entrapped into niosomes referred to the amount of drug present in the non-dialyzed sample and it was determined by di- luting 1 mL of dialyzed or 1 mL of non-dialyzed in 25 mL of a mixture of isopropanol/ethanol 50:50, to obtain the vesicle rupture. After, the measurement of absorbance at 252 nm of these solutions was performed. Absorption spectra were recorded with a UV ± Vis JASCO V-530 spectrometer using 1 cm quartz cells. Each experiment was carried out in triplicate and the results are expressed as mean ± standard deviation.

2.9. ^{2}H-NMR characterization of ACV LLC

The characterization of the mesophases was performed through the ^{2}H quadrupolar interaction using nuclear magnetic resonance (NMR) spectroscopy. The nanometric structural organization of LLC phases is reflected in the rotational and translational motion of water molecules at the interface with supramolecular surfactant aggregate. The orientation order of water was detected with ^{2}H-spectra which can be used not only to differentiate between lamellar, cubic and hexagonal phase, but also determine the directional order and the size of microcrystal.

In this study, ^{2}H-NMR experiments were performed at a resonance frequency of 46.53 MHz on deuterium a Bruker AVANCE 300 pulsed superconducting spectrometer working in Fourier Transform mode. The measurements were performed at 25 °C and 35 °C which is the temperature at which the release experiments were conducted to verify the maintenance of the lyotropic structure.

2.10. Polarized optical microscopy observation of ACV LLC

Polarized optical microscopy (POM) observations were typically used to detect the existence of LLC [24], and to identify the mesophases through their characteristic textures This type of analysis is very important to evaluate the crystalline ordered of the various mesophases that produce typical

birefringence effects. Phase characterization of the samples was performed with a Leica 12 Pol optical polarizing microscope.

2.11. Transdermal permeation and skin retention study

Ex-vivo skin permeation studies were performed using vertical diffusion Franz cells with an effective diffusion area of 0.416 cm2. The experiments were carried out using rabbit ear skin obtained from a local slaughterhouse. The skin, previously frozen at −18 °C, was pre-equilibrated in physiological solution at room temperature for 2 h before the experiments. The skin was mounted on the receptor compartment with the SC side facing upward into the donor compartment. The donor compartment was charged with an appropriate volume of sample and covered with Parafilm to prevent water loss. The receptor compartment was filled with 5.5 mL of distilled water. At predetermined time up to 24 h receptor solution were sampled for analysis and replaced with the same volume of prethermostated (37 °C ± 0.5 °C) fresh solution. Absorption spectra were recorded with a UV ± Vis JASCO V-530 spectrometer using 1 cm quartz cells.

At the end of permeation study, the skin surfaces were thoroughly cleaned with physiological solution, dried with tissue paper, chopped into tiny pieces and after that immersed in 10 mL of distilled water and bath-sonicated for 30 min. The extraction solutions were filtered using 0.22 μm Millipore membrane filter and the amount of ACV were determined by UV–Vis spectrometry. Each experiment was carried out in triplicate and the results are expressed as mean ± standard deviation.

2.12. Statistical analysis

All data were expressed as the mean ± SD of three independent experiments. Statistical analysis was performed using a Student's t-test and p values of ≤0.05 were considered statistically significant.

3. Results

3.1. Niosomes characterization

To our knowledge, niosomes based on Brij97 surfactant are not described in literature. The Brij97 surfactant is able to form vesicles spherical in shape with and without cholesterol, also when they were loaded with drug. Fig. 1 shows typical TEM micrograph obtained (Fig. 1). Visually niosomal suspensions of Brij97 appear opalescent as well as vesicular formulations. The ability of the surfactant to self-assembly in vesicles depends on its structure and, in particular, on the balance between its hydrophilic and hydrophobic portions. In fact, Brij97 has HLB value 12.4, which allows the

achievement of suitable molecular geometry and hydrophobicity for bilayer vesicle formation [25].

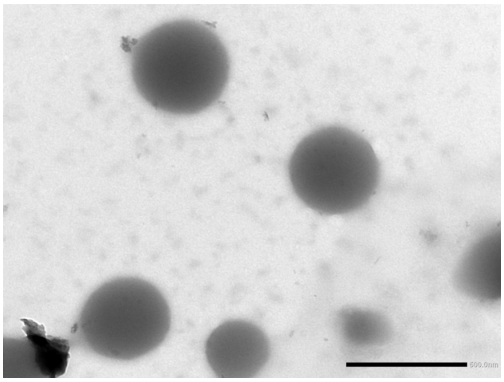

Fig. 1. Typical TEM photomicrographs for ACV loaded niosomes (N^A). Bar is 500 nm.

The presence of a large hydrophilic head group in the molecular structure determines a high surface energy and consequently high vesicles sizes [26]. The presence of cholesterol gave rise to less turbid suspensions depending on the amount, and to decreased niosomes size. This effect can be attributed to the decrease in surface energy because of the increase of hydrophobicity [27]. In Table 1, the size and some physico-chemistry properties of these systems are reported.

Moreover, the presence of ACV influenced significantly the characteristics of the carriers. In fact, the encapsulation of ACV into aqueous compartment led to increased vesicular diameter. Probably, this can be ascribed to the hydrophilic character of the drug. ACV is indeed deprotonated (pKa = 2.9) at neutral pH condition used in the preparation. The repulsion between the charged groups may explain the increase of vesicle diameter [25].

As reported in Table 1, the P. I. of the studied formulations were in the range 0.199 to 0.254 indicating that the vesicle population were relatively homogenous in size. The drug had a moderate affinity to the niosomal matrix, this result was evidenced by the values of the encapsulation efficiency from 44.00% to 56.54%.

Zeta-potential value of all the formulations was found to be negative and changes within a range of -13.2 ± 1.0 and -18.0 ± 1.4 mV. This may be due to the presence of free carboxyl groups in cholesterol and surfactant molecule. The zeta-potential values seemed to be in- dependent of the composition of the systems.

3.2. Emulsions and micro-emulsions characterization

Oil in water emulsions and micro-emulsions empty and loaded with different ACV concentration were prepared, as described above. Hydrodynamic diameters of ME and E oil droplets are reported in Table 2. When E and ME are visually observed, E appears milky and cloudy, while ME appear isotropic, transparent and optically clear due to smaller size of droplets [6].
The droplet-size range for the ME was within 13.6–20.8 nm, while for the E it was in the range 130.4–365.1 nm.
The loading of the drug led to a significant reduction of mean droplet size for both E and ME respectively. The exact mechanism of the observed phenomenon is not understood yet. Two different explanations can be found in literature. The first proposes that a certain amount of undissolved drug is located at the interface of the dispersed systems and it acts as emulsifying agent consequently the oil drop size de- creases. The second one attributes the decreasing of size to the reduction of surfactant mobility induced by the presence of the drug at the interface [28].
The P. I. of E and ME ranged between 0.11 and 0.25 indicating that the droplets size distribution was narrow and consequently the formulations were homogeneous in size for colloidal dispersion.

3.3. LLC characterization

As reported in literature, the mixtures Brij97/IPM/H2O are able to self-assembly in very rich mesophases with increasing surfactant content [20] and we tested their cubic, hexagonal and lamellar structures by ^{2}H-NMR spectra. These phases could be interesting and promising carriers for pharmaceutical delivery. We realized different LLC based on Brij97 as possible ACV drug delivery. The systems have been made with two different drug concentrations (0.1 and 1%) in order to check the effect of drug incorporation on the mesophases structure. For all samples, the visual and POM observations are different at various drug amounts. Visually, the empty and 0.1% ACV LLC appear as semi-solid transparent systems, while the LLC with the 1% of ACV present a milky turbidity, indicative only of a partial solubilisation of the drug. This effect was confirmed by the POM observations that revealed the presence of needles in all LLC samples containing 1% drug (POM images are not shown).
All samples showed a viscosity suitable for a topical application, LLC_1 showing higher viscosity than the other mesophases, according to the literature data for lamellar mesophase [29]. Furthermore, a rapid increase of fluidity was observed for the LLC_3 that appeared as a viscous gel at room temperature and it became liquid-like at 32 °C. The influence of temperature on the existence of mesophases has been widely demonstrated, the

measurement was done at 25 °C, storage temperature, and 35 °C that is the temperature at which the *ex-vivo* permeation studies have been carried out. ^{2}H-NMR spectra of LLC_1 sample without drug showed a quadrupolar splitting typical of a lamellar phase at 25 and 35 °C, as reported in the ternary phase diagram [20], and this structure was preserved when ACV at different concentration was loaded. Instead, ^{2}H-NMR spectra of LLC_2 showed a clear influenced of temperature and of the presence of ACV.

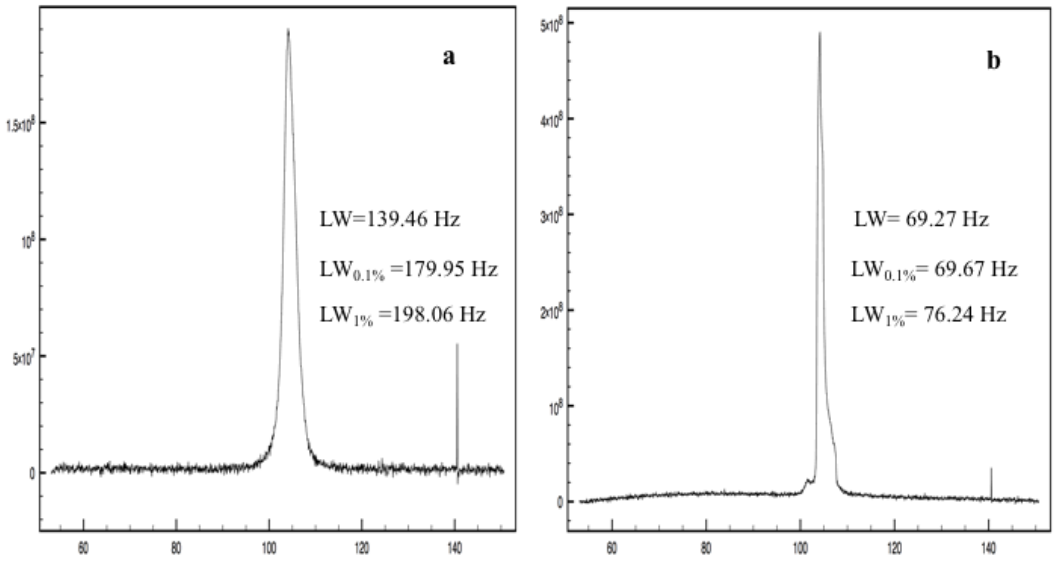

Fig. 2. ^{2}H-NMR spectra at 35 °C. (a) LLC_2 and (b) LLC_3. In the top the value of LW at different drug concentration.

The lineshape of ^{2}H-NMR spectrum of the LLC_2 without ACV was a typical of a hexagonal phase at 25 °C, as reported in [20], When the temperature increases the mixture as a viscous liquid appeared and its NMR spectrum showed isotropic lineshape. The same effect was observed with drug incorporation (Fig. 2a). In fact, the ACV presence in the systems changed the structural order of the hexagonal phase and already at 25 °C ^{2}H-NMR spectrum of LLC_2 was not typical of the hexagonal phase but on the contrary typical of isotropic phase. We hypothesized that is a cubic phase due to the high viscosity, the stiff consistency and the POM images where birefringence was not observed with the incorporation of the drug into the LLC_2 system.
In ternary phase diagram, the LLC_3 without ACV was reported as cubic phase and the ^{2}H-NMR spectrum recorded presented an isotropic peak typical of this structural organization. When ACV was loaded, we measured an increasing linewidth (LW) of spectrum recorded, the values are shown in

the top of Fig. 2b. This behavior could be ascribed to an increase structural order recorded at increasing of drug concentration.

3.4. Permeation and skin retention studies

The success of antiviral therapy depends on how much drug reach the basal epidermis. ACV has a very low topical bioavailability due to its partition coefficient (log P=−1,5) and limited aqueous and lipid bilayer solubility [30]. Multiple daily doses of the drug are consequently needed to suppress viral replication. New topical formulations therefore were developed in this research. The permeation experiments were, then, carried out in order to evaluate the effectiveness of the systems proposed. In particular, the focal point of our study is to realize systems able to improve the therapeutic efficacy of ACV in Herpes labialis disease. The formation of intracutaneous drug depot that would lead to prolonged drug release over the time is a crucial factor for the success of antiviral therapy. For this reason, the quantification of ACV in the skin layers may be useful.

3.4.1. Niosomal *ex-vivo* permeation and skin retention studies

The cumulative ACV permeation percentages versus time of all niosomal samples are shown in Fig. 3a. The permeation of ACV from solution used as control resulted lower respect to ones in niosomal formulations.

As illustrated, the higher cumulative amount of ACV permeated across rabbit skin after 24 h was obtained for NA formulations, equal to 17.1%. This value decreased to13.85% and 12.35% for N_1^A and N_2^A samples, respectively.

The ACV permeation depends on the lipophilicity of the systems: lower Ch content, higher permeation. Ch is one of the main factor affecting the skin permeation, an increase of Ch content reduces the bilayers fluidity of vesicles and thereby decrease the drug leakage and increase skin deposition [32].

The incorporation of ACV in the vesicular formulation led to a greatest accumulation of drug in the skin with respect to that obtained for the simple solution, for which the retention was almost negligible.

The quantities of drug accumulated in the skin are reported in Fig. 3b. ACV depot obtained with systems in presence of Ch was considerably higher with respect to that obtained with niosomes without Ch, as expected. In fact, a major lipophilicity of the formulation determined a high retention in the skin because of a better physicochemical similarity with the skin layers and a reduction of the systemic drug concentration. These characteristics are the basis for a formulation designed to guarantee a local pharmacological effect.

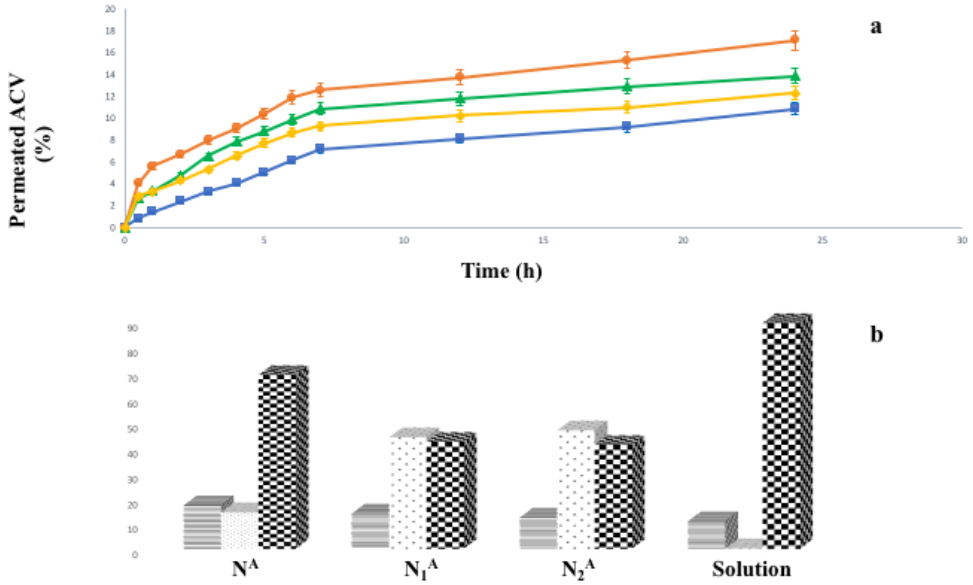

Fig. 3. A) ACV permeation from the different niosomal samples through rabbit ear skin at 37 °C: N^A (●); N_1^A (▲); N_2^A (♦); ACV solution (■); (mean ± SD; n=3); b) amount of ACV permeated (lines), depot (point), not permeated (square) from different niosomal formulation and control.

3.4.2.E and ME permeation and skin retention studies

The mean cumulative amount permeated per unit area for all E systems resulted to be greater than the commercial cream, as reported in Fig. 4a, demonstrating the enhancement effect of emulsion for topical delivery with respect to the classical formulations. While the E4, E5 and E6 formulations showed a permeation profile dependent on drug concentration, an anomalous ACV permeation was observed for E1, E2 and E3 samples. In fact, on increasing drug-surfactant ratio, the ACV permeation rate decreased. The slower drug release from E2 and E3 compared to E1 might be attributed to particular interactions that occurred between matrix and drug. In fact, it has been reported that basic drug-substrate interaction is a crucial factor in controlling drug release [34]. In particular, this interaction hinders the drug leakage from matrix and, consequently, reduces the drug skin permeation [35]. However, with the increase of drug content the interaction drug- matrix likely must be to the saturation and an increase in the drug permeation rate occurred. The same trends are observed with ME formulations. The results of ACV skin permeation study through rabbit ear skin from ME are depicted in Fig. 4b. All ME achieved an improvement of the permeation compared to commercial cream. The highest ACV permeation was obtained with ME3 that resulted 3 times higher than Zovirax® 5%. High permeation profile achieved from E and ME samples results are even more striking if we consider that the new proposed formulations have a much smaller amount of drug compared to the commercial specialty.

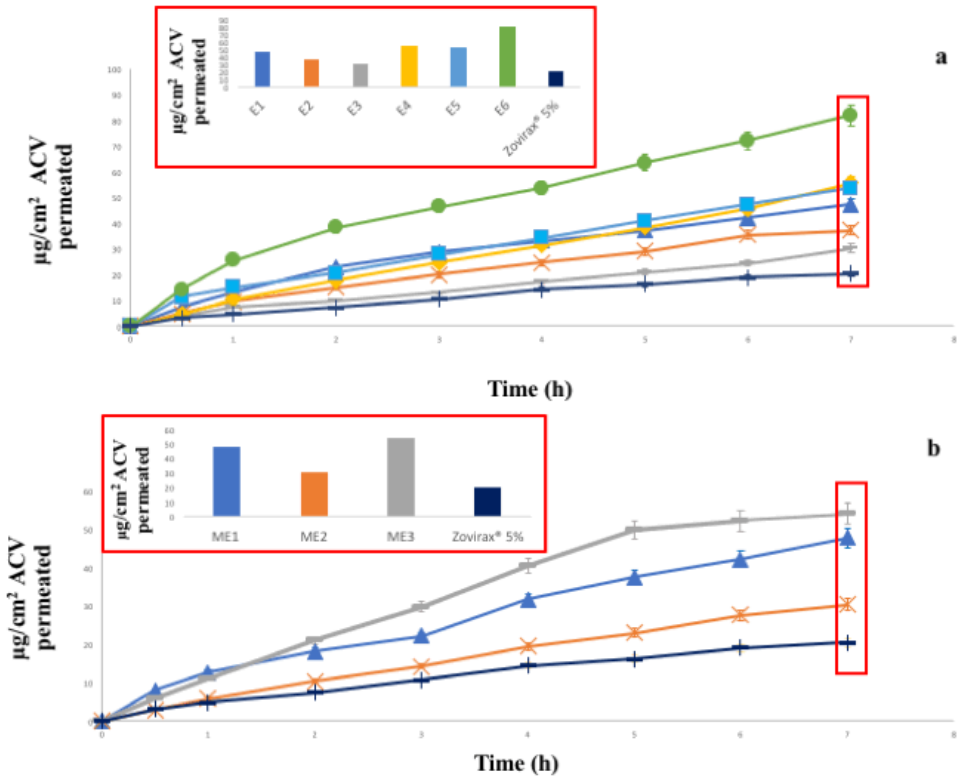

Fig. 4. Amount of ACV permeated at different concentration of drug through rabbit ear skin at 37 °C: a) Emulsion formulations E1 (▲); E2 (×); E3 (−); E4 (♦); E5 (■); E6 (●); Zovirax® 5% (+). B) micro-emulsion formulations: ME1(▲); ME2 (×); ME3 (−); Zovirax® 5% (+).

Table 2 reported the amount of ACV deposited in the skin layers after the *ex vivo* permeation studies. For all ME and E systems realized the amount of ACV retained was significantly higher compared to commercial specialty. Greater deposition was observed with E4, E5, E6 and ME3. In particular, the amount of drug deposited both E1 and ME1 was about twice higher than commercial cream despite containing a much lower quantity of drug. These results highlight the ability of such systems to promote permeation and create a drug reservoir in the skin. This reservoir is made available for protracted periods allowing a more efficient suppression of viral growth.

3.4.3. LLC permeation and skin retention studies

When the ACV were formulated as lyotropic liquid crystal samples the experimental data were dependent on the microstructures changes and as showed previously, these structural variations were related to drug amount. The cumulative quantities of drug permeated from LLC with 0.1 and 1% of ACV across the skin are plotted versus time in Fig. 5.

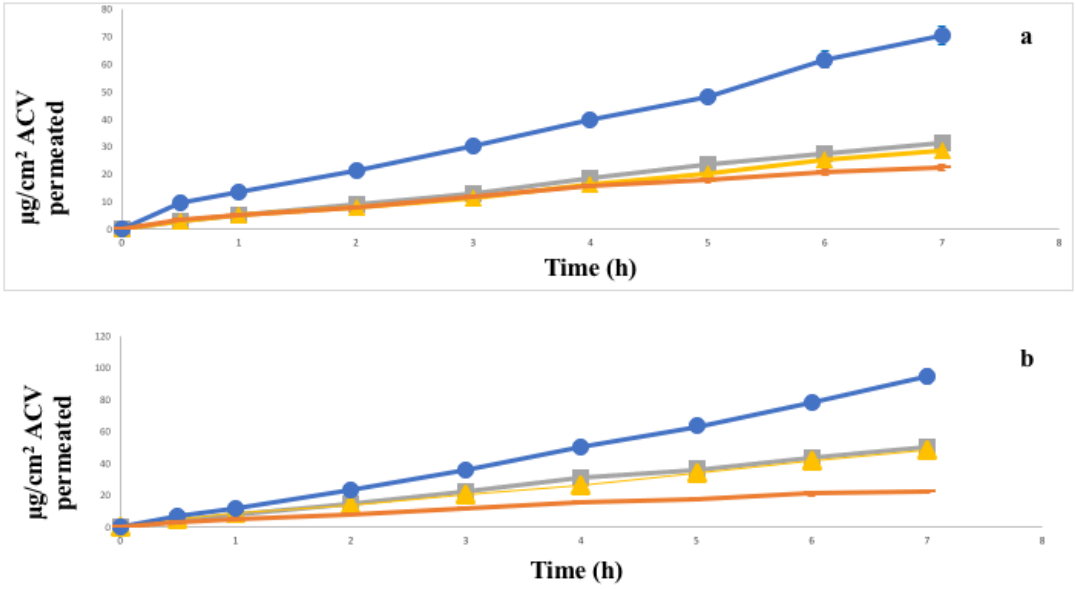

Fig. 5. Amount of ACV permeated from different samples through rabbit ear skin at 37 °C: LLC_1 (■); LLC_2 (▲); LLC_3 (●); Zovirax® 5% (−): a) at 0.1% and b) at 1% of drug.

For LLC1 and LLC2 with 0.1% of ACV, no significant difference in the permeation rate was observed when compared to the Zovirax® 5%. Nevertheless, the new realized systems provided a permeation similar to the commercial specialty despite containing an amount of ACV 50 times lower. On the other hand, the ACV permeation from LLC_3 was significantly higher than Zovirax® 5%. In fact, the permeated amount was already equal to 9.58 µg/cm^2 against 3.46 µg/cm^2 of the Zovirax®5% in the first half hour. Unlike the samples with 0.1% of ACV, the LLC with 1% showed a release profile significantly higher than the commercial cream (Fig. 5). The amount of ACV permeated after 7 h was 50.38, 48.9 and 94.53 µg/cm2 respectively from LLC_1, LLC_2, and LLC_3 against 22 µg/cm^2 permeated with the specialty Zovirax® 5%. This suggests that lyomesophases can successfully act as ACV permeation enhancer. It is worthy to observe the correlation between the width of the NMR signal and the permeation data. ACV loaded in the LLC_1 not change the initial microstructure, ACV concentration effect determined only a linewidth decrease that suggest a lower order of the system. Despite ^{2}H-NMR spectrum of LLC_2 and LLC_3 at 35 °C show lineshapes typical of cubic phases, they had completely different skin permeation profiles. The difference in permeation profiles may be related to two different cubic structures. That was confirmed by the different LW of NMR signal of the samples, as reported in the top of Fig. 2. While the LW of LLC_2 empty was 139.46 Hz, the LW of LLC_3 was much lower, equal 69.27 Hz. In fact, LLC_3 visually appeared more fluid than the LLC_2 sample at 35 °C. Such different fluidity of the system could explain the remarkable greater

permeation that was observed with LLC_3 mesophases. As reported in literature, it has widely been demonstrated the existence of an inverse correlation between the viscosity of a semisolid formulation and skin permeation. Generally, permeation decreases with the increase of viscosity [36]. The structural disorder of the lyophases and the ACV concentration promotes always the permeation compared to the control, the interesting observation is that in general the permeation increases with the disorder, the concentration and even more with fluidity of the system. All LLC systems realized provided higher and sustained skin con- centration of drug than Zovirax® 5% and Table 3 compares the ACV deposition for LLC at 0.1% and 1% of ACV. This deposition is probably due to structural similarity of the nanostructured lyophases with the particular arrangement of the skin layers which retard the diffusion of the drug. Greater deposition of drug for samples with 0.1% of ACV was observed for LLC_3 equal to 1.01×10^{-6} moles accumulated in the skin layers. While for the phases realized with 1% of ACV, the greatest depot was given by the LLC_1 equal to 1.4×10^{-6} moles. To confirm the accumulation of the drug in the skin, the permeation of ACV was monitored following removal of the samples from the skin surface for the next 24 h. A prolonged and slow drug release for all samples was detected and after 24 h the formulation released about 25 $\mu g/cm^2$ of drug. This confirmed the depot formation from which the drug is made available in high concentrations for prolonged periods and the possibility to cut down the frequency of administration and these results, then, could be optimal in the case of drug that should act topically, as in the case of ACV.

4. Conclusions

In this study, the effect of Acyclovir incorporation in several kinds of colloid systems on the permeation and skin deposition were evaluated. For this purpose, the surfactant Brij97 was selected due to its bio- compatibility, low toxicity, biodegradability and niosomes, emulsion, micro-emulsion and lyotropic liquid crystals based on it were designed and studied. The new formulations proposed were successfully able to significantly increase the amount of ACV able to cross the SC and lead to the formation of intracutaneous drug reservoir. They could represent, therefore, a valid alternative to the commercial cream. In fact, despite having significantly lower drug concentrations, they guarantee greater drug depot in the target site from which it is made available for pro- longed times.

The studies carried out, also, showed that the different structural organization of the surfactant has a different influence on the promotion of permeation: increasing hydrophobicity (due to the cholesterol) lowers the permeation and increases instead the skin deposition, while the higher amount of Acyclovir

permeated was obtained from liquid crystalline gel with a lower structural order. These results, therefore, suggest that the appropriate use of

References

[1] J.E. Malkin, Herpes 11 (2004) 2A.
[2] M. Jiang, S.A. Qureshi, K.K. Midah, J.P. Skelly, J. Pharm. Pharm. Sci. 1 (1998) 102.
[3] R. Muzzalupo, L. Tavano, F.P. Nicoletta, S. Trombino, R. Cassano, N. Picci, J. Drug Targeting 18 (2010) 404.
[4] G.E. Parry, P. Dunn, V.P. Shah, L.K. Pershing, J. Invest. Dermatol. 98 (1992) 856.
[5] P. Arora, B. Mukherjee, J. Pharm. Sci. 91 (2002) 2076.
[6] D.J. McClements, Soft Matter 8 (2012) 1719.
[7] T.P. Hoar, J.H. Schulman, Nature 152 (1943) 102.
[8] K. Kawakami, T. Yoshikawa, T. Hayashi, Y. Nishihara, K. Masuda, J. Control.Release 81 (2002) 75.
[9] L.B. Lopes, Pharmaceutics 6 (2014) 52.
[10] A. Dogrul, S.A. Arslan, F. Tirnaksiz, J. Microencapsul. 31 (2014) 448.
[11] W.L. Sim, M.Y. Han, D. Huang, J. Agric. Food Chem. 57 (2009) 3409.
[12] M. Azizi, F. Esmaeili, A. Partoazar, S. Ejtemaei Mehr, A. Amani, J. Microencapsul.34 (2017) 195.
[13] H. Mirhosseini, C.P. Tan, N.S.A. Hamid, S. Yusof, B.H. Chern, Food Hydrocoll. 23 (2009) 271.
[14] C. Wang, D. Chen, X. Jiao, Sci. Technol. Adv. Mater. 10 (2009).
[15] B. Mukherjee, B. Patra, B. Layek, A. Mukherjee, Int. J. Nanomed. Nanosurg. 2 (2007) 213.
[16] R. Cortesi, S.C. Ajanji, E. Sivieri, M. Manservigi, G. Fundueanu, E. Menegatti, E. Esposito, J. Microencapsul. 24 (2007) 445.
[17] C. Giannavola, C. Bucolo, A. Maltese, D. Paolino, M.A. Vandelli, G. Puglisi, V.H.L. Lee, M. Fresta, Pharm. Res. 20 (2003) 584.
[18] M. Bencini, E. Ranucci, P. Ferruti, J. Control. Release 126 (2008) 17.
[19] A.S. Zidan, N. Kamal, A. alayoubi, M. Seggel, S. Ibrahim, Z. Rahman, C.N. Cruz, M. Ashraf, J. Pharm. Sci. 106 (2017) 1805.
[20] Z. Wang, Z. Diao, F. Liu, G. Li, J. Colloid Interface Sci. 297 (2006) 813.
[21] A.D. Bangham, M.M. Standish, J.C. Watkins, J. Mol. Biol. 13 (1965) 238.
[22] S.W. Provencher, Comput. Phys. Commun. 27 (1982) 229.
[23] R. Xu, Particuology 6 (2008) 112.
[24] M.R. Kuzma, V. Skarda, M.M. Labes, Chemphyschem 81 (1984) 2925.
[25] A. Manosroi, P. Wongtrakul, J. Manosroi, H. Sakai, F. Sugawara, M. Yuasa, M. Abe, Colloid Surf. B Biointerfaces 30 (2003) 129.
[26] F. Uchegbu, A.T. Florence, Adv. Colloid Interface Sci. 58 (1995) 1.
[27] T. Yoshioka, B. Sternberg, A.T. Florence, Int. J. Pharm. 105 (1994) 1.
[28] G. Kantarci, I. Ozguney, H.Y. Karasulu, S. Arzik, T. Guneri, AAPS Pharm. Sci. Tech. 8 (2007) 75.
[29] M.W. Sulek, A. Bak, Int. J. Mol. Sci. 11 (2010) 189.
[30] D.M. Richards, A.A. Carmine, R.N. Brogden, R.C. Heel, T.M. Speight, G.S. Avery, Drugs 26 (1983) 378.
[32] R. Muzzalupo, L. Tavano, R. Cassano, S. Trombino, T. Ferrarelli, N. Picci, Eur. J. Pharm. Biopharm. 79 (2011) 28.
[34] M. Miyajima, A. Koshika, J. Okada, M. Ikeda, J. Control. Release 61 (1999) 295.

[35] G. Buckton, M. Efentakis, H. Al-Hmoud, Z. Rajan, Inter. J. Pharm. 74 (1991) 169.
[36] N. Dragicevic-Curica, S. Winterb, M. Stuparc, J. Milicc, D. Krajisnikc, B. Gitterd, A. Fahra, Inter. J. Pharm. 373 (2009) 77.

2.2 Innovative topical formulations from diclofenac sodium used as surfadrug: The birth of *Diclosomes*

Lorena Tavano[a], Elisabetta Mazzotta[a], Rita Muzzalupo[a]

[a] Department of Pharmacy, Health and Nutritional Sciences, University of Calabria, Via Savinio, Ed. Polifunzionale, 87036 Arcavacata di Rende, Italy

Pubblished on Colloids and Surfaces B: Biointerfaces , 164 (2018) 177–184.

GRAPHICAL ABSTRACT

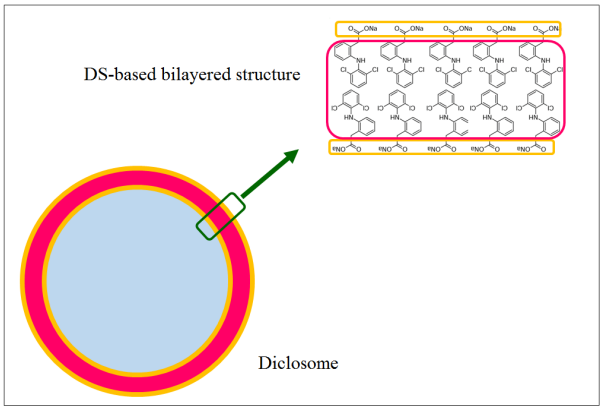

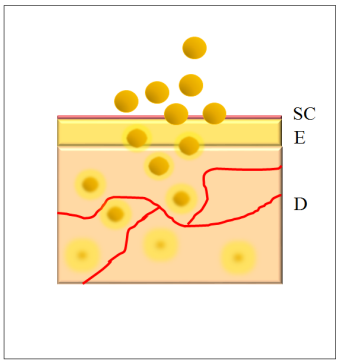

Diclofenac permeation mediated by diclosomes

ABSTRACT

Hypothesis: Due to the well-known surfactant-like properties of diclofenac sodium (DS), vesicular systems consisting exclusively of DS, named diclosomes, were designed with the aim to minimize or avoid the use of other excipients and to improve the formulation biocompatibility.

Experiments: Diclosomes were designed and characterized in terms of dimensions, polydispersity index, Z-potential, drug retained, stability as a function of storage time and *ex-vivo* percutaneous permeation profiles. Additionally, diclosomes were incorporated into gel dosage forms and their performance in terms of permeation enhancement were evaluated.

Findings: DS was found to form nanosized vesicular systems, both alone and in presence of cholesterol. Increasing hydrophobicity (due to the presence of cholesterol) resulted in smaller vesicles, always spherical and homogeneous in shape. Permeation of DS from free solution was found to be lower respect to ones obtained for all diclosomal formulations, allowing these aggregates to be considered as percutaneous permeation enhancers. DS

permeated from diclosomal gels was higher than that obtained with traditional niosomal gel, DS plain gel and commercial specialty Voltaren Emulgel® 1%, while containing a considerably lower drug amount.

1. Introduction

Drug delivery systems (DDS) are a class of nanodevices able to provide enhanced efficacy and to reduce adverse side effects of therapeutics agents [1]. DDS are typically inert and they only transport drugs by forming a carrier able to encapsulate hydrophobic or hydrophlilic drugs [2]. Moreover, they have been reported to target these compounds at desired site, with definite rate and timing. Unfortunately, despite the variety of nanocarriers developed to treat diseases (i.e. nanoparticles, liposomes, polymers and proteins), success is limited to just a few formulations [3]. The most important drawback of these nanocarriers is their low drug loading capacity [4,5]. To overcome this limitation, the direct use of drug molecules as components of nanocarriers has been recently proposed by several researchers, with the aim to substantially increase the drug loading content, to minimize the use of inactive materials, and suppress drug premature burst release [6].

Many pharmacologically active compounds are amphiphilic molecules, which tend to self-associate and to interact with bio- logical membranes likewise classical surfactants, whereby they have been defined as surfadrug (blend of surface active drug) [7]. Using an amphiphilic drug in the design of DDS would minimize or avoid the use of other excipients, improving the formulation safety and thus facilitate their clinical translation [8,9]. Thus, DDS made of sulfadrugs could represent a great innovation in the pharmaceutical field, because of their dual function: one related to the pharmacological nature of the molecule and the other related to the technological properties of the obtained carriers [10]. Additionally, these nanodevices may also serve as carriers of other drugs, to achieve combination therapy [10].

Classes of amphiphilic drugs including analgesics, tranquilizers, antibiotics, local anesthetics, non-steroidal antiinflammatory and chemotherapics have been extensively reviewed [8]. The structural features of amphiphilic drug molecules influence their association pattern in aqueous solution and consequently their interaction with biological membranes. Generally, sulfadrugs contain one or more flexible and hydrophobic aromatic nuclei, to which an ester group or a charge-bearing N atom is directly attached or which include a pyridine-like N atom [11]. The flexibility of the aromatic ring leads to these drugs may resemble typical surfactants in their association behaviour. In aqueous medium, surfadrugs can exist as monomers or can aggregate into micelles, bilayers and mesophases, depending on the

concentration, hydrophilic-hydrophobic balance and, obviously, method of preparation [11]. Additionally, the different structures can be interconverted as a function of pH, temperature, ionic strength and surfadrug concentration [12,13].

Since macromolecular aggregates obtained from surfadrugs have been reported to act as effective drug delivery systems [14], we decided to test the aggregation properties of a widely used amphihilic drug, the diclofenac sodium. The vehiculation of DS has been studied in depth by the scientific community and also our research group contributed to increase knowledge in this field, investigating the effect of its compartimentalization and vehiculation into different macromolecular drug delivery systems [15–17]. Considering the well-known surfactant-like properties of diclofenac sodium, we hypotized that its direct use to form diclosomes (blend of diclofenac sodium-based niosomes), could avoid the use of other excipients in the preparation of DDS and increase the amount of loaded drug. In this context, pure diclosomes were compared with diclosomes contained different mole ratio of drug and cholesterol in terms of dimensions, polydispersity index, Z-potential, retained DS and *ex-vivo* percutaneous permeation profiles. Additionally, to make diclosomes more exploitable for a direct application onto the skin, we incorporated vesicles into a gel dosage form and we evaluated its performance in terms of permeation enhancement, comparing with commercial specialty (Voltaren Emulgel® 1%).

2. Materials and methods

2.1. Chemicals

Diclofenac sodium (DS), cholesterol (Ch), Span 60 and carboxymethyl cellulose were purchased from Fluka (Sigma-Aldrich, Milan, Italy, 98% purity). All organic solvents were supplied from Sigma-Aldrich (Milan, Italy) and are of high performance liquid chromatography grade. Pharmaceutical specialty Voltaren Emulgel® 1% (Novartis FarmaSpA, Italy) was obtained commercially.

2.2. Preparation of vesicular systems and gels

Diclosomes were prepared by the hydration of lipidic film method. Accurately weighed amounts of DS and Ch were dissolved in ethanol in a round-bottom flask. After mixing, solvent was evaporated under reduced pressure and constant rotation to form a thin lipid film. This film was then hydrated with 10 mL of dis- tilled water at 60 ◦C for 30 min, to obtain multilamellar vesicles (MLV). After preparation, the dispersions were left to equilibrate at 25 ◦C overnight. Small unilamellar vesicles were obtained from MLV by sonication in an ultrasonic bath for 30 min at 60 ◦C. The purification

of diclosomes from untrapped materials was carried out by exhaustive dialysis for 4 h (details are reported in Section 2.3.3), using Visking tubing (Spectra/Por®, cut-off 12–14 kDa), manipulated before use in according to Fenton's method [18]. After purification, diclosomes were immediately used in subsequent experiments.

Formulation	Composition	DS (mg)±5	Ch (mg)±5	DS Concentration (M)
DS	DS:Ch/100:0	32.10	-	1.00×10^{-2}
DSCh/82	DS:Ch/80:20	24.40	9.03	7.76×10^{-3}
DSCh/55	DS:Ch/50:50	15.90	19.30	5.09×10^{-3}

Table 1. Composition of diclosomes at 25 ◦C. All formulations were prepared at 1×10^{-2} M of total lipid concentration. Values represent mean ± SD (n = 3).

Additionally, to make diclosomes more exploitable for a direct application onto the skin, we incorporated vesicles into gel dosage forms. Diclosomal gel and diclosomal gel 55 were prepared incorporating diclosomes obtaining from DS alone and DS/cholesterol in ratio 50:50 into the gel matrices, respectively. In DS plain gel, DS was incorporated directly into the gel, while DS niosomal gel were prepared incorporating Span 60-niosomes into the polymeric matrix. Details on the preparation procedures were reported below.

Diclosomal gels formulations were prepared adding 5 mL of diclosomal solutions to 0.150 g of carboxymethyl cellulose and magnetically stirring up to 3 h, to get homogeneous opalescent gels. DS plain gel formulation was prepared according to the same procedure, dissolving DS in 5 mL of distilled water and adding this solution to 0.150 g of carboxymethyl cellulose. This formulation was realized with a DS content of 1% w/w, to compare with the commercial specialty Voltaren Emulgel® 1%.

DS niosomal gel was prepared as follow. Firstly, traditional niosomes were prepared dissolving 43 mg of Span 60 in ethanol, evaporating the solvent to obtain a thin lipid film and then hydrating with 10 mL of DC aqueous solution (1.25 10−3 M corresponding to 3.94 mg of DS). A certain amount of niosomal suspension was lyophilized and 0.71 g of this powder (containing about 50 mg of DS) were added to 5 mL of distilled water, to obtain a DS content of 1% w/w. Afterwards, DS niosomal gel was obtained by adding this suspension to 0.150 g of carboxymethyl cellulose and proceeding as above reported.

2.3. Characterization of niosomes

2.3.1. Size distribution and Z-potential analysis

Vesicles diameter and size distribution were determined by dynamic light scattering (DLS), using a 90 Plus Particle Size Analyzer (Brookhaven Instruments Corporation, New York, USA) at 25.0 ± 0.1 ◦C. The autocorrelation function was measured at 90◦, while the laser beam was operating at 658 nm. The polydispersity index (P.I.) was used as a measure of the size distribution. It was directly obtained from the instrumental data fitting procedures by the inverse "Laplace transformation" and by Con- tin methods [19]. P.I. values 0.3 indicate homogenous and monodisperse populations in the case of colloidal systems. The Z-potential of the formulations was measured with the laser Doppler electrophoretic mobility measurements using the Zeta-sizer ZS (Malvern Instruments Ltd., Malvern, U.K.), at 25.0 ± 0.1 ◦C.

Z-potential values were calculated by the instrument software, using Helmholtz–Smoluchosky equation. All analyses were done in triplicate and expressed as mean ± standard deviation.

2.3.2. Morphology

The morphology of diclosomes was examined by Transmission Electron Microscopy (TEM) and the images were obtained with a TEM Jeol 1400 Plus electron microscope, operating at an acceleration voltage of 80 kV. A droplet of the vesicles suspension was placed on a Formvar/Carbon coated copper grid, forming a thin liquid film. Water in excess was removed by a piece of filter paper, followed by air-drying.

2.3.3. Evaluation of DS content into vesicles

The amount of DS retained in the vesicles was determined by exhaustive dialysis. 3 mL of diclosomes dispersion were dropped into a dialysis bag, immersed in 100 mL of distilled water and magnetically stirred. Samples were dialyzed for 60 min each time until no drug was detectable by UV–vis spectrometry. The percentage of DS retained into the vesicles (E%) was expressed as the percentage of the drug retained in the purified sample, referred to the total amount of drug present in the non-purified one. E% was determined by diluting 1 mL of purified and 1 mL of non-purified diclosomes in 25 mL of ethanol, followed by the measurement of maximum absorbance of these solutions at 276 nm, corresponding to the DS wavelength. Ethanol allows the breaking of vesicular membranes and the solubilizing of DS. Absorption spectra were recorded with a UV Vis JASCO V-530 spectrometer using 1 cm quartz cells. Each experiment was carried out in triplicate and the results are expressed as mean ± standard deviation.

2.3.4.Stability studies

The stability of diclosomes both in suspensions and in gels was evaluated by storing the formulation at 4 ◦C and 25 ◦C in the dark for a month, monitoring size, PI, Z-potential and retained DS percentages every 14 days. In the case of diclosomes incorporated in the hydrogels, 0.2 g of the diclosomal gel were diluted (1:10 w/w) with distilled water and mixed until a clear dispersion was obtained. After, the measurements were carried out as usual. Each analysis was carried out in triplicate and the results are expressed as mean ± standard deviation.

2.4. *Ex-vivo* DS permeation study

The experiments were carried out in the vertical Franz diffusion cells for 24 h at 37 ◦C, using rabbit ear skin obtained from a local slaughterhouse, as reported elsewhere [15]. The skin, previously frozen at 18 ◦C, was pre-equilibrated in physiological solution at room temperature for 2 h before the experiments. A circular piece of this skin was sandwiched securely between the receptor and donor compartments with the epidermal side in contact with the receiver medium. The donor compartment was charged with an appropriate volume of sample (so as to keep DS moles constant), covered with Parafilm® to prevent water loss and mantained in the dark, while the receptor compartment was filled with 5.5 mL of distilled water. At regular intervals up to 24 h, the medium was removed and replaced with an equal volume of prethermostated (37± 0.5 ◦C) fresh distilled water. The complete substitution of the medium was needed to ensure sink conditions and quantitative determination of the small amounts of drug permeated. The release of free diclofenac sodium was investigated by the same procedure and used as control. The content of drug in the samples was analyzed by UV–vis spectrophotometry. Each experiment was carried out in triplicate and the results are expressed as mean standard deviation.

2.5. Skin DS retention studies

For skin DS retention study, the pieces of skin were removed from the diffusion cell after 24 h, cleaned with physiological solution and then gently dried by pressing between two tissue papers. Skin was homogenized in 10 mL of distilled water for 2 h and after, extraction solutions were filtered. DS amounts were determined by UV–vis spectrophotometry. Each experiment was carried out in triplicate and the results are expressed as mean standard deviation.

2.6. Statistical analysis

Statistical analysis was performed using a Student's t-test. p values of 0.05 were considered statistically significant. Each experiment was carried out in triplicate and the results are expressed as mean ± standard deviation.

3. Results and discussion

2-[(2,6-Dichlorophenyl)amino] benzene-acetic acid sodium salt (DS) is a non-steroidal anti-inflammatory drug (NSAID) for pain control and treatment of rheumatic diseases. It is available in a number of administration forms which can be given orally, rectally, topically or intramuscularly [20].

DS undergoes an intramolecular cyclization under the acidic conditions found in gastric juices, which can cause its inactivation, so it is recommended to take it after meals. The drug has a relatively short elimination half-life (1.5 h), which limits the potential for drug accumulation and requires frequent administrations [21]. DS is not effectively absorbed after transdermal application, also because its photosensitivity, and its most frequent adverse effects were gastrointestinal [22,23].

Structurally, DS possesses two benzene rings and a carboxyl group and it is expected to aggregate in the aqueous solution when its concentration is large enough, due its surfactant-like structure. In contrast to what happens for other diclofenac salts, several researchers demonstrated that, despite DS is surface active, it is not capable of forming micelles, probably due to the effect of the counterion [24–26].

Since no information on the possibility to obtain vesicular systems exclusively from DS is currently available, diclosomes starting from 1:0 up to 1:1 of mixtures of DS and cholesterol were designed. These ratios have been set because cholesterol content is thus usually included in a 1:1 molar ratio in most formulations [27]. Details on vesicles compositions are reported in Table 1.

Despite the absence of CMC [28], this surfadrug was found to form vesicular systems both alone and in presence of cholesterol, at 8:2 and 5:5 mol ratios. Probably, this is favored by the preparation technique: by supplying mechanical and thermal energy, the thin layer evaporation method provides the DS film closes on itself, forming a bilayered structure surrounding an aqueous core.

Visually observed, diclosomal vesicles possess an opalescent appearance: the addition of Ch gave rise to milky and cloudy dispersions with increasing turbidity, as shown in Fig. 1.

As can be deduced from Table 2a, the presence of Ch may cause an improvement of diclosomes bilayer rigidity and cohesion, result- ing in a strong decrease of vesicles diameter.

Cholesterol is known to abolish the gel to liquid phase transition of vesicular systems and to influence the membrane permeability and encapsulation efficiency, resulting in niosomes that are less leaky [29]. In our case, increasing amounts of Ch may progressively convert the surfadrug gel phases to a liquid ordered states, whose properties are intermediate between those of the solid and of the liquid-disordered fluid bilayers.

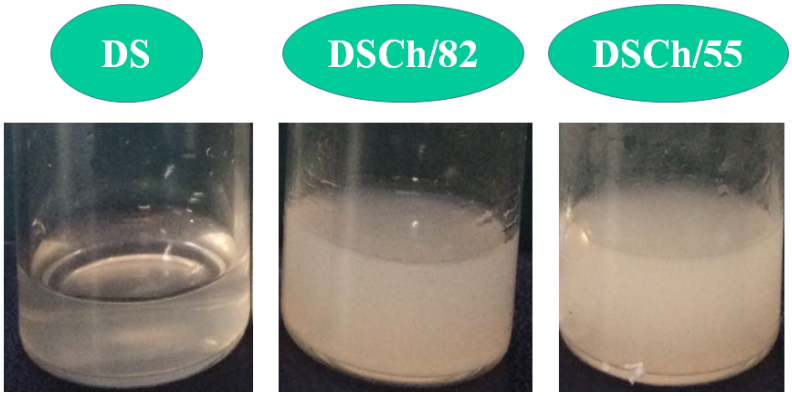

Fig. 1. Visual appearance of diclosomes

P.I. ranged from 0.190 to 0.250, and one narrow distribution was obtained for almost all formulations, indicating that the vesicles population is relatively homogeneous in size.

Z-Potential values were between −22.4 mV and −25.8 mV at 25 ◦C, indicating that there is a certain electrostatic repulsive force between the vesicles, giving appreciable stability. Thus, in the case of diclosomes, Z-potential could depend both on the contribution given by DS and Ch structured into the bilayer [30].

The morphological features of the diclosomes were evaluated by Transmission Electron Microscopy. TEM images showed that all the vesicular suspensions were spherical, homogenous in size and shape (Fig. 2), with regular and well-defined edges. The presence of Ch did not affect the vesicles morphology. These data are well correlated with DLS measurements.

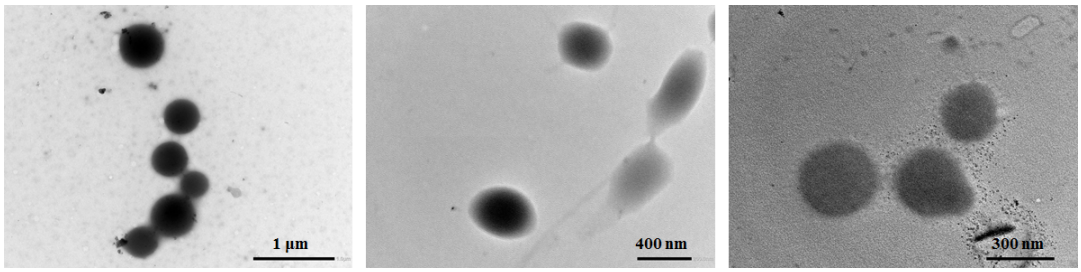

Figure 3. Typical TEM photomicrograph for A) DS; B) DSCh/82 and C) DSCh/55 samples.

As shown in Table 2, the amount of DS retained in each formulation were about 35%, 33% and 31%, for DS, DSCh/82 and DSCh/55, corresponding to 3.52 x10^{-6}, 2.57 x 10^{-6} and 1.57x 10^{-6} mol/mL, respectively. Obviously, the retained DS into the systems decreases proportionally with the decrement of the DS concentration in the stock solutions and with the increase of Ch content. Probably, this may be due to the competition between both amphiphilic molecules for the formation of the bilayer: the presence of increasing amount of Ch may limit the retention of DS in the lipophilic lamellae.

It is well known that niosomes properties and stability depend on several parameters such as bilayer composition and preparation methods [10,27]. For this reason, a multi experimental setup has been also designed in order to evaluate how small changes in the technical procedures may affect the physical-chemical characteristics of the vesicles.

It has been widely demonstrated that hydration temperature plays a fundamental role in the formation of vesicles, affecting their shape and size [27]. In our study, we fixed the hydration temperature at 60 ◦C and we also verified the possibility to obtain vesicles at 40 ◦C. An increase of vesicles size was detected, while no relevant changes in Z-potential were found (Table 2b). Concerning the amount of DS retained, pure diclosomes showed E% few percent- age points lower than that obtained by preparing the formulation at 60 ◦C. In presence of Ch, an opposite behavior was detected. The properties of the vesicular membranes may be manipulated to improve their performances (i.e. increase drug loading), by altering the composition of the bilayer [31]. Our formulations were prepared both at 10×10^{-3} M and 2.5×10^{-3} M of total lipid concentration at 60 ◦C, and results demonstrated that, as the total lipid level decreases, the amount of DS retained also decreases in a proportional manner, since the higher drug concentration gradient may promote an higher retention of DS into the bilayer. In fact, despite the highest values of E% obtained by the formulations prepared with 2.5 x 10^{-3} M of total lipid concentration, if we calculate the effectively retained DS moles, this trend appears clearer and more immediate (Table 2c). Also in this case, while Z-potential did not change significantly, vesicles diameter increased. Thus, the optimal pure diclosomal formulations in terms of size and E% were those prepared with 1×10^{-2} M of total lipid concentration at 60 ◦C, whereby we decided to use these samples in the subsequent percutaneous permeation experiments.

Formulation	Diameter (nm±SD)	P.I.	Z-potential (mV±SD)	E%	Retained DS mol/mL
2a					
DS	547.0±12	0.250	-25.8±1.9	35.19± 1.3	3.52×10^{-6}
DSCh/82	413.7±11	0.190	-23.1±1.8	33.17±1.21	2.57×10^{-6}
DSCh/55	357.2±14	0.222	-22.4±2.6	30.86±1.45	1.57×10^{-6}
2b					
DS	612.5±18	0.231	-22.4±2.0	27.50±1.6	2.75×10^{-6}
DSCh/82	462.6±14	0.283	-22.6±1.7	37.87±1.0	2.93×10^{-6}
DSCh/55	417.8±15	0.238	-24.7±1.8	43.86±1.3	2.22×10^{-6}
2c					
DS	761.9±15	0.203	-26.5±1.5	40.17±1.2	1.00×10^{-6}
DSCh/82	497.0±14	0.207	-23.9±1.8	46.77±1.7	9.06×10^{-7}
DSCh/55	408.6±11	0.167	-22.5±1.7	56.71±1.4	7.08×10^{-7}

Table 2. Hydrodynamic diameter, P.I., Z-potential and E% of diclosomes at 25 ◦C. All formulations were prepared at 1 x 10^{-2} M of total lipid concentration at 60 ◦C (2a), and 40 ◦C (2b). Hydrodynamic diameter, P.I., Z-potential and E% of diclosomes at 25 ◦C of formulations prepared at 2.5x 10^{-3} M of total lipid concentration at 60 ◦C (2c). Values represent mean ± SD (n = 3).

3.1. Diclosomes stability

One of the principal requirements of vesicular systems to enter the pharmaceutical market is a long-term stability during the storage period, consisting in the maintenance of physical and chemical characteristics until their use by the patient. Generally, the stability of vesicles is determined by monitoring their principal parameters, such as size distribution, Z-potential and encapsulation efficiency, whereby instability processes result in changes in size and drug loss. In this context, the stability of diclosomes was evaluated by storing the samples at 4 ◦C and 25 ◦C for a month, and monitoring the formulation physical-chemical parameters every 14 days. Results were collected in Table 3.

Formulation	T (°C)	Time (days)	Diameter (nm±SD)	P.I.	Z-potential (mV±SD)	E%
DS	**4**	14	678.6±19	0.270	-18.6±1.4	30.42±1.2
		28	693.8±16	0.311	-16.8±1.2	31.56±1.4
	25	14	731.6±22	0.282	-19.3±1.5	34.58±1.7
		28	774.0±35	0.512	-16.5±1.2	32.30±1.3
DSCh/82	**4**	14	472.3±13	0.258	-21.9±1.7	34.52±1.3
		28	461.2±10	0.211	-18.3±1.4	31.84±1.9
	25	14	478.6±15	0.246	-20.3±1.5	34.45±1.4
		28	440.5±11	0.252	-18.4±1.4	34.48±1.5
DSCh/55	**4**	14	436.8±17	0.247	-19.2±1.5	28.63±1.3
		28	389.9±12	0.173	-18.2±0.6	26.75±1.7
	25	14	445.0±14	0.226	-22.0±1.7	28.09±1.7
		28	430.0±15	0.210	-18.7±1.3	27.27±1.6

Table 3. Hydrodynamic diameter, P.I., Z-potential and E% of diclosomes prepared at 1 x 10^{-2} M of total lipid concentration at 60 ◦C (mean ± SD; n = 3), as a function of storage time.

As shown, generally the size of all diclosomal formulation is quite large already after 14 days, respect to the corresponding stock suspensions. The P.I. and E% did not change considerably after storage both at 25 ◦C and 4 ◦C up to 1 month, while Z-potential slightly decreased. It is worthy of note that a considerable variation in size and distribution occurred only with DS sample when stored at 25 ◦C, suggesting that a diclosomes aggregation happened. The same experimental setup was designed also for the formulations prepared at 40 ◦C or at lower lipid concentrations, to evaluate their stability as a function of storage time. Results are shown in Table 4.

Formulation	T (°C)	Time (days)	Diameter (nm±SD)	P.I.	Z-potential (mV±SD)	E%
DS_{40}	**4**	14	943.9±37	0.374	-20.1±1.5	28.56±0.9
		28	981.2±42	0.424	-22.4±1.7	29.98±1.3
	25	14	1088.6±34	0.401	-19.6±1.5	29.90±1.2
		28	1055.2±41	0.330	-17.4±1.3	29.31±1.2
$DSCh/82_{40}$	**4**	14	438.7±13	0.237	-23.5±1.8	38.36±1.6
		28	528.9±14	0.211	-22.2±1.7	40.30±1.3
	25	14	494.9±10	0.251	-23.3±1.8	40.70±1.2
		28	449.2±12	0.245	-22.3±1.7	39.65±1.9
$DSCh/55_{40}$	**4**	14	539.6±13	0.206	-20.3±1.5	44.05±1.4
		28	428.9±16	0.220	-25.6±2.0	46.87±1.3
	25	14	539.1±15	0.239	-21.4±1.6	45.95±1.9
		28	546.1±17	0.289	-19.9±1.5	42.75±1.8
$DS_{1/4}$	4	14	1006.4±21	0.256	-20.4±1.5	39.20±1.2
		28	936.9±18	0.242	-17.2±1.3	41.42±1.4
	25	14	1067.1±19	0.352	-17.7±1.3	42.70±1.3
		28	1089.1±20	0.267	-17.6±2.1	40.43±1.6
$DSCh/82_{1/4}$	4	14	573.3±13	0.231	-22.4±1.7	52.35±1.7
		28	555.0±11	0.164	-18.2±0.7	50.28±1.5
	25	14	436.6±11	0.241	-19.5±1.5	44.33±1.4
		28	592.3±10	0.190	-15.1±1.2	46.08±1.8
$DSCh/55_{1/4}$	4	14	376.9±12	0.209	-20.3±1.5	62.92±1.0
		28	393.1±11	0.228	-15.2±0.3	61.62±1.2
	25	14	402.8±14	0.221	-21.4±1.6	58.66±1.4
		28	378.8±13	0.223	-15.6±1.1	69.80±1.7

Table 4. Hydrodynamic diameter, P.I., Z-potential and E% of diclosomes prepared at 10 x 10^{-3} and 2.5 x 10^{-3} M of total lipid concentration at 60 ◦C (mean ± SD; n = 3), as a function of storage time.

Pure diclosomes size changed in a relevant manner both at 25 ◦C and at 4 ◦C, reaching almost double values compared to the initial ones, meaning that aggregation process occurred. Formulations containing Ch as membrane additive generally showed a modest increase of hydrodynamic diameter, while they generally preserved their physical-chemical parameters, without any significant differences during storage.

Given these results, pure diclosomes prepared at 1×10^{-2} M of total lipid concentration working at 60 ◦C were selected and used in the subsequent experiments.

3.2. Diclosomes stability after incorporation into the gel

The stability studies performed on diclosomal suspensions were also carried out on vesicles after their incorporation into the carboxymethyl cellulose hydrogel. This valuation is the primary tool used to assess preliminarly quality of the formulation in terms of storage time. The incorporation of diclosomes into the gels produced an opalescent and viscous system. Size distribution, Z-potential and E% were monitored from 24 h to 28 days of storage, performing tests every 14 days.

Results demonstrated that a progressive vesicles size increase occurred just after 24 h (average percentage increase of about 5%) with strong variations up to 28 days 24 h (average percentage increase of about 35%), probably due to the coordination between the vesicles and the polymeric chains that contributing to increase the hydrodynamic diameter.

4. *Ex-vivo* DS permeation studies

4.1. Diclosomes

In order to predict the behavior of diclosomes after topical administration, DS, DSCh/82 and DSCh/55 formulations were tested by using excised rabbit ear skin mounted in the Franz cell diffusion system. The permeation experiments were carried out under sink conditions, maintaining the apparatus at 37 ◦C. The accumulative permeation percentages versus time of all samples are shown in Fig. 3a and compared with DS solution.

As illustrated, almost 17% of the drug permeated within 24 h from DSCh/55: this value slightly decreased to 13.6% and 13.0% for DSCh/82 and DS, respectively. Anyhow, permeation percent- ages achieved by diclosomal formulation were always higher than that achieved by drug solution (9.7%). This suggests that diclofenac sodium can successfully act as surfadrug and it could be considered as percutaneous permeation enhancer, specially, when it is in the form of vesicular aggregates. Despite the efficacy of DS loaded niosomes in enhancing *ex-vivo* percutaneous penetration was well demonstrated, our project represents the first study demonstrating the effective promotion effect of bilayered structures made exclusively of DS, respect to classical vesicles obtained from traditional surfactants or phospholipids.

However, the DS permeation profiles obtained by diclosomes were biphasic. An initial fast permeation of the drug was observed up to 7 h, which could be due to some molecules of DS adsorbed on the vesicles surfaces or

beginning to leak out from the systems, because the fusion with the skin. After, a steady state was achieved until a plateau was reached.
As illustrated, the flux of DS across the skin clearly varies depending on the nature of the formulations: the higher Ch content, the higher the permeation. These results can be explained considering the physical-chemical similarity existing between diclosomes and stratum corneum (sc). The lipid composition of the sc is dominated for about 90% by ceramides, cholesterol and free fatty acids, whereby it is extremely lipophilic and able to ostacolate the passage to hydrophilic molecules [32]. In particular, Ch affects membrane permeability and trafficking, regulating its stability, fluidity and phase behavior [30]. For these reasons, Ch and its esters have been widely used also as penetration enhancers for transdermal delivery [33]. DSCh/82 and DSCh/55 samples contained increasing amount of Ch in the bilayer, contributing to the system lipophilicity. As reported in literature, hydrophilic-hydrophobic balance value of the carrier was one of the principal factors in determining the percutaneous penetration of a drug: generally, penetration increase gradually with the carrier lipophilicity, probably because of better interactions with the skin layers [34].
The effect of amphiphilic molecules in altering the skin barrier depends on their own structure [35]. Anionic surfactants have been reported to interact strongly with both keratin and lipids, dis- ordering the lipid layer of skin and making the membrane more permeable [36]. Due to the amphiphilic nature of DS, we may hypothesize that it behaves the same way of a classical anionic surfactant. Moreover, in the case of ionizable drugs, the chemical form of the most suitable candidate for permeation is the un-ionized one, since it has a lower polarity and high logP, providing higher affinity for the sc [37].
Diclofenac sodium is the sodium salt of the 2-(2,6- dichloranilino) phenylacetic acid, possessing a pka of 4.15 and a logP of 13.4 and about 1.0 for the un-ionized and ionized forms, respectively [38,39]. LogP estimates the partition coefficient of the drug between a hydrophobic (n-octanol) and hydrophilic vehicle (aqueous phase): when the drug is in the form of a salt, a dominant hydrophilicity of the drug is expected. In the case of DS, a certain hydrophobicity is retained even in the ionized form, due to the formation of ion pairs [40]. In fact, ion pairs formation may confer sufficient lipophilicity to ensure a flux across a membrane, as reported elsewhere for diclofenac diethylammonium salt [41]: the same behavior could be kept by sodium salt of diclofenac.
Generally, vesicles are considered as one of the best vesicular system for topical drug administration, as their function varies with type and composition. Their versatility lies in the ability to control the release of the medicinal agent according to the specific needs of the therapy. Vesicular

systems may provide a localized depot of drug within the skin, which ensure prolonged drug release over time, reducing systemic absorption and thus minimizing side effects [42]. Alternatively, vesicles may be designed in order to enhance transdermal drug delivery, to promote skin penetration and to increase systemic drug concentrations, bypassing the disadvantages of other administration routes [43]. Obviously, a more pronunced drug resevoir into the upper layers is preferred when a pharmacological local effect is required.

To perform a more in-depth study we also evaluated the percentages of DS retained into the skin within 24 h: data were reported into Table 5.

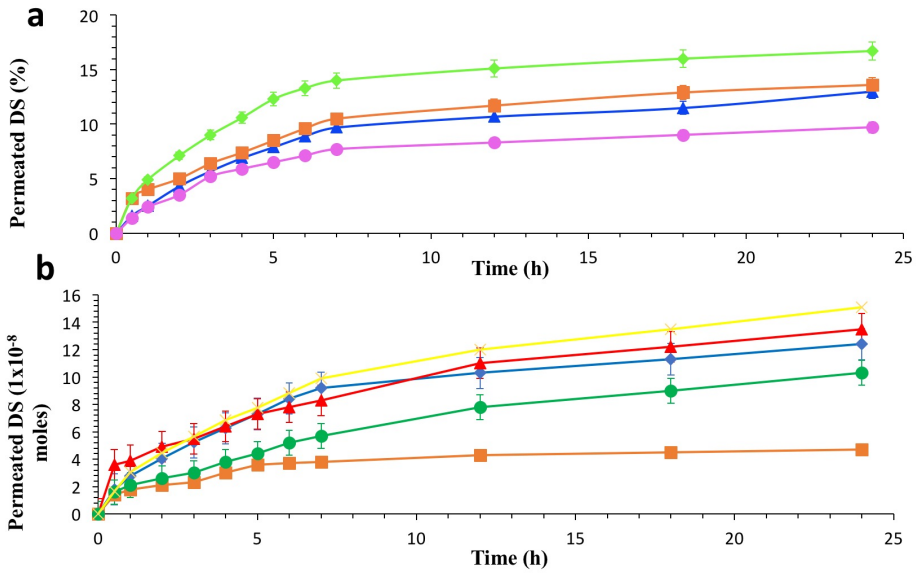

Fig. 3. (a) DS permeation from the different samples through rabbit ear skin at 37 ◦C: (a) (▲) DS; (■) DSCh/82; (♦) DSCh/55;(●) DS solution. (mean ± SD; n = 3).(b) DS permeation from the different samples through rabbit ear skin at 37 ◦C: (♦) diclosomal gel; (×) diclosomal gel 55; (■) DS plain gel 1%; (▲) traditional niosomal gel; (●) Voltaren Emulgel® 1%. (mean ± SD; n = 3).

As already mentioned, vesicular aggregates not only increased the drug permeation, but promoted the accumulation of DS into the sc and upper skin strata, creating a depot from which DS could move slowly. This means that diclosomes may provide a slow and extended DS permeation and they could be very useful when a pharmacological local effect is required.

4.2. Semisolid formulations

Considering these promising results, we decided to validate these findings by designing semisolid formulations for DS topical administration. Incorporation of vesicles into gel is the most common approach for the preparation of effective topical formulation, because the long retention time of the gel onto the skin has been reported to prolong the drug release rate and

reduce the dosing frequency [44]. Ex-vivo performances of diclosomal gels were compared with commercial specialty (Voltaren Emulgel® 1%), DS plain gel and Span 60-niosomal gel. The permeation profiles were illustrated in Fig. 3b.

As expected, the lowest drug permeation was observed for DS plain gel (4.71 10^{-8} mol), followed by commercial specialty (1.03 10^{-7} mol), because Voltaren Emulgel® 1% contains additional excipients acting as percutaneous permeation enhancers. The cumulative DS permeated from diclosomal gels were higher (1.24 10^{-7} and 1.51 10^{-7} mol for DSGel and DSCh/55Gel) than those obtained with the plain gel and commercial specialty, con- firming the drug permeation enhancing effects of vesicular systems across the skin. The amazing result is that, while plain gel and commercial specialty contains 1% of the drug (1.25 10^{-5} mol charged in the donor compartments), our systems provided greater permeations while containing an amount of DS 7.5 times lower (1.00 10^{-6} mol charged in the donor compartments). This finding is even more striking when compared with niosomal gel made of Span 60 (containing DS in the aqueous core). Despite 1.11 × 10^{-5} mol charged in the donor compartment, the amount of drug permeated up to 24 h was 1.35 10^{-7} mol. This means that DS in form of diclosomes may increase the drug accumulation in the sc and could promote its permeation better than when it is compartimentalized in the aqueous core of classical vesicles. Probably, this may be due to the fact that in classical vesicles, DS has firstly to overcome the vesicles bilayer and then the polymeric matrix to reach the skin, causing some slowdown in the permeation rate.

To confirm the hypothesis according to which diclosomal gel promoted the accumulation of DS into the sc creating a depot from which DS can move slowly, DS permeation even after removing the DSCh/55Gel (as significative sample) from the skin was monitored for the next 24 h.

Sample	Permeated DS (moles)	Permeated DS %	Skin DS (moles)	Skin DS %
DS	1.30×10^{-7}	13.00	2.30×10^{-7}	23.00
DSCh/82	1.36×10^{-7}	13.60	1.85×10^{-7}	18.50
DSCh/55	1.67×10^{-7}	16.70	2.53×10^{-7}	25.30
DS solution	9.70×10^{-8}	9.70	-	-

Table 5. Amount of DS (moles and%) permeated and retained in the skin after 24 h of *ex-vivo* permeation study.

A continous flow of DS was detected, reaching 47 μg/cm2 of permeated DS after this time. This means that diclosomal gels may provide a slow and

extended DS permeation and at the same time, they could temporarily accumulate the drug.

5. Conclusion

In summary, innovative topical formulations from diclofenac sodium named diclosomes were developed with or without cholesterol. The use of DS both as amphiphilic carrier constituent and pharmacologically active compound, may offer the possibility to bypass the use of additional excipients and improve the formulation safety. DS was found to form nanosized vesicular systems, both alone and in presence of cholesterol: increasing hydrophobicity (due to the cholesterol) resulted in smaller vesicles, always spherical and homogeneous in shape. Permeation of DS from free solution was found to be lower respect to ones obtained for all diclosomal formulations, that can be considered as percutaneous permeation enhancers. Additionally, to make diclosomes more exploitable for a direct application onto the skin and to improve patient compliance, we incorporated vesicles into a gel dosage form and we evaluated its performance in terms of permeation enhancement. As expected, DS permeated from diclosomal gels was higher than that obtained with traditional niosomal gel, DS plain gel and commercial specialty, while containing a considerably lower drug amount.
Therefore, diclosomes may represent the best option to increase the drug accumulation in the SC and promote its permeation across the skin, allowing us to propose the derived diclosomal gels as useful multi-component topical formulations.
These early results are a promising first step for the development of pharmacological devices in which DS could play the role of both carrier and drug, bypassing the use of additional excipients and increasing the system biocompatibility, for a more specific and efficient therapy.

References

[1] B. Mukherjee, Curr. Pharm. Biotechnol. 14 (2013) 1221.
[2] R. Savi´ c, A. Eisenberg, D. Maysinger, J. Drug Target. 14 (2006) 343.
[3] V.J. Venditto, F.C. Szoka Jr., Adv. Drug Deliv. Rev. 65 (2013) 80.
[4] R. Tong, J. Cheng, J. Angew. Chem. Int. Ed. Engl. 47 (2008) 4830.
[5] E.S. Lee, K. Na, Y.H. Bae, J. Control. Release 103 (2005) 405.
[6] Y. Shen, E. Jin, B. Zhang, C.J. Murphy, M. Sui, J. Zhao, J. Wang, J. Tang, M. Fan, E. Van Kirk, W.J. Murdoch, J. Am. Chem. Soc. 132 (2010) 4259.
[7] S. Schreier, S.V. Malheiros, E. de Paula, Biochim. Biophys. Acta 1508 (2000) 210.
[8] S. Hu, E. Lee, C. Wang, J. Wang, Z. Zhou, Y. Li, X. Li, J. Tang, D.H. Lee, X. Liua, Y. Shen, J. Control. Release 220 (2015) 175.
[9] M.S. Alam, D. Samanta, A.B. Mandal, Colloids Surf. B 92 (2012) 203.
[10] L. Tavano, A. Pinazoc, M. Abo-Riyad, M.R. Infantec, M.A. Manresae, R. Muzzalupo, L. Pérez, Colloids Surf. B 120 (2014) 160.
[11] D. Attwood, Adv. Colloid Interface Sci 55 (1995) 271.

[12] D. Attwood, V. Mosquera, J.L. Lopez-Fontan, M. Garcia, F. Sarmiento, J. Colloid Interface Sci. 184 (1996) 658.
[13] F. Gaboriau, M. Ch¨eron, L. Leroy, J. Bolard, Biophys. Chem. 66 (1997) 1.
[14] L. Tavano, F.P. Nicoletta, N. Picci, R. Muzzalupo, Colloids Surf. B 139 (2016) 132.
[15] L. Tavano, B. De Cindio, N. Picci, G. Ioele, R. Muzzalupo, Biomed. Microdevices 16 (2014) 851.
[16] R. Muzzalupo, L. Tavano, F.P. Nicoletta, S. Trombino, R. Cassano, N. Picci, J. Drug Target. 18 (2010) 404.
[17] E.F. Antunes, L. Gentile, C.O. Rossi, L. Tavano, G.A. Ranieri, Colloids Surf. B 87 (2011) 42.
[18] R.R. Fenton, W.J. Easdable, H. Meng, E.S.M. Omara, M.J. Mckeage, P.J. Russel, T.W. Hambley, J. Med. Chem. 40 (1997) 1090.
[19] S.W. Provencher, Comput. Phys. Commun. 27 (1982) 229.
[20] R.N. Brogden, R.C. Heel, G.E. Pakes, T.M. Speight, G.S. Avery, Drugs 20 (1980) 24.
[21] S.C. Sweetman, W. Martindale, Martindale: The Complete Drug Reference, 37th ed., Pharmaceutical Press, London (UK), 2011.
[22] G. Ioele, L. Tavano, M. De Luca, G. Ragno, N. Picci, R. Muzzalupo, Int. J. Pharm. 494 (2015) 490.
[23] R. Menassé, P.R. Hedwall, J. Kraetz, C. Pericin, L. Riesterer, A. Sallmann, R. Ziel, R. Jaques, Scand. J. Rheumatol. (Suppl. 22) (1978) 5.
[24] M.T. Ledwidge, O.I. Corrigan, Int. J. Pharm. 174 (1998) 187.
[25] E. Khalil, S. Najjar, A. Sallam, Drug Dev. Ind. Pharm. 26 (2000) 375.
[26] D. Attwood, A.T. Florence, Surfactant Systems: Their Chemistry, Pharmacy and Biology, Chapman & Hall, London (U.K.), 1983.
[27] I.F. Uchegbu, S.P. Vyas, Int. J. Pharm. 12 (1998) 33.
[28] K.M. O'Connor, O.I. Corrigan, Int. J. Pharm. 222 (2001) 281.
[29] B. Nasseri, Int. J. Pharm. 300 (2005) 95.
[30] D.Z. Liu, W.Y. Chen, L.M. Tasi, S.P. Yang, Colloids Surf. A Physicochem. Eng. Asp. 17 (2000) 57.
[31] G.P. Kumar, P. Rajeshwarrao, Acta Pharm. Sin. 1 (2011) 208.
[32] J.A. Bouwstra, P.L. Honeywell-Nguyen, G.S. Gooris, M. Pone, Progr. Lipid Res. 42 (2003) 1.
[33] I.A. Kravchenko, N.S. Novikova, V.B. Larionov, E.S. Pavlovskaya, Pharm. Chem. J. 43 (2009) 13.
[34] L. Tavano, P. Alfano, R. Muzzalupo, B. de Cindio, Colloids Surf. B 87 (2011) 333.
[35] K.A. Walters, W. Bialik, K.R. Brain, Int. J. Cosmet. Sci. 15 (1993) 260.
[36] I. Som, K. Bhatia, M. Yasir, J. Pharm. Bioallied Sci. 4 (2012) 2.
[37] J. Swarbrick, Surfactants in Pharmaceutical Products and Systems, Encyclopedia of Pharmaceutical Technology, 3rd ed., Informa Healthcare, New York, 2006.
[38] A. Fini, G. Bassini, A. Monastero, C. Cavallari, Pharmaceutics 4 (2012) 413.
[39] J.A. Cordero, L. Alarcon, E. Escribano, R. Obach, J. Domènech, J. Pharm. Sci. 86
[40] M.E. Palomo, M.P. Ballesteros, P. Frutos, J. Pharm. Biomed. Anal. 21 (1999) 83.
[41] A. Fini, G. Fazio, M. Gonzalez-Rodriguez, C. Cavallari, N. Passerini, L. Rodriguez, Int. J. Pharm. 187 (1999) 163.
[42] P. Arora, B. Mukherjee, J. Pharm. Sci. 91 (2002) 2076–2089.

[43] G.M. El Maghraby, A.C. Williams, B.W. Barry, Can drug-bearing liposomes penetrate intact skin? J. Pharm. Pharmacol. 58 (2006) 415.
[44] L. Tavano, Liposomal gels in enhancing skin delivery of drugs, in: N. Dragicevic, H.I. Maibach (Eds.), Percutaneous Penetration Enhancers Chemical Methods in Penetration Enhancement: Drug Manipulation Strategies and Vehicle Effects, Springer-Verlag, Berlin, 2015.

3

NANOCARRIERS FOR CANCER THERAPY

This section reviews the nanodevices for tumor target therapy developed during my PhD research, including a first part in which I reported two our reviews on the recent applications of nanotechnology approaches in cancer therapy.

3.1 Thermo-Sensitive Vesicles in Controlled Drug Delivery for Chemotherapy (Review)

Elisabetta Mazzotta[a], Lorena Tavano[a], Rita Muzzalupo[a].

[a] Department of Pharmacy, Health and Nutritional Sciences, University of Calabria, Via Savinio, Ed. Polifunzionale, 87036 Arcavacata di Rende, Italy

Published on Pharmaceutics, 2018, 10, 150

ABSTRACT

Thermo-sensitive vesicles are a promising tool for triggering the release of drugs to solid tumours when used in combination with mild hyperthermia. Responsivity to temperature makes them intelligent nanodevices able to provide a site-specific chemotherapy. Following a brief introduction concerning hyperthermia and its advantageous combination with vesicular systems, recent investigations on thermo-sensitive vesicles useful for controlled drug delivery in cancer treatment are reported in this review. In particular, the influence of bilayer composition on the *in vitro* and *in vivo* behaviour of thermo-sensitive formulations currently under investigation have been extensively explored.

Keywords: thermo-sensitivity; hyperthermia; liposomes; vesicles; drug delivery; cancer

1. Introduction to Novel Approaches for Chemotherapy

The treatment of cancer with antineoplastic drugs is known as chemotherapy [1]. Generally, chemotherapeutics are administered intravenously and, due to their systemic distribution, the therapeutic effect at the tumour site is achieved only after high dose administration, often causing resistance and severe adverse effects [2,3].

In recent decades, drug delivery systems (DDS) have been designated as the solution to systemic toxicity due to chemotherapy. DDS are versatile systems since they can be designed in order to encapsulate the opportune amount of drug that reaches the tumour site and releases a sufficient amount of chemotherapeutics to produce an effective therapeutic response [4]. Among several macromolecular carriers, vesicular systems such as liposomes and niosomes, have been widely investigated and proposed as the most promising [5]. First, vesicles were only designed to provide site-specific treatment, while the second-generation of such systems also possesses the ability to trigger drug release, assuring higher control of the therapy. Among stimuli-sensitive approaches, temperature-sensitive vesicles (TSV) have been

successfully developed, with the commercial ThermoDox® version currently undergoing phase III clinical trials. After being administered intravenously, ThermoDox® (TSL-Dox) in combination with radiofrequency ablation (RFA) leverages two typical features of tumour biology to deliver higher concentrations of drug directly to the tumour site. First, the rapidly growing tumours have a leaky vasculature and, therefore, are permeable to liposomes, enabling their accumulation within tumours. This mechanism is known as the enhanced permeability and retention (EPR) effect. Second, when the tumour tissue is heated at about 40 ◦C, the thermosensitive carriers rapidly change their structure and the selectively destabilized liposomal membrane releases the drug directly into the tumour and the surrounding vasculature [6]. Therefore, systemic delivery of an anticancer drug loaded into thermo-sensitive vesicles represents a strategy that allows both the local control of release using mild hyperthermia and the subsequent accumulation of the drug by diffusion in the tumour mass, ensuring minimal exposure to the drug in normal tissue [7]. There are several clinical trials with TSL-Dox, all with the formulation ThermoDox® in combination with various heating modalities. In human clinical trials, as heating sources, high-intensity-focused ultrasound (HIFU) in combination with magnetic resonance imaging (MRgHIFU), and for animal clinical trials microwave devices and various light sources, are used [8]. Recent investigations on thermo-sensitive vesicles useful for controlled drug delivery in cancer treatment, focusing on the influence of bilayer composition on the *in vitro* and *in vivo* behaviour of thermo-sensitive formulations, are reported here.

2. Hyperthermia and temperature-sensitive vesicles (TSV)

2.1 Hyperthermia and Cancer: General Remarks

Hyperthermia is defined as the procedure of raising the temperature of the tumour tissue to 40–43 ˚C, and it has been used in the treatment of several diseases, including cancer, showing many therapeutic benefits, as illustrated in Figure 1[9]. The most obvious advantage of hyperthermia is its direct cytotoxicity: it may kill or damage tumour cells, with limited effects on healthy cells. This is due to the disorganized and compact vascular structure of cancer cells, which prevents heat dissipation and, in combination with tumour oxygenation, can induce a cell final necrotic or apoptotic death [10,11]. When cells in the body are exposed to temperatures higher than normal (i.e., 42 ◦C), several changes occur, making them more sensitive to other treatments (such as chemotherapy and radiotherapy), due to synergistic action resulting in an enhanced cytotoxic effect [12]. Accordingly, hyperthermia is mainly used as an adjuvant therapy [13]. Additionally, hyperthermia treatment is claimed to

improve tumour blood flow and vascular permeability and to increase vessels pore size. Therefore, an intensified vesicle extravasation nearby the tumour site, improving drug delivery, has been demonstrated [14]. Obviously, killing the cells depends both on the length of treatment and temperature achieved during the therapeutic sessions and it has been reported that thermo-tolerance, consisting in a transient resistance to additional heat stress, occurs when hyperthermia sessions have been given in an interval shorter than 48–72 h [15]. For these reasons, hyperthermia must be carefully controlled and monitored. The higher the temperature and the longer the time that heat is applied to the tumour, the stronger is the lethal effect induced [15].

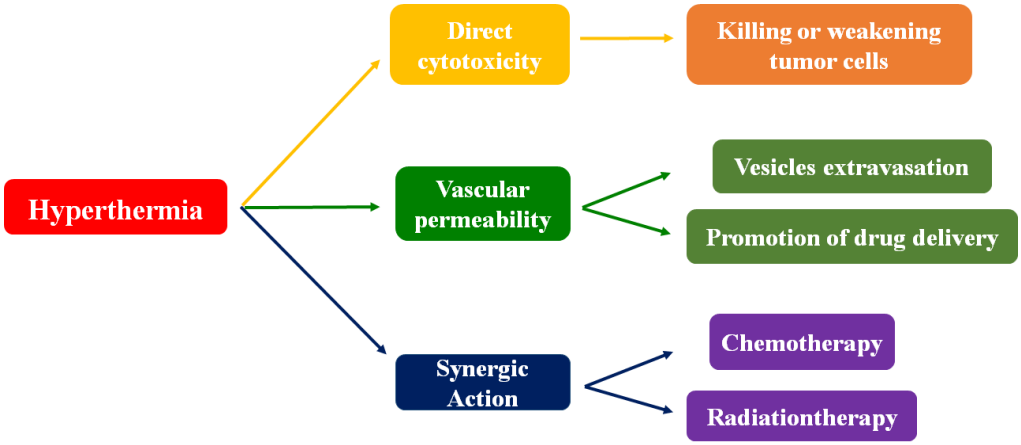

Figure 1. Hyperthermia most important therapeutic benefits.

According to the extension of the treatment area, hyperthermia can be local, regional or whole-body, giving heat delivery to localized, advanced or deep and widespread cancer, respectively [16]. Generally, a number of techniques including ultrasound, microwaves, radiofrequency, ferromagnetic seeds and resistive wire implants have been used to heat the tumour site. Local hyperthermia is used for small tumours located superficially or within an accessible body cavity (i.e., rectum or esophagus), while regional hyperthermia is often destined to treat advanced tumours affecting large parts of the body, organs or limbs or limbs (major and minor pelvis, abdomen or thighs). Widespread cancerous cells may be destroyed or sensitized to drugs by achieving a systemic temperature of 42.0 ◦C in the whole organism: this mechanism is called whole-body hyperthermia and can be administered only after deep analgesia and sedation or general anesthesia [17].

2.2Hyperthermia and Its Combination with Vesicular Systems

Vesicular systems able to release drugs after heating of few degrees above physiological temperature represent an attractive strategy to treat cancer, due to the possibility to control drug release by changing the heating focus and power [18]. The first temperature-sensitive formulation of such systems was designed in 1978 by Yatvin et al. [19], and since then, a lot of smart thermo-sensitive nanodevices have been proposed [20], with the first formulation demonstrating its *in vivo* efficacy in 2000 [7] and entering human clinical trials in 2011 as ThermoDox® [6].

In recent decades, additional and combined approaches to improve the performance of classical thermo-sensitive vesicles have been reported. For instance, a pre-hyperthermia treatment has been proposed to improve tumour vasculature permeability for passive carrier accumulation, followed by a second heat trigger producing interstitial drug release [21]. Additionally, surface modifications for active targeting of the tumour vasculature or tumour cells have been proposed [22].

2.3 Ideal Thermo-Sensitive Vesicles

An ideal thermo-responsive nanodevice should be obtained by materials that are safe and sensitive enough to respond to temperature changes between 39 ◦C and 42 ◦C. Furthermore, the device may be able to sequester a drug until it reaches the tumour site, where hyperthermia can promote carrier extravasation and a localized triggered release, ensuring minimal drug exposure for normal tissue (Figure2) [14].

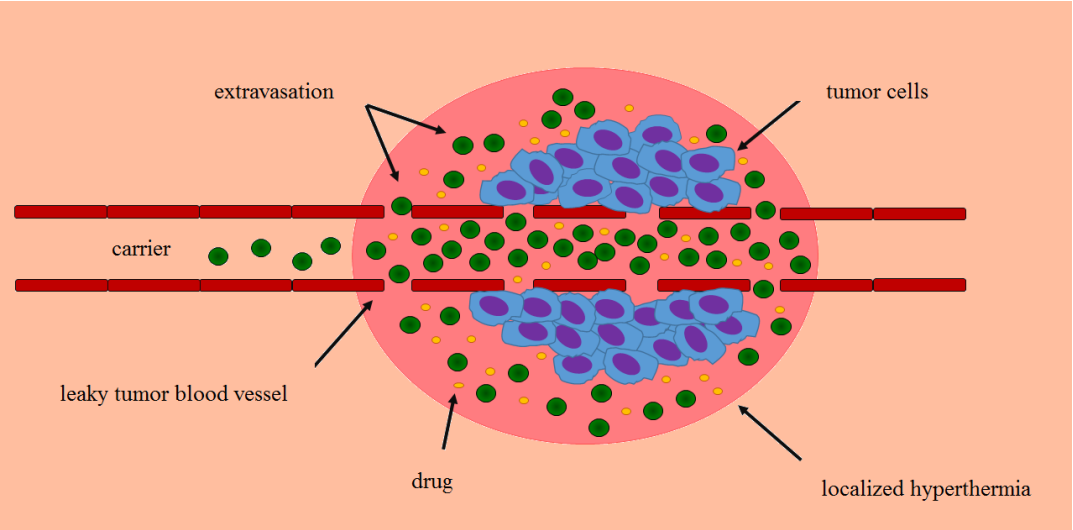

Figure 2. Schematic mechanisms involved in combining hyperthermia and thermo-sensitive devices therapy.

Traditional thermo-sensitive vesicles are composed of lipids or non-ionic surfactants that undergo a gel-to-liquid phase transition slightly above 37 ◦C, whereas more recently, temperature-sensitization of nanosized carriers has been demonstrated with the use of lysolipids and synthetic temperature-sensitive polymers, as illustrated in Figure 3 and extensively explored in the following section [18]. The most important feature of a phospholipidic or non-ionic surfactant membrane is the existence of a temperature-dependent reversible phase transition (T_m), in which the phospholipid or surfactant hydrocarbon chains undergo a transition from an ordered (gel) to a more disordered fluid (liquid crystalline) state. In the gel phase, lipid molecules are ordered and condensed with fully extended hydrocarbon chains, and are constrained to the two-dimensional plane of the membrane. Upon heating, the mobility of the lipid head groups gradually increases. As the temperature is further increased and is close to T_m, the orientation of the C–C single bonds in the hydrocarbon chains begins to switch from a *trans* to a *gauche* configuration.

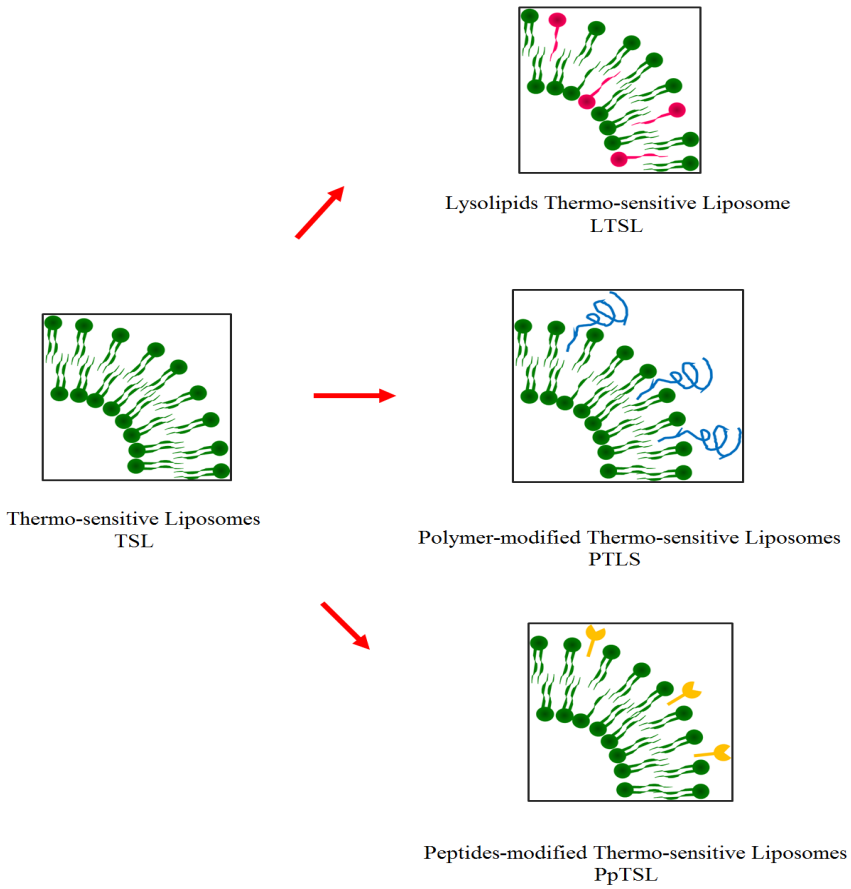

Figure 3. Schematic representation of different thermo-sensitive liposome (TSL) systems: lysolipids thermo-sensitive liposomes (LTSL), peptides thermo-sensitive liposomes (PpTSL), polymer thermo-sensitive liposomes (PTSL).

At temperatures higher than T_m, the bilayer exists in a fully liquid phase. Individual lipid molecules are still confined to the two-dimensional plane of the membrane as in the solid phase, but they are able to move freely and rapidly within the plane, as illustrated in Figure4[23]. Obviously, the physical state of the bilayer affects the permeability, leakage, and overall stability of the liposomes and the T_m is a function of the lipid mixture, whereby it can be altered by changing the bilayer composition [24].

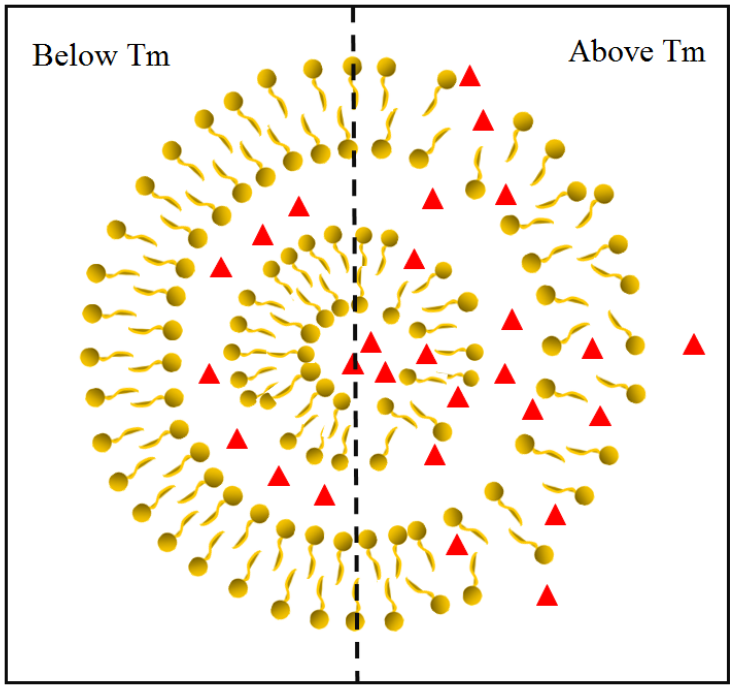

Figure 4. Phase transition behaviour of temperature-sensitive vesicles (TSV). Below *T*m, lipid membranes exist in solid phase and therefore no drug release is expected. When the temperature of lipid membrane passes through *T*m, the bilayer permeability increases, promoting drug release.

3. Recent Advances on Thermo-Sensitive Vesicles for Controlled Drug Delivery

Since the first temperature-sensitive formulation in 1978, several approaches were further developed in order to optimize carrier performances. Below, we report a detailed discussion on the most representative thermo-sensitive vesicular systems, which are classified and commented on according to the strategy for which why they were designed, and focus on the potential of their peculiarities.

3.1 Traditional Thermo-Sensitive Liposomes

To ensure the therapeutic success of TSL, the T_m must be preferably a few degrees above the physiological temperature and in the range of typical temperatures of the mild hyperthermia. 1,2-dypalmitoyl-*sn*-glycero-3-phosphocoline (DPPC) which has a T_m of 41.4 ◦C is used as a major component in most TSL formulations, despite this phospholipid has been reported to limit drug release [19,25].

The first thermo-sensitive liposome (TSL), introduced by Yatvin and collaborators in 1978 was made of DPPC and 1,2-distearoyl-*sn*-glycero-3-phosphocholine (DSPC) in 3:1 molar ratio. The T_m obtained depended on the lipid combination and it ranged between 42.5 and 44.5 ◦C, and in this temperature interval drug release occurred [19].

After the pioneering study of Yatvin [19], a lot of TSL formulations based on mixtures of DPPC and other phospholipids, have been designed and studied, with the objective to improve *in vitro* vesicles stability, to increase the drug release rate [26] and demonstrating that the combination of TSL and hyperthermia is really able to increase the level of several cytotoxic drugs at the tumour site and enhance their therapeutic effect [27,28].

As reported in Table1, the inclusion of other components such as cholesterol (CH) and modified-polyethylene glycol (PEGs) into the lipid bilayer, can prolong the liposome circulation time together with a significant enhancement in their content release upon heating. CH was introduced to optimize vesicle stability in serum [26]. The presence of CH in the bilayer is able to reduce the undesired drug leakage at 37 ◦C, when the temperature is below the T_m [29]. Another issue of TSL obtained by using conventional phospholipids is the rapid elimination by the reticuloendothelial systems (RES), that limits the bioavailability of the vehiculated drug. To overcome this drawback, the design of stealth liposomes by using PEG-lipids has been proposed [30].

Composition	Drug	Ref
DPPC/CH/DSPE-PEG2000)/DSPE-PEG(2000)-Folate	DOX	[31]
DPPC/HSPC/CH/DPPE-PEG2000/DOTA-DSPE	DOX + GD	[32]
DPPC/DSPC/DPPGOGDPPC/P-lyso-PC/DSPE-PEG2000	DOX	[33]
DPPC/P-lyso-PC/DSPE-PEG2000	DOX	[34,35]
DPPC/HSPC/CH/DSPE-PEG2000	DOX	[26]
DPPC/DSPC/DSPE-PEG200055:40:580:15:5	DOX	[36]
DPPC/DSPCDPPC/DSPC/DPPGOG	CF	[37]
DPPC:MSPC:DSPG:DSPE-mPEG200082:8:10:4	Epirubicin	[38]
DPPC:MSPC:DSPE-PEG2000:DSPG83:3:10:4	Paclitaxel	[39]
DPPC:DSPE:PEG2000:EPC:MSPC82:11:4:3:4	Docetaxel	[40]
DPPC:CHO:DSPE-PEG90:5:5	5-Fluorouracil	[41]
DPPC:MPPC:DSPE-PEG200086:5:4	Vinorelbine	[42]
DPPC: DSPE-PEG2000: MSPC75:17:8	DOX + Vincristine	[43]
DPPC:MSPC:DSPE-PEG200085.3:9.7:5.0	DOX + ProHance®	[44]

Table 1. Most used lipids in TSL preparation.

Interesting results have been obtained by Dicheva and collaborators by the introduction for the first time of cationic lipids in the bilayer composition. Indeed, cationic nanocarriers have been reported to deliver selectively anticancer drugs to angiogenic endothelial cells and tumour cells. This strategy provides an important targeting to endothelial and tumour cells compared to non-cationic formulations [45–47].

Other studies have been carried out by preparing TSL with a multifunctional target or loaded with different bioactive molecules. An interesting multi-functional approach was proposed by Pradhan in 2010. The researchers described folate receptor targeted thermo-sensitive magnetic liposomes, and showed that this formulation that integrate active targeting, magnetic field gradient targeting, drug temperature triggered release and pharmacological activity can be used advantageously for thermo-chemotherapy of cancers [31]. Traditional TSL have been also proposed for drug co-encapsulation, as reported by de Smet and collaborators in 2013, combining doxorubicin and gadolinium (GD) in 111In-labeled liposomes. In this study, the authors used high-intensity focused ultrasound (HIFU) to obtain deep and local hyperthermia combined with magnetic resonance imaging (MRI) to allow cancer diagnosis and treatment. The result has shown that HIFU-mediated hyperthermia of the tumour increased more than a 4-fold higher uptake of the radiolabeled TSL while the doxorubicin concentration increased about 8-fold in the tumour [32]. Another study that investigated the simultaneous release of Gemcitabine (Gem) and GD was realized by Affram et al. [48]. In this study the researchers prepared two TSL delivery systems with one encapsulated with Gem, a poor membrane-permeable drug, and another encapsulated only with GD. They demonstrated that this strategy improved the antitumour efficacy of Gem, and increased distribution of Gem and GD in tissues and organs. In addition to bilayer composition, the *in vitro* and *in vivo* drug release rate from TSL is influenced by many factors such as physico-chemical properties of the carriers (i.e., vesicles size), and chemical and biological characteristics of the environment in which they are located after the injection (i.e., the presence of serum and its composition). An in–depth study devoted to the evaluation of the vesicles size influence on drug release after intravenous application was proposed in 2010 by Hossann and collaborators [49] and they concluded that *in vitro* release properties of TSL are dramatically influenced by vesicle size in the range of 50 to 200 nm. With decreasing vesicle size the content release rates is increased due to the membrane curvature increasing, resulting in more packing defects and consequently more membrane permeability. Furthermore, TSL stability at 37 C in serum is also dramatically affected and several studies demonstrated how even the drug release is influenced by the presence of serum. In fact, as reported in literature, the components possess a destabilizing effect on the

bilayer of vesicles, because the interaction of serum components with the membrane bilayer appears to increase the diameter of packing defects or pores, followed by an increase in release rates of hydrophilic compounds [50]. The research group of Hossann in 2012 evaluated the effect of two major serum proteins, albumin (HSA) and immunoglobulin type G (IgG), on the stability and integrity of the following TSL formulations: DPPC/DSPC/DPPG2(DPPG2-TSL), DPPC/DSPC/DPPG2/DSPE-PEG2000 (DPPG2/PEG-TSL), DPPC/P-Lyso-PC/DSPE-PEG2000 (PEG/Lyso-TSL), and DPPC/DSPC/DSPE-PEG2000 (PEG-TSL). In particular, HSA was reported to increase the carboxyfluorescein (CF) release from all formulations around Tm, while IgG was found to affect only anionic TSL. Moreover, the CF release increased around or above the Tm, dependently on the HSA concentration, but below the Tm the protein stabilized the bilayer [51].

Unfortunately, the purported low stability of TSL in blood circulation limited also their capacity to reach the site action in effective doses, because of their reduced plasma half-life. A high stability in serum, associated to the enhanced permeability and retention (EPR) effect, may allow the drug to accumulate at the desired site in concentrations high enough to produce a therapeutic effect. With the aim of improving TSL-mediated drug delivery, the surface of liposomes is often modified with a hydrophilic polymer such as PEG that, as reported before, is able to provide steric protection to the carrier by increasing its surface hydrophilicity and consequently reducing the binding of serum component, preventing opsonisation and limiting its capture by the RES [52]. An exhaustive study on the use of DSPE-PEG_{2000} has been reported by Li and collaborators by incorporating this compound into the bilayer and evaluating the optimal concentration of grafted polymer on the liposomal surface to stabilize the vesicles in serum and to improve the release efficiency under mild hyperthermia. The results suggested that the incorporation of 5% mol DSPE-PEG_{2000} is sufficient to stabilize the lipid membrane in serum at physiological temperature and to enhance the kinetics release at 42 ◦C. Moreover, the authors demonstrated that the use of higher density DSPE-PEG_{2000} may cause the membrane integrity collapse, producing a significant CF release [53].

The main approaches developed to overcome the limited drug release occurring in traditional TSL include the incorporation of thermo-sensitive polymer or lysolipids into the bilayer, or a change in the methodology treatment [18]. Recently, Li and collaborators have proposed a novel two step mild hyperthermia approach to further improve the therapeutic performances of DPPC/DSPC/DSPE-PEG_{2000}-based TSL [36]. The first step of mild hyperthermia (41 ◦C) increases tumour vasculature permeability and maximizes intratumoral liposomal drug accumulation; the second step

promotes the drug release from TSL, with minimal drug redistribution through circulation. This type of heating protocol is known as the interstitial release approach. The authors observed that the liposome accumulation and DOX bioavailability at the tumour site obtained with the two-step approach is increased when compared to the one-step classical treatment, resulting in being particularly beneficial for large and deep-seated tumours [36]. The effect of heating protocol on drug release profile from TSL has been also investigated by Al-Ahmady et al. The research group developed a new type of TSV by inclusion of leucine zipper peptides within a lipid bilayer (Lp-Peptide hybrids) and investigated their activity *in vivo* using two different heating protocols: the first was an interstitial release approach; the second was an intravascular release protocol in which TSL are administered during the heating process, resulting in drug release inside blood vessels when reaching the heated area. Both methods proved to be effective, but the suppression of tumour growth was greater with the intravascular approach. This study, therefore, highlights the importance of the choice of the heating protocol that in turn depends on the physical-chemical characteristics and on the pharmacokinetic profile of the TSV to improve clinical efficacy [54].

3.2 Influence of Lysolipids on Thermo-Sensitive Liposome (TSL) Properties

Lysolipids (LP) are phospholipids in which one or both acyl group derivatives have been removed. Their non-cylindrical structure allows them to be easily incorporated into a lipid membrane and to alter the chemical and physical properties of the bilayer, such as membrane permeability, morphology and stability. The incorporation of a small amount of LP leads to a destabilization and reduction of membrane ability to act as a barrier, due to changes in membrane curvature caused by the particular geometry of lysolipids [55]. Moreover, the presence of a lysolipid in the bilayer has been reported to reduce the phase transition temperature of traditional thermo-sensitive liposomes from 43 ◦C to 39–40 ◦C and, furthermore, their accumulation at the grain boundaries and the formation of stabilized defects may result in an increased drug release rate [56]. The decrease of T_m is necessary and clinical trials recommend mild HT <43 ◦C because higher temperature can cause hemorrhage or damage to the surrounding healthy tissue [6]. The most frequently used lysolipids are shown in Figure 5. The first example of lysolipids-modified TSL was proposed in 1999 by Anyarambhatla and collaborators, incorporating LP in PEGylated TSL, with the aim to decrease the T_m phase transition and to promote a rapid drug release [57]. This first formulation originally comprised DPPC/MSPC/DSPE-PEG2000 in 90:10:4 molar ratio and since then slight bilayer modifications have been proposed, reviewed as well by Landon in

2011 [6]. Typically, traditional TSL were able to release a drug over 30 min, while after the lysolipids inclusion into liposomes bilayer, drug release occurs in a matter of seconds [58].

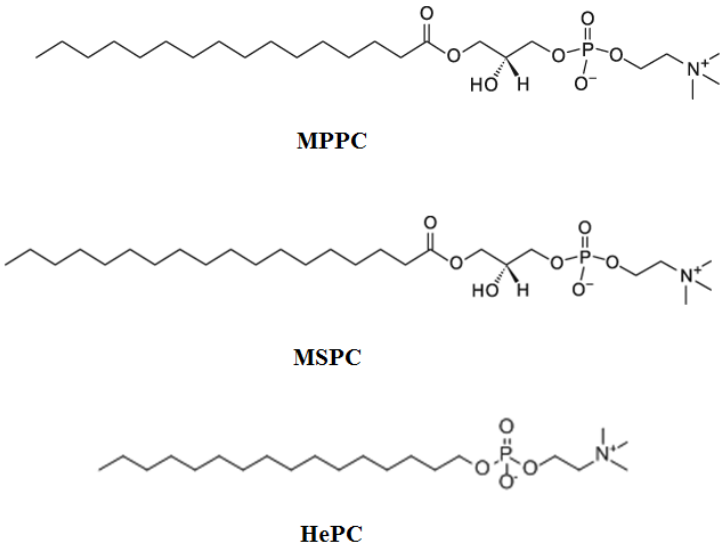

Figure 5. Most frequently used lysolipids.

In 2010, de Smet and collaborators [59] studied the simultaneous release of doxorubicin and gadolinium, a contrast agent for magnetic resonance image (MRI) guidance, co-encapsulating them in two different thermo-sensitive systems: a traditional liposomal sample made of DPPC/HSPC/CH/DPPE-PEG_{2000} and a LTSL system based on DPPC/MPPC/DPPE-PEG_{2000}. Drug release from LTSL formulation was faster than that obtained from the classical TSL formulation at 42 ◦C, as required by an ideal thermo-sensitive system, but unlike TSL, this formulation presented also an unwanted leakage of doxorubicin at 37 ◦C [59]. The presence of lysolipids, in fact, determined a certain vesicle's sensitivity to the serum, due to their ability to make the liposomal bilayer interact with HSA or exchange and incorporate themselves into cellular membranes [60]. This desorption from the bilayer led to a premature drug leakage at physiological temperature, invalidating the clinical success of low thermo-sensitive vesicles. Nevertheless, the co-encapsulation of MRI contrast agent did not influence the loading and release kinetics of DOX and this suggested that their simultaneous release makes possible the *in vivo* monitoring and control of the drug delivery process [60]. Different thermo-sensitive formulations encapsulating carboxyfluorescein (CF) were developed starting from mixtures of DPPC, DSPC, P-Lyso-PC, DSPE-PEG_{2000}, $DPPG_2$ and hexadecylphosphocholine (HePC). Results demonstrated that the CF release rate increased with decreasing liposomes

size, in the temperature range between 30 and 45 ◦C. Probably, this is due to an increase of membrane curvature, resulting in more packing defects and consequently in a higher membrane permeability, as reported in literature [61]. Nevertheless, release rate depended on the composition of the bilayer: while CF release from $DPPG_2$-TSL is strongly affected by vesicle size, a similar behaviour was not observed for $DPPG_2$/HePC-TSL [34]. Furthermore, the CF release appeared also to be higher in the presence of serum, due to the highest interaction of albumin with DPPC-TSL and DPPG-TSL, resulting in an increased diameter of packing defects and release rates.
In 2007, Hossann and collaborators proposed a novel TSL formulation with a prolonged plasma half-life without the use of PEGylated lipids, commonly used strategy, but based on DPPGOG [33]. Since the only TSL formulation in clinical trials applies DSPE-PEG2000 and lysophosphatidylcholine (P-lyso-PC), the main objective of this study was to compare the influence of DPPGOG, DSPE-PEG_{2000} and P-lyso-PC on *in vitro* vesicles stability and on thermal-triggered drug release. Three different formulations were developed and compared in presence of fetal calf serum: DPPC/DSPC/DPPGOG 50:20:30, DPPC/P-lyso-PC/DSPEPEG_{2000} 90:10:4 and PEGylated based TSL. The DPPGOG based formulation showed an improved stability at 37 ◦C compared to PEGylated liposomes. In DPPC/DSPC/DPPGOG sample, CF was retained up to 10 h at 37 ◦C in serum, whereas PEGylated TSL became unstable after 6 h. Furthermore, DPPGOG was reported to increase membrane permeability similarly to P-lyso-PC, releasing over the 70% of CF at their T_m. All these properties were retained when CF was replaced with DOX. In fact, DPPGOG-TSL retained 89% of DOX and released it completely only at 42 ◦C. In conclusion, DPPGOG was able to prolong the liposomes *in vivo* half-life, like DSPE-PEG_{2000}, and to increase the drug release like P-lyso-PC, without a negative effect on TSL stability [33].
Cisplatin-loaded LTSL were designed by Woo and collaborators in 2008, proposing a new drug encapsulation method, named passive equilibration, consisting in drug loading in preformed LTSL. The researchers demonstrated that cisplatin was released from LTSL at 42 ◦C within 5 min [62].
The potential of LTSL for high molecular weight molecule delivery was studied by Zhang and collaborators [63]. Fluorescein isothiocyanate conjugate-albumin was used as a model drug (MW 66 kDa) and incorporated into liposomes, demonstrating not only excellent stability at physiological temperature, but also a fast release behaviour at 42 and 44.5 ◦C [63].
In 2011, Tagami and collaborators hypothesized that Brij surfactants could replace the functions of MSPC, a single acyl chain lipid/surfactant, and DSPE-PEG2000, a PEGylated lipid/surfactant in the LTSL formulation, to obtain a simplified thermo-sensitive carrier [64]. The results showed that only Brij78, may be optimally incorporated both via the thin film method or

post-insertion approach, achieving formulations with better performances compared to traditional lysolipids-based thermo-liposomes. In particular, Brij78-based formulations showed stability at 37 ◦C comparable to that of LTSL and a fast DOX release at 40–42 ◦C already within 2–3 min [64].
More recently, new thermo-sensitive vesicles based on a alkylphosphocholines, a novel class of substances with anticancer and antiprotozoal activities (structurally related to lysophospolipids), have been designed [14]. Hexadecylphosphocholine (HePC) is one of the most representative molecules and presents increased metabolic stability compared with lysolipids. Additionally, unlike classical cytostatic drugs, HePC is not myelosuppressive and can stimulate leukopoiesis and thrombopoesis [65]. HePC is able to act at the same time as drug and carrier constituents, conferring peculiar and interesting functionality to the formulation, allowing the use of additional excipients to be bypassed, increasing system biocompatibility, and making them suitable candidates for special biomedical applications [14]. In 2008, Lindner and collaborators decided to investigate the HePC ability to induce a burst release from DPPGOG-based TSL by mild hyperthermia. As expected, HePC increased the CF release rate similarly to lysolipids and also it exerted stronger therapeutic efficacy against cancer cells when incorporated into liposomal membrane comparing micellar formulation [37].

3.3 Polymer-Modified and Peptides-Modified Thermo-Sensitive Liposomes

Thermo-sensitive polymers present a low critical solution temperature (LCST) that corresponds to their sharp coil-to-globule transition and phase separation. These polymers are water-soluble below their cloud point (CP) while, above it, hydrogen bonds between water molecules and the polymer hydrogen bond-forming groups become weaker, resulting in less hydrated polymer chains [66]. Consequently, the polymers undergo a coil-to-globule transition, causing their precipitation. The presence of a thermo-sensitive polymer in the vesicles bilayer leads to a destruction of the membrane and to the release of the drug above LCST [67]. Thermo-sensitive polymers can be incorporated into liposomes by coupling to a hydrophobic moiety that is able to dissolve in the liposomal bilayer [68]. Since temperature promotes changes in solubility, turning polymers from hydrophilic to hydrophobic molecules, this parameter may be used to control the stabilization and destabilization of PTSL, allowing control also of the drug release and interaction with cells and serum proteins [66,69].
This strategy has been investigated in depth and one of the first thermo-sensitive polymers incorporated into liposomal membrane was the poly(*N*-isopropylacrylammide) (pNIPAM) [70]. The main drawback of this polymer

is that it possesses a LCST around 32 ◦C in aqueous solution, which does not coincide with the basic requirement of an ideal pharmaceutical thermo-sensitive system [71]. Researchers have tried to overcome this problem through its copolymerization with appropriate co-monomers, in order to bring the LCST to a desired temperature range [70].

Even pH-sensitive monomers such as PAA may also be co-polymerized with NIPAM, conferring relevant targeting ability to different physiological districts [67]. Poly(NIPAM-*co*-propylacrylic acid) has been synthesized by reversible addition-fragmentation chain transfer giving products with a LCST of 42 ◦C (at pH 6.5). PTSL prepared with this polymer has been found to release 100% of loaded DOX at 42 ◦C within 5 min (95% of the content in 10 s at 42 ◦C), with a minimum release (less than 20%) at 37 ◦C within 30 min in serum [72].

DPPC liposomes modified with 5% of p(NIPAAm-*co*-PAA) are stable in serum and are able to release 70% and 100% of loaded DOX already after 5 min of heating at 40 ◦C and 42 ◦C, respectively. Additionally, the release from p(NIPAAm-*co*-PAA)-modified liposomes is higher at acid condition (typical of tumour cells) because of the pKa PAA (pKa = 6.7). At acid pH, in fact, the carboxyl group of PAA is protonated and promotes its coil-to-globule phase transition and consequently drug release [67].

Liposomes modified with co-polymers of NIPAM and acryloylpyrrolidine (pAPr) were already proposed by Kono and collaborators in 1999 [73].

Also, acrylamide (AAM) was used to modify the LCST of pNIPAM, as reported by Han and collaborators in 2006. Authors synthetized various co-polymers of NIPAM and AAM by changing the monomers ratio and observed that the variation of LCST depended on the acrylamide content [74]. Its incorporation increased the hydrophobicity of the polymer chains, resulting in the increase of LCST. Furthermore, the authors incorporated this copolymer into the bilayer of different TSL and observed that DPPC/HSPC/CHOL/DSPE-PEG_{2000}-PNIPAM-AAM_{17} formulation gave the highest DOX release rates in serum. These results highlighted that the increase in hydrophobicity of the polymer induces a stronger interaction with lipid membrane and consequently enhances the drug release from liposomes. Conversely, the presence of PEG on the liposomes surface decreases their interaction with serum proteins in the bloodstream and prolongs the *in vivo* stability of carriers compared with polymer unmodified liposomes [74].

Another polymer used for the polymer-modified TSL preparation has been poly[2-(2-ethoxy) ethoxyethyl vinyl ether] (p-EOEOVE). This polymer exhibits a LCST around 40 ◦C, undergoing a sharply structural transition from a highly hydrophilic coil to a hydrophobic globule [75]. These PTSL are stable and retain the drug inside them below physiological temperatures. However, they exhibit a higher release of the encapsulated DOX above 40

◦C reaching complete emptying within 1 min at 45 ◦C. Additionally, the copolymer-modified liposomes exhibit long circulating properties and biodistribution like that obtained by traditional PEG-modified liposomes [75]. Considering polymer EOEOVE potentiality in drug delivery, similar copolymers have been prepared. In particular, poly [2-(2-ethoxy) ethoxyethyl vinyl ether-block-octadecyl vinyl ether (p-EOEOVE-block-ODVE)] with a LCST around 40 ◦C has been synthesized: the poly(EOEOVE) block acts as the temperature-sensitive moiety, while the poly(ODVE) block behaves as anchor units [76]. In 2011, the performance of PTSL in terms of visualization and efficacy against a tumour was investigated by Katagiri et al. [77] In this study the authors incorporated hydrophobized Fe_3O_4 nanoparticles into the poly(EOEOVE-bODVE) liposomal bilayer via hydrophobic interactions. An alternating magnetic field was used to heat the Fe_3O_4 nanoparticles and to induce the release of a fluorescent marker. The potential of the same carrier as "theranostic" nanodevice has been successful investigated by Kokuryo et al. preparing PTSL loaded with an anticancer drug, a MRI contrast agent, and a fluorescent dye with the aim of monitoring drug delivery in cancer therapy [78].

The drug release rate from grafted-polymer-TSL depends on several variables as the polymer molecular weight and grafted density. Recently, van Elk and collaborators developed *N*-(2-hydroxypropyl) methacrylamide mono/dilactate (pHPMAlac)-grafted liposomes, varying polymer molecular weights, composition and anchoring it to cholesterol [68]. Results have shown that release starts at the polymer CP temperature, and that it increases with the decrease of CH-pHPMAlac molecular weight. Furthermore, the presence of CH contributes to reducing the polymer thermo-sensitivity. The release percentage of DOX from CH-pHMAlac-grafted liposomes, with a CP at 11.5 ˚C, is been about 89% at 42 ˚C after 5 min, while that obtained with the sample possessing a CP at 25 ˚C has reached the same value only at 52 ˚C. Moreover, authors have observed that the grafting density affects the liposomes thermo-sensitivity: only 5% polymer-grafting density CH-pHMAlac ensures a fast release at the desired temperature [68].

An innovative approach to prolong the plasma half-life of TSL relies on the incorporation onto the bilayer of a thermally responsive elastin-like polypeptide (ELP), consisting of a Val-Pro-Gly-Val-Gly units [79]. ELP is reported to act like a LCST polymer, swelling below the transition temperature, due to a hydrogen bonding interaction between ELP and water molecules, and drying out above LCST, due to hydrophobic interaction, making the bilayer less flexible [80]. In 2013, Park and collaborators [72] have used modified ELP to confer thermo-sensitivity to liposomes, producing a more rigid membrane at physiological temperatures and reducing vesicle instability during blood circulation. The ELP N-terminal portion has been conjugated with a single stearyl group (C18) for anchoring to the lipid bilayer of DPPC/DSPE-

PEG_{2000}/CH liposomes. The resulting formulation has shown a high stability at physiological conditions and has given a significant release of encapsulated DOX after mild heating. The authors have demonstrated that ELP-liposomes can release more than 95% of drug content in 10 s at 42 °C, while less than 20% is released within 30 min at 37 °C in serum. The designed formulation has shown a plasma half-life of 2.03 h compared to a half-life of 0.92 h reported for LTSL. A significant delay in tumour growth has been achieved by ELP-liposomes in combination with high intensity focused ultrasounds compared to LTSL, already after one intravenous injection [72].

3.4 Multifunctional Thermo-Sensitive Liposomes (MTSL)

In the field of drug-delivery systems, the use of a single strategy is not generally sufficient to enhance anticancer therapy efficacy. Therefore, the design and development of carriers that combine different strategies in the same system, making them clinically more efficacious, are needed [81]. The thermal triggering approach has been very successful when combined with active or passive targeting strategies to further enhance its efficacy. A synergistic combination is one that joins tumour vasculature targeting with temperature-triggered release. This is achieved by coating the thermo-sensitive vesicle surface with antigens expressed on angiogenic tumour vasculature, such as ligands for integrins vascular endothelian growth factor receptor (VEGFR), platelet-derived growth factor receptor (PDGFR), and CD13/aminopeptidase N [82]. A novel cyclic Asn-Gly-Arg (NGR) peptide not containing a disulfide bridge was synthesized by Negussie and collaborators and used to confer target properties to LSTS. *In vitro* fluorescence microscopy evaluation demonstrated that the peptide was actively taken up by a $CD13^+$ cancer cell, showing minimal binding to $CD13^-$ cells, and displayed 3,6-fold greater affinity than a linear form also when conjugated on the liposomal surface of a LSTL [22].

Kim and collaborators improved the performance of thermo-sensitive liposomes by coupling them with a cyclic arginine-glycine-aspartic acid (cRGD) peptide, able to enhance tumour accumulation through the targeting to $\alpha_v\beta_3$ integrin, overexpressed in tumour vasculature and in several malignant tumours. The cellular uptake of these multifunctional vesicles was 7-fold higher than that obtained with no-targeted liposomes. These results were also confirmed by *in vivo* tumour accumulation experiments [83].

The use of cationic lipids and temperature-triggered release represents another strategic combination for use in cancer treatment. Cationic nanocarriers have been reported to deliver selectively anticancer drugs to cancer cells thanks to the electrostatic interactions with overexpressed anionic glycoproteins, phospholipids and proteoglycans on the tumour vasculature [84,85]. Additionally, the vesicle accumulation at the cancer site is facilitated by the irregular and slow blood flow and hyperthermia, which promotes carrier extravasion [84]. Recently, as mentioned,

Dicheva and collaborators [47] have designed PEGylated cationic thermo-sensitive liposomes (CSTL) made of DPPC, DSPC, DSPE-PEG_{2000} and the cationic lipid DPTAP. These vesicles have displayed a high stability at physiological temperature and release kinetics of CF similar to that achieved by non-cationic thermo-sensitive liposomes (NCTSL). The levels of binding of CSTL to BML (benign metastatic Leiomyoma) and HUVEC (human umbilical vein endothelial cells) are higher at 37 °C compared to NCTSL. Upon binding due to their small size, CTSL are easily internalized into cancer cell and the release of CF is triggered by temperature increase and might occur both extracellularly and intracellularly, improving the therapeutic outcome. The same research group has demonstrated the effectiveness of this system by encapsulating DOX and the resulting effective mild hyperthermia-triggered drug release has confirmed the success of the dual targeting approach [46]. Additionally, the cytotoxicity of DOX-CTSL is higher than that obtained when loaded in TSL after treatment on several tumour cells lines. Furthermore, the decrease of cationic lipid in the bilayer from 10 to 7.5 mol % does not influence the cellular CTSL tumour targeting and related induction of cytotoxicity [47]. A new multifunctional formulation is also developed for the specific delivery of small interfering RNA (siRNA). To do this, Yang et al. in 2016 combined two main strategies into a single carrier to give rise to smart multifunctional TSL. The first involves direct conjugation of cell penetrating peptide (CPP) to siRNA via disulphide bonds (designated as siRNA-CPPs) which determines the carrier sensitivity to glutathione. In the second strategy, the siRNA-CPPs were encapsulated, to overcome their limitation *in vivo*, in TSL containing an Asparagine-Glycine-Arginine (NGR) peptide with vasculature target function. Under dual stimulus of hyperthermia and intracellular redox environment, the siRNS-CPPs/NGR-TSL has higher *in vivo* tumour efficacy and gene silencing efficiency rather than the free siRNA-CPPs under hyperthermia [86].

3.5 Thermo-Sensitive Niosomes (TSN)

Niosomes are non-ionic surfactant vesicles obtained on hydration of manufactured non-ionic surfactants, with or without joining of cholesterol or other lipids. They are vesicular systems like liposomes that can be utilized as carriers of amphiphilic and lipophilic drugs. Niosomes are promising vehicles for drug delivery and, being non-ionic, they are less dangerous and enhances the therapeutic index of the drug.

For the first time, in 2016, Tavano et al. have decided to investigate the natural characteristic of certain surfactants to transfer their thermo-sensitivity properties to niosomes. Pluronic L64 belonging to the class of poly (ethylene oxide)-poly (propylene oxide)-poly (ethylene oxide) blocks surfactants and its derivative were used to form thermo-sensitive vesicles either in the presence or absence of cholesterol, evaluating the effect of small changes in composition on the thermo-sensibility of the carriers [87]. The use of L64 as an amphiphilic constituent, with

claimed stealth and thermo-sensitive functionality, may give the possibility to bypass the use of additional excipients, increasing the system biocompatibility. The *in vitro* calcein release studies have been performed at 25, 37 and 42 °C, that are representative of storage, physiological conditions and mild hyperthermia, showing a more pronounced calcein release from L64-based niosomes at 42 °C. Due to these promising results, authors have validated the thermo-sensitivity of these by encapsulating 5-FU in the aqueous core. Also, 5-FU release has exhibited a temperature dependence, with a marked increase at 42 °C, confirming that the temperature-sensitivity of these niosomes depends only on the surfactant characteristics and it is not affected by the chemical nature of the drug [87].

3.6 Thermo-Sensitive Polymersomes (TSP)

Polymersomes (Ps), also known as polymeric vesicles, are based on the self-assembly of synthetic amphiphilic branch, graft and dendritic copolymers [88]. Compared to liposomes, Ps present countless advantages such a high stability, multi-drug loading capacity and membrane property versatility, due to the great variability of the starting materials [89]. Recently, the development of stimuli-responsive polymersomes to further control the release of drugs has attracted a lot of interest and is achieved through the use of thermo-sensitive amphiphilic polymer. Already in 2006, Li and collaborators prepared polymersomes from poly[*N*-(3-aminopropyl)-methacrylamide hydrochloride]-*b*-poly(*N*-isopropylacrylamide) (PAMPA-PNIPAAM): when temperature is raised above the LCST of the PNIPAAM chains, the polymer become insoluble in water and its monomers self-assembled into the vesicular structure [90]. In the same year, Qin and collaborators studied the influence of temperature on assembly and disassembly of polymersomes encapsulating DOX, obtained from PEG-*b*-PNIPAAm with 7–20% wt PEG content [91]. By increasing the temperature, polymer and monomers gave vesicles, easily destroyable by cooling because of the increased hydrophilic character. Unfortunately, this system required very high temperatures to form polymersomes and a reduction often below the 37 °C to promote drug release; thus, it could not be effectively used in combination with mild hyperthermia treatment. To by-pass this limitation and to encourage the formation of polymersomes at room temperature, mixtures of thermo-sensitive and hydrophobic polymer blocks have been proposed. Zhou and collaborators synthesized novel polymersomes based on star copolymers presenting a hydrophobic hyperbranched poly[3-ethyl-3-(hydroxymethyl)oxetane] (HBPO) core and several hydrophilic PEG arms [92]. Unlike classical thermo-sensitive Ps, these novel carriers have been formed at room temperature and destabilized above the LCST, enhancing membrane permeability and drug release. In 2015, Liu and collaborators, designed polymersomes from hydrophilic poly(*N*-vinylcaprolactam) (PVCL) attached to a long hydrophobic PDMS poly(dimethylsiloxane) core block, generating a thermo-responsive bola amphiphile, conducting an in depth and extensive study [93]. Several

poly(*N*-vinylcaprolactam)*n*-poly(dimethylsiloxane) 65-poly(*N*-vinylcaprolactam)*n*($PVCL_n$-$PDMS_{65}$-$PVCL_n$) copolymers have been synthesized with varying PVCL amounts, but only samples with a PVCL ratio between 0.36 and 0.52 are able to form stable vesicles at room temperature. Polymersomes size decreases with the temperature rise, dependently on the PVCL chain length. In fact, when the temperature increases from 25 °C to 55 °C, vesicle volume lowers with increasing PVCL length (from $PVCL_{10}$ to $PVCL_{15}$). Conversely, $PVCL_{19}$-$PDMS_{65}$-$PVCL_{19}$ shows an increase of hydrodynamic diameter from 300 to 800 nm. Furthermore, the authors have investigated the DOX release from $PVCL_{10}$-$PDMS_{65}$-$PVCL_{10}$, $PVCL_{15}$-$PDMS_{65}$-$PVCL_{15}$, and $PVCL_{19}$-$PDMS_{65}$-$PVCL_{19}$ based formulations both at 25 and 42 °C, in a fluid-simulating tumour environment, achieving released drug percentages of 86%, 29%, and 11% at 42 °C, respectively, and demonstrating a strong dependence on PVLC length [85]. After temperature increase, collapse and aggregation of PVLC block occurs, leading to a decrease of Ps size and to an improvement of membrane permeability, favouring the release of DOX. Also, hydration and dehydration of PVLC blocks linked to the hydrophobic PDMS block play an important role, since it is assumed that hydrophilic molecules may overcome the hydrophobic PDMS layers by the presence of transient pores at high temperature. Finally, the cytotoxicity of DOX-loaded $PVCL_{10}$-$PDMS_{65}$-$PVCL_{10}$ polymersomes has been evaluated on human alveolar adenocarcinoma A549 cell line, with the result that cell viability decreased from 85% to 59% and from 71% to 50% for polymersomes containing 0.1 and 0.5 μg mL^{-1} of drug, respectively. Therapeutic efficacy stopped after 48 h for 0.1 and 0.5 μg mL^{-1} DOX-loaded vesicles, while for vesicles containing 1 and 5 μg mL^{-1} of DOX it continued until 72 h, achieving cell cytotoxicity higher than 75% and 97%, respectively [93].

4. Conclusions

In the field of temperature-sensitive drug delivery systems, thermo-sensitive vesicles in combination with local hyperthermia represent a powerful tool for tumour specific drug delivery. This review has shown the considerable progress in the development of thermo-sensitive vesicle formulations for targeted cancer therapy developed since 1978. Mild hyperthermia exposure has been proved to be an ideal external stimulus able to trigger localized drug release. Therefore, the combination of this strategy with a carrier sensitive to temperature changes between 39 ◦C and 42 ◦C resulted in a promising strategy to improve therapeutic efficacy. The latest studies suggest that such a carrier could be able to release rapidly and extensively a hydrophilic drug when the temperature increases a few degrees above physiological temperature. The efficacy of TSV depends both on the specific vesicular formulation, on the encapsulated drug, and on the specific heating modality. The progress obtained in the last few years on the new formulations to improve the TSV efficacy are reported

in this review, but we recommend reading the recent review about the new heating modality [94]. One limitation of many current TSV formulations is the still relatively short plasma half-life, which limits the duration available for delivery, reduces the quantity of encapsulated drug available for release, and also negatively impacts systemic toxicities. Promising results are obtained by the synergistic effect due to the combination of several approaches in the same nanodevices. We are sure that the rational design of a multifunctional thermo-responsive system has remarkable potential in target cancer therapy. In summary, TSV represents a highly promising drug-delivery approach that has the potential for considerable clinical impact in the near future.

Abbreviations

AAM	acrylamide
C	Calcein
CF	carboxyfluorescein
CH	cholesterol
CP	cloud point
CPP	cell penetrating peptide
CTSL	cationic thermo-sensitive liposomes
DDS	drug delivery systems
DOX	Doxorubicin
DPPC	1,2-dypalmitoyl-*sn*-glycero-3-phosphocoline
$DPPG_2$	1,2-dipalmitoyl-*sn*-glycero-3-phosphoglyceroglycerol
DPPGOG	1,2-dipalmitoyl-*sn*-glycero-3-phosphoglyceroglycerol
DSPC	distearoyl phosphocholine
$DSPE\text{-}PEG_{2000}$	1,2-distearoyl-*sn*-glycero-3-phosphoethanolamine-Nmethoxy(PEG)-2000
FCS	fetal calf serum
GD	Gadolinium
Gem	Gemcitabine
HBPO	hydrophobic hyperbranched poly[3-ethyl-3-(hydroxymethyl)oxetane]
HePC	hexadecylphosphocholine
HAS	human serum albumin
HSPC	hydrogenated soyphosphocholine
IgG	immunoglobulin type G
LCST	low critical solution temperature
LP	Lysolipids
LTSL	lysolipids thermo-sensitive liposomes
LTST	low thermo-sensitive liposomes
MPPC	Monopalmitoylphosphatidylcholine
MSPC	monostearoylphosphatidylcholine
MTSL	multifunctional thermo-sensitive liposomes
NCTSL	non-cationic thermo-sensitive liposomes
PAA	propyl acrylic acid
PAMPA-PNIPAAM	poly[*n*-(3-aminopropyl)-methacrylamidehydrochloride]-*b*-poly(*n*-isopropylacrylamide)
PDGFR	patelet-derived growth factor receptor
PDMS	poly(dimethylsiloxane)
pEOEOVE	poly[2-(2-ethoxy)ethoxyethyl vinyl ether]
pEOEOVE-block-ODVE	poly [2-(2-ethoxy)ethoxyethyl vinyl ether-block-octadecyl vinyl ether]
EOEOVE-block-ODVE	
pHPMAlac	*N*-(2-hydroxypropyl)methacrylamide mono/dilactate
P-Lyso-PC	1-palmitoyl-2-hydroxy-*sn*-glycero-3-phosphocholine
pNIPAM	poly(*N*-isopropylacrylammide)
PpTSL	peptides thermo-sensitive liposomes
Ps	polymersomes
PTSL	polymer thermo-sensitive liposomes
PVCL	poly(*N*-vinylcaprolactam)

$PVCL_n$-$PDMS_{65}$-$PVCL_n$	poly(*N*-vinylcaprolactam)*n*-poly(dimethylsiloxane)65-poly(*N*-vinylcaprolactam)n
RES	reticulo-endothelial system
T_m	phase transition temperature
siRNA	small interfering RNA
TSL	thermo-sensitive liposomes
TSN	thermo-sensitive niosomes
TSP	thermo-sensitive polymersomes
TSV	temperature-sensitive vesicles
VEGFR	endothelian growth factor receptor

References

[1] Hanahan, D.; Weinberg, R.A. The hallmarks of cancer. *Cell* **2000**, *100*, 57–70.
[2] Skeel, R.T.; Khleif, S.N. *Handbook of Cancer Chemotherapy*, 8th ed.; Lippincott Williams and Wilkins: Philadelphia, PA, USA, 2011; ISBN 978-1-60831-782-0.
[3] Szakacs, G.; Paterson, J.K.; Ludwig, J.A.; Booth-Genthe, C.; Gottesman, M.M. Targeting multidrug resistance in cancer. *Nat. Rev. Drug Discov.* **2006**, *5*, 219–234.
[4] Minchinton, A.I.; Tannock, I.F. Drug penetration in solid tumours. *Nat. Rev. Cancer* **2006**, *6*, 583–592.
[5] Deshpande, P.P.; Biswas, S.; Torchilin, V.P. Current trends in the use of liposomes for tumor targeting. *Nanomedicine* **2013**, *8*, 1509–1528.
[6] Landon, C.D.; Park, J.Y.; Needham, D.; Dewhirst, M.W. Nanoscale drug delivery and hyperthermia: The materials design and preclinical and clinical testing of low temperature-sensitive liposomes used in combination with mild hyperthermia in the treatment of local cancer. *Open Nanomed. J.* **2011**, *3*, 38–64.
[7] Needham, D.; Anyarambhatla, G.; Kong, G.; Dewhirst, M.W. A new temperature-sensitive liposome for use with mild hyperthermia: Characterization and testing in a human tumor xenograft model. *Cancer Res.* **2000**, *60*, 1197–1201.
[8] Motamarry, A.; Asemani, D.; Haemmerich, D. *Thermosensitive Liposomes in Liposomes*; Angel, C., Ed.; IntechOpen: Rijeka, Croatia, 2017; Chapter 7.
[9] Hildebrandt, B.; Wust, P.; Ahlers, O.; Dieing, A.; Sreenivasa, G.; Kerner, T.; Felix, R.; Riess, H. The cellular and molecular basis of hyperthermia. *Crit. Rev. Oncol. Hematol.* **2002**, *43*, 33–56.
[10] Chicheł, A.; Skowronek, J.; Kubaszewska, M.; Kanikowski, M. Hyperthermia description of a method and a review of clinical applications. *Rep. Pract. Oncol. Radiother.* **2007**, *12*, 267–275.
[11] Sneed, P.K.; Stauffer, P.R.; Li, G.C.; Stege, G.J.J. Hyperthermia. In *Textbook of Radiation Oncology*, 2nd ed.; Leibel, S.A., Phillips, T.L., Eds.; Saunders: Philadelphia, PA, USA, 2004; p. 1596. ISBN 0-7216-0026-3.
[12] Storm, F.K. Clinical hyperthermia and chemotherapy. *Radiol. Clin. N. Am.* **1989**, *27*, 621–627.
[13] Issels, R.D.; Lindner, L.H.; Verweij, J.; Wust, P.; Reichardt, P.; Schem, B.C.; Abdel-Rahman, S.; Daugaard, S.; Salat, C.; Wendtner, C.M.; et al. Neo-adjuvant chemotherapy alone or with regional hyperthermia for localised high-risk soft-tissue sarcoma: A randomised phase 3 multicentre study. *Lancet Oncol.* **2010**, *11*, 561–570.
[14] Kneidl, B.; Peller, M.; Winter, G.; Lindner, L.H.; Hossann, M. Thermosensitive liposomal drug delivery systems: State of the art review. *Int. J. Nanomed.* **2014**, *9*, 4387–4398.
[15] Jones, E.L.; Samulski, T.V.; Vujaskovic, Z.; Prosnitz, L.R.; Dewhrist, M.W. Hyperthermia. In *Principles and Practise of Radiation Oncology*, 4th ed.; Perez, C.A., Brady, L.W., Halperin, E.C., Schmidt-Ullrich, R.K., Eds.; Lippincott Williams & Wilkins: Philadelphia, PA, USA, 2004; Chapter 24; pp. 699–735. ISBN 978-1-451-11648-9.

[16] Wust, P.; Hildebrandt, B.; Sreenivasa, G.; Rau, B.; Gellermann, J.; Riess, H.; Felix, R.; Schlag, P.M. Hyperthermia in combined treatment of cancer. *Lancet Oncol.* **2002**, *3*, 487–497.
[17] Kerner, T.; Deja, M.; Ahlers, O.; Löffel, J.; Hildebrandt, B.; Wust, P.; Gerlach, H.; Riess, H. Whole-body hyperthermia: A secure procedure for patients with various malignancies? *Intensive Care Med.* **1999**, *25*, 959–965.
[18] Ta, T.; Porter, T.M. Thermosensitive liposomes for localized delivery and triggered release of chemotherapy. *J. Control. Release* **2013**, *169*, 112–125.
[19] Yatvin, M.B.; Weinstein, J.N.; Dennis, W.H.; Blumenthal, R. Design of liposomes for enhanced local release of drugs by hyperthermia. *Science* **1978**, *202*, 1290–1293.
[20] May, J.P.; Li, S.D. Hyperthermia-induced drug targeting. *Expert Opin. Drug Deliv.* **2013**, *10*, 511–527.
[21] Li, L.; ten Hagen, T.L.; Bolkestein, M.; Gasselhuber, A.; Yatvin, J.; van Rhoon, G.C.; Eggermont, A.M.M.; Haemmerich, D.; Koning, G.A. Improved intratumoral nanoparticle extravasation and penetration by mild hyperthermia. *J. Control. Release* **2013**, *167*, 130–137.
[22] Negussie, A.H.; Miller, J.L.; Reddy, G.; Drake, S.K.; Wood, B.J.; Dreher, M.R. Synthesis and *in vitro* evaluation of cyclic NGR peptide targeted thermally sensitive liposome. *J. Control. Release* **2010**, *143*, 265–273.
[23] Lingwood, D.; Simons, K. Lipid rafts as a membrane-organizing principle. *Science* **2010**, *327*, 46−50.
[24] Lindner, L.H.; Hossann, M. Factors affecting drug release from liposomes. *Curr. Opin. Drug Discov. Dev.***2010**, *13*, 111–123.
[25] Mabrey, S.; Sturtevant, J.M. Investigation of phase-transitions of lipids and lipid mixtures by high sensitivity differential scanning calorimetry. *Proc. Natl. Acad. Sci. USA* **1976**, *73*, 3862–3866.
[26] Gaber, M.H.; Hong, K.; Huang, S.K.; Papahadjopoulos, D. Thermosensitive sterically stabilized liposomes: Formulation and *in vitro* studies on mechanism of doxorubicin release by bovine serum and human plasma. *Pharm. Res.* **1995**, *12*, 1407–1416.
[27] Iga, K.; Hamaguchi, N.; Igari, Y.; Ogawa, Y.; Gotoh, K.; Ootsu, K.; Toguchi, H.; Shimamoto, T. Enhanced antitumor activity inmice after administration of thermosensitive liposome encapsulating cisplatin with hyperthermia. *J. Pharmacol. Exp. Ther.* **1991**, *257*, 1203–1207.
[28] Yatvin, M.B.; Muhlensiepen, H.; Porschen, W.; Weinstein, J.N.; Feinendegen, L.E. Selective delivery of liposome-associated cis-dichlorodiammineplatinum (II) by heat and its influence on tumor drug uptake and growth. *Cancer Res.* **1981**, *41*, 1602–1607.
[29] Sadeghi, N.; Deckers, R.; Ozbakir, B.; Akthar, S.; Kok, R.J.; Lammers, T.; Storm, G. Influence of cholesterol inclusion on the doxorubicin release characteristics of lysolipid-based thermosensitive liposomes. *Int. J. Pharm.* **2017**, *17*, 778–782.
[30] Mishra, P.; Bismita, N.; Dey, R.K. PEGylation in anti-cancer therapy: An overview. *Asian J. Pharm. Sci.* **2016**, *11*, 337–348.
[31] Pradhan, P.; Giri, J.; Rieken, F.; Koch, C.; Mykhaylyk, O.; Döblinger, M.; Banerjee, R.; Bahadur, D.; Plank, C. Targeted temperature sensitive magnetic liposomes for thermo-chemotherapy. *J. Control. Release* **2010**, *142*, 108–121.
[32] de Smet, M.; Langereis, S.; van den Bosch, S.; Bitter, K.; Hijnen, N.M.; Heijman, E.; Grüll, H. SPECT/CT imaging of temperature-sensitive liposomes for MR-image guided drug delivery with high intensity focused ultrasound. *J. Control. Release* **2013**, *169*, 82–90
[33] Hossann, M.; Wiggenhorn, M.; Schwerdt, A.; Wachholz, K.; Teichert, N.; Eibl, H.; Issels, R.D.; Lindner, L.H. *In vitro* stability and content release properties of phosphatidylglyceroglycerol containing thermosensitive liposomes. *Biochim. Biophys. Acta* **2007**, *1768*, 2491–2499.

[34] Hosokawa, T.; Sami, M.; Kato, Y.; Hayakawa, E. Alteration in the temperature dependent content release property of thermosensitive liposomes in plasma. *Chem. Pharm. Bull.* **2003**, *51*, 1227–1232.
[35] Limmer, S.; Hahn, J.; Schmidt, R.; Wachholz, K.; Zengerle, A.; Lechner, K.; Eibl, H.; Issels, R.D.; Hossann, M.; Lindhner, L.H. Gemcitabine Treatment of Rat Soft Tissue Sarcoma with Phosphatidyldiglycerol-Based Thermosensitive Liposomes. *Pharm. Res.* **2014**, *31*, 2276–2286.
[36] Li, L.; ten Hagen, T.L.M.; Haeri, A.; Soullié, T.; Scholten, C.; Seynhaeve, A.L.B.; Eggermont, A.M.M.; Koning, G.A. A novel two-step mild hyperthermia for advanced liposomal chemotherapy. *J. Control. Release* **2014**, *174*, 202–208.
[37] Lindner, L.H.; Hossann, M.; Vogeser, M.; Teichert, N.; Wachholz, K.; Eibl, H.; Hiddemann, W.; Issels, R.D. Dual role of hexadecylphosphocholine (miltefosine) in thermosensitive liposomes: Active ingredient and mediator of drug release. *J. Control. Release* **2008**, *125*, 112–120.
[38] Wu, Y.; Yang, Y.; Zhang, F.C.; Wu, C.; Lu, W.L.; Mei, X.G. Epirubicin-encapsulated long-circulating thermosensitive liposome improves pharmacokinetics and antitumor therapeutic efficacy in animals. *J. Liposome Res.* **2011**, *21*, 221–228.
[39] Wang, Z.Y.; Zhang, H.; Yang, Y.; Xie, X.Y.; Yang, Y.F.; Li, Z.; Li, Y.; Gong, W.; Yu, F.L.; Yang, Z.; et al. Preparation, characterization, and efficacy of thermosensitive liposomes containing paclitaxel. *Drug Deliv.* **2016**, *23*, 1222–1231.
[40] Zhang, H.; Gong, W.; Wang, Z.Y.; Yuan, S.J.; Xie, X.Y.; Yang, Y.F.; Yang, Y.; Wang, S.S.; Yang, D.X.; Xuan, Z.X.; et al. Preparation, characterization, and pharmacodynamics of thermosensitive liposomes containing docetaxel. *J. Pharm. Sci.* **2014**, *103*, 2177–2183.
[41] Al Sabbagh, C.; Tsapis, N.; Novell, A.; Calleja-Gonzalez, P.; Escofre, J.M.; Bouakaz, A.; Chacun, H.; Denis, S.; Vergnaud, J.; Gueutin, C.; et al. Formulation and pharmacokinetics of thermosensitive stealth(r) liposomes encapsulating 5-fluorouracil. *Pharm. Res.* **2015**, *32*, 1585–1603.
[42] Wang, S.; Mei, X.G.; Goldberg, S.N.; Ahmed, M.; Lee, J.C.; Gong, W.; Han, H.B.; Yan, K.; Yang, W. Does thermosensitive liposomal vinorelbine improve end-point survival after percutaneous radiofrequency ablation of liver tumors in a mouse model? *Radiology* **2016**, *279*, 762–772.
[43] Li, M.; Li, Z.; Yang, Y.; Wang, Z.; Yang, Z.; Li, B.; Xie, X.; Song, J.; Zhang, H.; Li, Y.; et al. Thermo-sensitive liposome co-loaded of vincristine and doxorubicin based on their similar physicochemical properties had synergism on tumor treatment. *Pharm. Res.* **2016**, *33*, 1881–1898.
[44] Negussie, A.H.; Yarmolenko, P.S.; Partanen, A.; Ranjan, A.; Jacobs, G.; Woods, D.; Bryant, H.; Thomasson, D.; Dewhirst, M.W.; Wood, B.J.; et al. Formulation and characterization of magnetic resonance imageable thermally sensitive liposomes for use with magnetic resonance-guided high intensity focused ultrasound. *Int. J. Hyperther.* **2011**, *27*, 140–155.
[45] Dicheva, B.M.; ten Hagen, T.L.M.; Li, L.; Schipper, D.; Seynhaeve, A.L.B.; van Rhoon, G.C.; Eggermont, A.M.M.; Koning, G.A. Targeted and heat-triggered doxorubicin delivery to tumors by dual targeted cationic thermosensitive liposomes. *J. Control. Release* **2014**, *195*, 37–48.
[46] Dicheva, B.M.; Koning, G.A. Targeted thermosensitive liposomes: An attractive novel approach for increased drug delivery to solid tumors. Expert Opin. *Drug Deliv.* **2014**, *11*, 83–100.
[47] Dicheva, B.M.; ten Hagen, T.L.M.; Li, L.; Schipper, D.; Seynhaeve, A.L.B.; van Rhoon, G.C.; Eggermont, A.M.M.; Lindner, L.H.; Koning, G.A. Cationic Thermosensitive Liposomes: A Novel Dual Targeted Heat-Triggered Drug Delivery Approach for Endothelial and Tumor Cells. *Nano Lett.* **2013**, *13*, 2324−2331.

[48] Affram, K.; Udofot, O.; Singh, M.; Krishnan, S.; Reams, R.; Rosenberg, J.; Agyare, E. Smart thermosensitive liposomes for effective solid tumor therapy and *in vivo* imaging. *PLoS ONE* **2017**, *12*, e0185116.
[49] Hossann, M.; Wang, T.; Wiggenhorn, M.; Schmidt, R.; Zengerle, A.; Winter, G.; Eibl, H.; Peller, M.; Reiser, M.; Issels, R.D.; et al. Size of thermosensitive liposomes influences content release. *J. Control. Release* **2010**, *147*, 436–443.
[50] Sabín, J.; Prieto, G.; Ruso, J.M.; Messina, P.V.; Salgado, F.J.; Nogueira, M.; Costas, M.; Sarmiento, F. Interactions between DMPC liposomes and the serum blood proteins. HSA and IgG. *J. Phys. Chem.* **2009**, *113*, 1655–1661.
[51] Hossann, M.; Syunyaeva, Z.; Schmidt, R.; Zengerle, A.; Eibl, H.; Issels, R.D.; Lindner, L.H. Proteins and cholesterol lipid vesicles are mediators of drug release from thermosensitive liposomes. *J. Control. Release* **2012**, *162*, 400–406.
[52] Verhoef, J.J.F.; Anchordoquy, T.J. Questioning the use of PEGylation for drug delivery. *Drug Deliv. Transl. Res.***2013**, *3*, 499–503.
[53] Li, L.; ten Hagen, T.L.M.; Schipper, D.; Wijnberg, T.M.; van Rhoon, G.C.; Eggermont, A.M.M.; Lindner, L.H.; Koning, G.A. Triggered content release from optimized stealth thermosensitive liposomes using mild hyperthermia. *J. Control. Release* **2010**, *143*, 274–279.
[54] Al-Ahmady, Z.S.; Scudamore, C.L.; Kostarelos, K. Triggered doxorubicin release in solid tumors from thermosensitive liposome-peptide hybrids: Critical parameters and therapeutic efficacy. *Int. J. Cancer* **2015**, *137*, 731–743.
[55] Arouri, A.; Mouritsen, O.G. Membrane-perturbing effect of fatty acids and lysolipids. *Prog. Lipid Res.* **2013**, *52*, 130–140.
[56] Mills, J.K.; Needham, D. Lysolipid incorporation in dipalmitoylphosphatidylcholine bilayer membranes enhances the ion permeability and drug release rates at the membrane phase transition. *Biochim. Biophys. Acta* **2005**, *1716*, 77–96.
[57] Anyarambhatla, G.R.; Needham, D. Enhancement of the Phase Transition Permeability of DPPC Liposomes by Incorporation of MPPC: A New Temperature-Sensitive Liposome for use with Mild Hyperthermia. *J. Liposomes Res.* **1999**, *9*, 491–506.
[58] Al-Ahmady, Z.; Kostarelos, K. Chemical Components for the Design of Temperature-Responsive Vesicles as Cancer Therapeutics. *Chem. Rev.* **2016**, *116*, 3883–3918.
[59] De Smet, M.; Langereis, S.; van den Bosch, S.; Grüll, H. Temperature-sensitive liposomes for doxorubicin delivery under MRI guidance. *J. Control. Release* **2010**, *143*, 120–127.
[60] Sandström, M.C.; Ickenstein, L.M.; Mayer, L.D.; Edwards, K. Effects of lipid segregation and lysolipid dissociation on drug release from thermosensitive liposomes. *J. Control. Release* **2005**, *107*, 131–142.
[61] Hatzakis, N.S.; Bhatia, V.K.; Larsen, J.; Madsen, K.L.; Bolinger, P.Y.; Kunding, A.H.; Castillo, J.; Gether, U.; Hedegård, P.; Stamou, D. How curved membranes recruit amphipathic helices and protein anchoring motifs. *Nat. Chem. Biol.* **2009**, *5*, 835–841.
[62] Woo, J.; Chiu, G.N.; Karlsson, G.; Wasan, E.; Ickenstein, L.; Edwards, K.; Bally, M.B. Use of a passive equilibration methodology to encapsulate cisplatin into preformed thermosensitive liposomes. *Int. J. Pharm.* **2008**, *349*, 38–46.
[63] Zhang, X.; Luckham, P.F.; Hughes, A.D.; Thom, S.; Xu, X.Y. Development of lysolipid-based thermosensitive liposomes for delivery of high molecular weight proteins. *Int. J. Pharm.* **2011**, *421*, 291–292.
[64] Tagami, T.; Ernsting, M.J.; Li, S.D. Optimization of a novel and improved thermosensitive liposome formulated with DPPC and a Brij surfactant using a robust *in vitro* system. *J. Control. Release* **2011**, *154*, 290–297.
[65] Vehmeyer, K.; Eibl, H.; Unger, C. Hexadecylphosphocholine stimulates the colony-stimulating factor-dependent growth of hemopoietic progenitor cells. *Exp. Hematol.* **1992**, *20*, 1–5.

[66] Kono, K. Thermosensitive polymer-modified liposomes. *Adv. Drug Deliv. Rev.* **2001**, *53*, 307–319.
[67] Ta, T.; Convertine, A.J.; Reyes, C.R.; Stayton, P.S.; Porter, T.M. Thermosensitive liposomes modified with poly(*N*-isopropylacrylamide-co-propylacrylic acid) copolymers for triggered release of doxorubicin. *Biomacromolecules* **2010**, *11*, 1915–1920.
[68] van Elk, M.; Deckers, R.; Oerlemans, C.; Shi, Y.; Storm, G.; Vermonden, T.; Hennink, W.E. Triggered Release of Doxorubicin from Temperature-Sensitive Poly(*N*-(2-hydroxypropyl)-methacrylamide mono/dilactate) Grafted Liposomes. *Biomacromolecules* **2014**, *15*, 1002−1009.
[69] Ward, M.A.; Georgiou, T.K. Thermoresponsive polymers for biomedical applications. *Polymers* **2011**, *3*, 1215–1242.
[70] Hayashi, H.; Kono, K.; Takagishi, T. Temperature-controlled release property of phospholipid vesicles bearing a thermo-sensitive polymer. *Biochim. Biophys. Acta Biomembr.* **1996**, *1280*, 127–134.
[71] Schild, H.G. Poly(*N*-isopropylacrylamide): Experiment, theory and application. *Prog. Polym. Sci.* **1992**, *17*, 163–249.
[72] Park, S.M.; Kim, M.S.; Park, S.J.; Park, E.S.; Choi, K.S.; Kim, Y.S.; Kim, H.R. Novel temperature-triggered liposome with high stability: Formulation, *in vitro* evaluation, and *in vivo* study combined with high-intensity focused ultrasound (HIFU). *J. Control. Release* **2013**, *170*, 373–379.
[73] Kono, K.; Nakai, R.; Morimoto, K.; Takagishi, T. Thermosensitive polymer-modi¢ed liposomes that release contents. around physiological temperature. *Biochim. Biophys. Acta* **1999**, *1416*, 239–250.]
[74] Han, H.D.; Shin, B.C.; Choi, H.S. Doxorubicin-encapsulated thermosensitive liposomes modified with poly(*N*-isopropylacrylamide-co-acrylamide): Drug release behaviour and stability in the presence of serum. *Eur. J. Pharm. Biopharm.* **2006**, *62*, 110–116.
[75] Aoshima, S.; Kanaoka, S. A renaissance in living cationic polymerization. *Chem. Rev.* **2009**, *109*, 5245–5287.
[76] Kono, K.; Ozawa, T.; Yoshida, T.; Ozaki, F.; Ishizaka, Y.; Maruyama, K.; Aoshima, S. Highly temperature-sensitive liposomes based on a thermosensitive block copolymer for tumor-specific chemotherapy. *Biomaterials* **2010**, *31*, 7096–7105.
[77] Katagiri, K.; Imai, Y.; Koumoto, K.; Kaiden, T.; Kono, K.; Aoshima, S. Magnetoresponsive on demand release of hybrid liposomes formed from Fe3O4 nanoparticles and thermosensitive block copolymers. *Small* **2011**, *7*, 1683–1689.
[78] Kokuryo, D.; Nakashima, S.; Ozaki, F.; Yuba, E.; Chuang, K.H.; Aoshima, S.; Aoki, I. Evaluation of thermo-triggered drug release in intramuscular-transplanted tumors using thermosensitive polymer-modified liposomes and MRI. *Nanomedicine* **2015**, *11*, 229–238.
[79] Dreher, M.R.; Raucher, D.; Balu, N.; Michael Colvin, O.; Ludeman, S.M.; Chilkoti, A. Evaluation of an elastin-like polypeptide–doxorubicin conjugate for cancer therapy. *J. Control. Release* **2003**, *9*, 31–43.
[80] Zoonens, M.; Reshetnyak, Y.K.; Engelman, D.M. Bilayer interactions of pHLIP, a peptide that can deliver drugs and target tumors. *Biophys. J.* **2008**, *95*, 225–235.
[81] Tavano, L.; Muzzalupo, R. Multi-functional vesicles for cancer therapy: The ultimate magic bullet. *Colloid Surf. B Biointerfaces* **2016**, *147*, 161–171. Perche, F.; Torchilin, V.P. Recent Trends in Multifunctional Liposomal Nanocarriers for Enhanced Tumor Targeting. *J. Drug Deliv.* **2013**, *2013*, 705265.
[82] Perche, F.; Torchilin, V.P. Recent Trends in Multifunctional Liposomal Nanocarriers for Enhanced Tumor Targeting. J. Drug Deliv. 2013, 2013, 705265.
[83] Kim, M.S.; Lee, D.W.; Park, K.; Park, S.J.; Choi, E.J.; Park, E.S.; Kim, H.R. Temperature-triggered tumor-specific delivery of anticancer agents by cRGD-conjugated thermosensitive liposomes. *Colloid Surf. B Biointerfaces* **2014**, *116*, 17–25.

[84] Abu Lila, A.S.; Ishida, T.; Kiwada, H. Targeting anticancer drugs to tumor vasculature using cationic liposomes. *Pharm. Res.* **2010**, *27*, 1171–1183.
[85] Campbell, R.B.; Ying, B.; Kuesters, G.M.; Hemphill, R. Fighting cancer: From the bench to bedside using second generation cationic liposomal therapeutics. *J. Pharm. Sci.* **2009**, *98*, 411–429.
[86] Yang, Y.; Yang, Y.; Xie, X. Dual stimulus of hyperthermia and intracellular redox environment triggered release of siRNA for tumor-specific therapy. *Int. J. Pharm.* **2016**, *506*, 158–173
[87] Tavano, L.; Rossi, C.O.; Picci, N.; Muzzalupo, R. Spontaneous temperature-sensitive Pluronic based niosomes: Triggered drug release using mild hyperthermia. *Int. J. Pharm.* **2016**, *51*, 703–708.
[88] Lee, J.S.; Feijen, J. Polymersomes for drug delivery: Design, formation and characterization. *J. Control. Release* **2012**, *161*, 473–483.
[89] Liao, J.F.; Wang, C.; Wang, Y.J.; Luo, F.; Qian, Z.Y. Recent Advances in Formation, Properties, and Applications of Polymersomes. *Curr. Pharm. Des.* **2012**, *18*, 3432−344.
[90] Li, Y.; Lokitz, B.S.; McCormick, C.L. Thermally Responsive Vesicles and Their Structural "Locking" through Polyelectrolyte Complex Formation. *Angew. Chem. Int. Ed.* **2006**, *45*, 5792–5795.
[91] Qin, S.; Geng, Y.; Discher, D.E.; Yang, S. Temperature-Controlled Assembly and Release from Polymer Vesicles of Poly(ethylene oxide)-block-poly(*N*-isopropylacrylamide). *Adv. Mater.* **2006**, *18*, 2905–2909.
[92] Zhou, Y.; Yan, D.; Dong, W.; Tian, Y. Temperature-responsive phase transition of polymer vesicles: Real-time morphology observation and molecular mechanism. *J. Phys. Chem. B* **2007**, *111*, 1262–1270.
[93] Liu, F.; Kozlovskaya, V.; Medipelli, S.; Xue, B.; Ahmad, F.; Saeed, M.; Cropek, D.; Kharlampieva, E. Temperature-Sensitive Polymersomes for Controlled Delivery of Anticancer Drugs. *Chem. Mater.* **2015**, *27*, 7945−7956.
[94] Dou, Y.; Hynynen, K.; Allen, C. To heat or not to heat: Challenges with clinical translation of thermosensitive liposomes. *J. Control. Release* **2017**, *249*, 63–73.

3.2 Nanovesicular Formulations for Cancer Gene Therapy (Review)

Lorena Tavano[a], Elisabetta Mazzotta[a] and Rita Muzzalupo[a]

[a] Department of Pharmacy, Health and Nutritional Sciences, University of Calabria, Via Savinio, Ed. Polifunzionale, 87036 Arcavacata di Rende, Italy

Published on Current Pharmaceutical Design, 2017, 23, 1-9

ABSTRACT

In the last decades, gene therapy has become a novel therapeutic strategy for cancer treatment, including immunologic and molecular approaches. Among molecular avenue, the design of efficient and effective gene delivery systems, like cationic liposomes and niosomes, has been widely investigated and proposed as the most promising research area. The advantages of cationic vesicles rely on their natural ability to form complexes with anionic genetic molecules and deliver them into the cells via the endosomal pathway. Obviously, cationic vesicles-mediated gene delivery is affected by numerous factors, in particular composition, that strongly affects vesicle physical-chemistry characteristics and transfection effectiveness. This review will analyse the potential of cationic nanocarriers in cancer gene therapy, focusing on the role of liposomes and niosomes as vesicular devices and giving an exhaustive collection of the most representative investigations.

Keywords: Liposomes; Niosomes; Gene therapy; Cancer

1. Cancer gene therapy: current strategies

In the last decades, gene therapy (GT) has become a novel therapeutic approach for cancer treatment. GT involves the transfer of genetic material into cells to treat diseases caused by altered gene expression [1]. In particular, since cancer develops from mutations of critical genes regulating biochemical cellular processes, gene therapy has been proposed as a novel and effective strategy against tumor. Two different classes of mutated genes have been identified in cancer disease. The first group includes *oncogenes*, that are involved in the codification of proteins that enhance cell proliferation: their mutation leads to a constitutive activation [2]. The most frequent alterations refer to the *ras*, *c-myc*, *c-erbB-2*, *abl* and *bcl-2* genes. The second group includes tumor *oncosoppressors* encoding for proteins which normally either inhibit cellular proliferation or cause cell death. Deletions or mutations in these genes result in the loss of their functionalities [2]. The *oncosoppressor* gene more frequently involved in cancer development is the *p53,* called *the guardian of genome* [3-5]. In health conditions, the cellular replication cycle depends on the balance between oncogenes and oncosoppressors, whereby their inappropriate activation/inactivation leads to uncontrolled proliferation [3].

Gene therapy overcomes the common drawbacks of classical biological approaches, like cytotoxic capacity and poor selectivity, resulting in a more effective therapy with reduced side effects [1]. Cancer gene therapy includes several strategies, which can be divided into two main categories: immunologic treatments (including immune-enhancement genes and vaccines) and molecular treatments (including antisense oligonucleotides, gene silencing, suicide genes, anti-angiogenesis and drug resistance gene therapies) [6], as summarized in Fig. **1**.

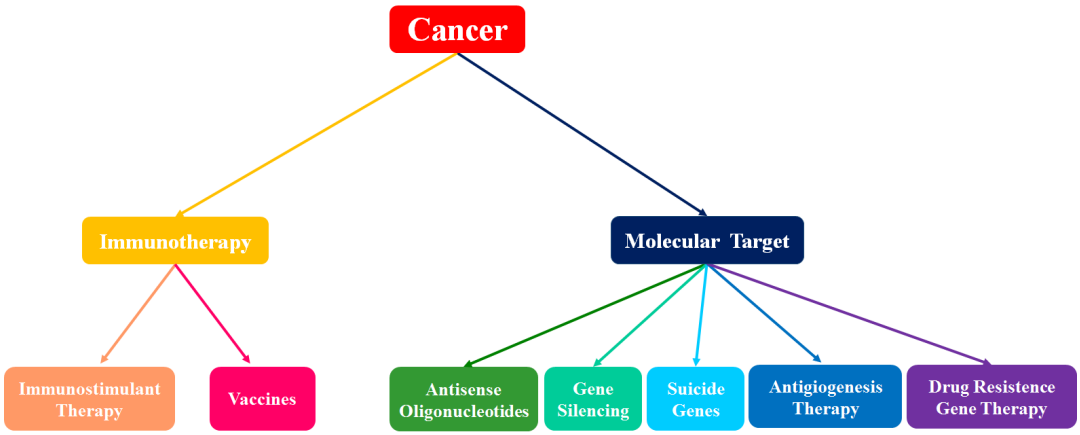

Fig.1 Most used approach for cancer gene therapy

1.1. Immunological Approach

Immunotherapy relies upon the enhancement of the immune system to target genes and vaccines and destroy cancer cells. Tumor cells are immunogenic, due to the secretion of immunosuppressive factors, the down-regulation of antigen expression and the lack of co-stimulation [7], so the normal immune response is not enough strong to eradicate cancer [8]. In this light, vaccine and immune-enhancement therapies have been proposed as immunomodulatory approaches against cancer. Both strategies rely on agents able to modulate the immune response to a desired level by potentiating or suppressing the tumor-induced immunologic tolerance [6]. Immune-enhancement therapy focuses on *checkpoints-molecules* located on certain immune cells that need to be activated (or inactivated) to start an immune response [9]. Common co-stimulatory molecules used in gene cancer therapy are cytokines such as Interleukin-12, leading to the activation of T lymphocytes and natural killer cells [10]. Conversely, one of the first inhibitory checkpoint molecules to be clinically targeted was Cytotoxic T-Lymphocyte-Associated protein 4 (CTLA-4). When the binding site of CTLA-4 on the lymphocytes is occupied, their cytotoxic action is inhibited [11]. Vaccination acts by inducing or increasing the specific recognition of tumor cells by the immune system that, therefore, is trained to respond and more effectively fight against malignant cells [12]. Gene based-vaccines and cell based-vaccines have been designed and developed. Gene based-vaccines consist in

the direct injection of tumor antigen encoding genes able to discriminate between healthy and cancer cells, while cell based-vaccines are antigen-presenting cells, which are manipulated *ex vivo* to enable a tumor antigen action [12].

1.2. Molecular Approach

Molecular approaches in gene therapy rely in the activation or inhibition of oncogenes, correction or silencing of mutated genes, use of antiangiogenesis or drug resistance genes, induction of cell cycle arrest or cell apoptosis. Below, a brief explanation of the most used strategies is reported.

1.2.1. Antioncogenes Strategy

Antioncogenes, as antisense or antigene oligonucleotides, are short nucleic acid segments that can bind to a specific sequence of the RNA or DNA, resulting in the inhibition of the oncogene activity [13]. Antisense oligonucleotides approach is based on the use of antisense oligonucleotides (AON), synthetic single stranded strings of nucleic acids that bind to RNA and thereby alter or reduce its expression, resulting in the inhibition of oncogenes [14]. When inserted into the cell, antisense oligonucleotides block the transduction at ribosome level, inducing the degradation and inhibition of proteins with proliferative action. The main drawback is that the genetic error needs to be corrected in all the tumor cells. Antigene oligonucleotides approach concerns the binding to the DNA, resulting in a non-functional triple helical structure and a block of gene expression at the transcription stage [15].

1.2.2. Gene Silencing Strategy

Gene silencing is a process of gene expression down-regulation, which finds its best expression in RNA interference (iRNA) therapeutic strategy [16]. iRNA is mediated by small interfering RNAs (siRNAs), which are intracellularly generated from double stranded RNA (dsRNA), through the cleavage activity of a ribonuclease III-type protein. siRNA interacts with RNA-induced silencing complex (RNA induced silencing transduction) and guides it to identify a complementary strand to degrade and silence the gene target [16]. The only limitation of this therapeutic strategy is the low availability of siRNA after systemic administration, due to the enzymatic degradation, phagocytosis, kidneys filtration and subsequent elimination.

1.2.3. Suicide Gene Strategy

The suicide gene strategy is based on the introduction into malignant cells of a viral or a bacterical gene, which allows the expression of an enzyme able to convert non-toxic prodrug into a lethal drug, causing cell death in directly or indirectly way [17]. p53 protein is the most studied cellular switch able to induce apoptosis. Suicide gene strategy makes cancer cells more vulnerable and sensitive to chemotherapy, improving its safety and effectiveness [18].

1.2.4. Antiangiogenesis Gene Therapy

Cancer tissue proliferation is associated with angiogenesis, providing the necessary nutrients to cancerous cells. Hence, antiangiogenesis gene therapy, which interferes with this process, could produce interesting therapeutic effects at the tumor site [19]. Both physiological and pathological angiogenesis are characterized by an increased release of proangiogenic cytokines from endothelial cells. Therefore, endothelial growth factor (VEGF), fibroblast growth factor (FGF), interleukin 4 (IL-4) and interleukin 8 (IL-8) could represent the main target of gene therapy [20]. Antiangiogenesis gene therapy is carried out not only by inhibition of angiogenic inducers, but also through the use of either angiogenic inhibitors such as angiostatin and endostatin, or cytotoxic drugs, like interferon and interleukin-12 [20]. Compared to conventional gene therapies, antiangiogenesis gene therapy shows a low systemic toxicity and the absence of drug resistance phenomena, whereby it represents a promising anticancer treatment [19].

1.2.5. Drug-Resistance Gene Therapy

A further approach of cancer gene therapy includes the prevention of the toxic effects of anticancer drugs by transferring the drug resistance genes into normal cells, making them resistant to chemotherapies [21]. This strategy avoids the toxic levels of drugs occurring in traditional chemotherapy and minimizes the appearance of side effects in healthy cells.

2. Vectors for cancer gene therapy

The success of gene therapy depends on the efficiency of gene transduction, which in turn is related to the chemical-physical properties of the carrier used to vehiculate and deliver the genetic material. An ideal vector for GT must possess some specific requirements: it should protect the nucleic acids from enzymatic degradation by nucleases and preserve small molecules, such as siRNA, from renal elimination. Moreover, it might promote the permeation of the nucleic acids across cell membranes, which is hindered by the electrostatic repulsions between the negatively charged groups of the genetic material and the membrane phospholipids [22]. Furthermore, the vector must be adequate to the gene size and the amount and duration of its product expression. Currently, gene therapy vehicles can be categorized into the two following groups: biological and non-biological systems (Fig. **2**) [23].

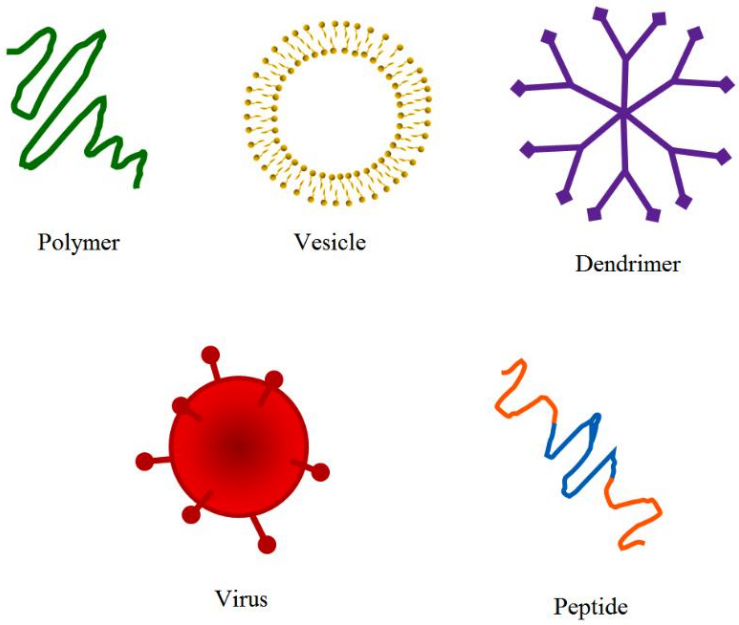

Fig. 2 Schematic representation of principal vectors for cancer gene therapy.

2.1. Biological Vectors

Biological carries are viruses, which naturally infect cells and transfer their genetic materials into the host cells. The advantages related to the use of these vectors rely in the prompt availability of natural and efficient systems for the insertion of DNA into the cells. Indeed, they have a high transfection efficiency in contrast to the non-viral vectors. Viruses used for this purpose are synthetically modified to eliminate their pathogenicity and retain their high efficiency in gene transfer. Obviously, viruses are immunogenic, difficult to modify, and with limited loading capacity [24]. Viruses used as gene vectors are divided into two classes ac-cording to survival and replication mechanisms. The first class includes the non-lytic viruses, such as retroviruses and lentiviruses, which produce virions leaving cells intact, while the second class consists of lytic viruses, such as adenoviruses and herpes simplex viruses, which destroy the infected cells after their replication and virions formation [25]. The non-lytic viruses (single stranded DNA) present several drawbacks such as the relatively small amount of genetic information that can be packaged into the vector, the uncontrolled integration of the virus into the genome, leading to a theoretical risk of mutations, and the possibility of homologous recombination between vectors and endogenous retroviruses, resulting in replication-competent new viruses [25]. Instead, double stranded DNA viruses (lytic viruses) have a higher packaging capacity and transfectability, but conversely, their immunogenicity makes repeated applications very problematic, due to the lack of integration into the cellular genome, leading to the loss of genetic information [24].

2.2. Non-biological Vectors

Cationic polymers, peptides, cationic lipids and vesicles represent the non-biological or non-viral vectors for cancer gene therapy [26-28]. These carriers present less limitations than the viral gene carriers, even if their efficiency is lower. They have been reported to possess high loading capacity and be very versatile vectors, because they may be designed and modified to enhance specificity [29]. In addition, they are biodegradable, low toxic and immuno-genic. They show a lower activation of complement than the viral vectors. Generally, non-viral carriers possess a positive charge promoting the complexation with the negative phosphate groups of the nucleic acids, and determining non-specific interactions with plasmatic proteins such as opsonines, which results in a rapid elimination and a reduction of their half-life [30]. This disadvantage is normally overcome by the use of cationic PEGylate molecules, which provide steric protection to the carriers [31]. This review analyses the potential of cationic nanocarriers in cancer gene therapy, focusing on the role of liposomes and niosomes as multi-functional vesicular devices and giving an exhaustive collection of the most representative investigations.

3. Cationic vesicles for gene delivery

3.1. Liposomal and Niosomal Nanocarriers

Gene therapy has become a promising approach for treating cancer by including not only therapeutic genes but also designing efficient and effective gene delivery systems [6]. Among non-viral vectors, liposomes and niosomes have been widely investigated and proposed as the most promising strategy [23]. Both systems are formed from the self-assembly of amphiphilic molecules in an aqueous environment, resulting in closed bilayer structures delimiting an internal aqueous core. Liposomes consist of phospholipid bilayers, whereas niosomes are constructed from surfactant molecules. Niosomes have greater stability, lower costs, higher availability and reduced purity problems than liposomes [32]. Due to their structure, these vesicular systems are able to encapsulate both hydrophilic molecules in the internal aqueous core and lipophilic sub-stances into the bilayer, compartment. They have been successful used as drug delivery systems to achieve controlled release, drug targeting and permeation enhancement [32]. Liposomes and niosomes improve the circulation, the distribution and the stability of loaded drugs and enhance the drug therapeutic efficacy [33]. These vesicular carriers were firstly proposed in cancer treatment by Gregoriadis and collaborators from 1974 [34], while their introduction in gene therapy came only 13 years later with the work of Felgner [35]. Since 1987 increased efforts have been made to develop of carriers for a more efficient delivery of nucleic acids, in both animals and humans [36].

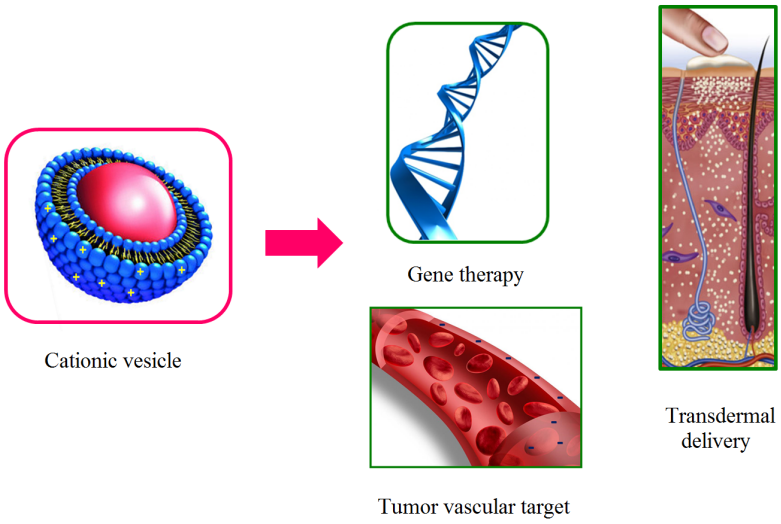

Fig. 3 Peculiarity of cationic vesicles exploitable in cancer treatments: ability to load genetic material, affinity for tumor vasculature and promotion of drug permeation across skin.

3.2. Versatility of Cationic Vesicles in Cancer Treatment

Essential requirement for liposomes and niosomes as effective tool for gene delivery is the presence of a positive charge on the vesicles surface. In fact, several researchers have outlined that cationic vesicles (CV) possess better physical-chemical characteristics for both gene and anticancer drug delivery than anionic and neutral carriers [37]. Cationic vesicles can form complexes with anionic genetic molecules and deliver them into cells via the endosomal pathway [38]. In particular, CV enter cells by adsorption/fusion with the cell membrane or endocytosis, and deliver the genetic material into the cell cytoplasm [39].

Positive charged nanocarriers have been reported to deliver therapeutic genes and cytotoxic drugs specifically to the tumor vasculature, rich in anionic glycoproteins, phospholipids and proteoglycans (Figure 3) [40]. This strategy, called neovascular therapy, was very successful also because angiogenesis is a consistent feature of tumors [41, 42]. Additionally, the slow and irregular blood flow in tumor vessels favour the interactions between the cationic carriers and anionic sites on the vasculature, whereby the development of devices that exhibit affinity to the cancer vasculature could improve drug/gene therapeutic effects by increasing its concentration at the tumor site [43-45]. Moreover, positive effects on skin permeation have been also reported by cationic vesicles [46]. Skin surface bears a net negative charge due to the presence of negatively charged molecules into the lipid layer of the stratum corneum, so positive charges at the vesicle surface could enhance the permeation rate of drugs and genes through the skin [47].

Unfortunately, cationic vesicles are far from to be ideal carriers, as several drawbacks have been found: fast elimination from blood, some cytotoxicity due to their positive charge, and non-specific interactions with cell components, serum

proteins and enzymes [48]. In order to overcome these inconvenients, several modifications have been done to improve their properties. The size, charge and surface characteristics of liposomes can be easily altered through the inclusion of specific compounds (helper lipids, stimuli-sensitive lipids) in the formulations by surface modifications. Aggregation of cationic carriers limits their interaction with blood proteins or blood cells, whereby PEGylation (or other procedures claimed to provide stealth properties), may be considered an efficient approach to avoid this inconvenient, and extend their half-life [49]. Stealth-cationic vesicles represent a potential solution to drawbacks associated with cationic lipoplexes while conjugation with targeting molecules has been reported to improve specific delivery [50-53].

3.3. Cationic Vesicles-Mediated Gene Delivery

In vivo complexes made of cationic vesicles-nucleic acid have been administered via numerous delivery routes including intravenous, intramuscular, intraperitoneal, subcutaneous, transdermal and mucosal route [54]. Compared to viral vectors, CV can be used to transfer DNA of unlimited size; moreover, they are simple and quick to formulate and possess low immunogenicity [55, 56].

Cationic vesicles-mediated gene delivery depends on numerous factors including composition, that strongly affects physical-chemical characteristics of vesicles such as size, charge, morphology, bilayer elasticity and pharmaceutical effectiveness [57]. It was reported that the transfection efficiency can be enhanced by varying the type and amount of cationic lipids and surfactants used in the preparation [58]. Generally, cationic amphiphilic molecules used as transfection reagents consist of a hydrophobic group, such as alkyl or fatty acid chains, and a positively charged head group, which is essential for binding nucleic acid phosphate groups, resulting in nucleic acids condensation [59]. The control or modification of the CV physical - chemical properties can be carried out through the synthesis of new cationic lipids or, more preferably, by mixing different commercial lipid molecules, avoiding additional and complicated chemical preparation steps [31, 60, 61]. As gene carriers, cationic niosomes are usually prepared from mixtures of single chain surfactant molecules, such as sorbitan fatty acid esters, polyoxyethylenesorbitan fatty acid ester, cholesterol, polyoxyethyl-ene alkyl ethers and quaternary ammonium compounds [62, 63].

3.3.1. Preparation Methods

Cationic vesicles can be produced through several methods, including ethanol injection (EI), detergent dialysis (DD) and thin film hydration (TF), but not all methods are feasible for gene loaded nanocarrier formation.

Ethanol injection is a simple vesicles formulation method based on the injection of ethanol-dissolved lipids into an aqueous phase to form liposomes or niosomes [64].

Clearly, EI is more efficient in encapsulating ethanol soluble molecules and since genetic material is neither lipophilic or ethanol-soluble, this method is not the best way to produce cationic vesicles for a later complexation with nucleic acids [65].
The detergent dialysis method consists in the conversion of a mixed micelles solution into bilayered vesicles, after detergent removal from the solution [66]. DD has been reported to be effective in encapsulating lipophilic drugs within its forming bilayer, and it is often used for production of lipoplexes [67, 68]. However, the most common method to produce vesicles is the thin film hydration, obtained by adding an aqueous solution to an adsorbed lipid film, which causes its detachment and to self-assembly in bilayer vesicles [69]. Both hydrophilic and lipophilic substances can be easily located in the inner aqueous core or in the lipophilic domain of the bilayer, respectively, making TF the most efficient and appropriate method for gene loading. Additionally, reverse phase evaporation (REV) and asymmetric vesicles formation (AVF), have been proposed to improve the encapsulation of large oligonucleotides [70]. REV vesicles are produced by introducing a drug aqueous solution into an organic phase containing lipids and sonicating this mixture to produce small drops of aqueous phase in the organic solvent. The amphiphilic lipids locate at the interface and, after organic phase evaporation, they form vesicles containing an aqueous core [71]. On the other site, AVF is an inverse emulsion method and has been used to encapsulate genetic material [72]. In this case, vesicles are prepared by producing reverse micelles around water drops within an oil phase. Afterwards these micelles are passed through a lipid monolayer that forms the outer vesicular layer, giving bilayer vesicles. This procedure allows to control the bilayer composition (as the inner and outer layers are added separately) and include additional functionality only outside the vesicles [72]. Unfortunately, the use of organic solvents during reverse phase evaporation and asymmetric vesicles formation could have adverse effects on the stability of oligonucleotides, and any residual solvent could introduce toxicity [73]. Recently, Yang and collaborators have carried out a comparative study on preparative methods of cationic lipoplexes, demonstrating that, among REV, EI and TF, the thin film hydration represents the best lipoplexes formation method in terms of quality and stability of the formulation [65]. Similar results were obtained by Levine *et al*., who found that TF method was best for gene encapsulation giving a higher yield and avoiding the use of organic solvents [74].

3.3.2. Physical-Chemical Characterization Methods

Quantification of genetic material encapsulated into liposomes or niosomes is basic for the evaluation of the lipoplexes pharmacological performances. Several methods have been proposed and used, but as most cationic vesicles do not need purification, no final quantification is required [74]. DNA content can be quantified by measuring the activity of radioactive labelled nucleotides, but the convenience of this methods limited by the associated risk of radio-active exposure [75]. Instead, PicoGreen DNA quantification method exploits the difference in fluorescence intensity before and

after vesicles disruption mediated by Triton X-100 [76]. PicoGreen is an intercalating dye, so proteins do not interfere with the resulting measurements [77]. Also, UV spectrophotometric analysis is classified as common DNA quantification tool, but it is not often used because it does not distinguish between DNA and RNA and it is sensitive to contaminations from lipids and surfactants [78, 79]. Additionally, several inconsistencies were found between PicoGreen analysis and UV absorbance measurement [80]. To over-come the limitations related to the most used quantification methods, covalently labelled RNA/DNA or fluorescently labelled DNA have been proposed [81, 82].

4. Recent advances in cationic vesicles-mediated gene delivery.

Cationic liposomes can be used as non-viral vectors for gene therapy due to their ability to easily promote complexation with nucleic acids, forming lipoplexes that are capable of transporting these nucleic acids into cells. In the late 80's a study by Felgner e al. [35] reported, for the first time, the ability of cationic liposomes to efficiently form complexes with DNA and transfect the COS-7 cell line. This study helped to understand the potential of liposomes for gene therapy. Felgner's lipoplexes were prepared starting from small unilamellar liposomes based on N-[1-(2, 3- dioleyloxy) pro-pyl-N, N, N-trimethylammonium chloride (DOTMA) after spontaneous interaction with DNA. This procedure gave large DNA aggregates surrounded by thin lipidic fibers, or condensed DNA coated by lipid bilayers, with a 100% DNA loading [35]. The dynamics of the lipoplex formation is not well known, but it has been demonstrated that the lipid packing parameters determines the structural organization. The lipoplex is obtained by the addition of a solution of cationic liposomes to an aqueous solution of DNA. The electrostatic interactions between negatively charged phosphate groups of the nucleic acid molecules, and the positively charged liposomes, drive the spontaneous formation [83]. These interactions lead to nucleic acid charge neutralization, and are followed by the disruption of liposomes and the condensation of nucleic acid molecules into lipoplexes. Ross and Hui [84], in 1999, reported that the lipoplex structure does not look like that of small unilamellar liposomes from which they derive. Lipoplexes consist of hydrated DNA layers alternating with cationic lipid bilayers (Fig. **4A**). A structural variant consists of a reverse hexagonal phase in which the DNA is allocated in the aqueous core (Fig. **4B**) [85]. magnetic cationic liposomes, giving a considerable drug accumulation at the tumor site, under magnetic field guidance. More recently, non-ionic surfactants have been incorporated into cationic liposomes bilayers as helper components for the delivery of plasmid DNA and oligodeoxyribonucleotides. Huang *et al*. pre-pared modified cationic liposomes with sorbitan monoesters and *in vitro* cellular uptake experiments showed that Span plays an important role in increasing the cellular uptake of encapsulated oligonu-cleotides [100]. In particular, the authors observed that cationic liposomes modified with Span 40 significantly facilitated the cellular uptake by COS-7 and HeLa cells and showed

some positive effects on gene expression. The same research group proposed polysorbate-based cationic niosomes by TF method as gene carriers [62]. These formulations included non-ionic surfactants (Tween®) and a modified cationic cholesterol. The cationic cholesterol, as a membrane additive, offers positive charges useful to bind genetic material and facilitate the access to the negative cellular membrane, improving intracellular transfer. Tween surfactants, particularly Tween 85, gave great stability to vesicles, high efficiency of gene transfer and strong bio-compatibility.

Zhou *et al*. [101] designed new surfactant vesicles for the delivery of siRNA. This novel vector, made of non-ionic surfactant, Span 80, DOTAP, and TPGS, was compared with DOPE/DOTAP and Span 80/DOTAP. Obtained data showed that the Span 80-based formulation was 6-fold more active than DOPE formulation in siRNA delivery.

Paecharoenchai *et al*. [102] obtained vesicular systems from Span 20, cholesterol, and novel synthesized spermine-based cationic lipids with different acyl chain length (C14, C16 and C18). The highest transfection efficiency, as well as the low cytotoxicity and the minimum haemolytic effect *in vitro,* was obtained by sper-mine-C18 based niosomes.

Sarker *et al*. [103] prepared cationic liposomes from synthesized hydrochloride salt arginine-based cationic lipids and trifluoroacetic acid salt arginine-based cationic lipids, without helper lipids. The transfection efficiency and the cytotoxicity of the arginine-based vesicles were evaluated on neuronal and human cervical cancer cells. Researchers observed that the counter ions in the arginine head groups did not influence the morphology of lipoplexes. In particular, the pDNA acted as a bridge among the cationic membranes and also stabilized the condensed lamellar phase.

Several studies have suggested that there is a simple and direct correlation between structure and transfection efficiency. Zuhorn *et al*. [86] have shown that formation of the hexagonal phase in lipoplexes (following interaction with anionic lipids) is essential for the translocation of nucleic acids across endosomes into the cytoplasm. Caracciolo *et al*. [87], however, have demonstrated that DO-TAP/DOPE/cholesterol liposomes with a multilayer structure in-crease the transgene expression in ovary adenocarcinoma cells, 4 folds more than compared with DC-Chol/DOPE liposomes. On the contrary, other researchers have demonstrated that DC-Chol/DOPE complexes transfect human tracheal epithelial cells more efficiently than other cationic lipid-DNA complexes [88]. It should be noted that the interactions of lipoplexes with cellular membrane lipids may result in a structural organization different from the original structure. Several studies have shown that the presence of helper lipids improved the transfection efficiency of liposomes and decreased the cytotoxicity associated with the high positive charge [58, 89-91]. For instance, helper or neutral lipids, such as DOPE, DOPC, Chol and MO, are often included in formulations to improve the characteristics of liposomes. These lipids were found able to change the liposome lamellar phase into a non-lamellar phase [92]. The

structured phases are able to promote fusion with endosomal mem-branes and destabilization of lipoplexes during transfection [93]. In particular, Yang *et al*. [65] developed cationic liposomes based on DOPE and 3β- [N-(N', N'-dimethylaminoethane) carbamoyl] cholesterol (DC-Chol). The samples were prepared with different methods, (TF, RPE and EI). through Morphology, particle size and zeta potential of the resulting samples were investigated. Samples by TF method showed better stability within 2 months, without aggregation at size increase and higher zeta potential values. On the basis of regression equations and response surface models, authors identified the optimal formulation giving the highest encapsulation efficiency [65]. Different gene delivery systems were developed starting from DOTAP or DC-CHOL in combination with other lipids including DPPC, DOPE, EPC and DPPE by Ramezani *et al*. in 2009 [94]. Researchers observed that DOTAP: DPPE, DC-CHOL: DOPE and DOTAP: DOPE: DPPE formulations showed the highest transfection activity.

An in-depth study on the influence of preparation methods on the lipoplexes characteristics were performed by Levine *et al*. [74] Liposomes and pDNA-encapsulated liposomes were prepared with DPPC, DPPE-PEG2000, and cholesterol with three different methods: TF, REV and AVF, pDNA concentration was determined by measuring activity from radioactively labelled pDNA. TF was evaluated the best preparation method as REV method provided no advantage over the TF in terms of overall pDNA yield, and the use of organic solvents could give adverse effects and toxicity concerns.

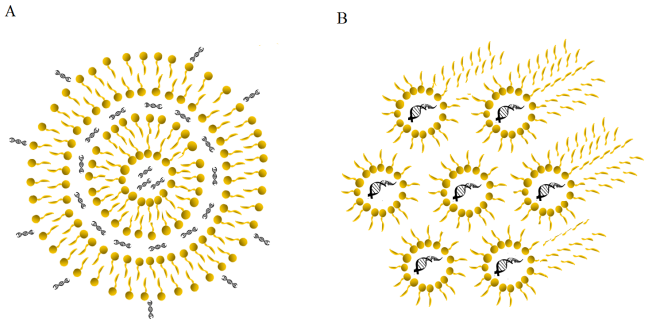

Fig. 4 Schematic representation of structure lipid-DNA arrangement in lipoplex: A complexed lamellar; B complexed reverse hexagonal structure.

It is worthy to note that the presence of uncomplexed cationic vesicles may influence the transfection activity and cytotoxicity, so formulations must be controlled by finely tuning the lipid film composition. This procedure implies modifications of positive/negative charge ratio. Sample may contain uncomplexed cationic liposomes. These vesicles may compete with lipoplexes for binding/uptake the cells, and give additional toxicity [95]. Therefore, in order to maximize the overall pDNA encapsulation, the lipid concentration should be increased, while in order to

minimize the number of uncomplexed carriers within the formulation, higher pDNA and lower lipid concentrations should be used [74].

One limitation for *in vivo* applications of lipoplexes is their short half-life, which decreases the possibility of liposomes to reach their site of action. The optimization of lipoplexes has been made by the inclusion of functionalities at the liposomes surface. A common method to increase the half-life of liposomes involves their surface modification with inert and biocompatible polymers, such as polyethylene glycol (PEG). PEG can be used to coat the vesicles surface, reducing the peripheral liposome charge and the proteins binding. As a consequence, the liposome recognition by opsonins decreases, avoiding clearance, increasing circulation time and reducing toxicity [96].

Nicolazzi *et al*. [97] prepared cationic lipoplexes inserting PEG-lipids into bilayers. In this case, PEG was not used to stabilize the particles by steric repulsions, since the stabilization was readily maintained by the cationic charges of complexes, but it was the shielding compound for preventing interactions with seric proteins. This strategy allowed authors to get lipoplexes with a lower blood clearance, a higher accumulation and a gene expression in the lung. Another approach relies in the simultaneous delivery of drug and gene in tumor treatments.

An exhaustive example was reported by Kang *et al*. [98], who combined hydrophobic drug and siRNA for the treatment of multidrug resistance in cancer. In this study the authors studied the co-delivery of anticancer small interfering RNA (siRNA) and a chemical MEK inhibitor using cationic liposomes, and they observed an increase of anticancer activity both *in vitro* and *in vivo*. Recently, a synergic combination between hydrophobic drug and pDNA for applications in cancer immunotherapy as well as for the enhancement of tumor was reported by Peng *et al*. [99]. Researchers developed a targeted thermosensitive co-delivery system based on magnetic cationic liposomes loaded with doxorubicin and SATB1-shRNA and evaluated its antitumor effect against gastric cancer both *in vitro* and *in vivo*. The results suggested that gene delivery efficiency and doxorubicin release could be improved with magnetic cationic liposomes, giving a considerable drug accumulation at the tumor site, under magnetic field guidance.

More recently, non-ionic surfactants have been incorporated into cationic liposomes bilayers as helper components for the delivery of plasmid DNA and oligodeoxyribonucleotides. Huang *et al*. prepared modified cationic liposomes with sorbitan monoesters and *in vitro* cellular uptake experiments showed that Span plays an important role in increasing the cellular uptake of encapsulated oligonucleotides [100]. In particular, the authors observed that cationic liposomes modified with Span 40 significantly facilitated the cellular uptake by COS-7 and HeLa cells and showed some positive effects on gene expression.

The same research group proposed polysorbate-based cationic niosomes by TF method as gene carriers [62]. These formulations included non-ionic surfactants (Tween®) and a modified cationic cholesterol. The cationic cholesterol, as a

membrane additive, offers positive charges useful to bind genetic material and facilitate the access to the negative cellular membrane, improving intracellular transfer. Tween surfactants, particularly Tween 85, gave great stability to vesicles, high efficiency of gene transfer and strong biocompatibility.

Zhou *et al*. [101] designed new surfactant vesicles for the delivery of siRNA. This novel vector, made of non-ionic surfactant, Span 80, DOTAP, and TPGS, was compared with DOPE/DOTAP and Span 80/DOTAP. Obtained data showed that the Span 80-based formulation was 6-fold more active than DOPE formulation in siRNA delivery. Paecharoenchai *et al*. [102] obtained vesicular systems from Span 20, cholesterol, and novel synthesized spermine-based cationic lipids with different acyl chain length (C14, C16 and C18). The highest transfection efficiency, as well as the low cytotoxicity and the minimum haemolytic effect *in vitro,* was obtained by sper-mine-C18 based niosomes. Sarker *et al*. [103] prepared cationic liposomes from synthesized hydrochloride salt arginine-based cationic lipids and trifluoroacetic acid salt arginine-based cationic lipids, without helper lipids. The transfection efficiency and the cytotoxicity of the arginine-based vesicles were evaluated on neuronal and human cervical cancer cells. Researchers observed that the counter ions in the arginine head groups did not influence the morphology of lipoplexes. In particular, the pDNA acted as a bridge among the cationic membranes and also stabilized the condensed lamellar phase.

Experimental results indicated that larger carriers showed elevated transfection efficiency, because of their higher contact with the cells, confirming that lipoplexes physical-chemical properties strongly affected the lipoplexes performance.

ABBREVIATIONS

Chol	Cholesterol
CV	Cationic vasicle
DC-Chol	3 β-[N-(N',N'-dimethylaminoethane)carbamoyl] cholesterol
DD	Detergent dialysis
DOTMA	N-[1-(2, 3- dioleyloxy)propyl-N, N, N-trimethylammonium chloride
DOPE	1, 2-dioleoyl-sn-glycero-3-phosphoethanolamine
DOPC	Dioleoylphosphatidylcholine
DOTAP	1, 2-dioleoyl-3-trimethylammonium-propane
DPPC	1, 2-dipalmitoyl-sn-glycero-3-phosphocholine
DPPE	1, 2-dipalmitoyl-sn-glycero-3-phosphoethanolamine
DPPE-PEG2000	N-(Carbonyl-methoxypolyethyleneglycol 2000)-1, 2-distearoyl-sn-glycero-3-phosphoethanolamine, sodium salt
EI	Ethanol injection
EPC	Egg L-α-phosphatidylcholine
GT	Gene therapy
MO	Monoolein
TF	Thin film hydration
TPGS	D-α-tocopheryl polyethylene glycol-1000 succinate

References

[1] Amer MH. Gene therapy for cancer: present status and future perspective. Mol Cell Ther 2014; 2: 27.

[2] Bertram JS. The molecular biology of cancer. Mol Aspects Med 2000; 21: 167-223.

[3] Levine AJ. p53, the cellular gatekeeper for growth and division. Cell 1997; 88: 323-31.

[4] Li Y, Li B, Li CJ, et al. Key points of basic theories and clinical practice in rAd-p53 (Gendicine ™) gene therapy for solid malignant tumors. Expert Opin Biol Ther 2015; 15: 437-54.
[5] Tazawa H, Kagawa S, Fujiwara T. Advances in adenovirusmediated p53 cancer gene therapy. Expert Opin Biol Ther 2013; 13: 1569-83.
[6] El-Aneed A. Current strategies in cancer gene therapy. Eur J Pharmacol 2004; 498: 1-8.
[7] Hanahan D, Weinberg RA. Hallmarks of cancer: the next generation. Cell 2011; 144: 646-74.
[8] Oettgen HF, Old LJ. The history of cancer immunotherapy, In: DeVita VT, Hellmann S, Rosenberg SA, Eds. Biological Therapy of Cancer: Principles and Practice. JB Lppincott Co, Philadelphia, PA, 1991; 87-119.
[9] Sharma P, Allison JP. Immune checkpoint targeting in cancer therapy: toward combination strategies with curative potential. Cell 2015; 161: 205-14.
[10] Saudemont A, Buffenoir G, Denys A, et al. Gene transfer of CD154 and IL12 cDNA induces an anti leukemic immunity in a murine model of acute leukemia. Leukemia 2002; 16: 1637-44
[11] Tarhini AA, Iqbal F. CTLA-4 blockade: therapeutic potential in cancer treatments. Onco Targets Ther 2010; 3: 15-25.
[12] Guo C, Manjili MH, Subjeck JR. Therapeutic cancer vaccines: past, present and future. Adv Cancer Res 2013; 119: 421-75.
[13] Emily Guo X, Ngo B, Sandaldjian Modrek A, et al. Targeting tumor suppressor networks for cancer therapeutics. Curr Drug Targets 2014; 15: 2-16.
[14] Castanotto D, Stein CA. Antisense oligonucleotides in cancer. Curr Opin Oncol 2014; 26: 584-89.
[15] Lila MAM, Siew JSK , Zakaria H, et al. Cell Targeting in Anti-Cancer Gene Therapy. Malays J Med Sci 2004; 11: 9-23.
[16] Lam JK., Chow MY, Zhang Y, et al. siRNA versus miRNA as therapeutics for gene silencing. Mol Ther Nucleic Acids 2015; 4: e252.
[17] Duarte S, Carle G, Faneca H, et al. Suicide gene therapy in cancer: where do we stand now? Cancer letters 2012; 324: 160-70.
[18] Zarogoulidis P, Darwiche K, Sakkas A, et al. Suicide gene therapy for cancer-current strategies. J Genet Syndr Gene Ther 2013; 4.
[19] Gardlik R, Celec P, Bernadic M. Targeting angiogenesis for cancer (gene) therapy. Bratisl Lek Listy 2011; 112: 428-34.
[20] Gasparini G, Harris AL. Does improved control of tumor growth require an anti-cancer therapy targeting both neoplastic and intratumoral endothelial cells? Eur J Cancer 1994; 30A: 201-6.
[21] Workman P, Al-Lazikani B, Clarke PA. Genome-based cancer therapeutics: targets, kinase drug resistance and future strategies for precision oncology. Curr Opin Pharmacol 2013; 13: 486-96.
[22] Seth P. Vector-mediated cancer gene therapy: an overview. Cancer Biol Ther 2005; 4: 512-7.
[23] El-Aneed A. An overview of current delivery systems in cancer gene therapy. J Control Release 2004; 94: 1-14.
[24] Luo J, Luo Y, Sun J, et al. Adeno-associated virus-mediated cancer gene therapy: Current status. Cancer Lett 2015; 356: 347-56.
[25] Kotterman MA, Chalberg TW, Schaffer DV. Viral vectors for gene therapy: Translational and clinical outlook. Annu Rev Biomed Eng 2015; 17: 63-89.
[26] Nayerossadat N, Maedeh T, Abbas- Ali P. Viral and nonviral delivery systems for gene delivery. Adv Biomed Res 2012; 1: 27.
[27] Pardakhty A, Moazeni E. Nano-niosomes in drug, vaccine and gene delivery: a rapid overview. Nanomed J 2013; 1: 1-12.

[28] Silva JPN, Oliveira, ACN, Casal M, et al. DODAB: monooleinbased lipoplexes as non-viral vector for transfection of mammalian cells. Biochim Biophys Acta 2011; 1808: 2440-9.
[29] Ramamoorth M, Narvekar A. Non viral vectors in gene therapy- an overview. J Clin Diagn Res 2015; 9: GE01-GE06.
[30] Shim G, Kim M-G, Park JY, et al. Application of cationic liposomes for delivery of nucleic acids. Asian J Pharm Sci 2013; 8: 72-80.
[31] HuangY, Chen J, Chen X. , et al. PEGylated synthetic surfactant vesicles (Niosomes): novel carriers for oligonucleotides. J Mater Sci Mater Med 2008; 19: 607-14.
[32] Abdelkader H, Alani AW, Alany RG. Recent advances in non-ionic surfactant vesicles (niosomes): self-assembly, fabrication, characterization, drug delivery applications and limitations. Drug Deliv 2014; 21: 87-100.
[33] Moghassemi S , Hadjizadeh A . Nano-niosomes as nanoscale drug delivery systems: an illustrated review. J Control Release 2014; 185: 22-36.
[34] Gregoriadis G, Wills EJ, Swain CP, et al. Drug-carrier potential of liposomes in cancer chemotherapy. Lancet 1974; 1: 1313-6
[35] Felgner PL, Gadek TR, Holm M, et al. Lipofection: a highly efficient, lipid-mediated DNA transfection procedure. Proc Natl Acad Sci USA 1987; 84: 7413-17.
[36] Perez-Herrero E, Fernandez-Medarde A. Advanced targeted therapies in cancer: Drug nanocarriers, the future of Chemotherapy. Eur J Pharm Biopharm 2015; 93: 52-79.
[37] Gao X, Huang L. Cationic liposome-mediated gene transfer. Gene therapy 1995; 2: 710-22.
[38] Simoes S, Filipe A, Faneca H, et al. Cationic liposomes for gene delivery. Expert Opin Drug Deliv 2005; 2: 237-54.
[39] Noguchi A, FurunoT, Kawaura C, et al. Membrane fusion plays an important role in gene transfection mediated by cationic liposomes. FEBS Letters 1998; 433: 169-73.
[40] Abu-Lila A, Suzuki T, Doi Y, et al. Oxaliplatin targeting to angiogenic vessels by PEGylated cationic liposomes suppresses the angiogenesis in a dorsal air sac mouse model. J Control Release 2009; 134: 18-25.
[41] Lila ASA, Ishida T, Kiwada H. Targeting anticancer drugs to tumor vasculature using cationic liposomes. Pharm Res 2010; 27: 1171-83.
[42] Allen TM, Cullis PR. Liposomal drug delivery systems: from concept to clinical applications. Adv Drug Deliv Rev 2013; 65: 36-48.
[43] Krasnici S, Werner A, Eichhorn ME, et al. Effect of the surface charge of liposomes on their uptake by angiogenic tumor vessels. Int J Cancer 2003; 105: 561-7.
[44] Campbell RB, Ying BO, Kuesters GM, et al. Fighting cancer: from the bench to bedside using second generation cationic liposomal therapeutics. J Pharma Scie 2009; 98: 411-29.
[45] Gabizon A, Papahadjopoulos D. Liposome formulations with prolonged circulation time in blood and enhanced uptake by tumors. Proc Natl Acad Sci 1998; 85: 6949-53.
[46] Song Y-K, Kim C-K. Topical delivery of low-molecular-weight heparin with surface-charged flexible liposomes. Biomaterials 2006; 27: 271-80.
[47] Katahira N, Murakami T, Kugai S, et al. Enhancement of topical delivery of a lipophilic drug from charged multilamellar liposomes. J Drug Target 1999; 6: 405-14.
[48] Knudsen KB, Northeved H, Ek PK, et al. *In vivo* toxicity of cationic micelles and liposomes. Nanomed Nanotechnol Biol Med 2015; 11: 467-77.
[49] Xin L, Cao J, Cheng H, et al. Stealth cationic liposomes modified with anti-CAGE single-chain fragment variable deliver recombinant methioninase for gastric carcinoma therapy. J Nanosci Nanotechnol 2013; 13: 178-83.
[50] Levine RM, Scott CM, Kokkoli E. Peptide functionalized nanoparticles for non viral gene delivery. Soft Matter 2013; 9: 985-1004.
[51] Pangburn TO, Petersen MA, Waybrant, B, et al. Peptide- and aptamer-functionalized nanovectors for targeted delivery of therapeutics. J Biomech Eng 2009; 131: 074005.

[52] Shroff K, Kokkoli E. PEGylated liposomal doxorubicin targeted to α5β1-expressing MDA-MB-231 breast cancer cells. Langmuir 2012; 28: 4729-36.
[53] Garg A, Kokkoli E. pH-Sensitive PEGylated liposomes functionalized with a fibronectin-mimetic peptide show enhanced intracellular delivery to colon cancer cells. Curr Pharm Biotechnol 2011; 12:1135-43.
[54] Templeton NS. Cationic liposome-mediated gene delivery *in vivo*. Biosci Rep 2002; 22: 283-95.
[55] Schmidt-Wolf GD, Schmidt-Wolf IG. Non-viral and hybrid vectors in human gene therapy: an update. Trends Mol Med 2003; 9: 67-72
[56] Niculescu-Duvaz D, Heyes J, Springer CJ. Structure-activity relationship in cationic lipid mediated gene transfection. Curr Med Chem 2003; 10: 1233-61.
[57] Qin G, Geng S, Wang L, et al. Charge influence of liposome on transdermal delivery efficacy. Soft Matter 2013; 9: 5649-56.
[58] Maitani Y, Igarashi S, Sato M, et al. Cationic liposome (DCChol/DOPE= 1: 2) and a modified ethanol injection method to prepare liposomes, increased gene expression. Inter J Pharm 2007; 342: 33-9.
[59] Brown MD, Schatzlein AG, Uchegbu IF. Gene delivery with synthetic (non-viral) carriers. Inter J Pharm 2001; 229: 1-21.
[60] Morille M, Passirani C, Vonarbourg A, et al. Progress in developing cationic vectors for non-viral systemic gene therapy against cancer. Biomaterials 2008; 29: 3477-96.
[61] Manosroi A, Thathang K, Werner, RG, et al. Stability of luciferase plasmid entrapped in cationic bilayer vesicles. Inter J Pharm 2008; 356: 291-9.
[62] Huang Y, Rao Y, Chen J, et al. Polysorbate cationic synthetic vesicle for gene delivery. J Biomed Mat Res 2011; 96: 513-9.
[63] Mamizuka EM, Carmona-Ribeiro AM. Cationic Liposomes as antimicrobial agents. Communicating current research and educational topics and trends in applied microbiology 2007; 2: 636-47
[64] Charcosset C, Juban A, Valour JP, et al. Preparation of liposomes at large scale using the ethanol injection method: Effect of scale-up and injection devices. Chem Eng Res Des 2015; 94: 508-15.
[65] Yang S, Chen J, Zhao D, et al. Comparative study on preparative methods of DC Chol/DOPE liposomes and formulation optimization optimization by determining encapsulation efficiency. Int J Pharm 2012; 434: 155-60.
[66] Dua JS, Rana AC , BhandariAK. Liposome: methods of preparation and applications. Int J Pharm Stud Res 2012; 3: 14-20.
[67] Huang Z, Li X, Zhang T et al. Progress involving new techniques for liposome preparation. Asian J Pharma Scie 2014; 9: 176-82.
[68] Tros de Ilarduya C, Sun Y, Dü zgü nes N. Gene delivery by lipoplexes and polyplexes. Eur J Pharm Sci 2010; 40: 159-70.
[69] Lasic DD. The mechanism of vesicle formation. Biochem J 1988; 256: 1-11.
[70] Szoka F, Papahadjopoulos D. Procedure for preparation of liposomes with large internal aqueous space and high capture by reverse-phase evaporation. Proc Natl Acad Sci USA 1978; 75:4194-8.
[71] Ko YT, Bickel U. Liposome-encapsulated Polyethylenimine/ oligonucleotide polyplexes prepared by reverse-phase evaporation technique. AAPS Pharm SciTech 2012; 13: 373-8.
[72] Whittenton J, Harendra S, Pitchumani R, et al. Evaluation of asymmetric liposomal nanoparticles for encapsulation of polynucleotides. Langmuir 2008; 24: 8533-40.
[73] Cortesi R, Esposito E, Gambarin S, et al. Preparation of liposomes by reverse -phase evaporation using alternative organic solvents. J Microencapsulation 1999; 16: 251-6.
[74] Levine RM, Pearce TR, Adil M, et al. Preparation and characterization of liposome-encapsulated plasmid DNA for gene delivery. Langmuir 2013; 29: 9208-15.

[75] Legendre JY, Szoka FC Jr. Delivery of plasmid DNA into mammalian cells using pH-sensitive liposomes. Pharm Res 1992; 9: 1235-42.
[76] Vonarbourg A, Passirani C, Desigaux L, et al. The encapsulation of DNA molecules within biomimetic lipid nanocapsules. Biomaterials 2009; 30: 3197-204.
[77] Singer VL, Jones LJ, Yue ST, et al. Characterization of PicoGreen reagent and development of a fluorescence-based solution assay for double stranded DNA quantitation. Anal Biochem 1997; 249: 223-38.
[78] Ausubel FM. Quantitation of DNA and RNA with absorption and fluorescence spectroscopy. Current Protocols in Molecular Biology. Ed John Wiley & Sons, New York, 2001.
[79] Bhat S, Curach N, Mostyn T, et al. Comparison of methods for accurate quantification of DNA mass concentration with traceability to the International System of Units. Anal Chem 2010; 82: 7185-92.
[80] Holden MJ, Haynes RJ, Rabb SA, et al. Factors affecting quantification of total DNA by UV spectroscopy and PicoGreen fluorescence. J Agric Food Chem 2009; 57: 7221-26.
[81] Tagawa T, Manvell M, Brown N, et al. Characterisation of LMD virus-like nanoparticles self-assembled from cationic liposomes, Adenovirus core peptide Mu and plasmid DNA. Gene Ther 2002; 9: 564-76.
[82] Holladay C, Keeney M, Newland B, et al. A reliable method for detecting complexed DNA *in vitro*. Nanoscale 2010; 2: 2718-23.
[83] Silva JPN, Coutinho PJG, Oliveira MECDR. Characterization of monoolein-based lipoplexes using fluorescence spectroscopy. J Fluoresc 2008; 18: 555-62.
[84] Ross PC, Hui SW. Lipoplex size is a major determinant of *in vitro* lipofection efficiency. Gene Ther 1999; 6: 651-9.
[85] Safinya CR. Structures of lipid-DNA complexes: supramolecular assembly and gene delivery. Curr Opin Struct Biolo 2001; 11: 440-8.
[86] Zuhorn IS, Bakowsky U, Polushkin E, et al . Non bilayer phase of lipoplex-membrane mixture determines endosomal escape of genetic cargo and transfection efficiency. Mol Ther 2005; 11: 801-10.
[87] Caracciolo G, Pozzi D, Caminiti R, et al. Structural characterization of a new lipid/DNA complex showing a selective transfection efficiency in ovarian cancer cells. Europ Phys J 2003; 10: 331-6.
[88] Colosimo A, Serafino A, Sangiuolo F, et al. Gene transfection efficiency of tracheal epithelial cells by DC-Chol-DOPE/DNA complexes. Biochim Biophys Acta (BBA)-Biomembranes 1999; 1419: 186-94.
[89] Balazs DA, Godbey WT. Liposomes for use in gene delivery. J Drug Deliv 2010; 2011.
[90] Silva JPN, Oliveira MR, Coutinho PJG. Characterization of mixed DODAB/monoolein aggregates using Nile Red as a solvatochromic and anisotropy fluorescent probe. J Photoch Photobio A Chem 2009; 203: 32-39.
[91] Hui SW, Langner M, ZhaoYL., et al. The role of helper lipids in cationic liposome-mediated gene transfer. Biophys J 1996; 71: 590.
[92] Madeira C, Loura LM, Prieto M, et al. Liposome complexation efficiency monitored by FRET: effect of charge ratio, helper lipid and plasmid size. Eur Biophys J 2007; 36: 609-20.
[93] Tenchov BG, Wang L, Koynova R, et al. Modulation of a membrane lipid lamellar-nonlamellar phase transition by cationic lipids: A measure for transfection efficiency. Biochim Biophys Acta (BBA)-Biomembranes 2008; 1778: 2405-12.
[94] Ramezani M, Khoshhamdam M, Dehshahri A, et al. The influence of size, lipid composition and bilayer fluidity of cationic liposomes on the transfection efficiency of nanolipoplexes. Colloids Surf B Biointerfaces 2009; 72: 1-5.
[95] Elouahabi A, Ruysschaert JM. Formation and intracellular trafficking of lipoplexes and polyplexes. Mol Ther 2005; 11: 336-47.

[96] Torchilin VP. Recent advances with liposomes as pharmaceutical carriers. Nat Rev Drug Discov 2005; 4: 145-60.
[97] Nicolazzi C, Mignet N, De la Figuera N, et al. Anionic polyethyleneglycol lipids added to cationic lipoplexes increase their plasmatic circulation time. J Control Release 2003; 88: 429-43.
[98] Kang SH, Cho HJ, ShimG, et al. Cationic liposomal co-delivery of small interfering RNA and a MEK inhibitor for enhanced anticancer efficacy. Pharm Res 2011; 28: 3069-78.
[99] Peng Z, Wang C, Fang E, et al. Co-delivery of doxorubicin and SATB1 shRNA by thermosensitive magnetic cationic liposomes for gastric cancer therapy. Plos one 2014; 9: e92924.
[100] Huang YZ, Gao JQ, Chen JL, et al. Cationic liposomes modified with non-ionic surfactants as effective non-viral carrier for gene transfer. Colloids and Surfaces B: Biointerfaces 2006; 49: 158-64.
[101] Zhou C, Mao Y, Sugimoto Y, et al. SPANosomes as delivery vehicles for small interfering RNA (siRNA). Mol Pharm 2011; 9: 201-10.
[102] Paecharoenchai O, Niyomtham N, Leksantikul L, et al. Non ionic surfactant vesicles composed of novel spermine-derivative cationic lipids as an effective gene carrier *in vitro*. AAPS Pharm SciTech 2014; 15: 722-30.
[103] Sarker SR, Aoshima Y, Hokama R, et al. Arginine-based cationic liposomes for efficient *in vitro* plasmid DNA delivery with low cytotoxicity. Int J Nanomed 2013; 8: 1361-75

3.3 Liposomes coated with multifunctional chitosan derivatives as potential carriers of anticancer drugs

Elisabetta Mazzotta[a], Antonia Marazioti[b], Spyridon Mourtas[b], Rita Muzzalupo[a], Sophia Antimisiaris[b,c]

[a] Department of Pharmacy, Health and Nutritional Sciences, University of Calabria, Via Savinio, Ed. Polifunzionale, 87036 Arcavacata di Rende, Italy

[b]Foundation for Research and Technology Hellas, Institute of Chemical Engineering Sciences, FORTH/ICE-HT, Rio 26504, Greece

[c]Laboratory of Pharmaceutical Technology, Department of Pharmacy, University of Patras, Rio 26510, Greece

Submitted on Langmuir

GRAPHICAL ABSTRACT

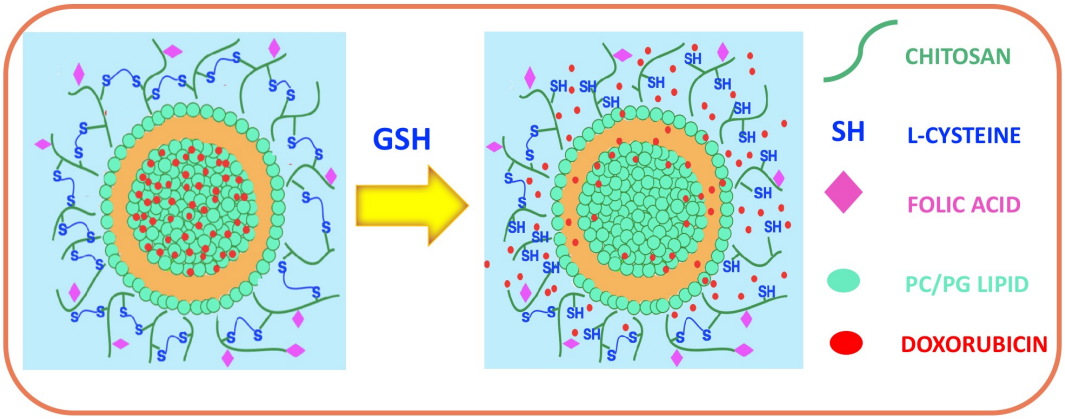

ABSTRACT

Liposomes coated with multifunctional polymers were proposed as innovative platform for tumor targeting drug delivery. Novel Folic-thiolated-chitosan (FTC) derivatives possessing active targeting and redox responsivity ability were developed, characterized and employed to coat liposomes made up of PC:PG:Chol. The physicochemical properties such as size, surface charge and drug encapsulation efficiency were evaluated before and after coating process. The formation of a coating layer on liposomal surface was confirmed by the slight increase of particle size and by the inversion of Zeta-potential values. FTC-coated liposomes showed a redox-dependent drug release profile: good stability at physiological conditions and a rapid release in presence of glutathione. Moreover, their cytotoxic activity after

loading with doxorubicin was evaluated on B16-F10 melanoma cancer cell lines. The results showed an enhanced antitumor efficacy of FTC-coated liposomes compared to chitosan-coated liposomes used as control. The increased cytotoxicity of FTC-coated liposomes could be attributed to higher cellular uptake via Folate receptor-mediated endocytosis and to the triggered drug release by the reductive microenvironment of tumor cells. Therefore, our formulations show great potential as nanocarriers for targeted cancer therapy.

Keywords

Liposomes, Folic acid, Redox responsive, Chitosan, Doxorubicin

1. Introduction

Multi-target drug delivery systems are innovative pharmaceutical devices emerging as one of the most promising challenge in cancer therapy. The major limitation of traditional chemotherapy is the low drug selectivity and the use of supramolecular carriers aiming to modify drug distribution and to improve pharmacokinetic and pharmacodynamic profiles has been extensively reported in literature [1]. Several approaches such as active and passive targeting have been, indeed, studied to achieve a controlled drug release, increased cellular uptake, enhanced drug distribution, prolonged half-life and reduced side effects. Anyway, the expected results were far from optimal and inadequate to obtain clinical efficacy. To further improve drug performance, the design of tailor-made carriers combining several targeting approaches in a single system has been actively pursued in the last years. Smart engineered nanocarriers exhibiting simultaneously multiple tumor targeting properties have shown great promise in clinic and could be used in the near future as tools for personalized cancer therapy. Different strategic combinations have demonstrated a high control of drug release at the site of action and reduced drug leakage avoiding toxic effects on healthy cells [2, 3]. Among the strategies adopted to increase tumor targeting capability, considerable efforts have been paid to the design of stimuli responsive nanodevices. Both biological/endogenous and non-biological/exogenous stimuli are currently investigated as triggers to activate a fast and localized drug release within the interested target site [4]. External stimuli-responsive nanoparticles offer some advantages including spatial, temporal and dose control of the drug release through a remote apparatus that can be switched on and off at will [5]. Common external signals used are temperature [6], magnetic field [7, 8], ultrasound[9] and light[10]. On the other hands, the drug release can also be triggered by specific biological signals of altered microenvironment of cancer cells. Tumors normally present low pH [11], high redox potential [12] and specific proteolytic enzymes [13] and, thus, carriers can be smartly engineered to undergo rapid changes in their structure only under exposure to these conditions. Among the

stimuli investigated for anticancer drug delivery, very interesting results have been achieved with glutathione (L-γ-glutamyl-L-cysteinylglycine, GSH), a natural antioxidant involved in cellular redox homeostasis [14]. GSH represents the major organic reducing agent in the human body protecting the cells from harmful effects of free radicals. Due to the role of GSH in tumor initiation, progression and drug resistance [15, 16], GSH concentrations inside cancer cells (2-20 mM) are, in fact, significantly higher (four-fold) than that in extracellular matrix (2-20 μM) or in normal healthy cells [17]. Therefore, the incorporation in nanocarriers of disulfide linkages cleavable by GSH is ongoing as a promising way to obtain a selective and localized drug release. Notably, disulfide bonds act as controlled gates, thus, preventing the premature drug leakage, decreasing the systemic toxicity and triggering the release only in the redox rich environment of the cancers cells [18]. Moreover, active targeting approach exhibits unique advantages in current cancer therapy. This strategy refers to a selective molecular recognition between ligands on carrier surface and specific receptors on tumor tissues. Many cancer cells, indeed, exhibit overexpression of specific receptors in response to their increased metabolic demand. The specific interaction of modified carriers with cell receptors allows an enhanced drug accumulation in the tumor microenvironment and, subsequently, an improved internalization via receptor mediated endocytosis. A large variety of molecules such as antibodies, proteins, cell penetrating peptides, sugar and small molecules were deeply investigated for active delivery of drugs to cancer tissues [19]. Folic acid (FA) is one of the most popular approaches because its receptors are overexpressed in a wide range of epithelial cancer cells such as ovary, breast, liver, brain, colon, lung and kidney [20] and exhibits high binding affinity with dissociation constant (Kd) < 1 nM [21]. On the contrary, folate receptor shows low expression frequency in normal healthy cells. Folate receptors actively internalize folate conjugated devices via receptor mediated endocytosis. Consequently, the surface functionalization of nanocarriers with folic acid represents an attractive strategy to increase the uptake and accumulation of the chemotherapeutic drug at the tumor site.

Liposomes are nanovesicular systems suitable for the design of multifunctional devices due to their excellent features such as biocompatibility, biodegradability, sustained and controlled release [22,23,24]. Their application in cancer treatment is still limited by various drawbacks related to the premature drug leakage, low physical and chemical stability and non-specific targeting [25,26]. Surface coating of liposomes with biocompatible polymers has been proposed as a potential way to overcome some of these limitations [27,28]. In particular, the coating of liposomes with multi-targeted polymers may be a strategic approach aiming to enhance target specificity towards cancer. A recent study focused on the design of liposomes coated with pH sensitive polymers demonstrated an enhanced anticancer activity and cellular uptake of them [29].

Herein, taking into account all these considerations, we reasoned the design of liposomes coated with polymer combining active targeting and redox-responsivity as innovative platform for intracellular anticancer drug delivery.
To achieve this goals, chitosan, a natural, biocompatible, easily modified (chemically) polymer was selected as starting material. In the first step, the polymer was functionalized with a targeting agent FA and L-cysteine (L-Cys) residues that can be easily oxidized by air to give inter- and intramolecular disulfide bonds. The synthesized polymers were characterized, used to coat Calcein loaded liposomes and the redox-responsive behavior was studied. After confirming the sensitivity to reduced environment, Doxorubicin (Dox), an anthracycline antibiotic with broad-spectrum antitumour activity, was loaded in liposomes and the cytotoxicity of the liposomes coated with the new conjugate was investigated in B16-F10 melanoma cancer cell lines.

2.0 Materials and Methods

Chemicals

Egg phosphatidylocholine (PC), Phosphatidylglycerol (PG) were purchased from Lipoid. Chitosan (low molecular weight), N-cyclohexyl-N-(2-morpholinoethyl) carbodiimide-metho-p-toluenesulfonate, L-cysteine, Folic acid, Doxorubicin hydrochloride, Glutathione, 3-[4,5-dimethylthiazol-2-yl]-2,5 diphenyl tetrazolium bromide and all other reagents used were purchased from Sigma- Aldhrich.

2.1 Preparation of Folic-thiolated-chitosan

Following the scheme shown in Figure 1, Folic-thiolated-chitosan (FTC) conjugates were synthetized through a two step-process. Firstly, L-Cys conjugation to chitosan backbone was achieved via amide formation. Three different thiolated chitosan (TC) derivatives were synthesized and the quantities used are reported in Table 1. Briefly, the carboxylic group on L-Cys was activated by PTCD in demineralized water for 1 hour. Next, CHT was dissolved in acetic acid 1 %(v/v) to obtain a 1% (w/v) polymer solution and added dropwise to the above solution under magnetic stirring. The pH of the reaction mixtures was carefully adjusted to 5 with NaOH 0.5 M. After that, the mixture was reacted in the dark at room temperature under stirring for 4 hours. The resulting solution was extensively dialyzed [molecular weight (MW) cutoff 12 kDa] for 3 days, first against 5 mM HCl, twice against 5 mM HCl containing 1% NaCl, and finally against 1 mM HCl. Finally, the polymers solutions were lyophilized and used for the synthesis of Folic-thiolated-chitosan (FTC).

Conjugate	Chitosan (mg)	L-Cysteine (mg)	PTCD (mM)
TC 1	150	150	50
TC 2	150	300	150
TC 3	150	600	150

Table 1. Amounts of reagents used (± 10%) for the synthesis of TC conjugates with different weight ratios of L-Cysteine.

In the second step, PTCD (0.04 mmol) was added to 2 mg $ml^{-1}$of FA (0.02 mmol) in dimethyl sulfoxide and stirred at room temperature for 1 hour. Then, 100 mg of TC was dissolved in 10 ml of acetic acid 1 % (v/v), added to the above solution and stirred in the dark at room temperature for 16 hours. The mixture was, thus, precipitated leading the pH to 9. The flocculent precipitate was collected and then dialyzed (molecular weight cut-off, 12 kDa) against the excess amount of 0.1 M sodium phosphate buffer (pH 7.4) for 3 days and, then, water for 3 days. Finally, after being freeze-dried, the resulting products were obtained and stored at 4°C until further use. ^{1}H-NMR (400 MHz, D_2O) δ (ppm): 1.97 (s, -$NHCOCH_3$), 2.63 (s, -CH_2SH), 3.07 (s, proton of Glucosamine unit of CHT), 3.25-3.80 (m, proton of Glucosamine unit of CHT), 6.95 (d, aromatic proton of FA), 7.65 (d, aromatic proton of FA), 8.74 (s, aromatic proton of FA).

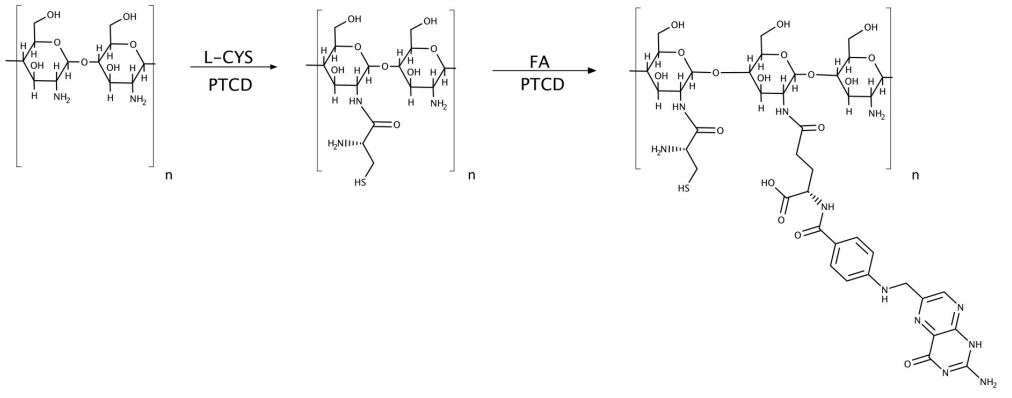

Figure1. Synthesis route of Folic-Thiolated Chitosan. Abbreviations: L-CYS, L-Cysteine; PTCD, N-cyclohexyl-N-(2-morpholinoethyl) carbodiimide-metho-p-toluenesulfonate; FA, Folic Acid.

2.2 Characterization of FTC conjugates

2.2.1 ^{1}H-NMR analysis

^{1}H NMR spectra were recorder at 25°C with a Varian Mercury 400 MHz instrument. The chitosan and three FTC polymers were each dissolved in deuterium oxide (D2O) acidified with 2 % (v/v) trifluoroacetic acid (CF_3COOH). The signals obtained were reported in parts per million.

2.2.2 Quantification of Folic acid

The amount of FA conjugated on CHT was evaluated using UV-Vis spectroscopy, considering its absorption at 285 nm. The conjugates were dissolved in 1 % acetic acid at the concentration of 2×10^{-2} mg/mL and the measurements of the absorbance of these solutions were performed. The FA concentration was calculated on the basis of a standard curve previously plotted from a stock solution of FA dissolved in a 0.1M NaOH solution, from which subsequently dilutions in 1% acetic acid were made in the range 0.2-2×10^{-2} mg/mL.

2.2.3 Determination of thiol and disulfide bond content

The amount of thiol groups on the polymers was determined via iodometric titration [30]. Firstly, a storage iodine solution was prepared at concentration 0.1 M by dissolving 0.63 g of I_2 and 1.93 g of KI in 25 ml of distilled water and diluted just before the assay. Each polymer was hydrated in 0.5 M acetate buffer pH 2.7 in different concentrations (0.5–0.05 mg/ml). Then, 1 ml of starch aqueous solution (1%, w/v) and 1 ml of iodine (1 mmol/l) were added to 2 ml of each sample. Iodine promotes the oxidation of free thiol groups. The excess of iodine reacts with starch giving a blue complex easily measured at 560 nm. The amount of thiol moieties was calculated from a standard curve of L-Cys in a concentration range of 20–70 mol/l. Disulfide bond content was measured after reduction with $NaBH_4$ and conversion to thiol groups. Control samples were elaborated with non-thiolated chitosan.

2.3 Liposomes preparation

Multilamellar (MLV) and small unilamellar (SUV) liposomes made up of PC/PG/Chol 9:1:5 (mol/mol/mol) were prepared by the thin film hydration technique as reported. In brief, accurately weighted amounts of lipid were dissolved in a Chloroform /Methanol (2:1 v/v) mixture in a round-bottom flask. The solvents were evaporated under reduced pressure and constant rotation to form a thin lipid film on the walls of the flask. Hydration of the lipid film was performed adding 1 ml of PBS buffer pH 7.4 at 42°C and applying bath sonication and intensive vortex. The obtained liposomes dispersion, thus, was left to equilibrate for 2 hours at a temperature above the transition temperature of the lipid (42°C) in order to allow complete annealing of any structural defects. SUVs were prepared from MLV applying probe sonication until the formation of clear dispersion. Titanium fragments released from probe as result of the high intensity of sonication were removed by centrifugation at 15000 rpm for 20 min. Finally, the liposome dispersions were stored at 4°C or used immediately.

2.4 FTC coating of liposomes

The coating of liposomes was performed using a polymer/lipid mass ratio equal to 0.1, reported as the best condition to achieve the maximum coating efficiency in a previous work [31]. Firstly, the coating solutions were prepared dissolving the polymers in isotonic acetate buffer (pH 4.4). The exact phospholipid content of the liposomes was measured by the Stewart assay in order to know the concentration of polymer solution necessary to achieve FTC/PC equal to 0.1 (mass ratio). The polymer solution was added dropwise into liposomes dispersion at equal volume, under continuous stirring for 1 hour. CHT-coated liposomes in the same conditions were prepared as control.

The coating efficiency (CE%) of the liposomes was determined as the ratio between the phospholipid content within the FTC-coated liposomal fraction and the total phospholipid content of liposomes. For this, the FTC-coated liposomes were subjected to centrifugation at 14.000 rpm for 20 min until complete sedimentation of the coated liposomes. The phospholipid concentration before and after centrifugation was determined by the Stewart assay. Thus, CE % was calculated using the following equations:

$$CE.\% = \frac{lipid\ content\ in\ pellet}{lipid\ content\ before\ the\ centrifugation} \times 100$$

2.5 Liposomes physicochemical characterization

2.5.1 Stewart assay

The lipid concentration of the liposomes dispersions was measured by the Stewart assay [32] based on the formation of a colored complex between phospholipids and ammonium ferrothiocyanate (485 nm). Firstly, the Stewart reagent was prepared by dissolving 27.03 g of $FeCl_3$ 6 H_2O and 30.4 g of ammonium thiocyanate in 1 L of double distilled water. Then, 20 µL of each liposomal suspension were mixed with 2 mL of Stewart reagent and 2 mL of $CHCl_3$. The resulting mixture was intensively vortexed for extraction of the lipid complex in the organic phase and, after that, centrifuged at 4000 rpm for 5 min. The lipid concentration was calculated on the basis of a standard curve prepared with known amount of each phospholipid.

2.5.2 Size distribution and Zeta potential measurements

The liposomes size and distribution before and after coating were measured by dynamic light scattering (DLS) technique (Malvern Nano-Zs; Malvern Instrument, UK) at 25 °C and an angle of 173°. The Polydispersity Index (P.I.) was used as a measure of the size distribution. P.I. less than 0.3 indicates a homogenous and monodisperse population in the case of colloidal systems [33]. Zeta potential was also measured at 25 °C by the same instrument using the Doppler electrophoresis technique.

2.6 *In vitro* redox responsive release studies

To evaluate the redox responsive nature of the designed liposomes, the release experiments were performed in presence or absence of GSH in order to simulate the intracellular compartment of cancer cells and the physiological environments. Calcein, a water soluble and fluorescent probe was used as release molecule and Calcein-loaded SUV liposomes were initially prepared as above described using a buffered solution containing Calcein in a quenched concentration (100 mM). Calcein liposomes were separated from non-entrapped drug by gel filtration on a Sephadex G-50 (1 cm × 30 cm) column eluted with PBS buffer. Subsequently the liposomes were coated using a 0.1 (w/w) FTC/lipid ratio by the method mentioned above. CHT-coated liposomes were also prepared and their release profiles were evaluated in the same conditions.

Aliquots of liposomes suspension were placed in dialysis bags (0.5 mL), manipulated before use (Visking dialysis tubes, 20/30 cut-off: 12,000–14,000 Da) and suspended in 20 mL of phosphate buffer saline (PBS, pH 7.4) with or without 10 mM GSH at 37 °C. At prescribed time intervals, 2 mL of the release medium were withdrawn maintaining the volume of the receptor compartment with an equal volume of fresh solution. The total amount of drug in the withdrawn samples was determined by the quantitative fluorescence spectrophotometric method (emission wavelength: 470 nm, excitation wavelength: 520 nm). The results were presented in terms of cumulative release as a function of time. All drug release studies were carried out in triplicate.

2.7 *In vitro* cytotoxicity assay

The cytotoxic effects of empty liposomes coated with new polymers were evaluated towards Human Embryonic Kidney 293 (HEK-293) cells using the 3-[4,5-dimethylthiazol-2-yl]-2,5 diphenyl tetrazolium bromide (MTT) dye test (cell viability) The cells were grown in RPMI medium (Gibco) supplemented with penicillin-streptomycin (100mg/ml), and 10% heat-inactivated FBS, at 37 °C, 5% CO2/saturated humidity. For the assay, the cells were seeded at a density of 5 $x10^4$ cells/ml in 24-well tissue culture plates for 24 h to allow the adhesion of the cells. The culture medium was, then, replaced with fresh medium and the different liposomal formulations were added at final polymer concentration of 0.6 and 1.8 µg/ml. After 3 h, the cells were washed and incubated with fresh medium for other 45 h. Untreated HEK-293 cells were used as control. At the end of the incubation time, 50 µl of MTT tetrazolium salt (5 mg/ml dissolved in PBS) were added to each well and the cells were incubated at 37°C and 5% CO_2 for additional 4 h, to allow the formation of violet formazan crystals. Acidic isopropanol (500 µl) was added to solubilize the formazan crystals in the cells. Viable cells (%) were calculated based on the formula (A570sample - A570background)/(A570control -A570background) x 100, where A570control is the OD-570 nm of untreated cells and A570background the OD-570 nm of MTT without cells.. Values of cell viability are expressed as the

mean of at least three different experiments ± S.D.

2.8 Doxorubicin Liposomes: Preparation and evaluation of anticancer activity.

Dox was loaded into the liposomes using the active loading technique. According to this method, PC/PG/Chol liposomes were prepared in ammonium sulfate ([NH4]2SO4, 120 mM) instead of PBS, as described above. The un-trapped external ammonium sulfate was removed by ultracentrifugation at 40000 rpm for 2 h and, then, the pellet was resuspended in PBS pH 7.4. Subsequently, a Dox solution (0.2 mg/mL) was added to the liposomes at a 7:1 phospholipid/ Dox weight ratio and incubated at 60 °C for 1 hour protected from the light. Finally, the liposomes were firstly purified from non-encapsulated drug by ultracentrifugation (40.000 rpm for 1 h) and then coated as described above.

Dox encapsulation in liposomes was determined as the molar ratio of drug over lipid [D/L (μmol/ μmol)] in the Dox encapsulating liposomes. The drug as well as the lipid content of each liposome preparation was measured as described below. For the measurement of the Dox amount, 200 μL of each liposomes dispersion was completely dissolved in 1.98 mL of PBS and 2 mL of Triton 10 %. Then the absorption of Dox at 481 nm wavelength was recorded on an UV–vis spectrometer and the concentration was calculated according to the standard curve constructed by standard solutions of Dox in PBS/Triton 10% (linear in the 2.5–40 ppm range). For the measurement of phospholipid concentration, instead, the Stewart assay was used.

The anticancer activity of liposomes coated with target polymer was evaluated in B16-F10 melanoma cancer cells. The cells were seeded at a density of 5 x10^4 cells/ml in 24-well tissue culture plates as above described. The cells were treated with Dox-loaded liposomes at two concentrations; 1 and 3 μM. After 3 h of incubation the cells were washed and incubated with fresh medium foranother 45 h. Values of cell viability are expressed as the mean of at least three different experiments ± S.D.

2.9. Statistical analysis

Data are expressed as mean ± S.D. of at least three independent experiments. Statistical analysis was performed using Student's t-test. P-values ≤ 0.05 were considered statistically significant.

3.0 Results

3.1 Characterization of FTC conjugates

In this study, novel folate redox-responsive chitosan derivatives were designed and characterized. The aim was to combine redox-responsivity and active targeting into a single polymer for improved specificity on targeting cancer cells. FTC conjugates were synthetized in a two-step synthesis pathway by covalent coupling of L-Cys and FA to CHT using the carbodiimide chemistry, as shown in Figure 1. ^{1}H-NMR and UV-vis spectroscopy were performed to characterize the chemical structure of the

resultant materials. The ^{1}H-NMR spectra of FTC conjugates showed a new peak at 2.63 ppm corresponding to methylene protons on $–CH_2SH$ confirming the successful L-Cys conjugation. Moreover, the appearance of peaks at 8.74 ppm, 7.65 ppm, 6.95 ppm which correspond to the aromatic ring of folate revealed the effective incorporation of this targeting molecule in CHT backbone. The successful FA conjugation was also confirmed by UV-vis spectroscopy. In fact, the typical absorption peak of FA at 280 nm was clearly observed and the content of FA conjugated resulted be 59.70± 4.60, 28.16 ± 1.04 and 45.85 ± 4.92 μmol /g polymer respectively for FTC1, FTC2 and FTC3. Iodometric titration was used to evaluate the free thiol groups and disulfide bonds content in the polymers and the results of quantitative assay are reported in Table 2. As can be observed, the highest degree of conjugation was achieved using a polymer:L-Cys ratio of 1:4 . Moreover, the 41.13%, 33.53% and 62.00% of the total amount of thiol groups were oxidized to the disulfide during conjugation process respectively for FTC1, FTC2 and FTC3 (Table 3) .

Conjugate	CHT:L-Cys:FA Ratio (wt:wt:wt)	-SH free total (μmol/g polymer)	-S-S bond (mol/g polymer)
FTC1	1:1:0.1	90.2 ± 4.5	37.0 ± 1.9
FTC2	1:2:0.1	122.0± 6.1	41.0 ± 2.1
FTC3	1:4:0.1	160.0± 7.9	99.2 ± 4.8

Table2. Amount of thiol groups and disulfide bonds grafted on chitosan obtained by iodine titration method.

3.2 Characterization of liposomes

Redox-responsive nanodevices were obtained by coating traditional liposomes made up of PC:PG:Chol with the multi-functional polymers synthetized. The physical polymer coating can give to liposomes some attractive features, such as an improved stability accompanied by prolonged circulation times and resistance to macrophage uptake, redox-responsivity and active targeting properties. Several studies were carried out in order to confirm the effective formation of a coating layer on liposomes surface and to evaluate its effect on vesicles physicochemical characteristics since are key aspects that contribute to the overall behavior of the systems *in vitro* and *in vivo.* The mean diameters, P.I. and Zeta-potential of liposomes before and after the coating are given in Tables 3. The designed liposomes showed a specific distribution size depending on the presence or absence of the coating layer. In fact, uncoated liposomes had a mean size ranged between 57.35 nm and 134.10 nm with a polydispersity index (PI) always ≤ 0.3 indicating a narrow size distribution. The

coating process, as expected, induced a slight increase in the vesicle size without negatively affecting the characteristics of the systems. The designed liposomes have an average diameter smaller ≤ 400 nm as shown in Table 3. This smaller size is a desirable feature for anticancer delivery systems since it is a crucial parameter in influencing their stability *in vivo*. Commonly, liposomes with small size are associated to extended bioavailability compared to larger liposomal formulations and higher tumor accumulation through EPR effect [34]. The mean diameter of liposomes coated with plain CHT was higher than FTC-coated ones. This could be explained by the presence in the new conjugate of disulfide bonds among thiol groups located close on different polymer chains. These intermolecular linkages may lead to decrease the vesicles size and the development of a dense and compact structure. positive nature of polymers employed which indicates successful conjugation on liposomes surface. The presence of a polymer coating on liposome surfaces was also confirmed by the inversion of the Zeta potential from negative to positive values. Uncoated liposomes showed a Zeta potential equal to -20.9 ± 1.1mV, while the polymer-coated liposomes had a Zeta potential ranged between +27.8 ± 0.4 and +31.2 ± 0.1 mV. The shift in Zeta potential towards positive side can be ascribed to particles leading, thus, a high stability of the systems designed with no appearance sedimentation and coagulation in 3 months. Moreover, the positive nature of the designed liposomes may improve their vascular targeting ability and tumor accumulation thanks to the electrostatics interactions with anionic molecules in the tumor microvasculature such as proteoglycans, glycoproteins and anionic phospholipids [35]. The coated polymer over liposome ratio is a key parameter to evaluate the coating ability. The CE% values measured for PC/PG/Chol liposomes coated using CHT resulted be 77.58% in good agreement to previous study [31]. In the case of new conjugates, the CE% was found to be 94.39%, 91.23 % and 88.47 % respectively for FTC1, FTC2 and FTC3 indicating a better coating ability compared to CHT.

Formulation	Size (nm)	P.I.	Zeta-potential (mV)
EMPTY LIPOSOMES			
Non-coated	80.10 ± 4.60	0.233	-20.9 ± 1.1
Chit-coated	157.40 ± 31.09	0.349	+29.2 ± 2.1
FTC1-coated	92.58 ± 10.85	0.306	+ 32.3 ± 2.9
FTC2-coated	120.90 ±9.41	0.222	+27.8 ± 0.4
FTC3 coated	103.60 ± 2.80	0.280	+31.2 ± 01
CALCEIN LIPOSOMES			
Non-coated	57.35 ± 0.78	0.221	-11.5 ± 0.4
Chit-coated	135.20 ± 3.44	0.281	+ 29.6 ± 3.7
FTC1-coated	104.20 ±1.61	0.334	+38.2 ± 1.0
FTC2-coated	89.37 ± 2.34	0.267	+17.8 ± 3.9
FTC3-coated	83.12 ± 4.65	0.352	+ 17.7 ± 4.5
DOX LIPOSOMES			
Non-coated	134.10 ± 1.35	0.260	-14.1 ± 1.5
Chit-coated	400.90 ±15.37	0.380	+ 25.6 ± 4.8
FTC1-coated	162.50 ± 3.93	0.326	+ 29.5 ± 2.2
FTC2-coated	225.04 ±17.33	0.324	+ 21.5 ± 0.8
FTC3-coated	159.92 ± 4.07	0.205	+27.9 ± 1.2

Table 3. Physicochemical properties (hydrodynamic diameter, polydispersity index and Zeta-potential) of empty, Calcein and Dox liposomes based on PC/PG/Chol before and after coating with CHT and FTC polymers.

3.3 *In vitro* release studies

Extended drug retention in blood circulation and triggered release at the target site are important items to achieve in order to develop an optimal intracellular drug delivery system. To this end, the physical coating of liposomes with polymers containing disulfide bonds has been proposed in this work. The disulfide bonds in

surface coating should be able to reduce drug leakage during blood circulation and allow a selectively and quickly payload release triggered by the presence of reducing agents in tumor microenvironment. We decided, thus, to perform the release studies using GSH as reducing agent. The experiments were carried out in PBS pH 7.4 in presence and absence of 10 mM of GSH considering the concentrations of reducing agents in the cancer cell cytosol and in the extracellular matrix/blood plasma, respectively. The release profiles of Calcein used as model molecule from FTC-coated liposomes are shown in Figure 2. It is clearly proved that the release rates were markedly influenced by GSH. The drug release at pH 7.4 was very low indicating a high stability of disulfide bonds in the polymer backbone at physiological conditions. The presence of intermolecular disulfide linkages protects the drug against premature leakage and maximizes its location on the site of application. On the contrary, in presence of GSH the trend was already different since the first hour. The Calcein release was significantly greater throughout the investigated time range in reductive conditions predicting a rapid release in reduced cytoplasm of cancer cells. This faster and sustained drug release can be attributed to cleavage of disulfide linkages due their sensitivity to GSH. These formulations satisfied, thus, basic requirements of redox-responsive delivery systems for cancer therapy: drug retention during circulation and promoted release in response to reductive stimuli. In particular, the three different polymers showed a different ability to minimize the drug release at physiological conditions. The drug release at pH 7.4 resulted to be inversely proportional to the amount of disulfide bond present in the polymer chains. These results clearly suggested that FTC-coated liposomes may control drug release in a redox-responsive manner. A control experiment using liposomes coated with CHT with neither disulfide bonds nor FA ligands was also performed under similar conditions. Calcein release from control liposomes did not exhibit GSH dependence. In fact, similar release kinetics in presence and absence of GSH were obtained. The current results confirmed our expectations and suggest that the presence of disulfide linkages could make nanocarriers highly stable before reaching tumor site but allow a complete and accelerated release after uptake in the redox environment of cancer cells.

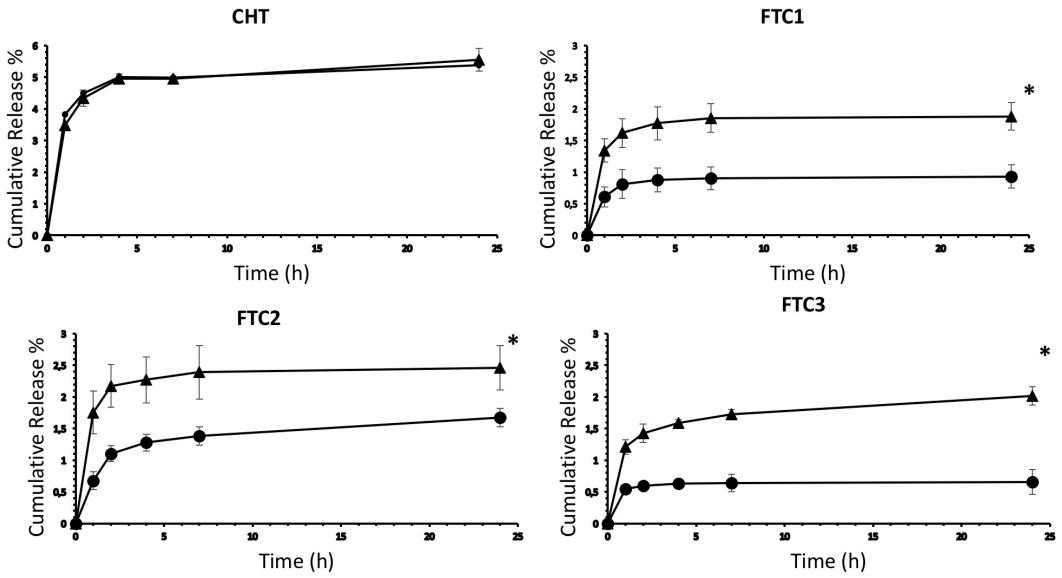

Figure 2. Redox-triggered release of Calcein from polymer coated liposomes in phosphate buffer pH 7.4 in absence (●) and presence of GSH 10 mM (▲) at 37 °C (mean ± standard deviation, n =3). CHT coated liposomes were used as a reduction insensitive control. In all cases, each value represents the mean ± S.D. of three independent experiments. At every sampling time, percentage of drug released in GSH 10 mM medium was statistically different ($p < 0.05$) from that recorded in medium without GSH.

3.4 *In vitro* evaluation of coated liposomes toxicity

Biocompatibility studies of liposomes coated with multifunctional polymers were performed by evaluating the cytotoxicity to HEK-293 cells. Blank polymer coated liposomes were tested in the 0.6 to 1.8 μg/mL polymer concentration range. As shown in Figure 3a, HEK-293 cells treated showed cell viability ~ 90% at all tested concentrations after 48 h indicating a good biocompatibility and non-toxic nature of FTC polymers.

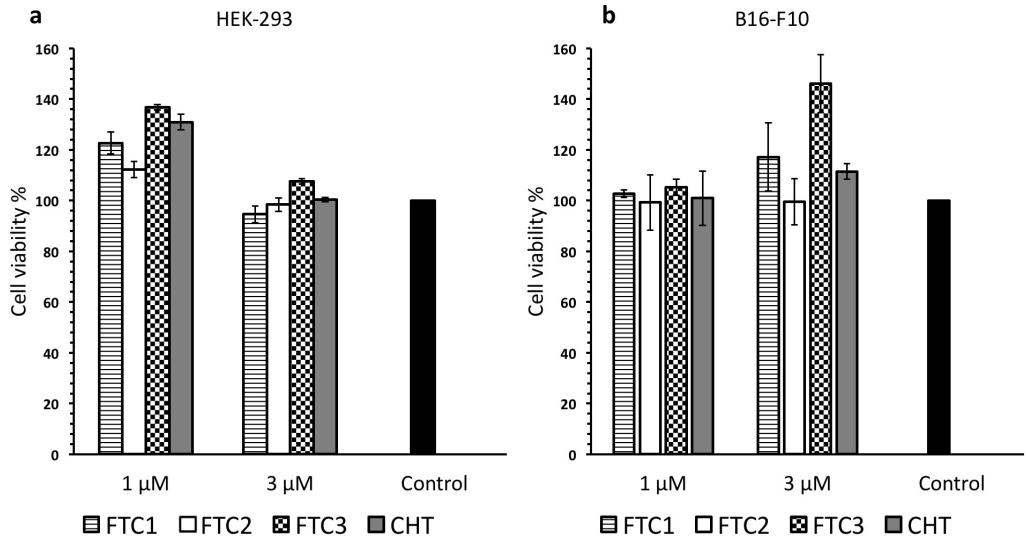

Figure 3. Biocompatibility assessment of empty polymer coated liposomes towards a) HEK-293 and b) B16-F10 cells after 48 h at different doses, which correspond to the doses of vesicles required to have DOX concentrations of 1.0 and 3.0 µM.

3.5 Dox-Loaded liposomes: physicochemical characterization and anticancer activity

At this point, we decided to evaluate the potential anticancer activity of these multifunctional liposomes by loading Dox, a potent anticancer agent.

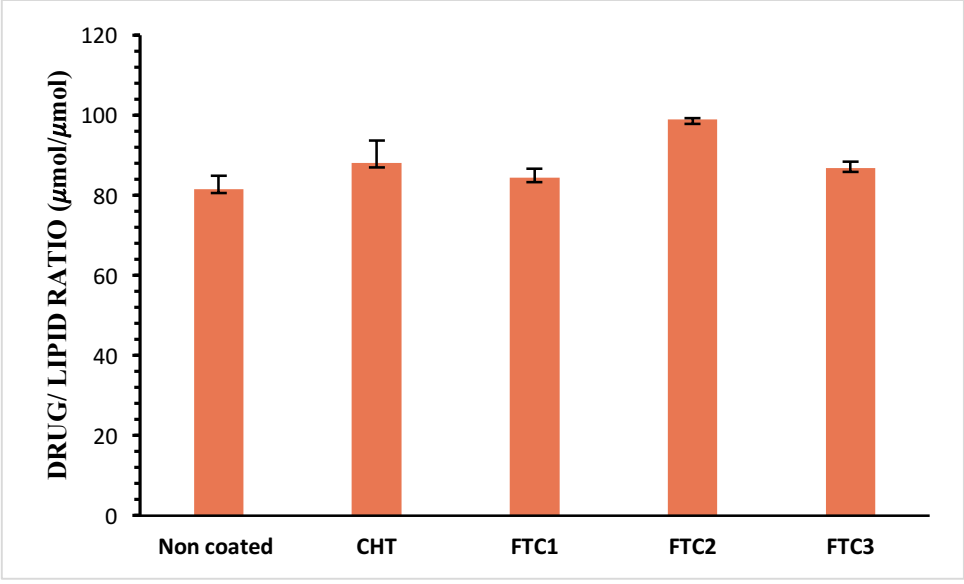

Figure 4. Dox encapsulation efficiency determined as the molar ratio of drug over lipid [D/L (µmol/ µmol)] of uncoated and coated liposomes.

Firstly, the drug was loaded in liposomes by the active loading method and, after, the coating process was performed.
The sizes of drug-loaded vesicles before and after coating were small enough to extravasate from the blood into the tumor interstitial space (Table 3).
The liposomes showed good capability in loading Dox and any leakage of encapsulated Dox wasn't observed during the coating process both with CHT and FTC, as shown in Figure 4. On the contrary, higher drug entrapment efficiency was obtained in polymer coated liposomes. This behavior is ascribed to the more compact layers on liposomal surface which prevent the drug lost [36].
B16-F10 cells were selected as models to evaluate the antitumor activity of Dox-loaded liposomes coated with FTC using non-target CHT-coated liposomes as control. To identify the best conditions for anticancer activity evaluation, two different Dox concentrations (1.0 and 3.0 μM) were tested. The results revealed that empty coated-liposomes (both CHT and FTC) were practically non-toxic (cell viability ≥ 88.3% at 48 h) under the conditions applied in the experiments (Figure 3b). On the contrary, a significant reduction of viability was observed in the cells exposed to liposomes coated with FTC and loaded with Dox. In fact, at the highest Dox concentration tested, a better cell-growth inhibition was observed for FTC-coated liposomes than the ones coated with CHT. In detail, the cell survival rate was reduced to 89.61 % after treatment with CHT-coated liposomes, while the value was 42.99, 32.24 and 46.99% with the use of FTC1, FTC2 and FTC3, respectively. This should be attributed to enhanced intracellular uptake by folate receptors and quickly intracellular release of Dox due to the sensitivity to high GSH levels present in cytoplasm of cancer cells.
The obtained results showed an enhancement of anticancer activity was achieved only at the highest Dox concentration (3 μM) used, but not at the lowest one (1 μM). This could be ascribed to the fixed ratio of FTC/Dox in liposomes that lead at higher amount of the new conjugates with targeting properties only with the increase of Dox concentrations. Consequently, a threshold amount of FTC is necessary to confer targeting properties to liposomes. However, it was demonstrated that the targeted liposomes had a higher anticancer activity compared to the non-targeted ones. This suggest that the developed nanoliposomes could penetrate inside the cells via endocytic processes and release the drug in the cytoplasm where GSH level is higher and the disulfide bonds can be broken, facilitating the drug release. Our formulations, thus, could be used in the future as multifunctional devices for controlled release of Dox.

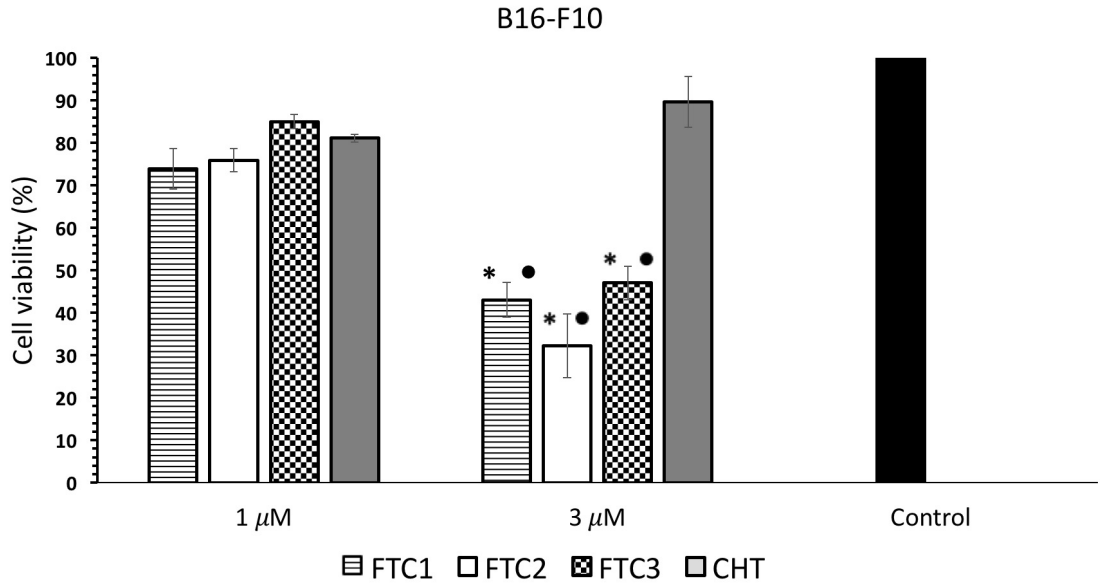

Figure 5 B16-F10 cell viability when exposed to Dox-loaded liposomes coated with different polymers after 48 h. Cell proliferation is expressed as mean ± S.D. of three experiments and as the percentage of the control assumed to be 100%. *p<0.05 vs control; • p<0.05 vs CHT-coated liposomes treated cells.

4.0 Conclusions

In summary, we have developed a multitarget liposomal platform for enhanced intracellular Dox delivery in anticancer therapy. To achieve this goal, novel multifunctional chitosan conjugates were synthetized by simultaneous combination of active targeting and redox responsivity and used to coat liposomal formulations. The designed liposomes showed a GSH dependent drug release profiles and enhanced cytotoxicity towards melanoma cell lines compared to non-target liposomes. We believe that physical coating of liposomes with the developed polymers enhanced tumor specificity of nanodevices and offers a promising approach for smart drug delivery. Anyway, these early results are a promising first step for the development of multi-functional devices and future research work is necessary to be performed to evaluate cellular uptake ability and to test these liposomal systems in animal models to obtain *in vivo* data.

References

[1] S. Senapati, A. K. Mahanta, S. Kumar, P. Maiti, Signal Transduct. Targeted. Ther. 3 (2018)7.

[2] X. Xu, W.H. Xiaoyang, Z. Xueqing, B. Nicolas, F. Omid, Trends Mol. Med. 21 (2015) 223.
[3] L. Tavano, R. Muzzalupo, Colloids Surf. B. 147 (2016)161.
[4] L. Li, W. W. Yang, D. G. Xu, J Drug Target. 27 (2019) 423.
[5] R. Cheng, F. Meng, C. Deng, H. A. Klok, Z. Zhong, Biomaterials 34 (2013) 3647.
[6] E. Mazzotta, L. Tavano, R. Muzzalupo, Pharmaceutics 10 (2018) 150.
[7] A. Skouras, K. Papadia, S. Mourtas, P. Klepetsanis, S. G. Antimisiaris, Eur J Pharm Sci. 15 (2018) 162.
[8] Z. H. Zhao, D. T. Huang, Z. Y. Yin, X. Q. Chi, X. M. Wang, J. H. Gao, J Mater Chem. 22 (2012) 15717.
[9] S. Mullick Chowdhury, T. Lee, J. K. Willmann, Ultrasonography. 36 (2017) 171.
[10] C. S. Linsley, B. M. Wu, Ther. Deliv. 8 (2017) 89.
[11] X. Guo, C. Shi, J. Wang, S. Di, S. Zhou, Biomaterials. 34 (2013) 4544.
[12] A. Raza, U. Hayat, T. Rasheed, M. Bilal, H.M.N. Iqbal, Eur J Med Chem. 157 (2018) 705.
[13] P. P. Deshpande, S. Biswas, V. P. Torchilin, Nanomedicine. 8 (2013) 1509.
[14] D. Liu, F. Yang, F. Xiong, N. Gu, Theranostics. 7 (2016) 1306.
[15] A. Bansal , M. C. Simon, J Cell Biol.2 (2018) 2291.
[16] N. Traverso, R. Ricciarelli, M. Nitti, B. Marengo, A. L. Furfaro, M. A. Pronzato, U. M. Marinari, C. Domenicotti, Oxid Med Cell Longev. 2013 (2013) 972913
[17] Cheng, R.; Meng, F.; Deng, C.; Klok, H. A.; Zhong, Z., Biomaterials 2013, 34, 3647-3657
[18] L. Sha, D. Wang, Y. Mao, W. Shi, T. Gao, Q. Zhao, S. Wang, Nanotechnology 29(2018)
[19] M. Srinivasarao, C.V. Galliford, P. S. Low, Nat. Rev. Drug Discov. 14 (2015) 203.
[20] A. R. Hilgenbrink, P.S. Low, J Pharm Sci. 94(2005) 2135.
[21] J. Lu, W. Zhao, Y. Huang, H.Liu, R. Marquez, R. B. Gibbs, J.Li, R.Venkataramanan, L. Xu, S. Li, S. Li, Mol. Pharmaceutics.11 (2014) 4164.
[22] A. Go´mez-Hens, J.M. Ferna´ndez-Romero, Trends Anal Chem 25 (2006)167.
[23] M. Coimbra, B. Isacchi, L. Van Bloois, J. S. Torano, A. Ket, X. Wu, F. Broere, J. M. Metselaar, C. J. Rijcken, G. Storm, R. Bilia, R. M. Schiffelers, Int J Pharm. 416 (2011) 433.
[24] M. K. Riaz, M. A. Riaz, X. Zhang, C. Lin, K. H. Wong, X. Chen, G. Zhang, A. Lu, Z. Yang, Int J Mol Sci.19 (2018) 195.
[25] M. Grit, J.H. de Smidt, A. Struijke, D. J. A Crommelin, Int J Pharm 50 (1989) 1.
[26] A. Graff, M. Winterhalter, W. Meier, Langmuir 17 (2001) 919.
[27] C. Tan, B. Feng, X. Zhang, W. Xia, S. Xia, Food Hydrocoll. 52 (2016) 774.
[28] R. Li, L. Deng, Z. Cai, S. Zhang, K. Wang, L. Li, S. Ding, C. Zhou, *Mater. Sci. Eng. C 80 (2017) 156.*
[29] L. Yan, S.H. Crayton, J.P. Thawani, A. Amirshaghaghi, A. Tsourkas, Z. Cheng, Small. 11 (2015) 4870.
[30] I. Osuna, D. Teutonico, S. Arpicco, C. Vauthier, G. Ponchel, Int J Pharm. 340 (2007) 173.
[31] M. Zaru, M. L. Manca, A. M. Fadda, S. G. Antimisiaris, Colloids Surf B Biointerfaces. 71(2009) 88.
[32] J. C. M. Stewart, Anal Biochem. 104 (1980) 10.
[33] L. Tavano, L, Gentile, C. Oliviero Rossi, R. Muzzalupo, Colloids Surf. B: Biointerfaces. 110 (2013) 281.
[34] P. P. Deshpande, S. Biswas, V.P. Torchilin, Nanomedicine (Lond). 8 (2013)1509.
[35] A. S. Abu Lila, T. Ishida, H. Kiwada, Pharm. Res. 27 (2010) 1171.
[36] A. Trapani, D. Mandracchia, G. Tripodo, S. Cometa, S. Cellamare, E. De Giglio, P. Klepetsanis, S.G. Antimisiaris, Colloids Surf. B: Biointerfaces. 170 (2018

3.4 Actively targeted and Redox responsive delivery of anticancer drug by chitosan nanoparticles

Elisabetta Mazzotta[a], Selene De Benedittis[b], Antonio Qualtieri[b], Rita Muzzalupo[a]

[a] *Department of Pharmacy, Health and Nutritional Sciences, University of Calabria Via Savinio, Ed. Polifunzionale, 87036 Arcavacata di Rende, Italy*
[b] *Institute for the Research and the Biomedical Innovation(IRIB)-CNR-Mangone (CS)*

Submitted on Pharmaceutics

GRAFICAL ABSTRACT

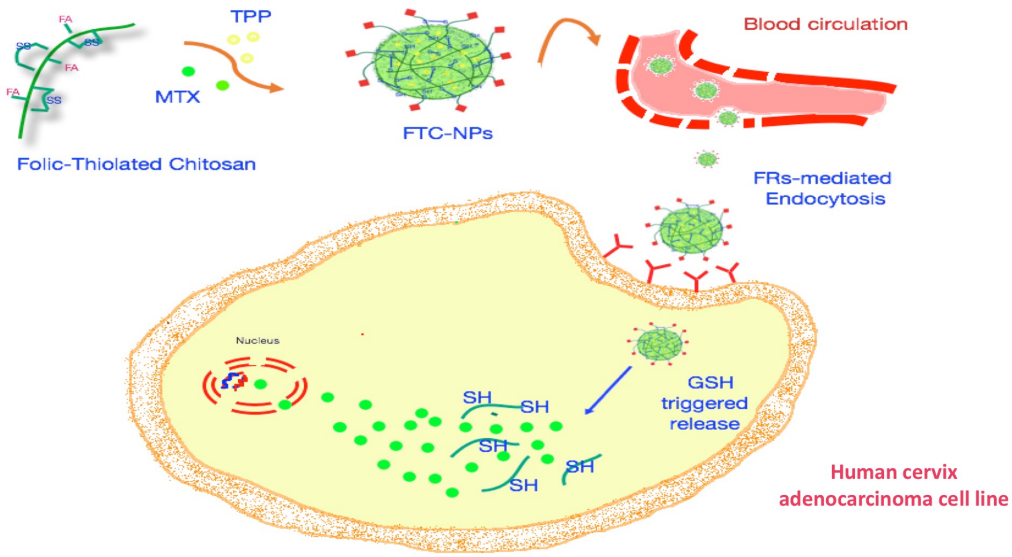

ABSTRACT

The clinical efficacy of Methotrexate (MTX) is limited by the poor water solubility, the low bioavailability and the development of resistance in cancer cells. Herein, we developed novel folate-redox responsive chitosan (FTC) nanoparticles for intracellular MTX delivery. L-cysteine and Folic acid molecules were selected to be covalently linked to chitosan in order to confer it redox responsiveness and actively targeting of folate receptors (FRs). NPs based on these novel polymers could possess tumor specificity and a controlled drug-release due to the overexpression of FRs and high concentration of reductive agents in the microenvironment of cancer cells. NPs were prepared using ionotropic gelation technique and characterized in terms of sizes, morphology and loading capacity. *In vitro* drug release profiles exhibited a GSH dependence: in normal physiological environment, NPs maintained good stability, whereas in a reducing environment similar to tumor cells, the encapsulated MTX was promptly released. The anticancer activity of MTX loaded FTC-NPs was also studied incubating HeLa cells with formulations for various time and

concentration intervals. A significant reduction in viability was observed in a dose and time dependent manner. Particularly, FTC-NPs showed a better inhibition effect on HeLa cancer cell proliferation compared to non-target chitosan based NPs used as control. The selective cellular uptake of FTC-NPs via FRs was evaluated and confirmed by fluorescence microscopy. Overall, the designed NPs provide an attractive strategy and potential platform for an efficient intracellular anticancer drug delivery.

Keyword

Redox-responsive, folate-targeting, chitosan nanoparticles, Methotrexate, intracellular drug release.

1.0 Introduction

Specific, effective and safe intratumoral delivery of active drug is one of the key issues in cancer therapy. Polymeric nanoparticles (NPs) are one of the most promising candidates to achieve this purpose and overcome the drawbacks of traditional chemotherapy. NPs, indeed, have gained increasing attention for their efficacy to improve pharmacokinetics and biodistribution drug profiles with higher degree of selectivity and specificity. NPs have several unique physical and biological properties that allow to target tumors and minimize side effects on healthy tissues [1]. The excellent features of NPs include prolonged systemic circulation, high preferential accumulation at the tumor sites by enhanced permeation and retention effect (EPR) and the ability to overcome P-glycoprotein-mediated multidrug resistance of cancer cells [2]. Among the most commonly used NPs, chitosan (CHT) based NPs play a pivotal role. CHT is a naturally occurring biopolysaccharide that has been extensively explored in pharmaceutical and biomedical fields due to unique biological activities including anti-oxidant, anti-inflammatory, antifungal and antimicrobial activity. This polysaccharide provides a profitable tool for the design of innovative delivery systems due to its biocompatibility, biodegradability, non-toxicity and mucoadhesivity [3]. Another interesting feature that promotes CHT as a promising material for effective drug delivery is its cationic nature. This is a special characteristic from the technological point of view because makes it a suitable material for electrostatic interactions with negatively charged molecules. Indeed, the common method used for NPs preparation is the ionic gelation technique, an easy method based on the electrostatic interaction between the positively charged chitosan chains and anionic crosslinking agents such as glutaraldehyde, tripolyphosphate and polyaspartic acid sodium salt [4]. Moreover, CHT is considered a natural anticancer polysaccharide. Many *in vitro* and *in vivo* studies have been published thanks to application of this polymer for the design of anticancer tools [5], [6], [7], but their efficacy is restricted due to the low efficiency of specific targeting [8]. However, the presence of reactive functional groups gives huge opportunities for chemical

modifications with a wide range of molecules in order to improve its targeting tumor ability.

NPs, indeed, can be designed to present well-defined properties according to the therapeutic purposes and to be able to respond and adapt to the surrounding pathological environment in order to release the payload only when it is necessary. Notably, the microenvironment within tumor is quite different from normal healthy cells such as its acidic and reductive conditions, different expression levels of some enzymes and receptors, etc. These distinctive features critically affect the success of NPs and, if opportunely considered in the design of nanocarriers, could be provide advantages for target cancer treatment. For instance, one important tumour hallmark is the overexpression of the specific receptors compared to normal cells [9]. In order to improve nanocarrier selectivity, several approaches have been advanced, mostly including the functionalization with ligands that are specifically recognized by receptors on cancer cell membrane. The tailorable chemistry of NPs allows them to be easily modified by conjugation of aptamers, antibodies, proteins, peptides, nucleic acids, or small molecules that specifically bind these receptors and promote cellular uptake via receptor-mediated endocytosis [10], [11]. In particular, Folic Acid (FA) is one of the most employed ligands for active targeting approach due to the countless advantages such as the low cost, the high stability and the broad library of conjugation reactions available [12]. In fact, FA can specifically bind to the folate receptors (FRs), overexpressed by many kinds of cancer cells, so it can be used as a drug-targeting ligand for cancer therapy [13], [14]. Various type of Folate based targeting drug delivery systems such as liposomes, nanoparticles, solid lipid nanoparticles and micelles have been designed and exerted greater anticancer activity than non-targeted systems [15], [16], [17], [18].

Once at the desired site of action, an ideal nanodevices for cancer therapy must still rapidly released the payload to effectively kill tumor cells. To enhance the intracellular drug release, a growing interest is currently focused in the design of functional polymers with reactivity to the tumor microenvironment [19].

The incorporation of stimuli responsive linkages in the polymeric network allows a triggered and localized drug release by responding to endogenous stimuli typical of tumor tissues. Various stimuli responsive nanosystems such as enzyme responsive, pH responsive, temperature responsive and redox responsive have been developed for controlled delivery applications [20], [21], [22], [23]. Among these, redox potential is of particular importance owing the fact that the concentration of intracellular glutathione (GSH 2-10 mM), a tripeptide responsible for reduction of disulfide linkages is approximately 2-3 order higher than that of the extracellular GSH (2-20 μM) [24]. Furthermore, cancer cells exhibit 4 folds-higher GSH levels as compared to normal healthy tissues [25] due to the rapid proliferation and the GSH-mediated phase II detoxification mechanism involved in drug resistance of cancer cells [26]. Accordingly, nano-systems can be tailor-made to be redox responsive by incorporation of disulphide linkages thanks to their stability in mildly

oxidizing environments (of atmospheric oxygen and bloodstream) and their lability in the presence of reducing agents. The reducing environment of tumors plays, thus, the role of internal signal that allows the destabilization of redox-responsive nanocarriers via the cleavage of disulphide bond into free thiols. Therefore, the use of redox-responsive NPs is an advantageous method to target the release of a drug inside of cells and improve consequently its efficacy.

Methotrexate (2,4-diamino-N-10-methyl propylglutamic acid, MTX) is a folic acid antagonist widely used in treatment of autoimmune disease and different cancers including acute lymphoblastic leukemia, head and neck cancer, lung cancer and breast cancer [27], [28]. MTX acts by inhibiting dihydrofolate reductase (DHFR) enzyme involved in the conversion of dihydrofolate (DHF) to tetrahydrofolate (THF) which is required for the synthesis of DNA and RNA. However, its clinical efficacy is often compromised by some limitations. First, undesirable side effects such as neurotoxicity, renal toxicity, bone marrow inhibition, liver toxicity, and acute and chronic obstructive pulmonary diseases are typical related to MTX. Moreover, bioavailability of MTX is low due to its poor water solubility and multidrug resistance in cancer cells due to cellular efflux of the molecule mediated by P-glycoprotein. In order to overcome these limitations, novel MTX delivery systems, such as nanoparticles [29], microspheres [30] and liposomes [31] have already been developed. Encapsulating drugs, in fact, in colloidal systems is a technique that allows to control pharmacokinetic and pharmacodynamic properties and increase therapeutic efficacy [32].

The objective of this research was, thus, the design of a multifunctional CHT derivative for targeted delivery of MTX to human cervix adenocarcinoma cell lines (HeLa). We decided to investigate the antitumor activity of a smart hybrid material possessing simultaneously folate active targeting properties and GSH responsiveness. Firstly, novel Folic-thiolated chitosan (FTC) derivatives were synthetized through the conjugation of L-cysteine (L-Cys) and FA to CHT. The resulting polymers were employed for the design of NPs as redox responsive platforms for the intracellular delivery of MTX. Via folate receptor-mediated endocytosis, the NPs can selectively enter tumor cells and, subsequently, the MTX can be rapidly released in response to the high reductive environment of the cytoplasm. Therefore, after NPs preparation with ionic gelation technique and physicochemical characterization, the release experiments were performed in reductive media mimicking the GSH concentrations in extra and intracellular space. By comparing with the redox-insensitive CHT-NPs, *in vitro* antiproliferative activity of FTC NPs were studied on HeLa by using MTT assay. Furthermore, the cellular uptake efficiency was evaluated by fluorescence microscopy. All the studies were carried out to evaluate the potential of the nanosystems proposed as devices for efficient intracellular MTX delivery.

2.0 Materials and method

Chemicals

5,5-dithiobis(2-nitrobenzoicacid) (DTNB, Ellman's reagent), MTX, methotrexate; CHT, chitosan; TPP, sodium triphosphate; PBS, phosphate buffer solution; HCl, hydrochloric acid; NaBH4, sodium borohydride; FA, folic acid; FRs, folate receptors; EDC, 1-ethyl-3-(3-dimethyllaminopropyl) carbodiimide hydrochloride; MTT, 3-(4,5-dimethylthiazol-2-yl)-2,5-diphenyltetrazolium bromide;

2.1 Preparation of Folic-thiolated-chitosan

The synthesis of Folic-thiolated-chitosan (FTC) was carried out as shown in Figure 1 via conjugation of L-Cys and FA to CHT backbone in a two step-process. Specifically, derivatives with three different weight ratios of CHT and L-Cys (1:1, 1:2, 1:4) were synthesized and the quantities used are reported in Table 1.

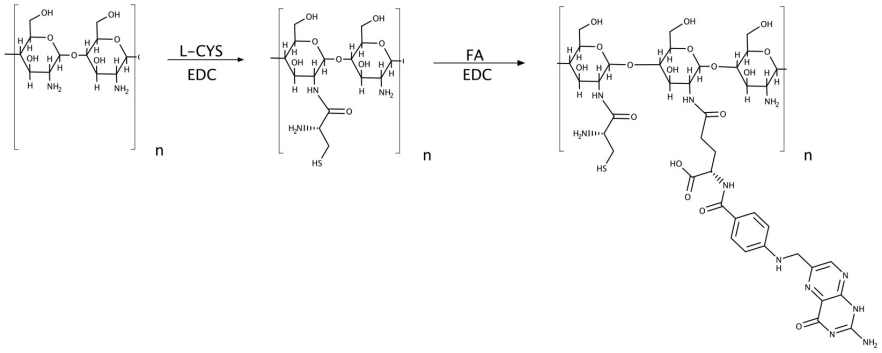

Figure1. Synthesis route of Folic-Thiolated Chitosan. Abbreviations: L-CYS, L-Cysteine; EDC, 1-ethyl-3-(3-dimethyllaminopropyl) carbodiimide hydrochloride; FA, Folic Acid.

Briefly, CHT was dissolved in acetic acid 1 %(v/v) to obtain a 1% (w/v) polymer solution. Separately, the carboxylic group on L-Cys was activated by EDC in demineralized water for 1 hour and, then, added dropwise to the above solution under magnetic stirring. The pH of the reaction mixtures was carefully adjusted to 5 with NaOH 0.5 M. This mixture was stirred for 4 hours in the dark at room temperature. After that, the reaction mixture was extensively dialyzed [molecular weight (MW) cutoff 12 kDa] for 3 days, first against 5 mM HCl, twice against 5 mM HCl containing 1% NaCl, and finally against 1 mM HCl. At the end, the polymers were lyophilized and stored at 4°C until further use.

The FA conjugation was performed in the following method. Briefly, EDC (0.04 mmol) was added to 2 mg $ml^{-1}$of folic acid (0.02 mmol) in dimethyl sulfoxide and stirred at room temperature for 1 hour. Separately, 100 mg of Thiolated-chitosan derivative was dissolved in 10 ml of acetic acid 1 % (v/v), added to above solution and stirred in the dark at room temperature for 16 hours. At the end of the reaction, the mixture was precipitated leading the pH to 9. The precipitate was collected and then dialyzed (molecular weight cut-off, 12 kDa) against the excess amount of 0.1 M sodium phosphate buffer (pH 7.4) for 3 days and, then, water for other 3 days. The resulting products were freeze-dried and subjected to ^{1}H nuclear magnetic resonance (NMR) characterization to demonstrate the successfull conjugation of L-CYS and FA to the CHT. ^{1}H-NMR (300 MHz, D_2O) δ (ppm): 1.75 (s, -$NHCOCH_3$), 2.55 (s, -CH_2SH), 2.87 (s, proton of Glucosamine unit of CHT), 3.30-3.76 (m, proton of Glucosamine unit of CHT), 7,17 (d, aromatic proton of FA), 7.56 (d, aromatic proton of FA), 8.51 (s, aromatic proton of FA).

2.2 FTC characterization

2.2.1 Ellman test

The amount of free thiol groups on FTC conjugates were determined with Ellman's reagent according to a previously reported method [33]. Briefly, 0.5 mg of each conjugate was hydrated in 500 µl of 0.5 M phosphate buffer pH 8.0. Then, 500 µl of 0.03 %(w/v) of DTNB dissolved in the same buffer were added to the sample and the resulted solution were incubated protected from the light for 2 h at 37°C. Finally, the absorbance of the supernatant was measured at 405 nm and the amount of thiol groups was calculated on the basis of a standard curve obtained using L-Cys. The content of disulfide bonds was measured after reduction with $NaBH_4$ and determined with Ellman's reagent as described above.

2.2.2 Quantification of FA

The amount of FA on novel designed polymers was evaluated using UV-Vis spectroscopy, considering its absorption at 285 nm. The FTC conjugates were dissolved in 1 % acetic acid at the concentration of 2×10^{-2} mg/mL and absorbance measurements of these solutions were performed. The FA concentration was calculated on the basis of a standard curve previously plotted from a stock solution of FA dissolved in a 0.1M NaOH solution, from which subsequently dilutions in 1% acetic acid were made in the range 0.2-2×10^{-2} mg/mL.

2.3 Nanoparticle preparation.

FTC nanoparticles were prepared according to ionic gelation technique which is based on the complexation of an anion crosslinking agent, sodium triphosphate (TPP), with cationic polymer. Briefly, FTC polymers were dissolved in acetic acid

1 % (v/v) achieving a concentration of 3 mg/ml. 0.5 ml of MTX alkaline solution (2.02×10^{-2} M) was added and the pH of the resulting solution was adjusted to 5.5 with NaOH 1 M. After that, NPs were immediately and spontaneously formed by adding dropwise 1 ml of aqueous solution of TPP (2 mg/ml) under constant stirring at room temperature. The purification of the resulting NPs was carried out by ultracentrifugation at 15000 rpm for 90 min.

2.4 Nanoparticles characterization

The mean particle size and distribution of the NPs were determined by dynamic light scattering (DLS) analysis using a 90 Plus Particle Size Analyzer (Brookhaven Instruments Corporation, New York, USA) at 25.0 ± 0.1 °C. We measured the autocorrelation function at 90°. The laser beam was operating at 658 nm. The size distribution was directly obtained from the instrumental data-fitting procedures through the inverse Laplace transformation and by Contin methods [34]. The samples were analyzed 24 h after preparation and appropriate dilution in distilled water. Each sample was measured six times, and the results were expressed as mean ± standard deviation (SD).

The Zeta potential values of NPs were measured with the laser Doppler electrophoretic mobility measurements using the Zeta-sizer ZS (Malvern Instruments Ltd., Malvern, U.K.), at 25.0 ± 0.1 °C. ZP evaluates the electric charge at the surface of the particles and it is an important index of the physical stability of colloidal systems. The measurements were performed in distilled water and the values were calculated through the instrument software, using Helmholtz–Smoluchosky equation. The results are reported as the means of three independent experiments performed in triplicate.

The morphology and size of the NPs were analyzed using transmission electron microscopy (TEM). A droplet of the NPs dispersion was stratified onto a carbon-coated copper grid and left to adhere on the carbon substrate for about 1 min. The dispersion in excess was removed by a piece of filter paper. A drop of 2% phosphotungstic acid solution was stratified and the solution in excess was removed by a tip of filter paper again. The sample was air-dried and observed under a ZEISS EM 10 electron microscope at an accelerating voltage of 80 kV.

2.5 Drug entrapment efficiency

MTX encapsulation efficiency was determined by indirect method measuring the amount of untrapped drug. Briefly, NPs were centrifuged at 15000 rpm for 90 min in order to separate the non-encapsulated drug from NPs and, then, the amount of free MTX in supernatant was analyzed using UV spectrophotometry at 306 nm. The entrapment efficiency was calculated according to the following equation:

$$EE\ \% = \frac{MTX\ tot - MTX\ free}{MTX\ tot}\ x\ 100$$

2.6 *In vitro* redox-responsive drug release

MTX release was carried out in phosphate buffer pH 7.4 in the absence and presence of 10 mM GSH to simulate the physiological conditions and reductive cytoplasm of cancer cells, respectively. Aliquots of NPs suspension (1 mL) were placed in dialysis bags (Visking dialysis tubes,20/30) and suspended in 25 mL of medium at 37 °C under gentle magnetic stirring. At predetermined time intervals, 2 mL of the medium was withdrawn while maintaining the volume of the receptor compartment with an equal volume of fresh release media. Samples were periodically analyzed using UV−visible spectrophotometry at 306 nm. MTX standard calibration curve was used to determine the concentration of released MTX. All experimental procedures were repeated three times, and the results were in agreement within ± 4% standard error.

2.7 Cell culture

The HeLa cells (a human cervix adenocarcinoma cell line) obtained from American Type Culture Collection (ATCC, Manassas, VA, USA) were grown in DMEM (Thermo-Fischer Scientific, MA, USA) supplemented with 10% (v/v) FBS, 2 mM L-glutamine, 100 UI/ml penicillin and 100 µg/ml streptomycin at 37 °C in a humidified incubator with 5% CO2. These cells were routinely cultured in 25 cm^2 flasks and were passaged using trypsin-EDTA when they reached approximately 80% confluence.

2.8 *In vitro* cytotoxicity assay

The *in vitro* cytotoxicity of the blank and MTX-loaded NPs was evaluated in HeLa cells by MTT assay. Briefly, the cells (8x104/ml) were allowed to settle by incubating the plates for 24 h at 37 °C and 5% CO_2. After the addition of 0.1, 1 and 10 µg/ml of free MTX, MTX-loaded FTC-NPs and MTX-loaded CHT-NPs. Then, the cells were incubated for 4 h and subsequently, washed and further cultured with fresh medium up to a total of 24, 48 and 72 h. Untreated HeLa cells were used as normal control. Moreover, the cytotoxicity of empty NPs towards the cells was evaluated under identical conditions. At the end of the incubation time, 100 µl of MTT (5 mg/ml) dissolved in Dulbecco's Phosphate Buffered Saline, pH 7.4 were added to each well and cells were incubated at 37°C and 5% CO_2 for additional 4 h, to allow the formation of violet formazan crystals. Then the medium was removed and a solubilization solution (100 µL, 16% SDS in 40% DMF, pH 4.7, prepared at 37 °C) was added to dissolve formazan crystal incubating the plate for another 30

min at 37 °C. The amount of formazan product was measured at 570 nm using a ELX800 microplate reader (Bio-Tek Instruments, Inc., VT, USA). Each experiment was performed in triplicate. The percentage of viable cells, directly proportional to the amount of formazan crystals formed, was calculated using the following equation:

$$cell\ viability = \frac{AT}{AU} x100$$

where AT is the absorbance of the treated cells and AU is the absorbance of the untreated cells. Cell viability values are expressed as the mean of at least three different experiments ± SD.

2.9 Cellular uptake studies

Sodium fluorescein (NaFl) loaded FTC-NPs were prepared using the same methods described above (for MTX) and then purified by ultracentrifugation at 15000 rpm for 90 min. NaFl was loaded to provide a final concentration of 0.03 mg/ml. Hela cells were seeded onto 6-wells plate on coverslip in DMEM (medium) and incubated overnight before the addition of NaFl loaded CHT-NP (100µl/ml). Free NaFl added to DMEM (0,003mg/ml) was used as control. Upon incubation at 37 °C for 4h, the media were removed, the cells were washed with PBS three times and fixed with 4% paraformaldehyde in PBS for 10 min at room temperature. All coverslips were mounted on clean glass slides with UltraCruz, a mounting medium containing DAPI, (Santa Cruz biotechnology, TX, USA) and examinated on a conventional fluorescent microscope, Nikon Microphot EPI-FL, (Nikon, JP) equipped with a mercury lamp.

2.10 Statistical analysis

The data are expressed as mean ± S.D. of at least three independent experiments. Statistical analysis was performed using Student's t-test. P-values ≤ 0.05 were considered statistically significant.

3. Results

3.1 FTC characterization

New multi-functional CHT-based NPs possessing redox responsiveness and folate-targeted properties were developed and investigated for a potential application in tumor target therapy. Nanocarriers responsive to the reductive conditions are particularly appealing for the intracellular drug delivery applications in cancer therapy. Notably chitosan, one of the biodegradable polymers most used for tumor drug delivery, was selected as starting material due to the presence of reactive amino

groups that make it an attractive biomaterial apt to several modifications in order to improve tumor targeting ability.
In this study, L-Cys and FA were functionalized and conjugated to CHT backbone through amide bonds in a two-step reaction. EDC was used as coupling agent and three different derivatives with various CHT/L-Cys w/w ratios of 1:1, 1:2 and 1:4 were synthetized.
These modifications had many advantages. The first was that L-Cys residues can be easily oxidized by air to give inter- and intramolecular disulphide bonds that are cleavable in a reductive environment. Consequently, the incorporation of disulphide linkages in NPs structure makes them to be redox responsive leading in a promptly and selective drug release only in response to reductive stimuli in a specially controlled manner. On the other hand, the FA was employed to functionalize NPs for an active tumor targeting and allow a preferential accumulation on tumor tissue via FRs mediated endocytosis. The combined activity of FRs targeting and redox responsiveness has been proposed in order to achieve an improved MTX delivery in cancer cells and, thus, high therapeutic efficacy.
Synthetic pathway of the FTC polymer is summarized in Figure 1 and the chemical structure was characterized by ^{1}HNMR analysis. The NMR spectra of synthesized FTC indicated a new peak at δ 2.75 ppm corresponding to methylene protons of L-Cys confirming the conjugation reaction and the successfully formation of a thiol functionalized polymer. Moreover, the coupling of FA residues with CHT was confirmed by the appearance of the peculiar signals at 7.17, 7.56 and 8.51 ppm, which are characteristic peaks attributed to the aromatic protons of folate ring. The successful conjugation of FA was also confirmed by UV− visible spectroscopy analysis and the amounts of FA conjugated are given in Table 1.

Conjugate	Chitosan (mg)	L-Cys (mg)	EDC (mM)	CHT:CYS:FOL Ratio (w:w:w)	-SH total μmol/g polymer	% disulfide bond	Folic acid μmol/g polymer
FTC1	150	150	50	1:1:0.1	114.0± 5.3	65.87	5.60± 0.28
FTC2	150	300	150	1:2:0.1	407.5± 9.5	92.29	5.05± 0.41
FTC3	150	600	150	1:4:0.1	141.9± 7.0	70.71	5.11± 0.18

Table 1. Amounts of reagents used (± 10%) for the synthesis of TC conjugates with different weight ratios of L-Cysteine and results of the amount of thiol groups and FA content obtained.

The numbers of free-thiol groups and disulfide bonds immobilized on FTC were determined using Ellman test and the results are shown in Table 1. FTC2 polymer

exhibited the higher disulfide content (92.29 %) among all polymers designed, followed by FTC3 (70.71 %) and FTC1 (65.87 %).

3.2 Nanoparticles characterization

Glutathione-responsive NPs were obtained by ionic gelation technique based on the complexation of positive charged FTC polymers with an polyanion cross-linking agent [35]. All the formulations developed were homogeneous and really stable in long term (more than 4 weeks, at room temperature and in the dark). The morphological features of NPs were evaluated by TEM. TEM pictures (Figure 2) revealed the presence of well-defined spherical NPs with smooth surface.

Physicochemical characteristics are important parameters from a pharmaceutical viewpoint and their evaluation plays a crucial role to predict the NPs *in vivo* stability. Consequently, NPs developed in this work have been widely characterized in terms of particle size, polydispersity index (P.I.), shape and Z-potential, and results are shown in Table 2.

NPs had a narrow size distribution as highlighted by P.I. values less than 0.3 reported in Table 2. The mean hydrodynamic diameters ranges between 202 nm and 378 nm and they are in good agreement with those evaluated with TEM analysis.

These small sizes (< 400 nm) make them suitable to be used as drug delivery carriers. The particle size, in fact, affects the drug release characteristics and the uptake in tumor tissues. In literature, it has widely been reported, indeed, that solid tumors show a hypervascular permeability and an impaired lymphatic drainage and thanks to this, NPs can significantly accumulate in tumors by EPR effect that typically operates in the range of 100–400 nm [37].

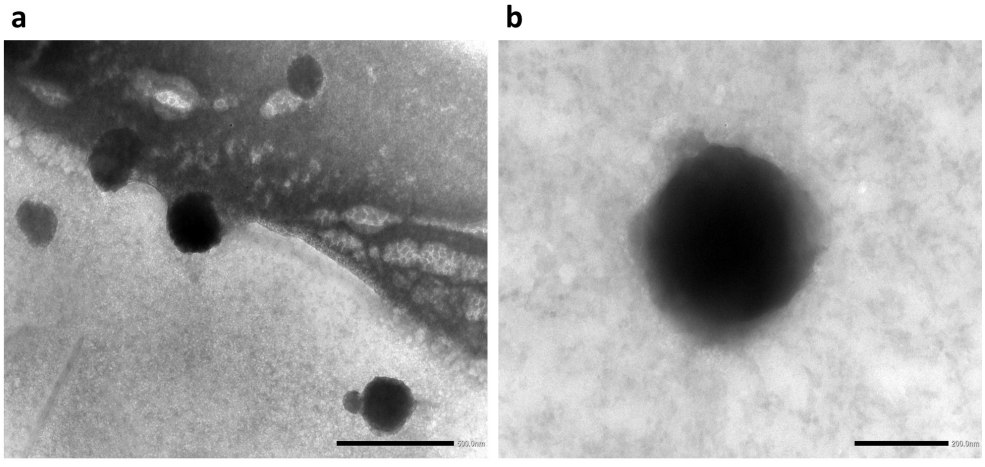

Figure 2. TEM micrographs of a) FTC2 and b) FTC1 NPs. Bar is a) 500 nm b) 200 nm

Commonly, the presence of disulphide intermolecular linkages in the polymer structure has proved to affect the NPs size [38]. The increase in disulphide content allows the formation of smaller devices. This trend conforms to the present experiments: in fact, smaller NPs are obtained by FTC2 polymers owing to be higher disulphide content compared to other polymers and plain CHT. DLS measurements of loaded samples demonstrated that, comparing to empty samples, no significant variation in particle size occurred after drug loading.

Formulation	Size (nm)	P. I.	Z-Potential (mV)	EE % MTX
FTC1	364.2 ± 3.1	0.167	+ 28.3 ± 1.04	-
FTC2	202.4 ± 5.8	0.254	+35.9 ± 0.36	-
FTC3	234.7 ± 7.9	0.234	+24.9 ± 1.4	-
CHT	378.4 ± 7.4	0.318	+30.7 ± 3.35	-
FTC1-MTX	363.9 ± 3.3	0.154	+26.3 ± 1.18	55.92 ± 2.88
FTC2-MTX	258.3 ± 4.9	0.153	+28.9 ± 0.47	37.44 ± 5.22
FTC3-MTX	302.0 ± 9.3	0.250	+26.8 ± 1.89	18.28 ± 9.87
CHT-MTX	364.1 ± 2.5	0.273	+26.7 ± 0.99	55.15 ±4.52

Table 2. Average size, polydispersity index, Z-potential and entrapment efficiency of empty and loaded NPs at 25 °C. Data are mean values ± S.D. (n = 3).

Zeta-potential is a measure of the electrical charge close to the NPs surface, thus Zeta-potential measurements are a powerful way to characterize electrostatic properties and predict NPs stability. Formulations investigated in this work showed positive Zeta-potential values ranging between +24.9 ± 1.4 and +35.9 ±0.36mV and presented high colloidal stability. Moreover, their cationic nature makes them effective devices for anticancer drug delivery to solid tumors. In fact, it has been found that positively charged nanoparticles showed high cellular uptake efficacy due to the electrostatic interactions with anionic molecules, such as proteoglycans, glycoproteins and anionic phospholipids in the tumour microvasculature [39].
The MTX entrapment efficiency values ranged from 18.28%to 55.92%. The three different derivatives showed different drug incorporation capacity. The reasons for that behavior are still obscure and could be probably ascribed to different interactions between drug and polymeric matrix.

3.3 *In vitro* release studies

A good stability in blood circulation and the ability to rapidly and thoroughly release the drug into the intracellular environment of cancer cells are important aims to be achieved for the design of an ideal drug delivery systems for tumor therapy.
To verify the redox responsive properties of the prepared NPs, the release studies were carried out at pH 7.4 PBS in presence and absence of 10 mM GSH to mimic the tumor tissue and physiologic environment, respectively. As is known, GSH concentration in the intracellular environment of tumor cells is about 4-fold higher than normal healthy cells. Hence, GSH was chosen as the reducing agent to evaluate the redox responsive nature of NPs. Drug release profiles for FTC3-NPs sample are given in Figure 3. A slow release of below 35% of MTX was observed within 24 h in PBS at pH 7.4, indicating a good stability in the extracellular medium of healthy tissues and only a little drug leakage during blood circulation. Oppositely, in presence of 10 mM of GSH, a faster drug release took place owing the breakage of the crosslinking points in the NPs structure, exhibiting a release equal to 59.85% in the first half hour and up to 88.4% in 24 h. These results demonstrated that cleavage of disulfide bridges led to a rapid and complete drug release. Redox-responsive NPs have, indeed, a high stability in bloodstream. On the other hand, FTC nanoparticles can be rapidly disassembled by GSH into high reductive cytoplasm of tumor, which results in a quick MTX release and an effectively inhibition of tumor growth.

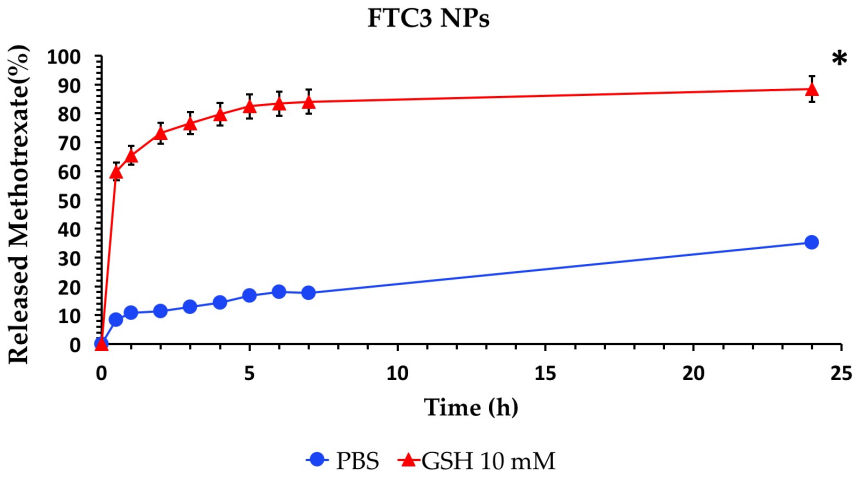

Figure 3. *In vitro* drug release profiles from MTX-FTC3 NPs in phosphate buffer in presence (▲) and absence (●) of GSH 10 mM at 25 °C (mean ± standard deviation, n = 3). Amount of MTX release in phosphate buffer in presence of GSH 10 mM at every time point was statistically different (*p< 0.05) from that recorded in absence of GSH.

The influence of disulfide contents on release was also investigated and the results were summarized in Figure 5. Previously, Hu et al. [40] reported that the redox reaction is a rate-dependent phenomenon and the reduction responsive ability could

be modulated by varying the amount of disulfide content depending on the application desired. In our studies, we also found that the drug release profile resulted be closely dependent on the amount of disulphide bond presents in polymer structure confirming the earlier studies. Higher degree of disulfide content in NPS are related to more high responsivity. In fact, FTC2 proved to be the polymer with the higher amount of disulfide bonds led to a drug release in presence of reducing agent 2.8 folds higher than that in physiological condition. The redox sensitivity decreased for FTC3 and FTC1 with an increase of drug release respectively 2.5 and 2.2 times higher in presence of GSH related to the lower crosslinking point content in NPs structure.

Overall, these results confirm our expectation since the nanocarriers were considerably stable before reaching tumor sites but achieved a complete and accelerated release in tumor cells. Therefore, the *in vitro* drug release studies confirmed the redox-responsive ability of the FTC nanocarrier and provided more supporting evidences for its great potential for intracellular tumor drug delivery.

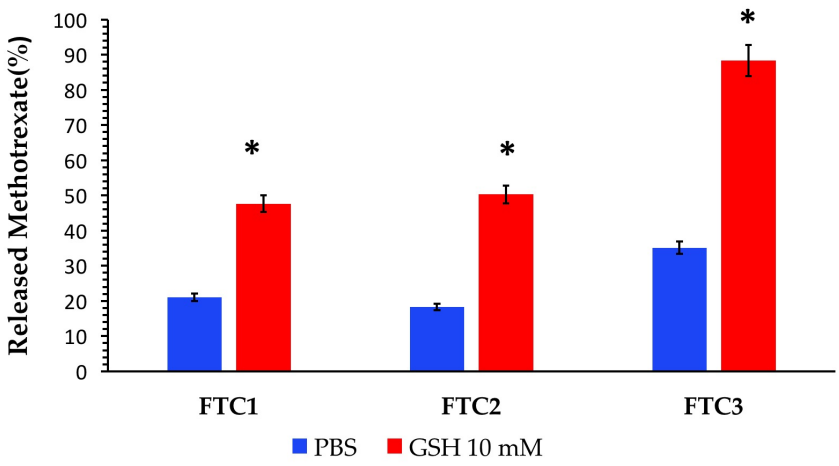

Figure 4. Percentage of MTX released from NPs based on FTC polymers with different amount of disulphide content (FTC1 65.87%; FTC2 92.29 %; FTC3 70.71 %) in phosphate buffer in presence (▲) and absence (●) of GSH 10 mM at 25 °C (mean ± standard deviation, n = 3). Amount of MTX release in phosphate buffer in presence of GSH 10 mM was statically different (* p< 0.05) from that recorded in absence of GSH.

3.4 *In vitro* cytotoxicity

In order to study the anticancer activity of designed formulations, cell viability was evaluated by the MTT assay in HeLa cells after being exposed to free MTX, MTX−FTC NPs and MTX-CHT NPs at different concentrations for 24, 48 and 72 h. The

results showed that cell viabilities remained higher than 80% after 72 h of incubation with empty systems in the range of concentration investigated indicating the biocompatible and non-toxic nature of FTC polymers.

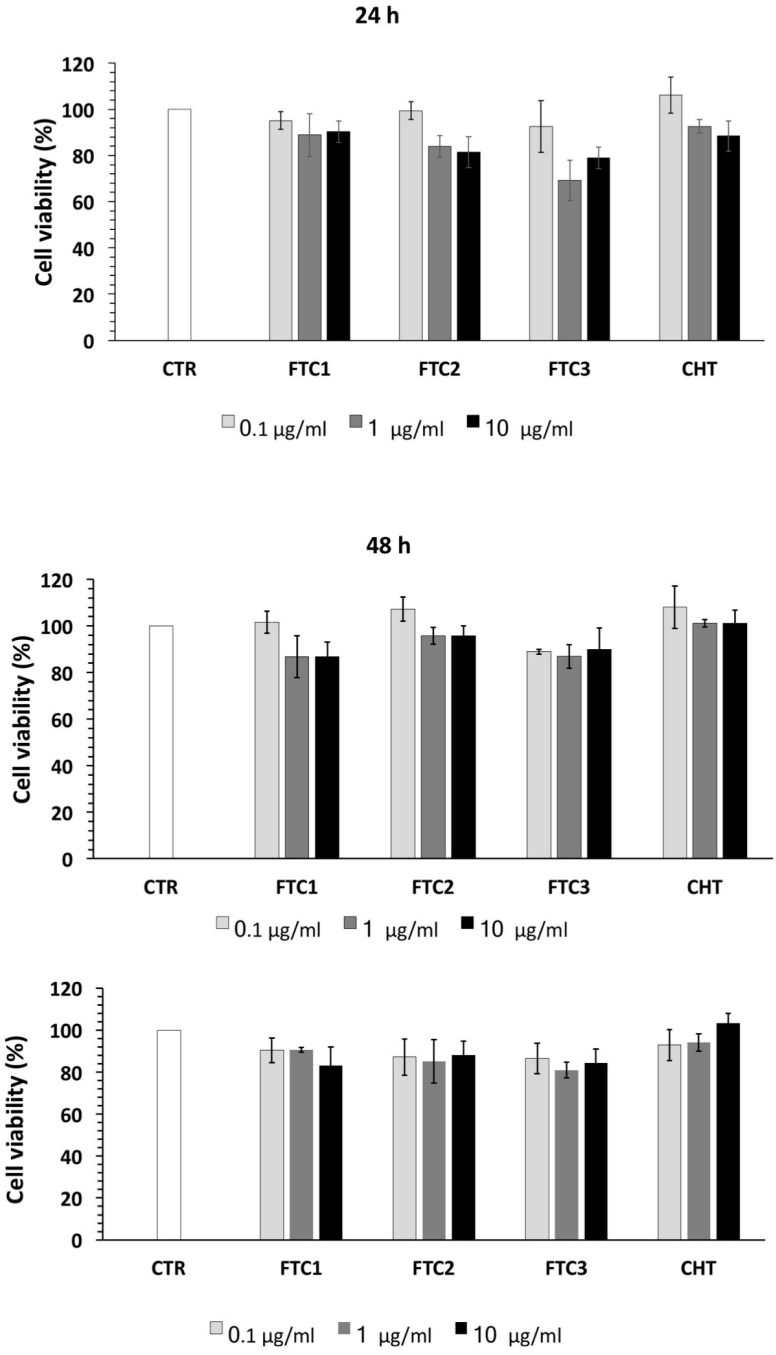

Figure 5. HeLa cell viability tested by MTT assay in triplicate. Cells were incubated with blank (CTR), FTC and CHT based NPs at different concentrations for 24, 48, and 72 h. The results are expressed as the percentage of the control assumed as 100%. Each value represents the mean ± S.D. of three independent experiments.

On the contrary, good cell growth inhibition effect was observed for drug loaded systems. As shown the Figure 6, the encapsulation of MTX in NPs greatly improved its anticancer efficacy and affected cell viability in a time and dose-dependent manner.

Both MTX-FTC NPs and MTX-CHT NPs, in fact, showed higher cytotoxicity toward HeLa cells than free MTX, this maybe because drug-loaded NP can enter the cell more accurately compared with free MTX. Typically, MTX clinical efficacy is compromised by the acquisition of resistance in cancer cells due to the efflux by P-glycoprotein and the availability at its intracellular site of action depends on a passive diffusion mechanism [41]. The enhanced cytotoxicity of MTX nano-sized carriers could be due to the improved drug cell internalization by endocytosis and lower drug efflux from cells [42]. Besides, our studies indicated that the cytotoxicity of MTX-FTC NPs was higher than that of the non-target MTX-CHT NPs used as control. In detail, the cell survival rate was reduced to 57.28% after treatment for 72 h with MTX-loaded CHT NPs, while the values were 45.92%, 34.81% and 41.23 % with the use of FTC1, FTC2 and FTC3 NPs, respectively. The increased cytotoxicity of MTX-FTC NPs highlighted that the redox-responsive and folate target NPs had better potential for MTX intracellular delivery in contrast with the non-target NPs.

This may be attributed to the high affinity of folate-modified NPs to tumour cells and a quick intracellular release of MTX under stimulation of GSH in cytoplasm of cancer cells. These devices can penetrate inside the cells via endocytic processes and release the drug in the cytoplasm where GSH level is higher and the disulfide bonds can be broken, facilitating the drug release. For these reasons, FTC-NPs may be a promising solution in delivering chemotherapeutic drugs to tumors. However, further studies are necessary to test these systems in an animal models to obtain important *in vivo* data.

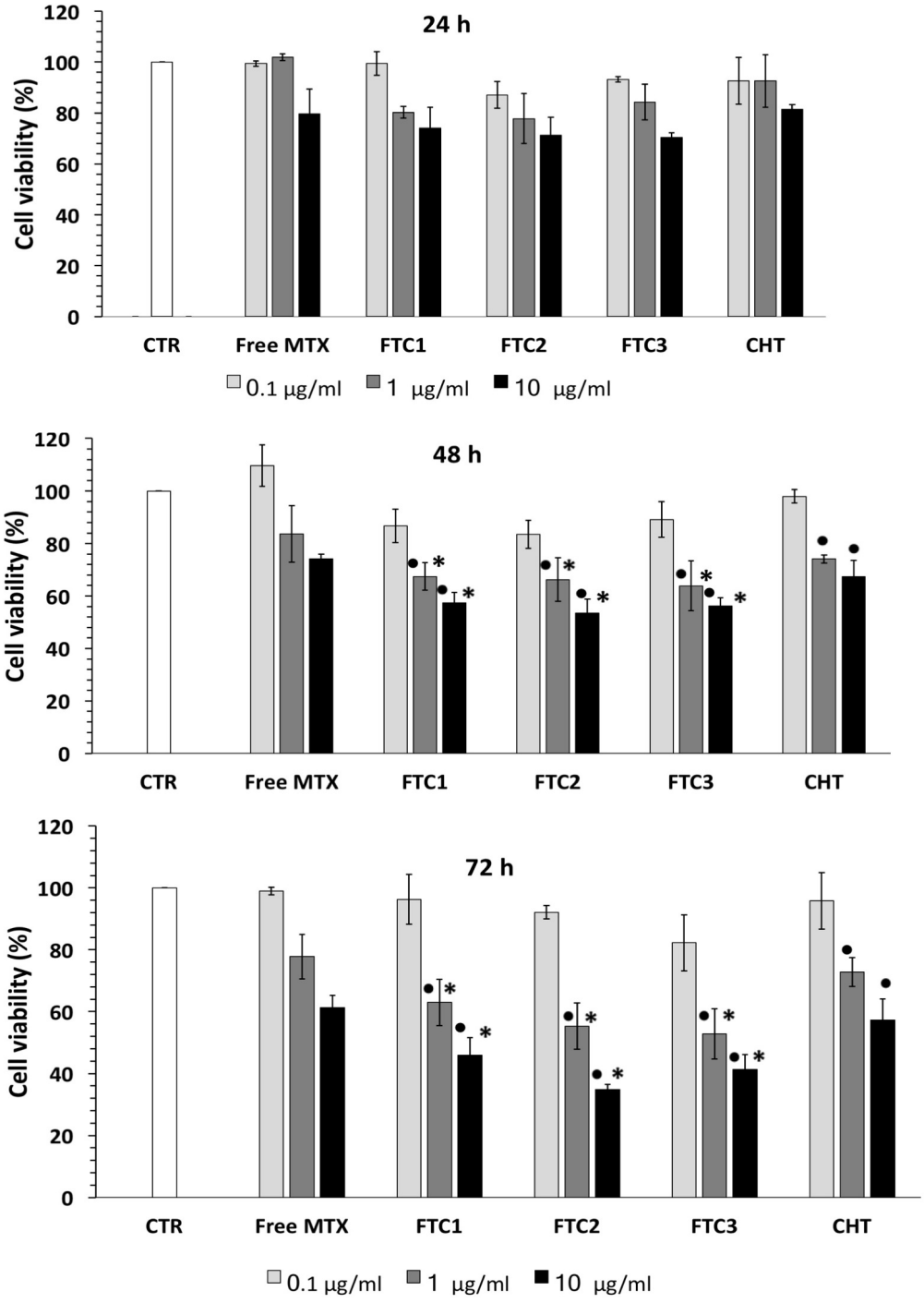

Figure 6. HeLa cell viability after incubation with free MTX, MTX loaded FTC-NPs and MTX loaded CHT-NPs at 0.1, 1 and 10 µM for 24, 48, and 72 h evaluated using MTT assay. The results are expressed as the percentage of the control assumed as 100%. Each value represents the mean ± S.D. of three independent experiments. • $p<0.05$ vs control; * $p<0.05$ vs CHT-coated liposomes treated cells.

3.5 Evaluation of FTC-NPs uptake using Fluorescence Microscopy Analysis.

To evaluate the cellular uptake ability of the designed devices in this work, green fluorescent NaFl was loaded in FTC-NPs. The evaluation of internalization ability of nanocarriers is essential to predict the *in vivo* performance. Consequently, evidence of cellular uptake was obtained by fluorescence microscopy analysis performed in HeLa cells after treatment with free NaFl and NaFl-loaded FTC-NPs for 4 h. As seen in Figure 7, nearly no green fluorescence was observed in HeLa cells incubated with free NaFl, which was due to the low permeability of fluorescein to cell membrane [43]. Conversely, the fluorescence of HeLa cells was greatly enhanced after treatment with FTC-NPs. This result showed that FTC-NPs were effective in the enhancement of NaFl uptake. This higher cellular uptake of folate conjugated NPs in the cancer cells can be ascribed to FRs mediated endocytosis of NPs. Our results are, thus, being in agreement with the previous cytotoxic studies according to which FTC-NPs were more effective than free drug in the inhibition of cancer cell. From these results, we can draw a conclusion that the FA-decorated redox-responsive NPs have the ability to convey anticancer drug to targeted cancer cells and enhance the intracellular release.

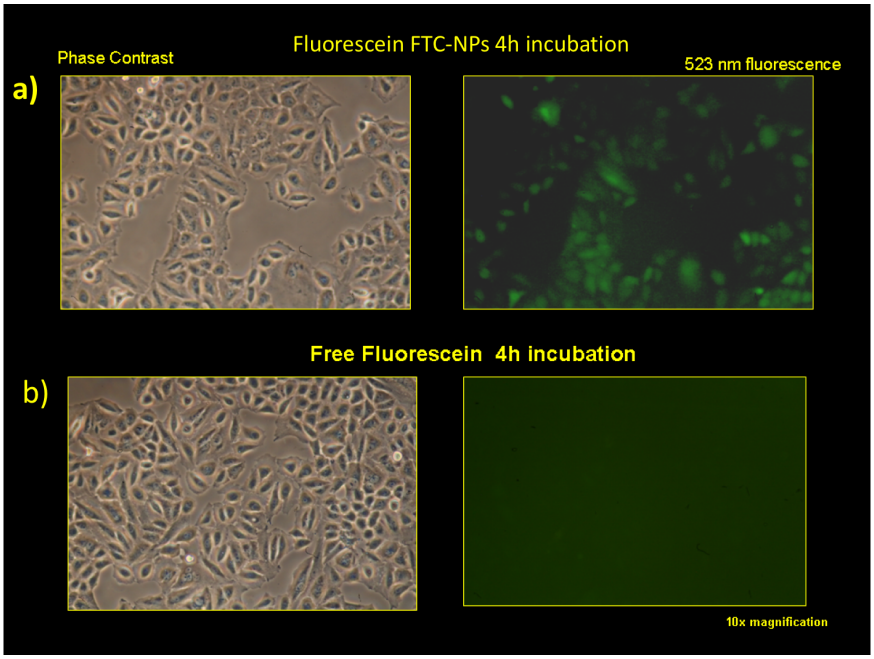

Figure 7. Fluorescence microscopic pictures (10 x) of HeLa cells after incubation over 4 h with culture medium containing NaFl loaded FTC-NPs a) and free NaFl b). The fluorescence of NaFl was excited at 475 nm and detected at a wavelength of 523 nm.

4.0 Conclusion

In this study, multifunctional CHT nanoparticles with Folate targeted and redox responsive properties were successfully developed as intracellular MTX delivery systems for improved antitumor activity. To achieve this goals, disulfide bonds were introduced in CHT backbone endowing a desirable redox-sensitivity to this system for triggering a selective and localize intracellular drug release in tumor microenvironment; the inclusion of folate ligands, instead, can enhance the selectivity to tumor cells. The FTC NPs exhibited an excellent physiological stability and a significant faster drug release in reductive environment. *In vitro* antitumor activity demonstrated that multifunctional NPs possess a better anticancer activity in contrast to the non-targeted NPs. Consequently, the designed NPs hold great promise as nanocarrier for target cancer therapy and further *in vivo* studies must be conducted in this field to prove their efficacy.

References

[1] Park, K.; Lee, S.; Kang, E.; Kim, K.; Choi, K.; Kwon, I. C. New generation of multifunctional nanoparticles for cancer imaging and therapy. Adv. Funct. Mater. 2009, 19, 1553–1566.

[2] Bertrand, N.; Wu, J.; Xu, X.; Kamaly, N.; Farokhzad, O. C. Cancer nanotechnology: the impact of passive and active targeting in the era of modern cancer biology. Adv. Drug Delivery Rev. 2014, 66, 2−25.

[3] Kim, S. Competitive Biological Activities of Chitosan and Its Derivatives: Antimicrobial, Antioxidant, Anticancer, and Anti-Inflammatory Activities. Inter. J. Polym. Sci. 2018, 1708172, 13

[4] Gan, Q.; Wang, T.; Cochrane, C.; McCarron, P. Modulation of surface charge, particle size and morphological properties of chitosan−TPP nanoparticles intended for gene delivery. Colloids Surf. B. 2005,44, 65−73.

[5] Mirzaie, Z. H.; Irani, S., Mirfakhraie, R.; Atyabi, S. M.; Dinarvand, M.; Dinarvand, R.; Varshician, R.; Atyabi, F. Docetaxel–chitosan nanoparticles for breast cancer treatment: cell viability and gene expression study. Chem. Biol. Drug Des. 2016, 88, 850–858.

[6]Yoon, H. Y.; Son, S.; Lee, S.J.; You, D. G.; Yhee, J. Y.; Park, J. H.; Swierczewska, M.; Lee, S.; Kwon, I. C.; Kim, S. H.; Kim, K.; Pomper, M. G.Glycol chitosan nanoparticles as specialized cancer therapeutic vehicles: sequential delivery of doxorubicin and Bcl-2 siRNA. Sci. Rep. 2015, 4, 1–12.

[7] Cheng, M.; Zhu, W.; Li, Q.; Dai, D.; Hou, Y. Anti-cancer efficacy of biotinylated chitosan nanoparticles in liver cancer. Oncotarget. 2017, 8, 59068–59085.

[8] Ji, J.; Wu, D.; Liu, L.; Chen, J.; Xu, Y. Preparation, characterization, and in vitro release of folic acid-conjugated chitosan nanoparticles loaded with methotrexate for targeted delivery. Polym Bull. 2012, 68, 1707–20.

[9] Akhtar, M. J.; Ahamed, M.; Alhadlaq, H. A.; Alrokayan, S. A.; Kumar, S. Targeted anticancer therapy: Overexpressed receptors and nanotechnology. Clin. Chim. Acta. 2014, 436,78–92

[10] Allen, T. M. Ligand-targeted therapeutics in anticancer therapy. Nat Rev Cancer. 2002, 2, 750-763.

[11] Peer, D.; Karp, J. M.; Hong, S.; Farokhzad, O. C.; Margalit, R.; Langer, R. Nanocarriers as an emerging platform for cancer therapy. Nat. Nanotechnol. 2007,2, 751-760.

[12] Low, P. S., Henne, W. A., Doorneweerd, D. D. Discovery and development of folic-acid based receptor targeting for imaging and therapy of cancer and inflammatory diseases. Acc. Chem. Res. 2008, 41,120–129.

[13] Kelemen, L. E. The role of folate receptor α in cancer development, progression and treatment: cause, consequence or innocent bystander? Int. J. Cancer. 2006,119,243–250.
[14] McGuire, J. J. Anticancer antifolates: current status and future directions. Curr. Pharm. Des. 2003,9,2593–2613.
[15] Liu, X.; Ma, S.; Dai, C.; Cai, F.; Yao, Y.; Yang, Y.; Feng, M.; Deng, K.; Li, G.; Ma, W.; Xin, B.; Lian, W.; Xiang, G.; Zhang, B.; Wang, R. Antiproliferative, antiinvasive, and proapoptotic activity of folate receptor α-targeted liposomal DOX in nonfunctional pituitary adenoma cells. Endocrinology. 2013,154,1414–1423.
[16] Pan, J.; Feng, S. S. Targeting and imaging cancer cells by folate-decorated, quantum dots (QDs)-loaded nanoparticles of biodegradable polymers. Biomaterials. 2009,30,1176–1183.
[17] Cui M.Y.;Dong, Z.; Cai, H.; Huang, K.; Liu, Y.; Fang, Z.; Li, X.; Luo, Y.Folate‑targeted polymeric micelles loaded with superparamagnetic iron oxide as a contrast agent for magnetic resonance imaging of a human tongue cancer cell line. Mol. Med. Rep. 2017,16, 7597-7602
[18] Rosière, R.; Van Woensel, M.; Gelbcke, M.; Mathieu, V.; Hecq, J.; Mathivet, T.; Vermeersch, M.; Van Antwerpen, P.; Amighi, K.; Wauthoz, N. New Folate-Grafted Chitosan Derivative to Improve Delivery of Paclitaxel-Loaded Solid Lipid Nanoparticles for Lung Tumor Therapy by Inhalation. Mol. Pharm. 2018, 5,15,899-910.
[19] Raza, F.; Zhu, Y.; Chen, L.; You, X.; Zhang, J.; Khan, A., Khan, M. W., Hasnat, M., Zafar, H., Wu J. Ge, L.Paclitaxel-loaded pH responsive hydrogel based on self-assembled peptides for tumor targeting. Biomater. Sci. 2019, 7, 2023–2036.
[20] Mazzotta, E.; Tavano, L.; Muzzalupo , R.; Thermo-Sensitive Vesicles in Controlled Drug Delivery for Chemotherapy Pharmaceutics. 2018,10, 150.
[21] Liu, J.; Huang, Y.; Kumar, A.; Tan, A.; Jin, S.; Mozhi, A.; Liang, X. J. pH-Sensitive nano-systems for drug delivery in cancer therapy. Biotechnol. Adv. 2014,32,693-710
[22] Hu, Q.; Katti, P. S.; Gu, Z. Enzyme-Responsive Nanomaterials for Controlled Drug Delivery. Nanoscale. 2014, 6, 12273–12286.
[23] Zhang, X.; Han, L.; Liu, M.; Wang, K.; Tao, L.; Wana, Q.; Wei, Y. Recent progress and advances in redox-responsive polymers as controlled delivery nanoplatforms. Mater. Chem. Front.2017, 1, 807
[24] Jia, L.; Cui, D.; Bignon, J.; Di Cicco, A.; Wdzieczak-Bakala, J.; Liu, J.; Li, M. H. Reduction-responsive cholesterol-based block copolymer vesicles for drug delivery. Biomacromolecules. 2014, 15, 2206−2217.
[25] Bao, Y.; Guo, Y.; Zhuang, X.; Li, D.; Cheng, B.; Tan, S.; Zhang, Z. D-α-tocopherol Polyethylene Glycol Succinate-Based Redox-Sensitive Paclitaxel Prodrug for Overcoming Multidrug Resistance in Cancer Cells. Mol. Pharmaceutics. 2014, 11, 3196−3209.
[26] Balendiran, G. K.; Dabur, R.; Fraser, D. The role of glutathione in cancer. Cell Biochem. Funct. 2004, 22, 343−352.
[27] Banerjee, D.; Mayer-Kuckuk, P.; Capiaux, G.; Budak-Alpdogan, T.; Gorlick, R.; Bertino, J. R. Novel aspects of resistance to drugs targeted to dihydrofolate reductase and thymidylate synthase. Biochim. Biophys. Acta 2002,1587,164-173.
[28] Yoon, S.; Choi, J. R.; Kim, J.-O.; Shin, J.-Y.; Zhang, X.; Kang, J.-H. Influence of reduced folate carrier and dihydrofolate reductase genes on methotrexate-induced cytotoxicity. Cancer Res. Treat. 2010, 42, 163−171
[29] Chen, Y. H.; Tsai, C. Y.; Huang, P. Y.; Chang, M. Y.; Cheng, P. C.; Chou, C. H.; Chen, D. H.; Wang, C. R.; Shiau, A. L.; Wu, C. L. Methotrexate conjugated to gold nanoparticles inhibits tumor growth in a syngeneic lung tumor model. Mol. Pharmaceutics 2007, 4, 713−722.
[30] Liang, L. S.; Jackson, J.; Min, W. X.; Risovic, V.; Wasan, K. M.; Burt, H. M. Methotrexate loaded poly (L-lactic acid) microspheres for intra-articular delivery of methotrexate to the joint. J. Pharm. Sci. 2004, 93, 943−956.

[31] Kuznetsova, N. R.; Sevrin, C.; Lespineux, D.; Bovin, N. V.; Vodovozova, E. L.; Meszaros, T.; Szebeni, J.; Grandfils, C. Hemocompatibility of liposomes loaded with lipophilic prodrugs of methotrexate and melphalan in the lipid bilayer. J. Controlled Release 2012, 160, 394−400.
[32] Kumari, A.; Singla, R.; Guliani, A.; S. K. Nanoencapsulation for drug delivery.Excli J. 2014, 13, 265–286.
[33] Schmitz, T.; Grabovac , V.; Palmberger , T. F.; Hoffer , M. H.; Bernkop-Schnürch A. Synthesis and characterization of a chitosan-N-acetyl cysteine conjugate. Int. J. Pharm. 2007,347, 79-85
[34] Provencher, S. W. A constrained regularization method for inverting data represented by linear algebraic or integral equations. Comput. Phys. Commun. 1982, 27, 213−227.
[35] Naskar, S.; Koutsu, K.; Sharma, S. Chitosan-based nanoparticles as drug delivery systems: a review on two decades of research. J. Drug Target. 2019,27, 379-393.
[36] Hillaireau, H.; Couvreur, P. Nanocarriers' entry into the cell: relevance to drug delivery. Cell. Mol. Life Sci. 2009, 66, 2873−96.
[37] Nakamura, Y.; Mochida, A.; Choyke, P. L.; Kobayashi, H. Nanodrug Delivery: Is the Enhanced Permeability and Retention Effect Sufficient for Curing Cancer? Bioconjugate Chem.2016,27,2225-2238.
[38] Trapani, A.; Mandracchia, D.; Tripodo, G.; Cometa, S.; Cellamare, S.; De Giglio, E.; Klepetsanis, P.; Antimisiaris, S.G. Protection of dopamine towards autoxidation reaction by encapsulation into non-coated- or chitosan- or thiolated chitosan-coated-liposomes. Colloid B surface. 2018, 70, 11-19.
[39] Abu Lila, A.S.; Ishida, T.; Kiwada, H. Targeting anticancer drugs to tumor vasculature using cationic liposomes. Pharm. Res. 2010,27, 1171–1183.
[40] Hu, Y. W.; Du, Y. Z.; Liu, N.; Liu, X.; Meng, T. T.; Cheng, B. L.; He, J. B.; You, J.; Yuan, H.; Hu, F. Q. Selective redox-responsive drug release in tumor cells mediated by chitosan based glycolipid-like nanocarrier J. Control. Release. 2015, 206,91–100.
[41] Nogueira, D. R.; Tavano, L.; Mitjans, M.; Perez, L.; Infante, M. R.; Vinardell, M. P. In vitro antitumor activity of methotrexate via pHsensitive chitosan nanoparticles. Biomaterials 2013, 34, 2758−2772
[42] Brigger, I.; Dubernet, C.; Couvreur, P. Nanoparticles in cancer therapy and diagnosis. Adv Drug Deliv Rev 2002, 54,631-651.
[43] Cercek, L.; Cercek, B.;, Ockey, C. H. Cell membrane permeability during the cell generation cycle in Chinese hamster ovary cells. Biophysik 1973, 10:195-197.

4

NANOCARRIERS FOR DRUG PHOTOPROTECTION

This section reviews the nanodevices for protection of photosensitive drugs developed during my PhD research, including a first part in which I reported our review on the nanotechnology strategies for the improvement of distribution, bioavailability and stability of reverse transcriptase inhibitors.

4.1 Reverse Transcriptase Inhibitors Nanosystems Designed for Drug Stability and Controlled Delivery (Review)

Fedora Grande[a], Giuseppina Ioele[a], Maria Antonietta Occhiuzzi[a], Michele De Luca[a], Elisabetta Mazzotta[a], Gaetano Ragno[a], Antonio Garofalo[a] and Rita Muzzalupo[a]

[a]*Department of Pharmacy, Health and Nutritional Sciences, University of Calabria, Via P. Bucci, 87036 Rende (CS)*

Published on Pharmaceutics 2019, 11, 197

ABSTRACT

An in-depth analysis of nanotechnology applications for the improvement of solubility, distribution, bioavailability and stability of reverse transcriptase inhibitors is reported. Current clinically used nucleoside and non-nucleoside agents, included in combination therapies, were examined in the present survey, as drugs belonging to these classes are the major component of highly active antiretroviral treatments. The inclusion of such agents into supramolecular vesicular systems, such as liposomes, niosomes and lipid solid NPs, overcomes several drawbacks related to the action of these drugs, including drug instability and unfavorable pharmacokinetics. Overall results reported in the literature show that the performances of these drugs could be significantly improved by inclusion into nanosystems.

Keywords

HIV; antiretrovirals; nanoformulations; drug degradation; drug protection

1. Introduction

The human immunodeficiency virus (HIV), belonging to the lentivirus genus of the large family of retroviridae, is the etiological agent of AIDS. The infection causes severe consequences to the immune system including a loss of CD4+T lymphocytes that leads to an increased susceptibility to even fatal opportunistic infections. The identification of various antiretroviral drugs allowed defining efficacious therapeutic regimens for the prevention and treatment of the disease by the combined administration of two, three or more different drugs acting on crucial steps of viral

replication. In particular, the targets of conventional drugs are proteins involved in the viral entry or specific enzymes necessary for the virus replication such as protease (PR), reverse transcriptase (RT) and integrase (IN). This approach known as HAART (highly active antiretroviral therapy) nowadays represents the most useful therapeutic treatment, even though it is affected by many drawbacks such as lifetime administration with a consequent reduced patients' compliance, severe side effects, and quick viral outbreak after drug resistance emergence.

Drug Class	Name (Acronym)	Year*	LS	OB (%)	t/2 (hours)	Side Effects
NRTIs	Stavudine (STV)	1996	low	86	1.3–1.4	Peripheral neuropathy, pancreatitis, asymptomatic acidosis, lipoatrophy, hepatic steatosis
	Zidovudine (AZT)	1986	low	60	0.5–3	Neutropenia, anemia, nausea, vomiting, asthenia, headache, insomnia, skin hyperpigmentation, acidosis, hepatic steatosis
	Lamivudine (3TC)	1995	low	86	5–7	Cough, diarrhea, fatigue, headache, malaise, nasal symptoms, lactic acidosis, hepatic steatosis
	Abacavir (ABV)	1998	low	83	0.8–1.5	Systemic respiratory hypersensitivity, gastrointestinal symptoms, fever, tiredness, sore throat
	Emtricitabine (FTC)	2006	low	93	8–10	Headache, nausea, upset stomach, diarrhea, trouble sleeping, dizziness, skin rash, strange dreams, cough, runny nose
	Zalcitabine (ZCT)	1992	low	85		Peripheral neuropathy, stomatitis, esophageal ulcerations, acidosis, hepatic steatosis
	Didanosine (DDN)	1991	low	30	2	Gastrointestinal intolerance, peripheral neuropathy, pancreatitis, asymptomatic acidosis, lipoatrophy, hepatic steatosis
	Tenofovir (TDF)	2001	low	25-39	12–15	Nausea, depression, confusion, headache, hitching, weakness, kidneys problems
NNRTIs	Nevirapine (NVR)	1996	moderate	92	25–30	Rash, Stevens-Johnson syndrome, elevated transaminases blood level, hepatitis, severe hypersensitivity reaction
	Etravirine (ETV)	2008	high		30–40	Rash, Stevens-Johnson syndrome, toxic epidermal necrosis and multiform erythema, hypersensitivity reactions, hepatic failure
	Etravirine (ETV)	2008	high		30–40	Rash, Stevens-Johnson syndrome, toxic epidermal necrosis and multiform erythema, hypersensitivity reactions, hepatic failure
	Rilpivirine (RPV)	2011	high	50	19	Rash, depression, liver problems, mood changes

Table 1. Relevant information of currently used RTI. *Year of FDA approval; LS = Lipid Solubility; OB = Oral Bioavailability; t/2 = Plasma Half-life.

HAART was demonstrated to be particularly effective in cutting down the overall number of viral particles, but is unable to completely eradicate infection in sanctuary sites, such as the brain, liver and lymphatic system [1–5]. Moreover, HAART always includes one or more nucleoside and non-nucleoside reverse transcriptase inhibitors (NRTI and NNRTI, respectively), which, despite a high antiviral efficacy, unavoidably show important clinical drawbacks. Relevant information on common RTI is summarized in Table 1 [6,7].In the light of these findings, the incorporation of new or customary anti-HIV drugs into supramolecular carriers could be particularly effective in suppressing viral replication. This strategy is corroborated by the possibility of encapsulating drugs or genes to not only be delivered next to the infected cells but also to target reservoir tissues to eradicate latent HIV [14]. This innovative strategy is suitable for improving the distribution of both hydrophilic and hydrophobic small molecules, as well as macromolecular drugs, which can be driven toward specific tissues thanks to the reduced size of the nanoscale delivery systems. Antiretroviral drugs can be carried as nanoparticles for their potential to better reach macrophages, CD4+T cells and latent reservoirs organs, such as brain and lymphnodes, that are particularly responsible of viral survival. [15–19]. Drug delivery systems (DDS) for RTI, developed in the last few years, are described in this survey and depicted in Figure 1, while their main properties are summarized in Table 2.

DDS		TARGET
Matrix	Surface	
Liposome NPs	Mannose	Liver, spleen, lung, brain, macrophages
Liposomes	Galactose	Liver
Chitosan NPs	Glycyrrhizin	Liver
NPs	Transferrin	Brain, endothelial cells
NPs	Serum albumin	Brain, liver, spleen
SLN	Phenylalanine	Blood brain barrier
Polymeric micelles	Anti-GP2 antibody	M-cell of gut-associated lymphoid tissue
Dendrimers	Tuftsin	Macrophages, monocytes, polymorph nuclear leukocytes

Table 2. Targets of DDS designed for anti-HIV therapy.

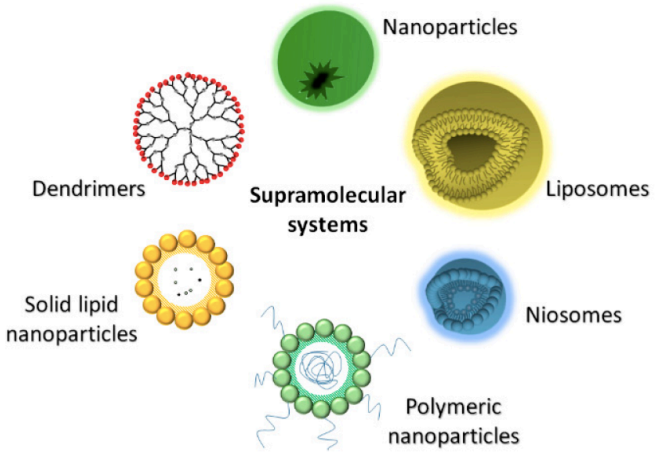

Figure 1. Drug delivery systems for RTI nanoformulations

Once the supramolecular system reaches the site of action, a controlled drug release provides high local concentration and longer residence time, resulting in an improved antiviral effect (Figure 2).

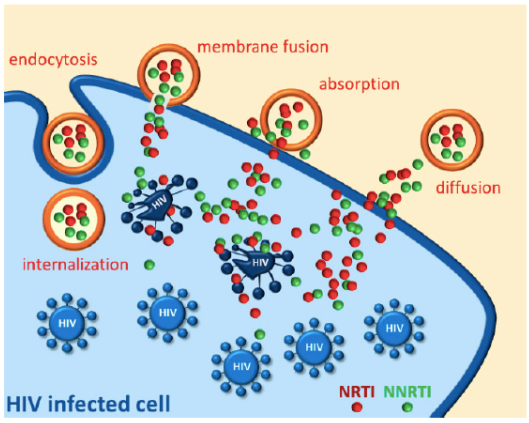

Figure 2. Representative delivery modalities for NRTI/NNRTI nanosystems to HIV resevoirs

The major advantages and limitations of known nanosystems are listed in Table 3. Several of these clinically used drugs show an undesirable stability profile when exposed to stressing conditions either in solution or in solid form [20,21]. Similarly, stress tests have been performed on supramolecular systems in order to confirm any improved stability, under different conditions [22]. In particular, studies published in the last few years on the RT inhibitors included in combined therapy have been taken into consideration [15,16,23].

DDS	Advantages	Limitations
Liposomes	Co-delivery of hydrophilic and lipophilic drug Selective uptake by mononuclear phagocytes Surface modification with target moiety of virus reservoir	Low drug loading capacity Physical and chemical instability Drug leakage Difficulty in sterilization Short half-life Poor scale up
Niosomes	Chemical stability Protection of drug from degradation Large uptake by mononuclear phagocytes and localization in virus reservoir organs Less expensive respect liposomes Functionalization with target ligand	Physical instability during the storage Difficulty in sterilization Difficulty in large-scale production
Polymeric NPs	High drug loading capacity Co-delivery of different drug for anti-HIV combination therapy Selective uptake by lymphoid organ Prolonged circulation time Surface functionalization with target moiety	Fast burst release Limited safe correlated to polymer toxicity High cost production
SLN	Higher stability and biological compatibility than liposomes and polymeric NPs Increase the bioavailability of poorly water soluble drug Avoidance of organic solvent Slow uptake by the RES Feasible-large scale production and sterilization Less expensive than polymeric and surfactant carriers	Low drug solubility in lipid matrix and loading capacity Drug leakage Particle growth Unpredictable gelation tendency
Dendrimers	Uniform particle size Large surface functional groups for the conjugation with target moieties	Toxicity problems

Table 3. Advantages and limitations of anti-HIV DDS

2. Drug Protection Nanosystems

Most of the protocols adopted for studying the drug stability are suggested by the ICH (International Conference on Harmonization) guidelines [24]. According to such rules, clearly defined drug storage conditions are required to prevent the degradation effects related to pH, temperature, light, air and humidity for either solution/suspension or commercial formulations/packaging [25]. The protection of sensitive drugs could often be assured by shielding with an adequate packaging [26]. When this simple precaution showed not to be sufficient, the stability of the drug, exposed to different environmental conditions, could be improved by suitable delivery devices, such as vesicular matrices (i.e., liposomes and niosomes), nanoparticles (NPs), and solid lipid nanoparticles (SLN).

Niosomal and liposomal vesicles consist of amphiphilic molecules and an aqueous compartment and differ for their structural chemical units. Both systems are very versatile. The hydrophilic drugs can be entrapped in their aqueous core while the lipophilic drugs can be partitioned into the bilayer domains. Liposomes are made of natural phospholipids, resulting in a greater stability, a low production cost and reduced toxicity [27–32], while niosomes are prepared by means of synthetic, non-ionic surfactants, as alkyl ethers, alkyl esters and pluronics copolymers, or fatty acid and amino acid compounds [31–33]. The preparation of these vesicles requires a

simple procedure based on a gentle agitation or sonication of an aqueous solution of phospholipid/surfactant and drug mixtures taken from an ultracentrifugation or low-pressure gel filtration chromatography to purify the formed systems [34].

More recent SLN have been proposed as alternative formulations for both hydrophilic and hydrophobic drugs. These systems are colloidal carriers based on a solid phase lipid and a surfactant and are characterized by a spherical shape in which the lipid portion is always solid and the surfactant acts as a stabilizing factor [22,35–40]. Fatty acids, monoglycerides, diglycerides, triglycerides, waxes and steroids can be applied in the preparation of SLN in the absence of organic solvent [35]. Low cost, good physical stability, large scale production, no toxicity and high biodegradability represent the greatest advantages in the use of these formulations with respect to the liposomes matrices [41].

Nanoparticles systems are known promising carriers for the improvement of solubility and pharmacokinetics of drugs as well as vaccines, nucleic acids and therapeutic proteins. These delivery devices can influence therapeutic efficiency of a drug, enhance its protection from degradation and reduce dose-limiting side effects. A variety of hydrophobic or hydrophilic active molecules can be dissolved, encapsulated, absorbed or conjugated to polymeric nanoparticles following different techniques [42]. Several natural and biodegradable materials like chitosan have been proposed for the realization of anti-HIV drug nanosystems. An alternative approach, based on the formation of crystalline complex with a fixed range size, was attempted by inclusion of the pure drug into a hydrophobic synthetic polymer [43]. Polymeric nanoparticles based on poly(lactic acid) (PLA) or poly(lactide-co-glycolide) (PLGA) are reported as ideal delivery systems, showing an improved therapeutic efficacy with lower incidence of side effects [42,44–49].

A higher local concentration of active molecules is often reached by integration of classic antiretroviral drugs in different NPs of metals [50]. According to a relative inertness and low toxicity, silver or gold NPs have been explored in biomedicine as multifunctional scaffolds. In particular, the application of gold NPs has been employed to conjugate biomolecules on the outer surface. Alternative inorganic multifunctional materials, such as silver NPs coated with poly(vinyl)pyrrolidone, have also been exploited as drug carriers [51].

Synthetic well-defined nanopolymers with a three-dimensional architecture, known as dendrimers, have been proposed for the vehiculation of several drugs. Generally, a dendrimer is a symmetric and hyper-branched macromolecule characterized by the presence of reactive groups in the central core, repeated branching units in the interior layers of the core and functional groups spanning from the outer surface. The drug molecule can be either entrapped inside the structure or linked to the external functional groups. This approach was proposed for the carrying of several anti HIV agents [52–55]. Some of these matrices are also able to improve the stability of drugs. Several studies described the use of niosomes, metal based and

polymeric NPs to prevent the degradation effects caused by stressing conditions [33,50,56].

3. Nucleoside Reverse Transcriptase Inhibitors Nanosystems

The therapy based on the administration of nucleoside antiviral derivatives such as stavudine, zidovudine, lamivudine and emtricitabine represented a first and effective approach adopted for the management of HIV infection (Figure 3). Due to the structural similarity to purine or pyrimidine nucleosides, the mode of action of these drugs consists of the competition for the incorporation into viral DNA, catalyzed by RT, so causing chain termination (Figure 4, panel b). Nowadays the most common nucleoside derivatives used in therapy are lamivudine, abacavir, emtricitabine, tenofovir and tenofovir alafenamide [57]. Stavudine and zidovudine, not yet recommended in first-line therapy, were early examples of NRTIs included in nanoformulations designed for limiting their severe side effects and improving pharmacokinetics.

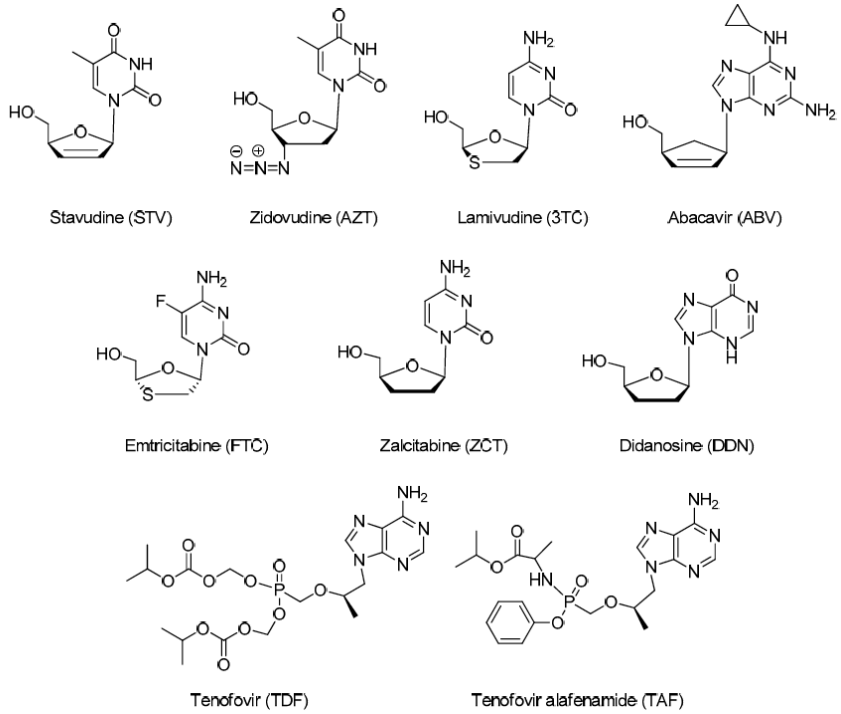

Figure 3. Chemical structures of NRTIs.

3.1. Stavudine

Stavudine (1-((2R,5S)-5-(hydroxymethyl)-2,5-dihydrofuran-2-yl)-5 methylpyrimidine-2,4(1H, 3H)-dione, STV) is one of the most commonly used forms of NRT approved by FDA in 1996 and its use was recommended in association with other antiretroviral agents. The drug showed major side effects, such as high blood lactate, pancreatitis and hepatomegaly. STV was characterized by a serum half-life of 1h only, while that of its phosphorylated active metabolite was calculated as being 3.5 h [27]. Thus, STV loaded

formulations able to concomitantly increase cellular uptake and sustain release should reduce unwanted effects. Accordingly, galactosyl or mannosyl coated liposomes loaded with STV were described. These formulations reached the desired results showing an increased *in vitro* anti-HIV activity together with a remarkable decrease of side effects. The efficacy was tested in a mononuclear phagocyte system, a major reservoir of HIV, proving advantages in terms of bio-stability, site-specific and ligand-mediated delivery, compared to free drug and uncoated liposomes [27,28]. More recently, STV-containing nanoformulations were proposed for the dual utilization to control the residual viremia as well as to target the reservoir sites. To achieve this aim, gelatin nanoformulations containing very low dosage of the drug were prepared through a simple desolvation process and loaded into soya lecithin based liposomes [29]. A study on STV degradation under different stress conditions (hydrolysis, oxidation, photolysis and thermal stress) was initially reported. A stability-indicating reversed-phase HPLC assay method showed the hydrolysis of the drug to thymine in acidic, neutral, alkaline and under oxidative stress conditions [20]. In order to improve the stability of this drug, STV-loaded SLN for intravenous injection were produced by high-pressure homogenization of drug lipid melt dispersed in hot surfactant solution [22]. This SLN formulation was also studied for its active delivery to lymphatic tissues by *ex vivo* cellular uptake evaluation in macrophages. Reported experiments confirmed an improved cellular uptake together with a prolonged activity next to the delivery site of the formulation compared to the simple drug solution. This could account for an efficient and safe therapeutic profile of the drug-carrier system [58].

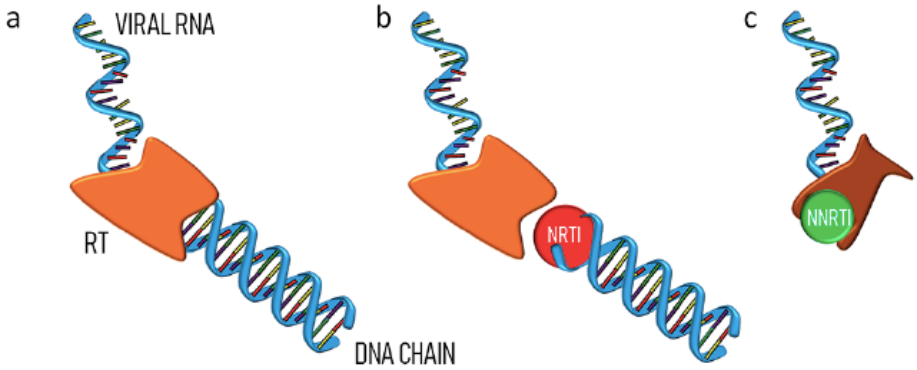

Figure 4. (a) RT catalyzes the conversion of viral RNA into pro-viral DNA before its incorporation into the target cell genome; (b) NRTIs are incorporated into the DNA causing chain termination; (c) NNRTIs bind the enzyme inhibiting its function.

3.2. Zidovudine

Zidovudine, also known as azidothymidine (1-((2R,4S,5S)-4-azido-5-(hydroxymethyl)tetra hydrofuran-2-yl)-5-methylpyrimidine-2,4(1H,3H)-dione, AZT), the first antiretroviral medication proposed to prevent and treat HIV/ AIDS, has been approved in 1986. An extensive first pass metabolism often requires an in vein administration. This feature and a long list of severe side effects limit the use of this drug, which is however still present in many therapeutic anti-HIV regimens. Its incorporation into supramolecular matrices was extensively exploited in order to increase bioavailability and to reduce dose-dependent unwanted effects. Positively and negatively charged liposomes based on stearylamine and diacetyl phosphate were used as AZT carriers. In order to enhance localization to lymph nodes and spleen, these systems were even coated with a site-specific mannose-terminated stearylamine ligand. Fluorescent microscopy images showed an enhanced uptake and localization of these liposomes in the target tissues [59]. In an early paper, a dispersed system comprising polyoxypropylene, polyoxyethylene, oleic acid, water and cetyl alcohol as surfactant, was described as a potential DDS. The release profile experimental analysis showed that the delivery of AZT could be controlled this way, in accordance with a mathematical theoretical approach [60]. This system has been proposed as a carrier, which potentially could overcome the main drawbacks of conventional pharmaceutical formulations [61]. AZT loaded in polymeric NPs based on PLA and poly(l-lactide)poly(ethyleneglycol) (PLA/ PEG) were prepared by double emulsion solvent evaporation and thoroughly investigated *in vitro* for uptake into polymorphonuclear leucocytes of rat peritoneal exudate. The cells activation by NPs was assessed by a chemiluminescence assay suggesting a more favorable behavior of PLA vs. PLA/ PEG complexes [62]. On the other hand, the drug release increased proportionally to the PEG amount in the blend [63]. AZT was encapsulated in alginate-glutamic acid amide based NPs obtained by an emulsion solvent evaporation method. The polymeric NPs were coated with pluronic F-68 to favor cellular internalization through the endocytosis mechanism. As a result, the antiviral drug loaded in these nanosystems was released in a prolonged manner. Intracellular uptake and cell viability assays also confirmed an efficient uptake of AZT in glioma cell lines [64]. Solid lipid NPs based on modified stearic acid and Aloe vera extract were described as an alternative drug delivery carrier for controlled release and targeting of AZT. The plant extract was used because of its high content of polysaccharides that showed synergistic antiretroviral activity with AZT. The described nanocarriers did not interact with plasma proteins and showed high drug loading and entrapment e ciency. Moreover, fluorescent microscopy images suggested that the natural gel facilitated the cellular uptake of AZT in brain cells [36].

The drug proved to decompose when exposed to light or under hydrolytic conditions, while it was more stable toward oxidation agents and thermal stress [65]. In particular, the acid degradation induced the formation of a pyrimidine derivative endowed with higher toxicity when compared to AZT, as demonstrated by a mutagenicity and an aerobic biodegradability assay [21]. Recently, three novel prodrugs of AZT, obtained by functionalization with dicarboxylic acids, were designed in order to enhance pharmacokinetics, chemical stability and a nity for human serum albumin [66].

3.3. Lamivudine

The oral agent lamivudine, (4-amino-1-((2S,5R)-2-(hydroxymethyl)-1,3-oxathiolan-5-yl)pyrimidin-2(1H)-one, 3TC), an analogous of nucleoside cytidine, was approved by FDA for the combined therapy with AZT in 1995 and for monotherapy in 2002. However, the emergence of drug resistance, associated to the gene mutation of RT, limited its clinical application [67,68]. Several nanocarriers were prepared by mixing biodegradable networks (i.e. PEG, pluronicpolyethyleneimmine (PEI), glycyrrhizin conjugated chitosan, mannosylated-PLGA) or dendritic networks (i.e. starPEG-PEI, poly(amidoamine)dendrimer-PEI-PEG) or nanogels with AZT or didanosine triphosphates under a freeze-drying method, to specifically deliver the antiviral agent next to macrophages in the CNS. All nano-NRTIs demonstrated high efficacy in inhibiting HIV at low M drug concentration. The major cause of NRTI neurotoxicity, consisting in the mitochondrial DNA depletion, was also reduced 3-fold compared to uncoated NRTIs [69]. Acid or alkaline conditions as well as an oxidative environment caused the degradation of the drug into five different products. On the other hand, light exposure or thermal stress did not affect drug stability [70,71]. More recently, a mass spectrometry study evidenced the formation of an additional degradation product when the solid drug was exposed to oxidative conditions [72]. 3TC was incorporated into polymethacrylic acid NPs in dierent drug/polymer ratio by nanoprecipitation method in order to overcome some drug limitations, such as accumulation during multi dose therapy and poor patient compliance. These polymers offer several advantages, including high stability and simple preparation route compared to remaining colloidal carriers. Moreover, these nanocarriers were shown to increase drug bioavailability and optimize the release time to the target site without significant chemical interactions between the drug and matrix [73]. An alternative encapsulation for 3TC was exploited by using PLGA NPs coated with bovine serum albumin through a double emulsion procedure. It was then demonstrated that PLGA NPs were rapidly internalized into the human liver cells after oral administration, at different drug concentrations, confirming their high potential as ideal 3TC delivery systems [74]. The PLGA/ 3TC system was also investigated for the formulation of a thermosensitive vaginal gel. The system was

obtained in the form of NPs by the formation of an amide bond between the biodegradable polymer and the free amine group of the drug. An analogue formulation was prepared using emtricitabine as an alternative NRTI. The NPs were finally incorporated into a thermosensitive gel for vaginal administration. The nanoformulations showed to be non-toxic in HeLa cells assay up to a 100 g/ mL concentration. Similar preparations containing fluorescent NPs were found to be active for up to 5 days, suggesting a potential long-lasting application in therapy [75]. A similar approach was adopted for the achievement of transdermal formulation of PLGA/ 3TC complex. NPs obtained resulted in an ideal spherical shape and an external smooth shell. The high drug entrapment rate resulted in an improved physical stability of the drug together with an efficient delivery after skin permeation. This last property was enhanced after microneedles skin pre-treatment [76]. Mannosylated-PLGA NPs were prepared to ensure an efficient delivery of 3TC into brain macrophages. The experimental data confirmed the increased drug release from nanocarriers and this e ect may be due to the presence of sugar receptors on the luminal surface of blood-brain barrier (BBB) [77]. 3TC was also entrapped into PLA/ chitosan (CS) NPs by an emulsion technique. The drug was e caciously entrapped and protected at low values of pH, while it was rapidly released at higher pH values, thus allowing the drug to be selectively absorbed in the intestinal tract. These NPs were also proven to be non-toxic in a mouse fibroblasts model. Efficient biomedical applications could be accordingly envisaged for such an inclusion system [78]. Similar results were obtained for 3TC-CS NPs prepared by ionic gelation of CS with tripolyphosphate anions. These formulations o er several advantages with respect to conventional dosage forms of the drug, particularly in terms of bioavailability [79]. The CS functionalization with glycyrrhizin was realized for a liver targeting and a 3TC controlled release. In fact, the results of this research confirmed a lower drug release and an augmented level of 3TC in hepatocyte tissues, if compared with CS NPs or the free-drug solution [80]. Successively, 3TC was loaded into poly(ε-caprolactone) through a double emulsion spray-drying method giving rise to NPs with spherical morphology. This system also proved to be effective in improving drug bioavailability and reducing side effects [81]. Multiple drugs combined in a single nanosystem showed significant advantages over therapy based on a single drug. Accordingly, an example of polymeric NPs based on methyl methacrylate or ε-caprolactone was designed for the release of four different anti HIV drugs, AZT, 3TC, nevirapine and the IN inhibitor raltegravir [82]. In a recent paper, the incorporation of 3TC into CS with sodium alginate/ calcium chloride by the above gelation method, in different experimental conditions, was described and showed an impressive drug release rate lasting up to 24 h. The method proved to furnish highly homogenous particles capable of improve bioavailability together with a constant drug release, following a first order mechanism, with diffusion of the drug after swelling of the polymer [83]. Protein-based NPs were prepared using lactoferrin for the controlled release of 3TC combined with AZT and EFV, after its

application for a single DDS. The lactoferrin possesses itself antiviral activity and therefore acts synergistically with the entrapped drugs. The assessment of pharmacokinetic profile for each entrapped drug and *in vitro* data suggested that these NPs are able to release drugs intracellularly in a controlled and sustained manner [84,85]. Alternative nanotechnologies used for anti-HIV drugs release included the use of inorganic components such as iron or silica. Preliminary results suggested a potential application for these new formulations. In particular, chemical-physical characterization of SiO_2 NPs coated with magnetic Fe_2O_3 loaded with 3TC were investigated for their pharmacokinetic and cytotoxic profiles showing more favorable features compared to the free drug [86]. A similar preparation was attempted for 3TC and zalcitabine both in form of triphosphosphates. Preliminary results showed that these nanosystems of dideoxynucleoside triphosphates/SiO_2 NPs were useful transport systems for delivering these drugs to target cells with increased antiviral efficiency [87]. Moreover, the co-encapsulation of 3TC and AZT, both in form of triphosphates, into iron carboxylate mesoporous NPs gave biocompatible systems endowed with peculiar delivery properties. In particular, the drugs were released with different kinetics: 3TC showed accelerated release, while AZT was released more slowly. This vector protected drug from degradation, conferring at the same time improved *in vitro* anti-HIV activity. In fact, these formulations contribute to stabilizing the drugs since no alterations were detected after two-month storage and freeze-drying reconstitution [50]. High drug bioavailability and patient compliance were recorded after the administration of the of 3TC encapsulated into a new gum odina based biopolymer obtained by a multiple water-in-oil-in-water emulsion approach. The long-term stability study showed the improvement of the stability of the emulsions after a 90-day storage compared to a similar emulsion comprising Tween 80 as a stabilizer [88]. 3TC was also loaded in nanovesicles based on phospholipids or non-ionic surfactants (niosomes and liposomes). The best components and reparation methods able to produce formulations with suitable size, improved drug encapsulation efficiency and release profile were formulated for these systems [89,90].

3.4. Abacavir

Abacavir ((1S,4R)-4-(2-amino-6-(cyclopropylamino)-9H-purin-9-yl)cyclopent-2-en-1-yl)methanol, ABV) introduced in 1998, represented an alternative nucleoside derivative administered orally in solid or solution form for the prevention and treatment of HIV infection. Similarly to other nucleoside analogous, its use is recommended in combination therapy because of its severe side effects like hypersensitivity, liver damage and lactic acidosis, which all preclude monotherapy. ABV and its congener 3TC, after transformation into the corresponding thiol ending ester derivatives, were conjugated to glucose-coated gold NPs, which were investigated for their pH dependent drug release performances. This drug-delivery

system was in turn studied for new multifunctional devices since such gold NPs, themselves endowed with microbicide properties, proved useful for the loading of more than one active agent differently targeting the viral replication cycle, and therefore representing a multivalent therapeutic approach [51]. Albumin NPs loaded with ABV sulfate were prepared by solvation method and studied for their mechanism of drug release. Results obtained revealed a remarkable drug loading capacity together with a sustained and controlled release within 24 h in HIV reservoir organs [91]. A myristoylated ABV prodrug entrapped into poloxamers was evaluated for the pharmacokinetic properties after injection in mice. Comparison of such nanoformulation with the free drug was performed on human monocyte-derived macrophages by proton nuclear magnetic resonance studies in terms of anti-HIV activity.

As a result, an efficacy comparable to that of the native drug was detected for the encased polymer, which showed a two-week lasting release [92]. A detailed study described the formation of innovative nanocarriers named ProTide (PROdrug and nucleotide) obtained by the loading of L-alanine and L-phenylalanine ester phosphoramidates of ABV into PLGA and poloxamer NPs. Such formulations showed sustained retention and antiretroviral activities for up to one month [93].

3.5. Emtricitabine

Emtricitabine (4-amino-5-fluoro-1-((2S,5R)-2-(hydroxymethyl)-1,3-oxathiolan-5-yl) pyrimidin-2(1H)-one, FTC), is a deoxycytidine nucleoside analogous approved in 2006 for anti-HIV therapy. Even if it showed reduced side effects when compared to other NRTIs, FTC is largely used in triple or quadruple drug combinations.

A customary PLGA nanoformulation of this water soluble drug was achieved through the water-in-oil-in-water emulsion method and showed a sustained release profile in rats, with adequate drug concentration up to two weeks [94,95]. The large volume distribution, beside a short plasma half-life, suggests the use of FTC in alternative formulations, such as PLGA NPs. This particular administration form proved to be able in enhancing drug stability and intracellular retention time, as demonstrated by an *ex vivo* endosomal assay. A once-biweekly dosing for HIV infection prevention or treatment was accordingly hypothesized [96]. In addition, eight degradation products were separated and characterized by LC–MS/MS from ABV sulfate when subjected to forced degradation under hydrolysis, oxidation, photolysis and thermal stressing conditions [97]. More recently, a solution state study showed the formation of eleven degradation products [98].

The thermal decomposition of FTC was well investigated by applying different methods. FTC largely decomposed to small molecules and insoluble substances. A small amount decomposed to 5-fluorocytosine due to an oxidation reaction [99]. When the drug was exposed to the action of acids or bases as well as oxidative stress conditions, an additional degradation product was detected [100].

3.6. Tenofovir

Tenofovir disoproxil fumarate ((R)-(((((1-(6-amino-9H-purin-9-yl) propan-2-yl)oxy)methyl) phosphoryl)bis(oxy))bis(methylene) diisopropyl dicarbonate, TDF) is a more recently approved NRTI (2001) used in the treatment of chronic hepatitis B and in the prevention and treatment of HIV infection. Successively its prodrug tenofovir alafenamide fumarate ((isopropyl 2-((((((R)-1-(6-amino-9H-purin-9-yl) propan-2-yl)oxy)methyl)(phenoxy)phosphoryl)amino)propanoate, TAF) was launched in the market due to its more favorable properties after oral administration. TAF has greater antiviral activity and better distribution into lymphoid tissues than TDF. Both drugs are recommended in combination therapy along with other antiretroviral agents.

3.6.1. Tenofovir SLN

Lipid NPs loaded with NRTI and NNRTI agents including TDF or TAF were extensively studied for the improvement of bioavailability and long lasting drug release. Several lipid matrices were designed and showed a very promising behavior under different experimental conditions [37,101,102].

Toxic effects of TDF loaded in nanoemulsions on liver and kidney were assessed using an animal model. Although any behavioral toxicity and mortality were not detected, moderate alterations were however observed on both organs [103]. Extensive chemical-physical studies were performed on hybrid inclusion complexes obtained by encasement of TDF into lipid and polymer matrices by engineered melt emulsification-probe sonication technique. The carrier obtained by combining TDF, lauric acid and pemulen polymer was shown to promote a noteworthy increase of TDF trans-nasal flux, so potentially useful for nasal administration [104]. Nanocarriers based on a hydrogel-core and a lipid-shell were designed for the controlled loading and topical vaginal release of TDF and maraviroc, a virus entry inhibitor. These nanolipogels proved to be efficient systems and robust carriers for the encapsulation and the prolonged *in vivo* release of antiretroviral drugs, showing solubility concerns that are useful during the prevention and treatment of HIV infection [105].

3.6.2. Tenofovir/ Dendrimers Complexes

A drug combination including TDF into dendrimers was designed for the evaluation in an *in vitro* model of semen-enhanced viral infection. The results obtained suggested that this therapeutic strategy could bypass the detrimental effects of amyloid fibrils, present in semen, which seem responsible of the failure of topical vaginal gels action [54]. An approach to the treatment of neuro-AIDS was based on the use of co-encapsulated drugs into ultra-small iron oxide NPs with the addition of dextran sulfate. The inclusion complex of TDF and vorinostat, a latency-breaking agent, was assembled by magnetically guided layer-by-layer method and a noteworthy blood–brain barrier transmigration of drugs was then observed. This

strategy, aimed to the activation of latent virus and its simultaneous killing, would result in a high efficacy to eradicate completely the infection from the CNS [106]. Nanosystems such as carbosilane dendrimers seem themselves able to inhibit HIV replication with a potential as local antiviral agents. Nevertheless, the concomitant administration of specific antiretroviral agents led to a potent synergistic activity. TDF, along with AZT and EFV or with maraviroc was encapsulated into anionic carbosilane dendrimers, bringing sulfated and naphthyl sulfonated groups to generate potential microbicides to prevent the sexual transmission of HIV [55 ,107 –110]. An innovative therapeutic strategy could be based on the TDF prolonged release from NPs obtained by hyaluronic acid (HA) cross-linked with adipic acid dihydrazide. This nanosystem did not show detectable toxicity under the control of hyaluronidase enzyme. Comparative experiments with a simple TDF/ HA gel suggested an essential role of the enzyme during the HA degradation and TDF release. The potential of these formulations for topical delivery of antiviral agents for the prevention of sexually transmitted diseases was accordingly hypothesized [111].

3.6.3. Chitosan based TDF Nanoparticles

TDF was also used as a model drug in a CS based nanopreparation coated with sodium acetate, an aggregation-preventing agent, realized by the freeze-drying method. The NPs cytotoxic profile on macrophages was assessed by neutral red, resazurin, nitrite oxide and cytokines assays. Satisfactory encapsulation rate together with a good stability of the colloidal dispersions was observed for the formulation. Moreover, a sustained drug release beside a lack of cytotoxicity and a pro-inflammatory effect was recorded [112]. Further improvements in terms of mucoadhesive performance were obtained by a formulation based on TDF-loaded CS NPs dispersed in vaginal thermogels [113]. CS based oral NPs loaded with TDF were prepared by the ionic gelation technique and studied for their potential in preventing esterase metabolism and facilitate active transport uptake. Both processes were affected as confirmed by *in vitro* experiments. Moreover, data obtained suggested that a clathrin-mediated mechanism is involved in the enhancement of drug oral absorption [114].

A triple combination of TDF, FTC and bictegravir, an integrase inhibitor, was loaded into trimethyl CS to generate a nanoconjugate with improved cellular uptake. The efficiency of the nanocarrier was determined by spectrophotometry while XTT and ELISA tests were used to determine cytotoxicity and anti-retroviral efficiency, respectively. As a result, this formulation proved to inhibit viral replication at lower concentrations than the free drugs combination, without a significant cytotoxicity, therefore resulting in a lower drug resistance [115]. Colloids based on polyelectrolyte complexes of CS and chondroitin sulfate were loaded with TDF and examined for the stability at physiological conditions.

This property was assured by the use of Zn(II) throughout the formulation procedure. *In vitro* studies did not reveal toxicity of such NPs on human peripheral blood mononuclear cells, while a remarkable dose-dependent antiretroviral activity was detected [116]. TDF was loaded into thiolated CS core/shell nanofibers in order to investigate the rate of drug loading, mucoadhesion properties and *in vivo* safety. The formulation was fabricated by assembling poly(ethylene oxide) with the CS component and PLA by a coaxial electrospinning technique. An enhanced drug loading together with a prolonged drug release and an increased mucoadhesion were assessed by *in vitro* studies, whereas a significant toxicity was not detected in neither *in vitro* nor *in vivo* experimental models. These new formulations could be therefore considered promising tools for the local delivery of microbicide agents [117].

3.6.4. Alternative Polymeric TDF NPs

An original formulation to be used for vaginal administration was fabricated by oil-in-water emulsification of the inclusion product of TFV into PLGA and sodium deoxycholate as an ion-pairing agent and a thermosensitive gel. Sustained release properties in humanized BLT mice were shown for these nanoformulations when instilled locally [118]. Similar results were obtained by loading TFV into PLGA/ stearylamine and incorporating such NPs into a hydroxypropyl methylcellulose/ PVA-based film [119 ,120]. TAF and FTC entrapped NPs were prepared for subcutaneous administration during pre-exposure prophylaxis. Drugs were included into the PLGA/ PVA system and investigated for their long-acting potency detectable even after 14 days by a humanized mice model [121 ,122]. A similar approach was exploited for the incorporation of TAF and elvitegravir, an integrase inhibitor, during the fabrication of devices to be used during vaginal prevention [123 ,124]. The drug absorption following oral administration were also positively affected by the use of TAF/ PGLA loaded NPs, as highlighted by a statistical model study [125]. Formulations containing mono- or by-layered films of PVA and pectin were coupled with Eudragit NPs loaded with TDF/ FTC, by nano spray-drying technique. These systems were designed for vaginal use with a better patient compliance. The time of disintegration and drug release was evaluated in a simulated vaginal fluid, showing favorable results. The by-layered films equipped with NPs loaded with drugs showed the best performances in terms of drug release delay. Moreover, this topic formulation was shown particularly safe by MTT and lactate dehydrogenase assays using different cervical cell lines [126]. Multifunctional magneto-plasmonic liposomes charged with TDF were obtained with the aim to study guided systems for enhancing efficiency of antiviral treatment. The distribution of such a hybrid system can be monitored by image technique and activated magnetically into the brain. The gold shell of such nanocomplexes can be followed by computed tomography. This way, these particular systems proved to be efficient against HIV in infected microglia cells after adequately crossing the BBB [127]. A nanosuspension of drug combination particles consisting of TDF, ritonavir

and lopinavir, two protease inhibitors, and lipids were prepared for the development of innovative topical formulations. This system was highly efficient in targeting lymphocytes during anti-HIV therapy with a long-lasting action after a single subcutaneous administration [128]. Similar results were described after the addition of 3TC to the previously combination to give a four-drug components nanosuspension [129]. Similar results were obtained for alternative combinations of TDF and other RTI. In all cases, a persistent drug concentration was detected after single subcutaneous injection in different HIV reservoir cells [130 ,131].
A stability study was performed on TAF and compared with the stress degradation behavior of TDF. Gastrointestinal stability studies were conducted on both drugs, showing the formation of six degradation products. These studies revealed a higher stability of TAF, except for with the acid condition, where the drug was extensively degraded [132].

4. Non-Nucleoside Reverse Transcriptase Inhibitors Nanosystems

An alternative approach to anti-HIV treatment with RTIs is represented by the combined therapy using both NRTIs and NNRTIs, exploiting the synergism of the two distinct classes of drugs. Accordingly, the multi-therapy is nowadays the most widely adopted strategy for the treatment of HIV infection in the clinic. NNRTI act directly by binding the enzyme, so preventing its DNA polymerase function. In fact, their heterogeneous structures do not resemble those of nucleobases, the natural substrate of RT (Figure 4, panel c). After a first generation NNRTI drugs introduced in the 90s (i.e. nevirapine, delavirdine, efavirenz) approved for anti-HIV therapy, recently some new and effective compounds entered the market (i.e. etravirine, rilpivirine). Some more interesting compounds are currently under clinical investigation. The structures of representative NNTRI are reported in Figure 5.

4.1. Nevirapine

Nevirapine (11-cyclopropyl-4-methyl-5H-dipyrido[3,2-b:20,30-e] [1,4]diazepin-6(11H)-one, NVR) was the first NNRTI approved by FDA in 1996 for the treatment of HIV infection. In order to improve the pharmacokinetics of this hydrophobic drug, NVR was loaded into liposomes prepared by thin film hydration and extrusion method to give uniform spherical vesicles. The matrix, obtained from egg phospholipid and cholesterol, proved to release the drug during 22 h at physiological pH values. The presence of proteins into the medium or the exposition of the system to ultrasounds greatly impair the delivery mode of the drug. However, this encapsulation method could optimize the efficacy of NVR in terms of drug stability and controlled release to the target tissues [30]. Transferrin grafted PLGA NPs have been designed in order to facilitate NVR in crossing vascular endothelial cells of the human brain. This particular nanosystem allowed a favorable drug loading with a desired controlled release, so proving to act as an efficient carrier to promote vascular diffusion of the compound [133]. Nanoparticles of

PLA/PEG, the surface of which was modified with serum albumin, were prepared to improve release of the drug to the target tissues. This favorable feature was measured after i.v. injection in rats, showing an improved bioavailability, cellular uptake and drug accumulation in the brain, liver and spleen, compared to pure drug solution or uncoated nanoformulations. Moreover, no additional cytotoxicity was recorded. The capability to cross the BBB makes these formulations potentially useful for the treatment of AIDS related dementia [134,135]. The stability of NVP was well investigated by a stability-indicating ultra-high performance liquid chromatography (UHPLC) method. Drug product efficacy, safety and quality were verified in different degradation conditions by using acids, bases, water, metal ions, heat, light and oxidation agents. The tests were applied on the pure compound and on its tablet formulation leading to the formation of five degradation products [136]. A physically stable formulation of NVP was prepared by forming a crystalline inclusion complex with biodegradable and hydrophobic poly(ε-caprolactone). Compared to pure NVP crystals, the formulation assured a sustained drug release at physiological conditions in PBS solution up to 6 weeks, due to the reduction of drug solubility [43].

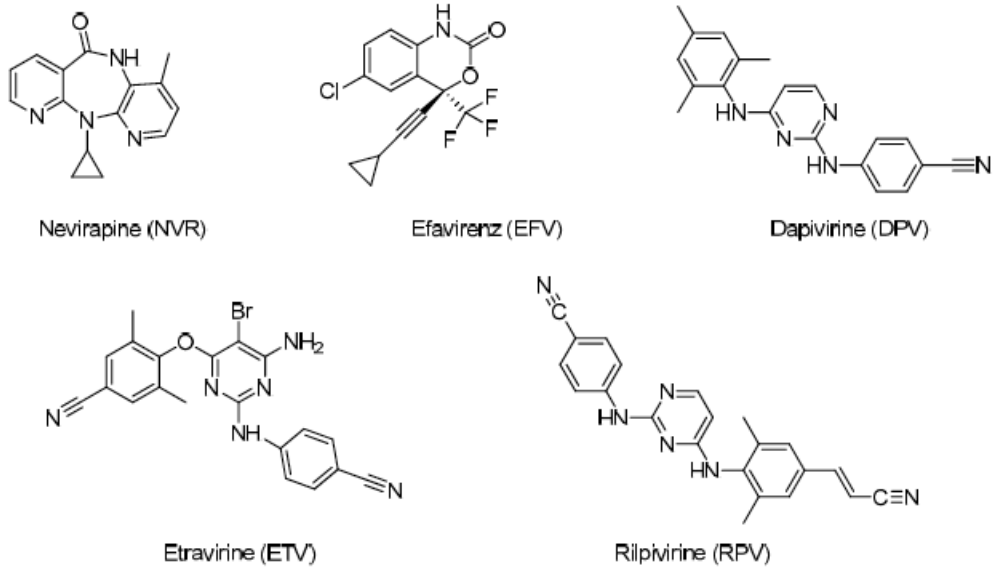

Figure 5. Chemical structures of NNRTI

4.2. Efavirenz

Efavirenz, ((S)-6-chloro-4-(cyclopropylethynyl)-4-(trifluoromethyl)-1H-benzo[d][1,3]oxazin- 2(4H)-one, EFV) was approved in 1998 and is largely utilized with other drugs for anti-HIV association therapies. However, its potential was limited by a low bioavailability due to its high lipophilicity and other drawbacks related to irritant effects on mucosae [137,138]. A strategy devoted to the improvement of EFV pharmacokinetics resides in its incorporation into SLN, which

should drive the delivery of the drug next to the lymphoid system and brain [38]. Phenylalanine anchored SLN (PA-SLN) were used to encapsulate EFV and the resulting nanocomplex was tested for its potential to cross BBB. Phenylalanine was chosen in order to exploit the aromatic amino acid transporter active within the barrier. The nanocomplex showed good entrapment efficiency and a favorable drug release, with a remarkable accumulation in brain assuring a long-lasting therapeutic effect [139].

4.2.1. Efavirenz SLN

SLN of selected lipids as matrix medium and EFV were prepared with the addition of a surfactant by high-pressure homogenization technique and evaluated in vivo for their enhanced bioavailability and brain targeting. In particular, such properties were assessed after an intranasal administration route, which could be useful for therapy devoted to the complete eradication of HIV [39]. As an example, EFV was loaded into SLN assembled with the use of mono- and tri-glycerides with the aid of a surfactant. This particular formulation allowed the drug to partly by-pass liver metabolism after oral administration and in doing so increasing bioavailability and accumulation into spleen [140]. A prolonged drug release together with a lower incidence of side effects, consequent to a reduced drug dosage, was achieved after EFV incorporation into SLN.

4.2.2. Polymeric EFV NPs

Efavirenz was loaded into NPs based on methacrylate polymers, which conferred an increased drug uptake in monocytes and macrophages [141,142]. Emulsion or nanoprecipitation methods allowed loading EFV into biodegradable PLGA NPs. The effects of the resulting formulations administered in combination with other free or encapsulated anti-HIV drugs were investigated. As a result, the new formulations proved more efficient compared to the free drugs and also a noteworthy synergistic effect was recorded for encapsulated EFV combined with TDF, a second NRTI [143]. EFV was dispersed with -tocopherol polyethylene glycol succinate and PVA by an emulsion-templated freeze-drying technique to realize solid inclusion NPs. Dry monoliths charged with these NPs proved to be stable for several months. Their reconstitution in water furnished nanodispersions, which showed reduced cytotoxicity together with an improved bioavailability and pharmacokinetics [49]. A nanoformulation was obtained by combining EFV with cellulose acetate phthalate, acting as an HIV entry inhibitor, by the nanoprecipitation method. The resulting NPs were formulated into a thermosensitive gel, which resulted in an efficient nanomicrobicide for long-term HIV prophylaxis [144]. Polymeric micelles based on pluronic F127 loaded with EFV and bio-conjugated with anti-M-cell-specific antibodies were prepared in order to evaluate their preferential target delivery to gut micro fold cells of lymphoid tissue, one of the major HIV reservoirs in the body. The

efficiency of such nanosystem was showed to be higher than the free drug and a possible oral application by enteric-coated capsule was accordingly hypothesized [145]. EFV was loaded into eudragit, pluronic and alginate sodium polymeric based NPs by solvent evaporation method. Cytotoxicity and antiviral characterization was investigated by syncytium inhibition assay. The polymeric nanocarrier was proven to be more effective than the pure free drug by an enhanced drug dissolution and bio-distribution, especially after BBB crossing. A reduced toxicity was also detected [146,147]. NPs to be used during intranasal administration were prepared by the encasement of EFV into CS grafted hydroxypropyl beta cyclodextrin matrices.
The results obtained confirmed a better CNS access due to an improved cellular permeation consequent to both a higher drug solubility and a concomitant beneficial action of CS on cell membrane [148]. Rectal polymeric formulations were prepared by incorporation of EFV into PLGA NPs coated with PEG. This particular form assured a prolonged drug residence in the lower colon with a long lasting prophylactic action against HIV transmission [149]. A better BBB crossing together with a reduction of side effects incidence was attempted by the preparation of transferrin functionalized PLGA NPs loaded with EFV. Although a higher deposition rate of the drug to the targeted site was recorded, the formulation did not improve drug membrane permeation [150]. Lactoferrin NPs were fabricated for oral or vaginal administration giving raise to significant results in terms of drug release and bioavailability. A combination of EFV and curcumin was also attempted in order to reach synergism for the two-microbicide agents. The results obtained confirmed an improved pharmacokinetic profile for the drug combination nanoformulation with respect to free drugs [151 ,152].

4.2.3. Efavirenz/ Dendrimer Complexes

EFV was incorporated into t-Boc–glycine and mannose conjugated dendrimer-based poly(propyleneimine) (PPI). These branched three-dimensional polymers were shown to be less toxic than free PPI and could allow the drug to reach monocytes and macrophages, both reservoirs of HIV in the body. In fact, it is known that inhibitors targeting only lymphocytes are ineffective in completely eradicating the infection. These formulations demonstrated to be particularly effective since they are able to promote a significant increase of EFV cellular uptake [153]. The same authors loaded EFV into dendrimer-based PPI complexed with tuftsin (Tu). This latter is a tetrapeptide coming from the cleavage of immunoglobulin G and showed to be capable of selectively target and activate macrophages, monocytes and polymorph nuclear leukocytes. This strategy would help EFV in avoiding unwanted effects acting in a synergistic fashion with the peptide. Such an option was suggested by the fact that the TuPPI complex showed no toxicity and prolonged EFV cellular uptake in HIV infected macrophages with respect to uninfected cells [154].

4.2.4. Alternative Supramolecular EFV NPs

Vesicular systems consisting of gold NPs entrapped inside the aqueous core were loaded with EFV in the bilayer membrane. The niosomes so formed were dispersed in carrageenan/hyaluronic acid/poloxamer based thermogel after coating with an opportunely functionalized mannose, in order to combine the action of the protein and the sugar for an effective prophylactic vaginal application. A remarkable inhibition of viral transmission as well as a drastic reduction of side effects was recorded [31]. A soya lecithin/cholesterol and PEG liposomal DDS was designed in order to overcome the limited solubility, dissolution rate and bioavailability of EFV [32]. Similar results were achieved by the entrapment of EFV into boron nitride and carbon nanotubes as delivery vehicles. Both the systems showed a favorable behavior. Between the two distinct formulations, carbon nanotubes assured a higher drug adsorption [155]. Enhanced solubility and dissolution of the drug were also obtained by inclusion complex with hydroxypropyl--cyclodextrin. The solubility of the complex was further increased by the addition of l-Arginine [156]. Degradation behavior of the drug in water solution was assessed by HPLC analyses, detecting a total twelve degradation products under acidic conditions. Alkaline stress resulted in the formation of only two degradation products, whereas oxidative and photolytic conditions did not promote any degradation of the drug. All the degradation derivatives showed remarkable toxicity, including carcinogenicity, mutagenicity and skin irritation, as confirmed by in silico experiments [72]. The thermal behavior of glass EFV was evaluated in different experimental conditions, showing a good stability only at room temperature [157].

4.3. Dapivirine

Dapivirine (4-((4-(mesitylamino) pyrimidin-2-yl)amino)benzonitrile, DPV) is a new, sparingly soluble NNRTI, under investigation for vaginal application during the prevention of HIV sexual transmission. This compound was shown to be a non-competitive inhibitor of RT that is particularly useful for topic treatments. In order to improve efficacy, a microbicide film for vaginal delivery was formulated by loading DPV into PLGA NPs and the nanosystems were in turn coupled to a PVA in a cellulose based platform film using solvent casting technique. TDF was also added to the formulation to achieve a synergist antiviral effect. A rapid release of active principles was accordingly recorded suggesting an ideal behavior of such a formulation as prophylactic microbicide [158,159]. Some advantages were also obtained by alternative formulations of this drug. In particular, surface-engineered poly(ε-caprolactone) NPs were manufactured and evaluated in pig vaginal and rectal mucosa, resulting in favorable drug release properties [160]. Physical–chemical properties of these nanocarriers were evaluated upon one-year storage to a variable temperature range. Colloidal instability affected the *in vitro* drug release of the NPs, although no detectable degradation was observed for the entrapped drug [56].

4.4. Etravirine

Etravirine (4-((6-amino-5-bromo-2-((4-cyanophenyl)amino)pyrimidin-4-yl)oxy)-3,5-dimethylbenzonitrile, ETV) is a NNRTI approved in 2008 for monotherapy against HIV, also clinically used in combination with other antiviral agents in antiretroviral treatment-experienced adult patients with onset of resistance. A combination of ETV, maraviroc and raltegravir was loaded into PLGA by emulsion-solvent evaporation technique. The antiviral potency of the resulting NPs was compared to the free triple drug combination in an *in vitro* cells assay and on a macaque cervicovaginal explant model *in vivo*. The nanoformulation provided a prolonged release by extension of the half-life of drugs, leading to an enhanced synergistic antiviral action [161]. An innovative approach for the design of NPs overcoming the drawback, consisting in low drug retention and massive leakage, was undertaken by the preparation of NP-releasing nanofiber vaginal devices. Mucoadhesive PVA fibers coupled to PEGylated NPs should ensure an adequate retention together with a rapid mucus diffusion. These composite nanoformulations proved to assure a sustained ETV release for up to seven days [162].

4.5. Rilpivirine

Rilpivirine ((E)-4-((4-((4-(2-cyanovinyl)-2,6-dimethylphenyl)amino)pyrimidin-2-yl)amino) benzonitrile, RPV) is a second-generation NNRTI, approved in 2011, possessing increased potency, longer half-life and lesser side-effects with respect to former non-nucleoside agents, today mainly used in combination with other anti-HIV drugs [163]. RPV met therapeutic success either in combination with other anti-HIV agents or in long-acting injectable nanoformulations during maintenance therapy. Its use could also be advantageous for the prophylactic treatment of high-risk uninfected individuals [164,165]. In two separate papers, the potential use of long acting RPV NPs associated with cabotegravir, an HIV integrase inhibitor, was described and an innovative monthly dosing therapeutic regimen was accordingly proposed. Recently, the result of a phase IIb study was reported on the effectiveness of this combination nanoformulation in maintaining adequate drug concentration in plasma or vaginal mucus for up to one month [166–168]. RPV-loaded PLGA NPs were fabricated by emulsion-solvent evaporation method. A sustained release in plasma as well as faster clearance were observed in animal models, suggesting a prophylactic use after the preparation of thermosensitive gels as well as long acting injectable nanosuspensions [169]. Biodistribution of tri-modal theranostic NPs was studied by single-photon emission computed tomography, magnetic resonance imaging and fluorescence techniques. These devices were prepared by the incorporation of Indium radiolabeled, europium doped cobalt-ferrite particles and RPV loaded into a poly("-caprolactone) matrix included into a lipid shell. A sustained drug release and antiretroviral activity were observed in HIV infected macrophages. These multi-functional NPs represent a platform for the monitoring and optimization of the antiretroviral drug pharmacokinetic profile [170].

5. Conclusions

There is a high level of interest in nanotechnologies for their relevant roles in the design and development of innovative anti-HIV formulations either for oral or topical administration. In the first case, a more specific targeted delivery together with a sustained release represents the major goal in the field. Mucoadhesive performance, prolonged retention time and improved patients' compliance were desired for vaginal or rectal application of microbicide nanoformulated antiretroviral agents. A large number of diversely assembled nanocarriers loaded with different classes of antiviral drugs were then developed and deeply investigated to improve both pharmacokinetic characteristics and stability behavior. Overall results demonstrated a potential success of such an approach for monotherapy, even though more profitable applications were recorded for the combination therapy, the most diffused method nowadays. In fact, anti-HIV therapeutic regimens today comprise multiple daily doses of more drugs acting at different stages of viral replication, which lead to poor patient compliance. Although the use of protease, integrase and viral entry inhibitors has become customary, NRTIs and NNRTIs remain pivotal tools during the infection management. In the light of these findings, this overview focuses mainly on the application of nanotechnology applied to RTI as vehicles for challenging virus eradication from depot organs and/or as a platform for the design of modern prophylactic devices for stable or stressing conditions.

References

[1] Vandamme, A.M.; Van Vaerenbergh, K.; De Clercq, E. Anti-human immunodeficiency virus drug combination strategies. Antivir. Chem. Chemoth. 1998, 9, 187–203.
[2] Lisziewicz, J.; Toke, E.R. Nanomedicine applications towards the cure of HIV. Nanomed-Nanotechnol. 2013, 9, 28–38.
[3] Bangsberg, D.R.; Hecht, F.M.; Charlebois, E.D.; Zolopa, A.R.; Holodniy, M.; Sheiner, L.; Bamberger, J.D.; Chesney, M.A.; Moss, A. Adherence to protease inhibitors, HIV-1 viral load, and development of drug resistance in an indigent population. Aids 2000, 14, 357–366.
[4] Schrager, L.K.; D'Souza, M.P. Cellular and anatomical reservoirs of HIV-1 in patients receiving potent antiretroviral combination therapy. JAMA 1998, 280, 67–71.
[5] Richman, D.D. HIV chemotherapy. Nature 2001, 410, 995–1001.
[6] Yilmaz, A.; Price, R.W.; Gisslen, M. Antiretroviral drug treatment of CNS HIV-1 infection. J. Antimicrob. Chemother. 2012, 67, 299–311.
[7] Guidelines for the Use of Antiretroviral Agents in Adults and Adolescents with HIV. Available online: http:// aidsinfo.nih.gov/guidelines/html/1/adult-and-adolescent-treatment-guidelines/0 (accessed on 10 April 2019).
[8]. Rohit, S.; Ramesh, J.; Karan, G.; Raman, K.; Anil, K.S. Nanotechnological interventions in HIV drug delivery and therapeutics. Biointerface Res. Appl. Chem. 2014, 4, 820–831.
[9]. Harrigan, P.R.; Hogg, R.S.; Dong, W.W.; Yip, B.; Wynhoven, B.;Woodward, J.; Brumme, C.J.; Brumme, Z.L.; Mo, T.; et al. Predictors of HIV drug-resistance mutations in a large antiretroviral-naive cohort initiating triple antiretroviral therapy. J. Infect. Dis. 2005, 191, 339–347.
[10] Chun, T.W.; Davey, R.T., Jr.; Engel, D.; Lane, H.C.; Fauci, A.S. Re-emergence of HIV after stopping therapy. Nature 1999, 401, 874–875.
[11] Marsden, M.D.; Zack, J.A. Eradication of HIV: current challenges and new directions. J. Antimicrob. Chemother. 2009, 63, 7–10.

[12] Nie, S.; Xing, Y.; Kim, G.J.; Simons, J.W. Nanotechnology applications in cancer. Annu. Rev. Biomed. Eng. 2007, 9, 257–288.
[13] Mazzuca, P.; Caruso, A.; Caccuri, F. HIV-1 infection, microenvironment and endothelial cell dysfunction. New. Microbiol. 2016, 39, 163–173.
[14. Mahajan, S.D.; Aalinkeel, R.; Law, W.C.; Reynolds, J.L.; Nair, B.B.; Sykes, D.E.; Yong, K.T.; Roy, I.; Prasad, P.N.; Schwartz, S.A. Anti-HIV-1 nanotherapeutics: promises and challenges for the future. Int. J. Nanomed. 2012, 7, 5301–5314.
[15] Vyas, T.K.; Shah, L.; Amiji, M.M. Nanoparticulate drug carriers for delivery of HIV/AIDS therapy to viral reservoir sites. Expert Opin. Drug Deliv. 2006, 3, 613–628.
[16] Amiji, M.M.; Vyas, T.K.; Shah, L.K. Role of nanotechnology in HIV/AIDS treatment: potential to overcome the viral reservoir challenge. Discov. Med. 2006, 6, 157–162.
[17] Ferrari, M. Cancer nanotechnology: opportunities and challenges. Nat. Rev. Cancer 2005, 5, 161–171.
[18] Farokhzad, O.C. Nanotechnology for drug delivery: the perfect partnership. Expert Opin. Drug Deliv. 2008, 5, 927–929.
[19] Farokhzad, O.C.; Langer, R. Impact of nanotechnology on drug delivery. ACS Nano 2009, 3, 16–20.
[20] Dunge, A.; Sharda, N.; Singh, B.; Singh, S. Establishment of inherent stability of stavudine and development of a validated stability-indicating HPLC assay method. J. Pharm. Biomed. Anal. 2005, 37, 1115–1119.
[21] Devrukhakar, P.S.; Shiva Shankar, M.; Shankar, G.; Srinivas, R. A stability-indicating LC-MS/MS method for zidovudine: Identification, characterization and toxicity prediction of two major acid degradation products. J. Pharm. Biomed. Anal. 2017, 7, 231–236.
[22] Shegokar, R.; Singh, K.K.; Muller, R.H. Production & stability of stavudine solid lipid nanoparticles–from lab to industrial scale. Int. J. Pharm. 2011, 416, 461–470.
[23]. Nowacek, A.; Gendelman, H.E. NanoART, neuroAIDS and CNS drug delivery. Nanomedicine (Lond) 2009, 4, 557–574.
[24] ICH Q1A(R2)- Stability Testing of New Drug Substances and Products; International Council for Harmonisation of Technical Requirements for Pharmaceuticals for Human Use (ICH): Geneve, Switzerland, 2003.
[25] Tonnesen, H.H. Photostability of Drugs and Drug Formulations; CRC Press: New York, NY, USA, 2004.
[26] De Luca, M.; Ioele, G.; Spatari, C.; Ragno, G. Photostabilization studies of antihypertensive 1,4-dihydropyridines using polymeric containers. Int. J. Pharm. 2016, 505, 376–382.
[27] Garg, M.; Asthana, A.; Agashe, H.B.; Agrawal, G.P.; Jain, N.K. Stavudine-loaded mannosylated liposomes: in-vitro anti-HIV-I activity, tissue distribution and pharmacokinetics. J. Pharm. Pharmacol. 2006, 58, 605–616.
[28] Garg, M.; Dutta, T.; Jain, N.K. Reduced hepatic toxicity, enhanced cellular uptake and altered pharmacokinetics of stavudine loaded galactosylated liposomes. Eur. J. Pharm. Biopharm. 2007, 67, 76–85.
[29] Nayak, D.; Boxi, A.; Ashe, S.; Thathapudi, N.C.; Nayak, B. Stavudine loaded gelatin liposomes for HIV therapy: Preparation, characterization and *in vitro* cytotoxic evaluation. Mater. Sci. Eng. C Mater. Biol. Appl. 2017, 73, 406–416.
[30] Ramana, L.N.; Sethuraman, S.; Ranga, U.; Krishnan, U.M. Development of a liposomal nanodelivery system for nevirapine. Int. J. Biomed. Sci. 2010, 17, 57.
[31] Malik, T.; Chauhan, G.; Rath, G.; Kesarkar, R.N.; Chowdhary, A.S.; Goyal, A.K. Efaverinz and nano-gold-loaded mannosylated niosomes: a host cell-targeted topical HIV-1 prophylaxis via thermogel system. Artif. Cells Nanomed. Biotechnol. 2018, 46, 79–90.
[32] Rao, M.R.P.; Babrekar, L.S. Liposomal Drug Delivery for Solubility and Bioavailability Enhancement of Efavirenz. Indian J. Pharm. Sci. 2018, 80, 1115–1124.

[33] Abdelkader, H.; Alani, A.W.; Alany, R.G. Recent advances in non-ionic surfactant vesicles (niosomes): self-assembly, fabrication, characterization, drug delivery applications and limitations. Drug Deliv. 2014, 21, 87–100.
[34] Khan, R.; Irchhaiya, R. Niosomes: a potential tool for novel drug delivery. J. Pharm. Investig. 2016, 46, 195–204.
[35] Naseri, N.; Valizadeh, H.; Zakeri-Milani, P. Solid Lipid Nanoparticles and Nanostructured Lipid Carriers: Structure, Preparation and Application. Adv. Pharm. Bull. 2015, 5, 305–313.
[36] Joshy, K.S.; Chandra, P.S.; Nandakumar, K.; Sandeep, K.; Sabu, T.; Laly, A.P. Evaluation of in-vitro cytotoxicity and cellular uptake eciency of zidovudine-loaded solid lipid nanoparticles modified with Aloe Vera in glioma cells. Mater. Sci. Eng. C Mater. Biol. Appl. 2016, 66, 40–50.
[37] Freeling, J.P.; Koehn, J.; Shu, C.; Sun, J.; Ho, R.J. Anti-HIV drug-combination nanoparticles enhance plasma drug exposure duration as well as triple-drug combination levels in cells within lymph nodes and blood in primates. AIDS Res. Hum. Retroviruses 2015, 31, 107–114.
[38] Mishra, N.; Mishra, M.; Padh, H. Formulation Development and Optimization of Efavirenz Loaded SLNs and NLCs using Plackett- Burman Design and its Statistical Elucidation. Int. J. Pharm. Res. Health Sci. 2018, 6, 2379–2388.
[39] Gupta, S.; Kesarla, R.; Chotai, N.; Misra, A.; Omri, A. Systematic Approach for the Formulation and Optimization of Solid Lipid Nanoparticles of Efavirenz by High Pressure Homogenization Using Design of Experiments for Brain Targeting and Enhanced Bioavailability. Biomed. Res. Int. 2017, 2017, 5984014.
[40] Madhusudhan, A.; Bhagavanth, R.G.; Venkatesham, M.; Veerabhadram, G. Design and Evaluation of Efavirenz loaded Solid Lipid Nanoparticles to Improve the Oral Bioavailability. Int. J. Pharm. Pharm. Sci. 2012, 2, 84–89.
[41] Pardeshi, C.; Rajput, P.; Belgamwar, V.; Tekade, A.; Patil, G.; Chaudhary, K.; Sonje, A. Solid lipid based nanocarriers: an overview. Acta Pharm. 2012, 62, 433–472.
[42] Date, A.A.; Destache, C.J. A review of nanotechnological approaches for the prophylaxis of HIV/AIDS. Biomaterials 2013, 34, 6202–6228.
[43] Yang, X.; Yu, B.; Zhong, Z.; Guo, B.H.; Huang, Y. Nevirapine-polycaprolactone crystalline inclusion complex as a potential long-acting injectable solid form. Int. J. Pharm. 2018, 543, 121–129.
[44] Cao, S.; Woodrow, K.A. Nanotechnology approaches to eradicating HIV reservoirs. Eur. J. Pharm. Biopharm. 2018, 138, 48–63.
[45] Singh, L.; Kruger, H.G.; Maguire, G.E.M.; Govender, T.; Parboosing, R. The role of nanotechnology in the treatment of viral infections. Therap. Adv. Infect. Dis. 2017, 4, 105–131.
[46] Parboosing, R.; Maguire, G.E.; Govender, P.; Kruger, H.G. Nanotechnology and the treatment of HIV infection. Viruses 2012, 4, 488–520.
[47] das Neves, J.; Amiji, M.M.; Bahia, M.F.; Sarmento, B. Nanotechnology-based systems for the treatment and prevention of HIV/AIDS. Adv. Drug Deliv. Rev. 2010, 62, 458–477.
[48] Patel, B.K.; Parikh, R.H.; Patel, N. Targeted delivery of mannosylated-PLGA nanoparticles of antiretroviral drug to brain. Int. J. Nanomed. 2018, 13, 97–100.
[49] McDonald, T.O.; Giardiello, M.; Martin, P.; Siccardi, M.; Liptrott, N.J.; Smith, D.; Roberts, P.; Curley, P.; Schipani, A.; Khoo, S.H.; et al. Antiretroviral solid drug nanoparticles with enhanced oral bioavailability: production, characterization, and *in vitro-in vivo* correlation. Adv. Healthc. Mater. 2014, 3, 400–411.
[50] Marcos-Almaraz, M.T.; Gref, R.; Agostoni, V.; Kreuz, C.; Clayette, P.; Serre, C.; Couvreurb, P.; Horcajada, P. Towards improved HIV-microbicide activity through the co-encapsulation of NRTI drugs in biocompatible metal organic framework nanocarriers. J. Mater. Chem. B 2017, 5, 8563–8569.

[51] Chiodo, F.; Marradi, M.; Calvo, J.; Yuste, E.; Penades, S. Glycosystems in nanotechnology: Gold glyconanoparticles as carrier for anti-HIV prodrugs. Beilstein J. Org. Chem. 2014, 10, 1339–1346.
[52] Peng, J.; Wu, Z.; Qi, X.; Chen, Y.; Li, X. Dendrimers as potential therapeutic tools in HIV inhibition. Molecules 2013, 18, 7912–7929.
[53] Ionov, M.; Ciepluch, K.; Klajnert, B.; Glinska, S.; Gomez-Ramirez, R.; de la Mata, F.J.; Munoz-Fernandez, M.A.; Bryszewska, M. Complexation of HIV derived peptides with carbosilane dendrimers. Colloids Surf. B Biointerfaces 2013, 101, 236–242.
[54] Garcia-Broncano, P.; Cena-Diez, R.; de la Mata, F.J.; Gomez, R.; Resino, S.; Munoz-Fernandez, M.A. Efficacy of carbosilane dendrimers with an antiretroviral combination against HIV-1 in the presence of semen-derived enhancer of viral infection. Eur. J. Pharmacol. 2017, 811, 155–163.
[55] Cena-Diez, R.; Vacas-Cordoba, E.; Garcia-Broncano, P.; de la Mata, F.J.; Gomez, R.; Maly, M.; Munoz-Fernandez, M.A. Prevention of vaginal and rectal herpes simplex virus type 2 transmission in mice: mechanism of antiviral action. Int. J. Nanomed. 2016, 11, 2147–2162.
[56] das Neves, J.; Amiji, M.; Bahia, M.F.; Sarmento, B. Assessing the physical-chemical properties and stability of dapivirine-loaded polymeric nanoparticles. Int. J. Pharm. 2013, 456, 307–314.
[57] Nucleoside Reverse Transcriptase Inhibitors (NRTIs or nukes). Available online: https://www.hiv.va.gov/ patient/treat/nrtis.asp (accessed on 10 April 2019).
[58] Shegokar, R.; Singh, K.K. Stavudine entrapped lipid nanoparticles for targeting lymphatic HIV reservoirs. Pharmazie 2011, 66, 264–271.
[59] Kaur, C.D.; Nahar, M.; Jain, N.K. Lymphatic targeting of zidovudine using surface-engineered liposomes. J. Drug Target 2008, 16, 798–805.
[60] Weibull,W. A statistical distribution function of wide applicability. J. Appl. Mech. 1951, 18, 293–297.
[61] Carvalho, F.C.; Sarmento, V.H.; Chiavacci, L.A.; Barbi, M.S.; Gremiao, M.P. Development and *in vitro* evaluation of surfactant systems for controlled release of zidovudine. J. Appl. Mech. 2010, 99, 2367–2374.
[62] Mainardes, R.M.; Gremiao, M.P.; Brunetti, I.L.; da Fonseca, L.M.; Khalil, N.M. Zidovudine-loaded PLA and PLA-PEG blend nanoparticles: influence of polymer type on phagocytic uptake by polymorphonuclear cells. J. Pharm. Sci. 2009, 98, 257–267.
[63] Mainardes, R.M.; Gremiao, M.P. Nanoencapsulation and characterization of zidovudine on poly(l-lactide) and poly (l -lactide)-poly(ethylene glycol)-blend nanoparticles. J. Nanosci. Nanotechnol. 2012, 12, 8513–8521.
[64]. Joshy, K.S.; Susan, M.A.; Snigdha, S.; Nandakumar, K.; Laly, A.P.; Sabu, T. Encapsulation of zidovudine in PF-68 coated alginate conjugate nanoparticles for anti-HIV drug delivery. Int. J. Biol. Macromol. 2018, 107, 929–937.
[65] Dunge, A.; Sharda, N.; Singh, B.; Singh, S. Validated specific HPLC method for determination of zidovudine during stability studies. J. Pharm. Biomed. Anal. 2005, 37, 1109–1114.
[66] Schenfeld, E.M.; Ribone, S.R.; Quevedo, M.A. Stability and plasmatic protein binding of novel zidovudine prodrugs: Targeting site ii of human serum albumin. Eur. J. Pharm. Sci. 2018, 115, 109–118.
[67] Perry, C.M.; Faulds, D. Lamivudine. A review of its antiviral activity, pharmacokinetic properties and therapeutic ecacy in the management of HIV infection. Drugs 1997, 53, 657–680.
[68] Vogenthaler, N.S. Lamivudine and second-line antiretroviral regimens. Clin. Infect. Dis. 2007, 44, 1387.

[69] Vinogradov, S.V.; Poluektova, L.Y.; Makarov, E.; Gerson, T.; Senanayake, M.T. Nano-NRTIs: ecient inhibitors of HIV type-1 in macrophages with a reduced mitochondrial toxicity. Antivir. Chem. Chemother. 2010, 21,1–14.
[70] Bedse, G.; Kumar, V.; Singh, S. Study of forced decomposition behavior of lamivudine using LC, LC-MS/TOF and MS(n). J. Pharm. Biomed. Anal. 2009, 49, 55–63.
[71] Konari, N.S.; Jacob, J.T. Stability indicating validated UPLC technique for the simultaneous analysis of raltegravir and lamivudine in pharmaceutical dosage forms. HIV AIDS Rev. 2016, 15, 161–169.
[72] Kurmi, M.; Sahu, A.; Singh, D.K.; Singh, I.P.; Singh, S. Stability behaviour of antiretroviral drugs and their
combinations. 8: Characterization and in-silico toxicity prediction of degradation products of efavirenz. J. Pharm. Biomed. Anal. 2018, 148, 170–181.
[73] Tamizhrasi, S.; Shukla, A.; Shivkumar, T.; Rathi, V.; Rathi, J.C. Formulation and evaluation of lamivudine loaded polymethacrylic acid nanoparticles. Int. J. Pharmtech Res. 2009, 1, 411–415.
[74] Bing, W.; Guan Qun, C.; Zheng Wei, M.; Yu Ying, Z.; Da Hai, Y.; Chang You, G. Preparation and cellular uptake of PLGA particles loaded with lamivudine. Chin. Sci. Bull. 2012, 57, 3985–3993.
[75] Rajca, A.; Li, Q.; Date, A.; Belshan, M.; Destache, C. Thermosensitive Vaginal Gel Containing PLGA-NRTI conjugated nanoparticles for HIV prophylaxis. NSTI-Nanotech 2013, 3, 293–296.
[76] Ramadan, E. Transdermal microneedle–mediated delivery of polymeric lamivudine loaded nanoparticles. J. Pharm. Technol. Drug Res. 2016, 5.
[77] Hatami, E.; Mu, Y.; Shields, D.N.; Chauhan, S.C.; Kumar, S.; Cory, T.J.; Yallapu, M.M. Mannose-decorated hybrid nanoparticles for enhanced macrophage targeting. Biochem. Biophys. Rep. 2019, 17, 197–207.
[78] Dev, A.; Binulal, N.S.; Anitha, A.; Nair, S.V.; Furuike, T.; Tamura, H.; Jayakumar, R. Preparation of poly(lactic acid)/chitosan nanoparticles for anti-HIV drug delivery applications. Carbohydr. Polym. 2010, 80, 833–838.
[79] Nesalin, J.A.J.; Smith, A.A. Stability study of chitosan nanoparticles containing some antiretroviral drugs. Res. J. Pharm. Biol. Chem. Sci. 2014, 5, 193–203.
[80] Deepak, M.; Nivrati, J.; Vaibhav, R.; Ashish, K.J. Glycyrrhizin conjugated chitosan nanoparticles for hepatocyte-targeted delivery of lamivudine. J. Pharm. Pharmacol. 2014, 66, 1082–1093.
[81] Tshweu, L.; Katata, L.; Kalombo, L.; Swai, H. Nanoencapsulation of water-soluble drug, lamivudine, using a double emulsion spray-drying technique for improving HIV treatment. J. Nanopart. Res. 2013, 15.
[82] Oluwaseun, O.; Namita, K.; Kahli, A.S.; Oleg, B.; Simeon, A.; Ayele, G.; Winston, A.A.; Sergei, N.; Emmanuel, O.A. Antiretroviral Drugs-Loaded Nanoparticles Fabricated by Dispersion Polymerization with Potential for HIV/AIDS Treatment. Inf. Dis. Res. Treat. 2016, 9, 21–32.
[83] Pravalika, R.P.; Madhava, R.B.; Prakash, D.J.; Latha, K.; Prashanthi, D. Formulation and characterisation of chitosan based lamivudine nanoparticles. Eur. J. Pharm. Med. Res. 2017, 4, 377–383.
[84] Kumar, P.; Lakshmi,Y. S.; C, B.; Golla, K.; Kondapi, A.K. Improved Safety, Bioavailability and Pharmacokinetics of Zidovudine through Lactoferrin Nanoparticles during Oral Administration in Rats. PLoS ONE 2015, 10, e0140399.
[85] Kumar, P.; Lakshmi, Y.S.; Kondapi, A.K. Triple Drug Combination of Zidovudine, Efavirenz and Lamivudine Loaded Lactoferrin Nanoparticles: an Eective Nano First-Line Regimen for HIV Therapy. Pharm. Res. 2017, 34, 257–268.

[86] Shahabadia, N.; Khorshidia, A.; Zhalehc, H.; Kashaniand, S. Synthesis, characterization, cytotoxicity and DNA binding studies of Fe3O4@ SiO2 nanoparticles coated by an antiviral drug lamivudine. J. Drug Deliv. Sci. Technol. 2018, 46, 55–65.
[87] Vasilyeva, S.V.; Shtil, A.A.; Petrova, A.S.; Balakhnin, S.M.; Achigecheva, P.Y.; Stetsenko, D.A.; Silnikov, V.N. Conjugates of phosphorylated zalcitabine and lamivudine with SiO2 nanoparticles: Synthesis by CuAAC click chemistry and preliminary assessment of anti-HIV and antiproliferative activity. Bioorg. Med. Chem. 2017, 25, 1696–1702.
[88] Kumar, J.A.; Kumar, A.N.; Arnab, D.; Debmalya, M.; Amalesh, S. Development of lamivudine containing multiple emulsions stabilizedby gum odina. Future J. Pharm. Sci. 2018, 4, 71–79.
[89] Suma, U.S.; Parthiban, S.; Senthil, K.G.P.; Tamiz, M.T. Eect of span-80 in the formulation lamivudine niosomal gel. Asian J. Res. Biol. Pharm. Sci. 2015, 4, 35–45.
[90] Godbole, M.D.; Mathur, V. Selection of phospholipid and method of formulation for optimum entrapment and release of lamivudine from liposome. J. Drug Deliv. Ther. 2018, 8, 175–183.
[91] Wilson, B.; Paladugu, L.; Priyadarshini, S.R.; Jenita, J.J. Development of albumin-based nanoparticles for the delivery of abacavir. Int. J. Biol. Macromol. 2015, 81, 763–767.
[92] Corbo, C.; Molinaro, R.; Parodi, A.; Toledano Furman, N.E.; Salvatore, F.; Tasciotti, E. The impact of nanoparticle protein corona on cytotoxicity, immunotoxicity and target drug delivery. Nanomedicine (Lond.) 2016, 11, 81–100.
[93] Lin, Z.; Gautam, N.; Alnouti, Y.; McMillan, J.; Bade, A.N.; Gendelman, H.E.; Edagwa, B. ProTide generated long-acting abacavir nanoformulations. Chem. Commun. 2018, 54, 8371–8374.
[94] Singh, G.; Pai, R.S. Pharmacokinetics and *in viv*o biodistribution of optimized PLGA nanoparticulate drug delivery system for controlled release of emtricitabine. Drug Deliv. 2014, 21, 627–635.
[95] Singh, G.; Pai, R.S. Optimization (central composite design) and validation of HPLC method for investigation of emtricitabine loaded poly(lactic-co-glycolic acid) nanoparticles: *in vitro* drug release and *in vivo* pharmacokinetic studies. Sci. World J. 2014, 2014, 583090.
[96] Mandal, S.; Belshan, M.; Holec, A.; Zhou, Y.; Destache, C.J. An Enhanced Emtricitabine-Loaded Long-Acting Nanoformulation for Prevention or Treatment of HIV Infection. Antimicrob. Agents Chemother. 2017, 61.
[97] Rao, R.N.; Vali, R.M.; Ramachandra, B.; Raju, S.S. Separation and characterization of forced degradation products of abacavir sulphate by LC-MS/MS. J. Pharm. Biomed. Anal. 2011, 54, 279–285.
[98] Kurmi, M.; Sahu, A.; Singh, S. Stability behaviour of antiretroviral drugs and their combinations. 5: Characterization of novel degradation products of abacavir sulfate by mass and nuclear magnetic resonance spectrometry. J. Pharm. Biomed. Anal. 2017, 134, 372–384.
[99] Wang, X.J.; Youa, J.; Yub, F. Study on the thermal decomposition of emtricitabine. J. Anal. Appl. Pyrolysis 2015, 115, 344–352.
[100] Kurmi, M.; Singh, S. Stability behavior of antiretroviral drugs and their combinations. 7: Comparative degradation pathways of lamivudine and emtricitabine and explanation to their dierential degradation behavior by density functional theory. J.Pharm. Biomed. Anal. 2017, 142, 155–161.
[101] Duan, J.; Freeling, J.P.; Koehn, J.; Shu, C.; Ho, R.J. Evaluation of atazanavir and darunavir interactions with lipids for developing pH-responsive anti-HIV drug combination nanoparticles. J. Pharm. Sci. 2014, 103, 2520–2529.
[102] Freeling, J.P.; Koehn, J.; Shu, C.; Sun, J.; Ho, R.J. Long-acting three-drug combination anti-HIV nanoparticles enhance drug exposure in primate plasma and cells within lymph nodes and blood. Aids 2014, 28, 2625–2627.
[103] Peter, A.I.; Naidu, E.C.; Akang, E.; Ogedengbe, O.O.; Oor, U.; Rambharose, S.; Kalhapure, R.; Chuturgoon, A.; Govender, T.; Azu, O.O. Investigating Organ Toxicity

Profile of Tenofovir and Tenofovir Nanoparticle on the Liver and Kidney: Experimental Animal Study. Toxicol. Res. 2018, 34, 221–229.
[104] Pokharkar, V.B.; Jolly, M.R.; Kumbhar, D.D. Engineering of a hybrid polymer-lipid nanocarrier for the nasal delivery of tenofovir disoproxil fumarate: physicochemical, molecular, microstructural, and stability evaluation. Eur. J. Pharm. Sci. 2015, 71, 99–111.
[105] Ramanathan, R.; Jiang, Y.; Read, B.; Golan-Paz, S.; Woodrow, K.A. Biophysical characterization of small molecule antiviral-loaded nanolipogels for HIV-1 chemoprophylaxis and topical mucosal application. Acta Biomater. 2016, 36, 122–131.
[106] Jayant, R.D.; Atluri, V.S.; Agudelo, M.; Sagar, V.; Kaushik, A.; Nair, M. Sustained-release nanoART formulation for the treatment of neuroAIDS. Int. J. Nanomed. 2015, 10, 1077–1093.
[107] Vacas-Cordoba, E.; Galan, M.; de la Mata, F.J.; Gomez, R.; Pion, M.; Munoz-Fernandez, M.A. Enhanced activity of carbosilane dendrimers against HIV when combined with reverse transcriptase inhibitor drugs: searching for more potent microbicides. Int. J. Nanomed. 2014, 9, 3591–3600.
[108] Briz, V.; Sepulveda-Crespo, D.; Diniz, A.R.; Borrego, P.; Rodes, B.; de la Mata, F.J.; Gomez, R.; Taveira, N.; Munoz-Fernandez, M.A. Development of water-soluble polyanionic carbosilane dendrimers as novel and highly potent topical anti-HIV-2 microbicides. Nanoscale 2015, 7, 14669–14683.
[109] Sepulveda-Crespo, D.; Sanchez-Rodriguez, J.; Serramia, M.J.; Gomez, R.; De La Mata, F.J.; Jimenez, J.L.; Munoz-Fernandez, M.A. Triple combination of carbosilane dendrimers, tenofovir and maraviroc as potential microbicide to prevent HIV-1 sexual transmission. Nanomedicine (Lond) 2015, 10, 899–914.
[110] Sepulveda-Crespo, D.; Gomez, R.; De La Mata, F.J.; Jimenez, J.L.; Munoz-Fernandez, M.A. Polyanionic carbosilane dendrimer-conjugated antiviral drugs as ecient microbicides: Recent trends and developments in HIV treatment/therapy. Nanomed.- Nanotechnol. Biol. Med. 2015, 11, 1481–1498.
[111] Agrahari, V.; Zhang, C.; Zhang, T.; Li,W.; Gounev, T.K.; Oyler, N.A.; Youan, B.B. Hyaluronidase-sensitive nanoparticle templates for triggered release of HIV/AIDS microbicide *in vitro*. AAPS J. 2014, 16, 181–193.
[112] Ngo, A.N.; Ezoulin, M.J.; Murowchick, J.B.; Gounev, A.D.; Youan, B.B. Sodium Acetate Coated Tenofovir-Loaded Chitosan Nanoparticles for Improved Physico-Chemical Properties. Pharm. Res. 2016, 33, 367–383.
[113] Timur, S.S.; Sahin, A.; Aytekin, E.; Ozturk, N.; Polat, K.H.; Tezel, N.; Gursoy, R.N.; Calis, S. Design and *in vitro* evaluation of tenofovir-loaded vaginal gels for the prevention of HIV infections. Pharm. Dev. Technol. 2018, 23, 301–310.
[114] Shailender, J.; Ravi, P.R.; Reddy Sirukuri, M.; Dalvi, A.; Keerthi Priya, O. Chitosan nanoparticles for the oral delivery of tenofovir disoproxil fumarate: formulation optimization, characterization and *ex vivo* and *in vivo* evaluation for uptake mechanism in rats. Drug Dev. Ind. Pharm. 2018, 44, 1109–1119.
[115] Shohani, S.; Mondanizadeh, M.; Abdoli, A.; Khansarinejad, B.; Salimi-Asl, M.; Ardestani, M.S.; Ghanbari, M.; Haj, M.S.; Zabihollahi, R. Trimethyl Chitosan Improves Anti-HIV Eects of Atripla as a New Nanoformulated Drug. Curr. HIV Res. 2017, 15, 56–65.
[116] Wu, D.; Ensinas, A.; Verrier, B.; Primard, C.; Cuvillier, A.; Champier, G.; Paul, S.; Delair, T. Zinc-Stabilized Chitosan-Chondroitin Sulfate Nanocomplexes for HIV-1 Infection Inhibition Application. Mol. Pharm. 2016, 13, 3279–3291.

[117] Meng, J.; Agrahari, V.; Ezoulin, M.J.; Zhang, C.; Purohit, S.S.; Molteni, A.; Dim, D.; Oyler, N.A.; Youan, B.C. Tenofovir Containing Thiolated Chitosan Core/Shell Nanofibers: *In Vitro* and *in Vivo* Evaluations. Mol. Pharm. 2016, 13, 4129–4140.
[118] Destache, C.J.; Mandal, S.; Yuan, Z.; Kang, G.; Date, A.A.; Lu, W.; Shibata, A.; Pham, R.; Bruck, P.; Rezich, M.; et al. Topical Tenofovir Disoproxil Fumarate Nanoparticles Prevent HIV-1 Vaginal Transmission in a Humanized Mouse Model. Antimicrob. Agents Chemother. 2016, 60, 3633–3639.
[119] Machado, A.; Cunha-Reis, C.; Araujo, F.; Nunes, R.; Seabra, V.; Ferreira, D.; das Neves, J.; Sarmento, B. Development and *in vivo* safety assessment of tenofovir-loaded nanoparticles-in-film as a novel vaginal microbicide delivery system. Acta Biomater. 2016, 44, 332–340.
[120] Cunha-Reis, C.; Machado, A.; Barreiros, L.; Araujo, F.; Nunes, R.; Seabra, V.; Ferreira, D.; Segundo, M.A.; Sarmento, B.; das Neves, J. Nanoparticles-in-film for the combined vaginal delivery of anti-HIV microbicide drugs. J. Control. Release 2016, 243, 43–53.
[121] Mandal, S.; Kang, G.; Prathipati, P.K.; Fan, W.; Li, Q.; Destache, C.J. Long-acting parenteral combination antiretroviral loaded nano-drug delivery system to treat chronic HIV-1 infection: A humanized mouse model study. Antiviral Res. 2018, 156, 85–91.
[122] Mandal, S.; Kang, G.; Prathipati, P.K.; Zhou, Y.; Fan, W.; Li, Q.; Destache, C.J. Nanoencapsulation introduces long-acting phenomenon to tenofovir alafenamide and emtricitabine drug combination: A comparative pre-exposure prophylaxis ecacy study against HIV-1 vaginal transmission. J. Control. Release 2019, 294, 216–225.
[123] Mandal, S.; Prathipati, P.K.; Kang, G.; Zhou, Y.; Yuan, Z.; Fan,W.; Li, Q.; Destache, C.J. Tenofovir alafenamide and elvitegravir loaded nanoparticles for long-acting prevention of HIV-1 vaginal transmission. Aids 2017, 31, 469–476.
[124] Prathipati, P.K.; Mandal, S.; Pon, G.; Vivekanandan, R.; Destache, C.J. Pharmacokinetic and Tissue Distribution Profile of Long Acting Tenofovir Alafenamide and Elvitegravir Loaded Nanoparticles in Humanized Mice Model. Pharm. Res. 2017, 34, 2749–2755.
[125] Shailender, J.; Ravi, P.R.; Saha, P.; Dalvi, A.; Myneni, S. Tenofovir disoproxil fumarate loaded PLGA nanoparticles for enhanced oral absorption: Eect of experimental variables and *in vitro, ex vivo* and *in vivo* evaluation. Colloids Surf. B Biointerfaces 2017, 158, 610–619.
[126] Cautela, M.P.; Moshe, H.; Sosnik, A.; Sarmento, B.; das Neves, J. Composite films for vaginal delivery of tenofovir disoproxil fumarate and emtricitabine. Eur. J. Pharm. Biopharm. 2018, 138, 3–10.
[127] Tomitaka, A.; Arami, H.; Huang, Z.; Raymond, A.; Rodriguez, E.; Cai, Y.; Febo, M.; Takemura, Y.; Nair, M. Hybrid magneto-plasmonic liposomes for multimodal image-guided and brain-targeted HIV treatment. Nanoscale 2017, 10, 184–194.
[128] Kraft, J.C.; McConnachie, L.A.; Koehn, J.; Kinman, L.; Sun, J.; Collier, A.C.; Collins, C.; Shen, D.D.; Ho, R.J.Y. Mechanism-based pharmacokinetic (MBPK) models describe the complex plasma kinetics of three antiretrovirals delivered by a long-acting anti-HIV drug combination nanoparticle formulation. J. Control. Release 2018, 275, 229–241.
[129] McConnachie, L.A.; Kinman, L.M.; Koehn, J.; Kraft, J.C.; Lane, S.; Lee, W.; Collier, A.C.; Ho, R.J.Y. Long-Acting Profile of 4 Drugs in 1 Anti-HIV Nanosuspension in

Nonhuman Primates for 5 Weeks After a Single Subcutaneous Injection. J. Pharm. Sci. 2018, 107, 1787–1790.
[130] Koehn, J.; Iwamoto, J.F.; Kraft, J.C.; McConnachie, L.A.; Collier, A.C.; Ho, R.J.Y. Extended cell and plasma drug levels after one dose of a three-in-one nanosuspension containing lopinavir, efavirenz, and tenofovir in nonhuman primates. Aids 2018, 32, 2463–2467.
[131] Perazzolo, S.; Shireman, L.M.; Koehn, J.; McConnachie, L.A.; Kraft, J.C.; Shen, D.D.; Ho, R.J.Y. Three HIV Drugs, Atazanavir, Ritonavir, and Tenofovir, Coformulated in Drug-Combination Nanoparticles Exhibit Long-Acting and Lymphocyte-Targeting Properties in Nonhuman Primates. J. Pharm. Sci. 2018, 107, 3153–3162.
[132] Golla, V.M.; Kurmi, M.; Shaik, K.; Singh, S. Stability behaviour of antiretroviral drugs and their combinations. 4: Characterization of degradation products of tenofovir alafenamide fumarate and comparison of its degradation and stability behaviour with tenofovir disoproxil fumarate. J. Pharm. Biomed. Anal. 2016, 131, 146–155.
[133] Kuo, Y.C.; Lin, P.I.; Wang, C.C. Targeting nevirapine delivery across human brain microvascular endothelial cells using transferrin-grafted poly(lactide-co-glycolide) nanoparticles. 134. Shegokar, R.; Singh, K.K. Nevirapine nanosuspensions for HIV reservoir targeting. Die Pharmazie 2011, 66, 408–415.
[135] Shegokar, R.; Singh, K.K. Surface modified nevirapine nanosuspensions for viral reservoir targeting: *In vitro* and *in vivo* evaluation. Int. J. Pharm. 2011, 421, 341–352.
[136] Reis, N.F.; de Assis, J.C.; Fialho, S.L.; Pianetti, G.A.; Fernandes, C. Stability-indicating UHPLC method for determination of nevirapine in its bulk form and tablets: identification of impurities and degradation kinetic study. J. Pharm. Biomed. Anal. 2016, 126, 103–108.
[137] Aungst, B.J.; Nguyen, N.H.; Taylor, N.J.; Bindra, D.S. Formulation and food eects on the oral absorption of a poorly water soluble, highly permeable antiretroviral agent. J. Pharm. Sci. 2002, 91, 1390–1395.
[138] Csajka, C.; Marzolini, C.; Fattinger, K.; Decosterd, L.A.; Fellay, J.; Telenti, A.; Biollaz, J.; Buclin, T. Population pharmacokinetics and eects of efavirenz in patients with human immunodeficiency virus infection. Clin. Pharmacol. Ther. 2003, 73, 20–30.
[139] Vyas, A.; Jain, A.; Hurkat, P.; Jain, A.; Jain, S.K. Targeting of AIDS related encephalopathy using phenylalanine anchored lipidic nanocarrier. Colloids Surf. B Biointerfaces 2015, 131, 155–161.
[140] Makwana, V.; Jain, R.; Patel, K.; Nivsarkar, M.; Joshi, A. Solid lipid nanoparticles (SLN) of Efavirenz as lymph targeting drug delivery system: Elucidation of mechanism of uptake using chylomicron flow blocking approach. Int. J. Pharm. 2015, 495, 439–446.
[141] Gaur, P.K.; Mishra, S.; Bajpai, M.; Mishra, A. Enhanced Oral Bioavailability of Efavirenz by Solid Lipid Nanoparticles: *In Vitro* Drug Release and Pharmacokinetics Studies. BioMed Res. Int. 2014, 2014, 363404.
[142] Vedha Hari, B.N.; Dhevendaran, K.; Narayanan, N. Development of Efavirenz nanoparticle for enhanced efficiency of anti-retroviral therapy against HIV and AIDS. In Proceedings of the First International Science Symposium on HIV and Infectious Diseases (HIV SCIENCE 2012), Chennai, India, 20–22 January 2012; Springer-Verlag GmbH: Heidelberg, Germany, 2012.
[143] Chaowanachan, T.; Krogstad, E.; Ball, C.; Woodrow, K.A. Drug synergy of tenofovir and nanoparticle-based antiretrovirals for HIV prophylaxis. PLoS ONE 2013, 8, e61416.

[144] Date, A.A.; Shibata, A.; McMullen, E.; La Bruzzo, K.; Bruck, P.; Belshan, M.; Zhou, Y.; Destache, C.J. Thermosensitive Gel Containing Cellulose Acetate Phthalate-Efavirenz Combination Nanoparticles for Prevention of HIV-1 Infection. J. Biomed. Nanotechnol. 2015, 11, 416–427.
[145] Roy, U.; Ding, H.; Pilakka-Kanthikeel, S.; Raymond, A.D.; Atluri, V.; Yndart, A.; Kaftanovskaya, E.M.; Batrakova, E.; Agudelo, M.; Nair, M. Preparation and characterization of anti-HIV nanodrug targeted to microfold cell of gut-associated lymphoid tissue. Int. J. Nanomed. 2015, 10, 5819–5835.
[146] Haria, V.B.N.; Lu, C.L.; Narayananc, N.; Wang, R.R.; Zheng, Y.T. Engineered polymeric nanoparticles of Efavirenz: Dissolution enhancement through particle size reduction. Chem. Eng. Sci. 2016, 155, 366–375.
[147] Hari, B.N.V.; Narayanan, N.; Dhevendaran, K.; Ramyadevi, D. Engineered nanoparticles of Efavirenz using methacrylate co-polymer (Eudragit-E100) and its biological eects in-vivo. Mater. Sci. Eng. C. Mater. Biol. Appl. 2016, 67, 522–532.
[148] Belgamwar, A.; Khan, S.; Yeole, P. Intranasal chitosan-g-HPbetaCD nanoparticles of efavirenz for the CNS targeting. Artif. Cells Nanomed. Biotechnol. 2018, 46, 374–386.
[149] Nunes, R.; Araujo, F.; Barreiros, L.; Bartolo, I.; Segundo, M.A.; Taveira, N.; Sarmento, B.; das Neves, J. Noncovalent PEG Coating of Nanoparticle Drug Carriers Improves the Local Pharmacokinetics of Rectal Anti-HIV Microbicides. ACS Appl. Mater. Interfaces 2018, 10, 34942–34953.
[150] Martins, C.; Araújo, F.; Gomes, M.J.; Fernandes, C.; Nunes, R.; Li,W.; Santos, H.A.; Borges, F.; Sarmento, B. Using microfluidic platforms to develop CNS-targeted polymeric nanoparticles for HIV therapy. Eur. J. Pharm. Biopharm. 2018, 138, 111–124.
[151] Kumar, P.; Lakshmi, Y.S.; Kondapi, A.K. An oral formulation of efavirenz-loaded lactoferrin nanoparticles with improved biodistribution and pharmacokinetic profile. HIV Med. 2017, 18, 452–462.
[152] Lakshmi, Y.S.; Kumar, P.; Kishore, G.; Bhaskar, C.; Kondapi, A.K. Triple combination MPT vaginal microbicide using curcumin and efavirenz loaded lactoferrin nanoparticles. Sci. Rep. 2016, 6, 25479.
[153] Dutta, T.; Agashe, H.B.; Garg, M.; Balakrishnan, P.; Kabra, M.; Jain, N.K. Poly (propyleneimine) dendrimer based nanocontainers for targeting of efavirenz to human monocytes/macrophages *in vitro*. J. Drug Target. 2007, 15, 89–98.
[154] Dutta, T.; Garg, M.; Jain, N.K. Targeting of efavirenz loaded tuftsin conjugated poly(propyleneimine) dendrimers to HIV infected macrophages *in vitro*. Eur. J. Pharm. Sci. 2008, 34, 181–189.
[155] Hong, X.; Long, L.; Guohong, F.; Xiangfeng, C. DFT study of nanotubes as the drug delivery vehicles of Efavirenz. Comput. Theor. Chem. 2018, 1131, 57–68.
[156] Suvarna, V.; Thorat, S.; Nayak, U.; Sherje, A.; Murahari, M. Host-guest interaction study of Efavirenz with hydroxypropyl--cyclodextrin and L-arginine by computational simulation studies: Preparation and characterization of supramolecular complexes. J. Mol. Liq. 2018, 259, 55–64.
[157] Moura Ramos, J.J.; Piedade, M.F.M.; Diogo, H.P.; Viciosa, M.T. Thermal Behavior and Slow Relaxation Dynamics in Amorphous Efavirenz: A Study by DSC, XRPD, TSDC, and DRS. J. Pharm. Sci. 2019, 108, 1254–1263.
[158] das Neves, J.; Sarmento, B.; Amiji, M.M.; Bahia, M.F. Development and validation of a rapid reversed-phase HPLC method for the determination of the non-nucleoside reverse

transcriptase inhibitor dapivirine from polymeric nanoparticles. J. Pharm. Biomed. Anal. 2010, 52, 167–172.
[159] Akil, A.; Devlin, B.; Cost, M.; Rohan, L.C. Increased Dapivirine tissue accumulation through vaginal film codelivery of dapivirine and Tenofovir. Mol. Pharm. 2014, 11, 1533–1541.
[160] das Neves, J.; Araújo, F.; Andrade, F.; Michiels, J.; Ariën, K.K.; Vanham, G.; Amiji, M.; Bahia, M.F.; Sarmento, B. *In Vitro* and *Ex Vivo* Evaluation of Polymeric Nanoparticles for Vaginal and Rectal Delivery of the Anti-HIV Drug Dapivirine. Mol. Pharm. 2013, 10, 2793–2807.
[161] Jiang, Y.; Cao, S.; Bright, D.K.; Bever, A.M.; Blakney, A.K.; Suydam, I.T.; Woodrow, K.A. Nanoparticle-Based ARV Drug Combinations for Synergistic Inhibition of Cell-Free and Cell-Cell HIV Transmission. Mol. Pharm. 2015, 12, 4363–4374.
[162] Krogstad, E.A.; Ramanathan, R.; Nhan, C.; Kraft, J.C.; Blakney, A.K.; Cao, S.; Ho, R.J.Y.; Woodrow, K.A. Nanoparticle-releasing nanofiber composites for enhanced *in vivo* vaginal retention. Biomaterials 2017, 144, 1–16.
[163] Goebel, F.; Yakovlev, A.; Pozniak, A.; Vinogradova, E.; Boogaerts, G.; Hoetelmans, R.; de Béthune, M.P.; Peeters, M.; Woodfall, B. Short-term antiviral activity of TMC278 – a novel NNRTI – in treatment-naive HIV-1-infected subjects. Aids 2006, 20, 1721–1726.
[164] Jackson, A.; McGowan, I. Long-acting rilpivirine for HIV prevention. Curr. Opin. HIV AIDS 2015, 10, 253–257.
[165] Viciana, P. Rilpivirine: The Key for Long-term Success. AIDS Rev. 2017, 19, 156–166.
[166] Spreen, W.R.; Margolis, D.A.; Pottage, J.C. Long-acting injectable antiretrovirals for HIV treatment and prevention. Curr. Opin. HIV AIDS 2013, 8, 565–571.
[167] Margolis, D.A.; Boto, M. Long-acting antiviral agents for HIV treatment. Curr. Opin. HIV AIDS 2015, 10, 246–252.
[168] Ferretti, F.; Boto, M. Rilpivirine long-acting for the prevention and treatment of HIV infection. Curr. Opin. HIV AIDS 2018, 13, 300–307.
[169] Kovarova, M.; Council, O.D.; Date, A.A.; Long, J.M.; Nochi, T.; Belshan, M.; Shibata, A.; Vincent, H.; Baker, C.E.; Thayer, W.O.; et al. Nanoformulations of Rilpivirine for Topical Pericoital and Systemic Coitus-Independent Administration Eciently Prevent HIV Transmission. PLoS Pathog. 2015, 11, e1005075.
[170] Ottemann, B.M.; Helmink, A.J.; Zhang,W. , Mukadam, I.; Woldstad, C.; Hilaire, J.R.; Liu, Y.; McMillan, J.M.; Edagwa, B.J.; Mosley, R.L.; et al. Bioimaging predictors of rilpivirine biodistribution and antiretroviral activities. Biomaterials 2018, 185, 174–193.

4.2 Photostability and *ex-vivo* permeation studies on Nabumetone in topical microemulsion gel.

Manuscript in preparation

GRAFICAL ABSTRACT

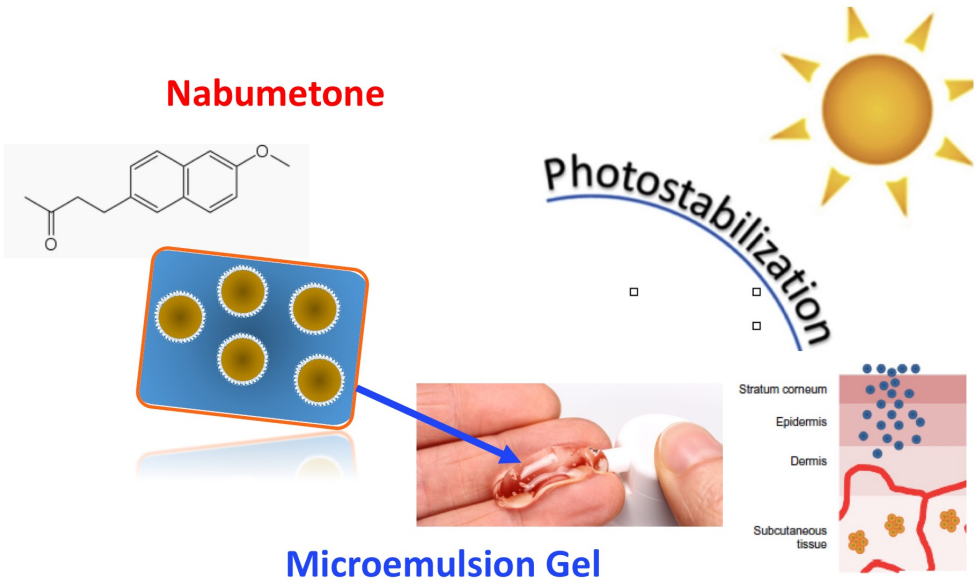

ABSTRACT.

Photostability studies were performed on topical formulations containing Nabumetone, an anti-inflammatory drug used in the treatment of osteoarthritis and rheumatoid arthritis that commonly undergoes a photodegradation process to give the 6-methoxy-naphthalene-aldehyde as the main photoproduct. In this work, drug inclusion in micro-emulsions was proposed to achieve an improved stability to light and at the same time a sustained release systems for topical application. The photodegradation experiments were realized under stressed conditions according with the ICH rules and monitored by spectrophotometry. The spectral data were processed by Multivariate Curve Resolution (MCR), able to estimate spectra and concentration profiles of the components involved in the kinetic process. NA entrapped in microemulsion and formulated in solution and gel preparations was exposed to an irradiance power of 350 W/m^2. A complete photostability was achieved when the drug was entrapped in microemulsion systems compared to ethanol solution and plain gels. Moreover, *ex-vivo* permeation experiments highlighted the potentiality of designed systems as retarded drug delivery systems.

Keywords

Anti-inflammatory Drug; Micro-emulsion; Photodegradation; MCR analysis; Topical permeation

1. Introduction

Photosensitivity is a severe drawback that affects the drug safety during production, storage, distribution and use by patients [1]. In particular, the exposure to light could modify the physicochemical properties of active compounds with loss or reduction of their pharmacological activity and, in some cases the formation of toxic by-products. Photostability of the drugs, in fact, is a very important topic in pharmaceutical research and photostability tests for new drugs are included as integral part of stress testing in the ICH guidelines [2]. Consequently, the development of advanced strategies aimed to avoid or minimize drug photodegradation is still required. The most customary method involved in the drug photostabilization strategies are the use of appropriate protective containers or packaging [3]. Anyway, when the pharmacokinetic behavior of a drug is not favorable and the absorption through the skin take too long, an active compound should be also protected after application, allowing a prolonged exposure to sunlight. In these cases, several approaches of encapsulation into supramolecular systems such as cyclodextrin (CD) complexes, liposomes and niosomes have been proposed, very often combined with antioxidants and solar filters [4-7]. Recent investigations, also, involve the use of microemulsions as encapsulation matrices to realize photoprotective carriers [8-10]. Microemulsions (ME) are optically isotropic and thermodynamically stable solutions with droplet sizes in the submicron range. In general, they consist of oil phase, surfactant, cosurfactant and aqueous phase. Some advantages offered by microemulsions include a high drug solubilizing capability and enhanced skin permeation for both hydrophobic and hydrophilic drugs, an easy manufacture and a long shelf life [11-12].

In this work, the light stability of Nabumetone (4-(6-methoxy-2-naphthyl)butan-2-one) (NA) and ability of ME as photoprotective agents were investigated. The photostabilty studies were performed according to the ICH rules; the photodegradation profiles were monitored by spectrophotometry and the spectral data were processed by Multivariate Curve Resolution (MCR). This chemometric procedure was chosen because particularly suitable for following transformation kinetic processes as it is able to estimate spectra and concentration profiles of the involved components [11-14]. Specifically, the proposed systems were designed for topical application since this route of administration contributes to a higher exposure to sunlight and no topical preparation of NA is currently available. Skin is, indeed, an attractive and accessible route of drug delivery that offers many advantages such as avoiding the first-pass effect associated with oral or parenteral administration, an easy use, reduced side effects and a better patient compliance. *Ex-vivo* permeation

studies, using rabbit ear skin and vertical Franz diffusion cells, were, thus, performed to evaluate the skin permeation ability of new formulations.

2. Material and methods

2.1. Chemicals, Instruments and software

NA, propylene glycol, microcrystalline cellulose, Brij97 were purchased from Sigma-Aldrich (Milan, Italy). Ethanol and methanol were from J.T. Baker (Holland). UV spectra were recorded by using a Perkin-Elmer Lambda 40P Spectrophotometer by setting the following instrumental conditions: range 200–450 nm, scan rate 1 nm/s; time response 1 s; spectral band 1 nm. Spectral acquisition and elaboration were made by using the dedicate software UV WinLab® (Perkin-Elmer, Waltham, MA). A light cabinet Suntest CPS+ (Heraeus, Milan, Italy) equipped with a Xenon lamp was used to perform the photodegradation experiments. The ID65 standard filter was set to simulate sunlight in a spectral range between 300 and 800 nm.
Multivariate analysis was performed by the software Matlab® computer environment (Mathwork Inc., version 7).

2.2 Samples preparation

NA standard solutions were prepared in ethanol at the concentration of 5.0 μg /ml in consideration of the low drug solubility in water.
For ME preparation, the composition was chosen considering the ternary diagram phase BRIJ97/IPM/H_2O [15] and details are given in Table 1. In the first step, the oil phase (Isopropyl myristate, IPM) and BRIJ97 surfactant were mixed and heated at 70°C for 3 min. The drug was dissolved in this mixture and, then, added dropwise to aqueous phase. Finally, the samples were subject to different cycles of centrifugation at 3500 rpm for 10 min, followed by 4 min of vortex mixing at 2200 rpm. The final drug concentration in ME was 0.7% w/w. Moreover, in order to make the formulation suitable for topical application, ME were incorporated into a gel matrix. ME gels (5 g) were prepared according to the European Pharmacopoeia [16] by the procedure reported below: 4.35 g of NA-micro-emulsions were added to 0.5 g of propylene glycol and 0.15 g of cellulose and stirred magnetically up to 15 min to get opalescent homogenous gels. Furthermore, NA plain gels were prepared by emulsifying 0.035 g NA in propylene glycol and cellulose and then 4.35 g of distilled water were added stirring for 15 min.

Component	Weight (g) for 5 g of formulation
BRIJ97	0.95
IPM	0.25
H_2O	3.80

Table 1. Composition of micro-emulsion formulation.

2.3 Size and distribution analysis

The mean particle size of ME was measured by dynamic light scattering (DLS) using a 90 Plus Particle Size Analyzer (Brookhaven Instruments Corporation, New York, USA) at 25.0 ± 0.1 °C. Before measurement, ME were appropriately diluted in distilled water and the results were directly obtained from instrument data fitting through the inverse "Laplace transformation" and the Contin methods [17]. The polydispersity index (PI) was used as a measure of the width of size distribution. The PI values lower than 0.3 indicated a homogenous population for colloidal systems. All the measures were done in triplicate and expressed as mean ± standard deviation.

2.3. Photodegradation test

The photodegradation tests were made on all the prepared liquid and gel formulations under the following conditions: irradiation power 450 W/m^2, corresponding to 27 kJ/m^2 min, temperature 25 °C. The samples were analysed just after preparation (t= 0 min) and at the several exposure times (10-30-50-70-100-130-150-210-270-300 min) by UV spectrophotometry. All laboratory experiments were carried out in a dark room to minimize drug photodegradation.

Drug content in gel along the photodegradation experiments was measured by MCR applied on the UV data of the methanol extracts. At this aim, gel 0.5 g was uniformly stratified on a glass plate to form a layer thickness of 0.25 mm and then exposed to forced irradiation. After each irradiation dose, the glass plate was sonicated in acetonitrile 25 mL for 10 min at room temperature. 10 ml of the obtained suspension were centrifuged at 5000 rpm for 10 min and the supernatant was analysed after 1:10 dilution with methanol.

2.4 *Ex-vivo* permeation studies

Ex-vivo permeation studies were carried out using vertical diffusion Franz cells for 7 h at 37°C, through rabbit ear skin obtained from local slaughterhouse. The skin, previously frozen at −18 °C, was pre-equilibrated in physiological solution at room temperature for 2 h before the experiments. A circular piece of this skin was securely placed between the receptor and donor compartments with the dermal side in contact with the receiver medium and the epidermis side in contact with the donor chamber (contact area = 0.416 cm^2). The donor compartment was charged with an appropriate volume of samples to keep constant the drug moles. The receptor compartment was filled with 5.5 ml of fresh hydroalcoholic solution (water:ethanol /50:50) which was maintained at 37 ± 0.5 ◦C and stirred by magnetic bar. At regular time points up to7 h, the receptor solution was removed for analysis and replaced with an equal volume of pre-thermostated (37 °C ± 0.5 °C) fresh one.

The drug content in the samples was analyzed by UV–vis spectrometry. Each experiment was carried out in triplicate and the results were in agreement within ± standard deviation.

3. Results and discussion

3.1 Micro-emulsion characterization

The interest of pharmaceutical industry in the design of new dosage formulations for light-sensitive drug has clearly increased over the last few years. The encapsulation of photo-labile drugs in supramolecular systems represents an approach able to increase the drug stability and, at once, ensure optimal permeation across the skin.
In this light, ME have shown interesting and attractive advantages like high thermodynamic stability, ability to deliver both hydrophilic and lipophilic drug, increased drug solubility and, not least, photoprotective capability. Taking all these considerations, ME for the delivery of NA were prepared selecting an accurate ratio between oil, surfactant and water in ternary diagram phase BRIJ97/IPM/H_2O studied by Wang [15].
Oil in water ME empty and loaded with NA visually appeared as isotropic and translucent solutions. The samples were highly stable and no sedimentation, creaming and flocculation were observed during 6 months. The average oil droplet size of plain and drug-loaded ME was 20.16 ±1.70 and 23.64 ± 3.21 nm respectively. The NA loading did not change the physicochemical features of the designed colloidal systems. In addition, the polydispersity index of plain and NA-loaded ME was respectively 0.214 and 0.169 indicating a narrow oil droplet size distribution and, consequently, that formulations were relatively homogenous in size.

3.2. Photodegradation of NA samples

An ethanol solution of NA 5.0 μg/ml was subdued to forced photodegradation, under the standard conditions above reported. The spectra, depicted in Figure 1, were recorded just after the preparation and at several exposure times up to five hours.

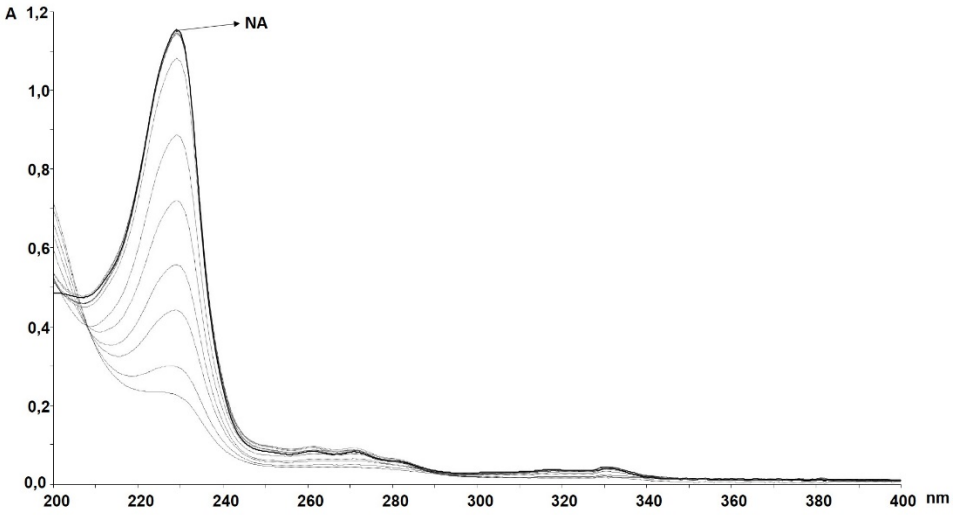

Figure 1. Absorbance spectra recorded for the ethanol solution of NA at several exposure times.

The spectral data, as average of five experiments collected during the photodegradation tests, were used to construct the data matrix to be analysed by MCR-ALS. The results reported in Figure 2 showed the NA photodegradation profiles and its photoproducts (A) and the respective absorbance spectra (B).
In accordance with the results reported in literature, data elaboration confirmed the formation of one major photoproduct (NA-P1) and traces of another by-product (NA-P2). Valero et al. [18] reported the photo-oxidation of the side chain to 6-methoxy-2-naphthaldehyde, as a major product, in butanol solution and the formation of the (4-(6-methoxy-2-naphthyl)-3-buten-2-one). In this solvent, the process seemed to be more efficient than in water [19].
In our experiment, a full degradation of the drug was observed after about 30 min. The degradation process proceeded via first-order kinetics, described by the equation:

$$\ln [\%NA] = - k \cdot t + 4.6$$

where %NA was the percentage of residual drug, k the photodegradation rate constant, t the time (min), and 4.6 the logarithm of the starting concentration (100%). The parameter $t_{0.1}$ (time to cause 10% degradation) was chosen as a criterion to compare the degradation behaviour of the tested samples. This parameter is conventionally adopted because a drug could no longer be used when its purity falls below 90%. Table 2 summarizes the degradation rate constants and the values of $t_{0.1}$ for all the studied matrices.
The value of k for NA solution was 0.0482 and $t_{0.1}$ resulted to be 2.08 min, as reported in Table 2.

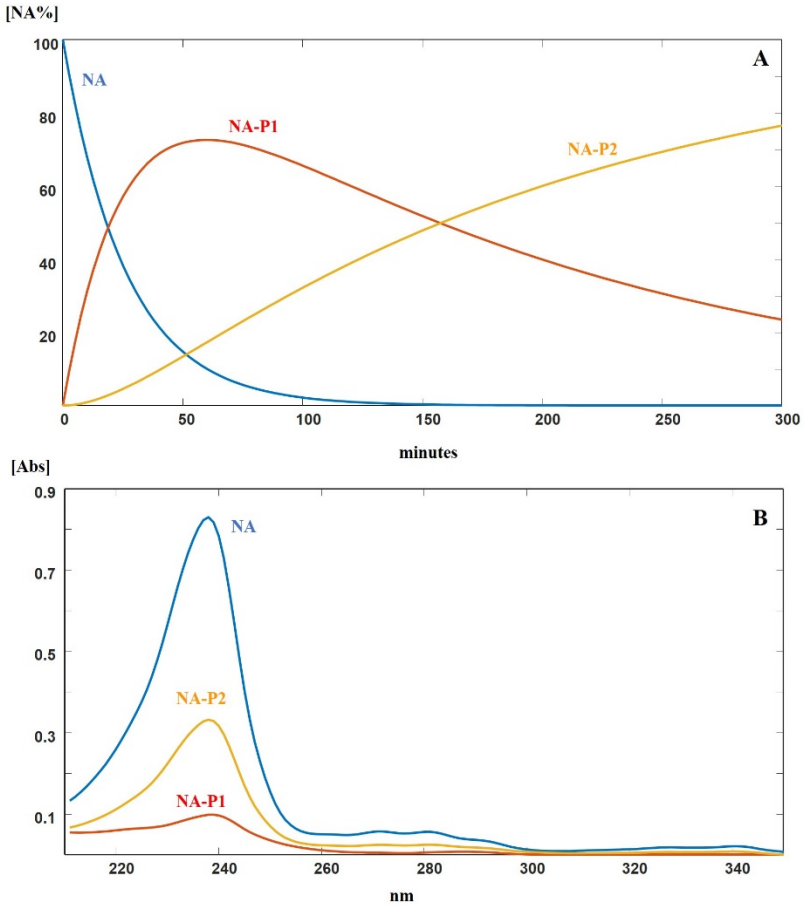

Figure 2. Photodegradation profiles of NA and its photoproducts (A) and their absorbance spectra (B)

Samples	K x 10^{-3}	$t_{0.1}$ (min)	R^2
NA-free	48.2	2.08	0.999
NA-gel	23.4	4.27	0.977
NA- ME	0.20	500.95	0.910
NA- ME gel	0.005	-	0.947

Table 2. Degradation kinetic parameters calculated for NA in different samples.

Photodegradation tests were then applied on the above described formulation prepared in gel. Gel formulation was made with 0.7% of the pure drug and exposed to light. The obtained data from the photodegradation experiments were processed by MCR method and the kinetics parameters are given in Table 2. Also in this formulation, the drug resulted very sensitive to light showing a $t_{0.1}$ value of 4.27 min.

In order to minimize the light degradation, the NA stability was investigated by entrapping the drug in ME. In this case, a clear decrease of NA degradation was measured, with a very successful $t_{0.1}$ value of 500.95 min.
This light-stable formulation was then performed in gel as above described, by showing a complete photoprotection of NA. The photodegradation profile of this formulation followed the first-order kinetics and was compared in Figure 3 to that of the other prepared formulations.

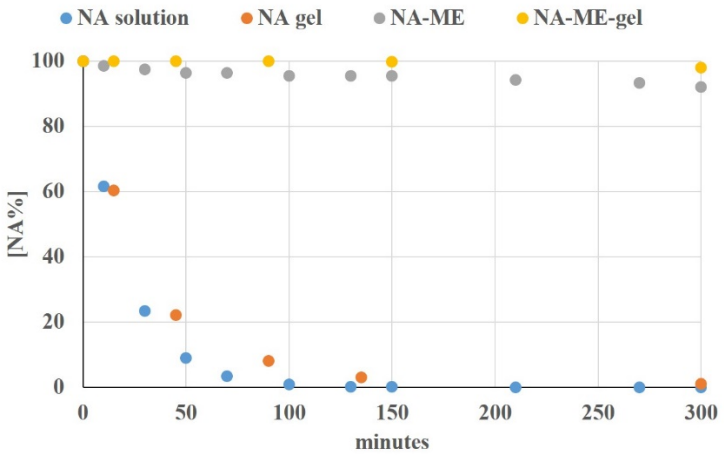

Figure 3. Photodegradation profiles of NA in all the prepared formulations.

3.4 Ex-vivo permeation studies

In order to evaluate the influence of the different type of formulations on NA skin permeation, *ex-vivo* percutaneous experiments were carried out using Franz cell diffusion system.
The cumulative amount of NA permeated from ME, ME gel and plain gel are plotted versus time in Figure 4. The obtained results clearly showed that NA skin permeation from ME systems was slowed down respect the plain gel. In fact, the amount of NA permeated after 7 h was 283.50 and 201.49 μg/cm^2 respectively from plain gel and ME. This trend could be ascribed to the lipophilic nature of the NA which has a very high partition coefficient (log P =3.08). In fact, it can be assumed that NA being lipophilic is located in the inner phase of ME and must firstly partition between the oil droplets and the continuous aqueous phase and, then, further onto the skin. So, this led to more slow drug permeation and higher drug retention capacity compared to plain gel where the NA is only embedded into polymeric network and, then, more available. This confirmed previous results reported in literature: ME can create drug reservoir into the skin from which the dug is released slowly for long-time [21]. This behaviour is interesting because suggests that the designed formulation could be used as retarded drug delivery systems. Afterwards, to further improve the formulation characteristics for topical delivery, we decided to entrap ME-NA in a gel matrix. In

fact, one of the major limits of ME is their low viscosity that is not suitable for topical application. The incorporation of ME in a gel network improves their rheological features increasing the residence time in the application site and ensuring an appropriate release. However, the high viscosity of polymeric network slows the drug diffusion. As expected, the NA permeation across skin from ME gel appeared be slower respect liquid ME. This delay could be attributed to the fact that the drug has further barrier in skin partitioning representing by the high viscosity of gel dosage that decreases drug mobility. *Ex vivo* percutaneous permeation experiments showed that ME gel may control and prolong the NA release, increasing skin retention. The creation of a drug reservoir into the skin is able to cut down the frequency of the applications, thus, improving patient compliance. The obtained results clearly suggest that the new topical dosage forms may be potentially useful as retarded drug delivery systems.

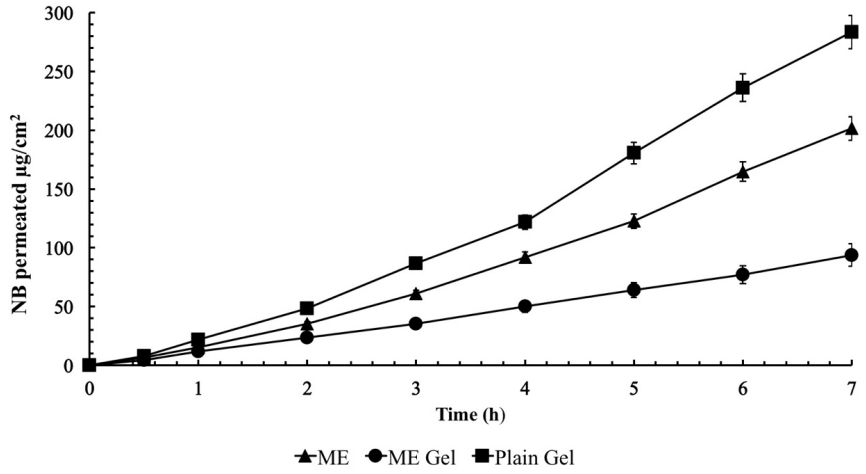

Figure 4. Cumulative amount of NB permeated from different samples through rabbit ear skin at 37°C: micro-emulsion (▲), micro-emulsion gel (●), plain gel (■) at 0.7 % of drug (mean ± SD; n = 3).

4. Conclusions

In this work, the anti-inflammatory drug Nabumetone, either in solution or in gel formulations, was demonstrated to undergo photodegradation. The study was performed by adopting photostability tests defined by international rules. In particular, under an irradiance power of 350 W/m^2, corresponding to 21 kJ/m^2 min and at a constant temperature of 25° C, the drug resulted degraded of 10% in only 2.08 and 4.27 min in ethanol and gel, respectively. The design of photoprotective pharmaceutical matrices for topical application is particularly important due to the greater probability of light exposure that can cause a lower drug bioavailability and, at the same time, can increase the risk of toxic photoproducts formation. In this study, the drug entrapment into ME was the adopted approach to reduce drug

photodegradation, reaching a very satisfactory value of 500 min for $t_{0.1}$, and a complete photoprotection when the ME was prepared in gel. The proposed system which has been shown to be particularly effective in reducing the drug photodegradation could be considered a valuable starting point for the development of innovative pharmaceutical formulations for Nabumetone topical use.

References

[1]Tonnesen H H, 2001 *Int.J. Pharm.* Formulation and stability testing of photolabile drugs, **225 (1-2)**, 1-14.
[2]ICH harmonized tripartite guideline, 1997 *Federal Register*. Photostability testing of new drug substance and products, 62, 27115–27122.
[3] Ragno G, Risoli A, Ioele G, Cione E, De Luca M, 2006 *J. Nanosci. Nanotechnol.* Photostabilization of 1,4-dihydropyridine antihypertensives by incorporation into β-cyclodextrin and liposomes, **6**, 2979-2985.
[4] Ragno G, Cione E, Garofalo A, Genchi G, Ioele G, Risoli A, Spagnoletta A 2003 *Int.J. Pharm.*, Design and monitoring of photostability systems for amlodipine dosage forms, **265(1-2)** 125-132.
[5] Ioele G, De Luca M, Ragno G 2014 *Future Med. Chem*. Photostability of barnidipine in combined cyclodextrin-in-liposome matrices, **6(1)** 35-43.
[6] Ioele G, De Luca M, Garofalo A, Ragno G 2017 *Drug deliv* Photosensitive drugs: a review on their photoprotection by liposomes and cyclodextrins, **24 (sup1)**, 33-44
[7] Coelho L, Almeida I F, Sousa Lobo J M, Sousa E S J P 2018 *Int.J. Pharm*, Photostabilization strategies of photosensitive drugs, **541(1-2)** 19-25.
[8] Xia L, Zhongxiao C, Zhihao L, Xiaodong M, Ming X, Yan T, Xinyi Z, Bingqing X, Jianbin Z, Zeyao T 2018 *J Drug Deliv Scien Technol,* Improvement of the solubility, photostability, antioxidant activity and UVB photoprotection of trans-resveratrol by essential oil based microemulsions for topical application, 48, 346-354
[9] Vicentini, F T, Fonseca, Y M, Pitol, D L, Lyomasa, M M, Bentley, M V, Fonseca M J 2010 *J Pharm Pharmaceut Sci,* Evaluation of Protective Effect of a Water-In-Oil Microemulsion Incorporating Quercetin Against UVB-Induced Damage in Hairless Mice Skin, 13(2) 274 - 285.
[10] Patel, M R, Patel, R B, Parikh, J R, Patel, B J 2011 *ISRN Pharmaceutics*, Improving the Isotretinoin Photostability by Incorporating in Microemulsion Matrix 6 pages
[11] Cmrr N, Ponto T, Abd E, Grice JE, Hae B, Roberts MS. Topical Nano and Microemulsions for skin delivery. Pharmaceutics. 2017;9(4):37–62.
[12] Goswami P, Choudhury A, Kumar Dey B 2019 *International Journal of Pharmaceutical & Biological Archives,* Microemulsion – A Potential Carrier for Improved Bioavailability 10(2):69-77
[13] De Luca M, Mas S, Ioele G, Oliverio F, Ragno G, Tauler R, 2010 *Int.J. Pharm.*Kinetic studies of nitrofurazone photodegradation by multivariate curve resolution applied to UV-spectral data, **386(1-2)** 99-107.
[14] De Luca M, Tauler R, Ioele G, Ragno G, 2013 *Drug Test. Anal.*Study of photodegradation kinetics of melatonin by multivariate curve resolution (MCR) with estimation of feasible band boundaries, **5(2)** 96-102.
[15] Wang Z, Diao Z, Liu F, Li G, 2006 *J. Colloid Interface Sci.* Microstructure and rheological properties of liquid crystallines formed in Brij 97/water/IPM system. 297(2) 813-818.
[16]*Council of Europe,* 2010 *European pharmacopoeia*.
[17] Provencher S W, *Comput. Phys. Commun.*1982 A constrained regularization method for inverting data represented by linear algebraic or integral equations. 27, 229.

[18] Valero M., 2004 *J. Photochem. Photobiol. A: Chemistry* Photodegradation of Nabumetone in n-butanol solutions**,163(1-2)**, 159-164.
[19] Valero M, Costa S M B 2003 *J. Photochem. Photobiol. A: Chemistry* Photodegradation of Nabumetone in aqueous solutions, **157(1, 21)** 93-101.
[20] Higuchi T, Connors K 1985 *Adv. Anal. Chem. Instr.* Phase solubility techniques, **4**, 127-212.
[21] Mazzotta E, Rossi C O, muzzalupo R 2019 *Colloids and Surfaces B: Biointerfaces* Different BRIJ97 colloid systems as potential enhancers of acyclovir skin permeation and depot. 173, 623–631